Energy, Environment, and Sustainability
Series Editors: Avinash Kumar Agarwal · Ashok Pandey

Franz Winter
Rashmi Avinash Agarwal
Jan Hrdlicka
Sunita Varjani *Editors*

CO_2 Separation, Purification and Conversion to Chemicals and Fuels

Springer

Energy, Environment, and Sustainability

This books series publishes cutting edge monographs and professional books focused on all aspects of energy and environmental sustainability, especially as it relates to energy concerns. The Series is published in partnership with the International Society for Energy, Environment, and Sustainability. The books in these series are editor or authored by top researchers and professional across the globe. The series aims at publishing state-of-the-art research and development in areas including, but not limited to:

- Renewable Energy
- Alternative Fuels
- Engines and Locomotives
- Combustion and Propulsion
- Fossil Fuels
- Carbon Capture
- Control and Automation for Energy
- Environmental Pollution
- Waste Management
- Transportation Sustainability

More information about this series at http://www.springer.com/series/15901

Franz Winter · Rashmi Avinash Agarwal
Jan Hrdlicka · Sunita Varjani
Editors

CO_2 Separation, Purification and Conversion to Chemicals and Fuels

Springer

Editors
Franz Winter
Institute of Chemical, Environmental and Bioscience Engineering
Technische Universität Wien
Vienna, Austria

Rashmi Avinash Agarwal
Department of Civil Engineering
Indian Institute of Technology Kanpur
Kanpur, Uttar Pradesh, India

Jan Hrdlicka
Department of Energy Engineering
Czech Technical University in Prague
Prague, Czech Republic

Sunita Varjani
Gujarat Pollution Control Board
Gandhinagar, Gujarat, India

ISSN 2522-8366 ISSN 2522-8374 (electronic)
Energy, Environment, and Sustainability
ISBN 978-981-13-3295-1 ISBN 978-981-13-3296-8 (eBook)
https://doi.org/10.1007/978-981-13-3296-8

Library of Congress Control Number: 2018961229

This Springer imprint is published by the registered company Springer Nature Singapore Pte Ltd.
The registered company address is: 152 Beach Road, #21-01/04 Gateway East, Singapore 189721, Singapore

Preface

Energy demand has been rising remarkably due to increasing population and urbanization. Global economy and society are significantly dependent on the energy availability because it touches every facet of human life and its activities. Transportation and power generation are two major examples. Without the transportation by millions of personalized and mass transport vehicles and availability of 24×7 power, human civilization would not have reached contemporary living standards.

The International Society for Energy, Environment and Sustainability (ISEES) was founded at Indian Institute of Technology Kanpur (IIT Kanpur), India, in January 2014 with the aim of spreading knowledge/awareness and catalysing research activities in the fields of energy, environment, sustainability and combustion. The society's goal is to contribute to the development of clean, affordable and secure energy resources and a sustainable environment for the society and to spread knowledge in the above-mentioned areas and create awareness about the environmental challenges, which the world is facing today. The unique way adopted by the society was to break the conventional silos of specializations (engineering, science, environment, agriculture, biotechnology, materials, fuels, etc.) to tackle the problems related to energy, environment and sustainability in a holistic manner. This is quite evident by the participation of experts from all fields to resolve these issues. ISEES is involved in various activities such as conducting workshops, seminars and conferences in the domains of its interest. The society also recognizes the outstanding works done by the young scientists and engineers for their contributions in these fields by conferring them awards under various categories.

The second international conference on "Sustainable Energy and Environmental Challenges" (SEEC-2018) was organized under the auspices of ISEES from 31 December 2017 to 3 January 3 2018 at J N Tata Auditorium, Indian Institute of Science Bangalore. This conference provided a platform for discussions between eminent scientists and engineers from various countries including India, USA, South Korea, Norway, Finland, Malaysia, Austria, Saudi Arabia and Australia. In this conference, eminent speakers from all over the world presented their views

related to different aspects of energy, combustion, emissions and alternative energy resources for sustainable development and a cleaner environment. The conference presented five high-voltage plenary talks from globally renowned experts on topical themes, namely "Is It Really the End of Combustion Engines and Petroleum?" by Prof. Gautam Kalghatgi, Saudi Aramco; "Energy Sustainability in India: Challenges and Opportunities" by Prof. Baldev Raj, NIAS Bangalore; "Methanol Economy: An Option for Sustainable Energy and Environmental Challenges" by Dr. Vijay Kumar Saraswat, Hon. Member (S&T), NITI Aayog, Government of India; "Supercritical Carbon Dioxide Brayton Cycle for Power Generation" by Prof. Pradip Dutta, IISc Bangalore; and "Role of Nuclear Fusion for Environmental Sustainability of Energy in Future" by Prof. J. S. Rao, Altair Engineering.

The conference included 27 technical sessions on topics related to energy and environmental sustainability including 5 plenary talks, 40 keynote talks and 18 invited talks from prominent scientists, in addition to 142 contributed talks, and 74 poster presentations by students and researchers. The technical sessions in the conference included Advances in IC Engines: SI Engines, Solar Energy: Storage, Fundamentals of Combustion, Environmental Protection and Sustainability, Environmental Biotechnology, Coal and Biomass Combustion/Gasification, Air Pollution and Control, Biomass to Fuels/Chemicals: Clean Fuels, Advances in IC Engines: CI Engines, Solar Energy: Performance, Biomass to Fuels/Chemicals: Production, Advances in IC Engines: Fuels, Energy Sustainability, Environmental Biotechnology, Atomization and Sprays, Combustion/Gas Turbines/Fluid Flow/Sprays, Biomass to Fuels/Chemicals, Advances in IC Engines: New Concepts, Energy Sustainability, Waste to Wealth, Conventional and Alternate Fuels, Solar Energy, Wastewater Remediation and Air Pollution. One of the highlights of the conference was the rapid-fire poster sessions in (i) Energy Engineering, (ii) Environment and Sustainability and (iii) Biotechnology, where more than 75 students participated with great enthusiasm and won many prizes in a fiercely competitive environment. More than 200 participants and speakers attended this four-day conference, which also hosted Dr. Vijay Kumar Saraswat, Hon. Member (S&T), NITI Aayog, Government of India, as the chief guest for the book release ceremony, where 16 ISEES books published by Springer, under a special dedicated series "Energy, Environment, and Sustainability" were released. This is the first time that such significant and high-quality outcome has been achieved by any society in India. The conference concluded with a panel discussion on "Challenges, Opportunities & Directions for Future Transportation Systems", where the panellists were Prof. Gautam Kalghatgi, Saudi Aramco; Dr. Ravi Prashanth, Caterpillar Inc.; Dr. Shankar Venugopal, Mahindra and Mahindra; Dr. Bharat Bhargava, DG, ONGC Energy Centre; and Dr. Umamaheshwar, GE Transportation, Bangalore. The panel discussion was moderated by Prof. Ashok Pandey, Chairman, ISEES. This conference laid out the road map for technology development, opportunities and challenges in energy, environment and sustainability domains. All these topics are very relevant for the country and the world in the present context. We acknowledge the support received from various funding agencies and organizations for the successful conduct of the second ISEES

conference SEEC-2018, where these books germinated. We would therefore like to acknowledge SERB, Government of India (special thanks to Dr. Rajeev Sharma, Secretary); ONGC Energy Centre (special thanks to Dr. Bharat Bhargava); TAFE (special thanks to Sh. Anadrao Patil); Caterpillar (special thanks to Dr. Ravi Prashanth); Progress Rail, TSI, India (special thanks to Dr. Deepak Sharma); Tesscorn, India (special thanks to Sh. Satyanarayana); GAIL, Volvo; and our publishing partner Springer (special thanks to Swati Meherishi).

The editors would like to express their sincere gratitude to a large number of authors from all over the world for submitting their high-quality work in a timely manner and revising it appropriately at short notice. We would like to express our special thanks to all our reviewers who reviewed various chapters of this book and provided very valuable suggestions to the authors to improve their manuscript.

The book covers different aspects of CO_2 separation, purification and conversion to chemicals and fuels. It gives an excellent overview of the importance to control CO_2 emissions and to utilize CO_2 as a carbon source. A special focus is given on the mitigation of climate change.

Vienna, Austria — Franz Winter
Kanpur, India — Rashmi Avinash Agarwal
Prague, Czech Republic — Jan Hrdlicka
Gandhinagar, India — Sunita Varjani

Contents

Editors and Contributors

About the Editors

Prof. Franz Winter is Professor and Head of the Chemical Process Engineering and Energy Technology Research Division and the Reaction Engineering & Combustion Research Group at the Institute of Chemical, Environmental and Biological Engineering at the TU Wien in Austria, where he also completed his Ph.D. His research interests include mathematical modelling and experimental work in energy conversion, CO_2 utilization, combustion chemistry for waste utilization and engine technology and design, and high-temperature gas–solid processes. He has published more than 90 journal articles, 190 conference papers, and 40 chapters and patents.

Dr. Rashmi Avinash Agarwal is Senior Researcher at IIT Kanpur. She completed her doctoral degree in inorganic chemistry at IIT Kanpur in 2014; her M.Sc. in organic chemistry at Rajasthan University, Jaipur, in 2002; and B.Sc. in chemistry from Kanoria College, Rajasthan University, in 2000. She has expertise in coordination chemistry, coordination polymers, organic synthesis, inorganic synthesis, crystal structure determination, supramolecular chemistry, porous materials, topology, fluorescence, SC (single crystal)-to-SC transformation and synthesis of nanoparticles. She has published over 20 research papers in leading international journals.

Assoc. Prof. Jan Hrdlicka is Associate Professor at the Faculty of Mechanical Engineering, Czech Technical University, Prague. His research interests include combustion processes, fluidized bed combustion, emission control, CCS (oxyfuel combustion, chemical looping), energy conversion of biomass, alternative fuels and energy sources and industrial energy sources. He completed his Ph.D. at the University of Chemistry and Technology, Prague. He has received a DAAD fellowship, Marie Curie fellowship and Erasmus fellowship.

Dr. Sunita Varjani is Scientific Officer at Gujarat Pollution Control Board, Gandhinagar, Gujarat, India. She holds an M.Sc. in microbiology and Ph.D. in biotechnology. Her major areas of research are industrial and environmental microbiology/biotechnology. She has authored more than 60 publications, including research and review papers, books and chapters. She has won several awards and honours, including Young Scientist Award—2018 by International Society for Energy, Environment and Sustainability; Certificate of Appreciation—2017 from EPFL, Lausanne, Switzerland; Top Reviewer Award—2017 from *Bioresource Technology Journal*, Elsevier; Young Scientist Award at AFRO-ASIAN Congress on Microbes for Human and Environmental Health, New Delhi (2014); and Best Paper Awards in national and international conferences in 2008, 2012 and 2013. She is Member of the editorial board of *Journal of Energy and Environmental Sustainability* and has served as Guest Editor of special issues of *Bioresource Technology Journal*, *Journal of Energy and Environmental Sustainability* and *Indian Journal of Experimental Biology*. She is the recipient of visiting scientist fellowship from EPFL, Lausanne, Switzerland (2017).

Contributors

Mohammad R. M. Abu Zahra Department of Chemical Engineering, Khalifa University of Science and Technology, Masdar City, Abu Dhabi, United Arab Emirates

Rashmi A. Agarwal Department of Civil Engineering, Indian Institute of Technology Kanpur, Kanpur, UP, India

E. J. Anthony Cranfield University, Cranfield, UK

Mukesh Kumar Awasthi College of Natural Resources and Environment, Northwest A&F University, Yangling, Shaanxi, China

Sanjeev Kumar Awasthi College of Natural Resources and Environment, Northwest A&F University, Yangling, Shaanxi, China

P. Thirumala Bai Department of Chemical Engineering, National Institute of Technology Warangal, Warangal, Telangana, India

Hongyu Chen College of Natural Resources and Environment, Northwest A&F University, Yangling, Shaanxi, China

Raghuram Chetty Department of Chemical Engineering, Indian Institute of Technology Madras, Chennai, India

P. T. Clough Cranfield University, Cranfield, UK

Abdallah Dindi Department of Chemical Engineering, Khalifa University of Science and Technology, Masdar City, Abu Dhabi, United Arab Emirates

Tomáš Dlouhý Department of Energy Engineering, Faculty of Mechanical Engineering, Czech Technical University, Praha 6, Czech Republic

Yumin Duan College of Natural Resources and Environment, Northwest A&F University, Yangling, Shaanxi, China

František Hrdlička Department of Energy Engineering, Faculty of Mechanical Engineering, Czech Technical University, Praha 6, Czech Republic

Jan Hrdlicka Department of Energy Engineering, Faculty of Mechanical Engineering, Czech Technical University, Praha 6, Czech Republic

Asha Humbal Central University of Gujarat, Gandhinagar, Gujarat, India

G. Keerthiga Department of Chemical Engineering, Indian Institute of Technology Madras, Chennai, India

Tao Liu College of Natural Resources and Environment, Northwest A&F University, Yangling, Shaanxi, China

Ashok Pandey CSIR-Indian Institute of Toxicology Research, Lucknow, UP, India

P. S. Sai Prasad Indian Institute of Chemical Technology, Hyderabad, India

Dang Viet Quang Department of Chemical Engineering, Khalifa University of Science and Technology, Masdar City, Abu Dhabi, United Arab Emirates

K. S. Rajmohan Department of Chemical Engineering, Indian Institute of Technology Madras, Chennai, India; Department of Chemical Engineering, National Institute of Technology Warangal, Warangal, Telangana, India

Xiuna Ren College of Natural Resources and Environment, Northwest A&F University, Yangling, Shaanxi, China

Pavel Skopec Department of Energy Engineering, Faculty of Mechanical Engineering, Czech Technical University, Praha 6, Czech Republic

S. Srinath Department of Chemical Engineering, National Institute of Technology Warangal, Warangal, Telangana, India; Gujarat Pollution Control Board, Gandhinagar, Gujarat, India

Vijay Kumar Srivastava Sankalchand Patel University, Visnagar, Gujarat, India

Sunita Varjani Gujarat Pollution Control Board, Gandhinagar, Gujarat, India

Matěj Vodička Department of Energy Engineering, Faculty of Mechanical Engineering, Czech Technical University, Praha 6, Czech Republic

Franz Winter Institute of Chemical, Environmental and Bioscience Engineering, Technische Universität Wien, Vienna, Austria

Zengqiang Zhang Gujarat Pollution Control Board, Gandhinagar, Gujarat, India

Junchao Zhao College of Natural Resources and Environment, Northwest A&F University, Yangling, Shaanxi, China

Chapter 1
Introduction to CO_2 Separation, Purification and Conversion to Chemicals and Fuels

Franz Winter, Rashmi A. Agarwal, Jan Hrdlicka and Sunita Varjani

Abstract Carbon dioxide, i.e. CO_2, is the most important greenhouse gas and considered to contribute significantly to climate change and global warming. Besides the reduction of CO_2 emissions, there is also a high potential to integrate CO_2 in terms of a carbon conversion cycle to products using it as the carbon source. This book deals with the effects of CO_2 on climate change and global warming and with the whole process chain from CO_2 separation, purification and conversion to chemicals and fuels. CO_2 which is a final product can also be considered as an initial material for product formation like chemicals and fuels like in nature where CO_2 is used from the atmosphere to produce with water and sunlight sugar and oxygen by photosynthesis.

Keywords CO_2 · Separation · Purification · Conversion · Chemicals Fuels

This chapter gives an introduction and overview of the book. CO_2 is the most important greenhouse gas and is considered to contribute most significantly to climate change and global warming. An excellent source of information is the Intergovermental Panel on Climate Change (IPCC) which is continuously assessing

F. Winter (✉)
Institute of Chemical, Environmental and Bioscience Engineering, Technische Universität Wien, Getreidemarkt 9/166, 1060 Vienna, Austria
e-mail: franz.winter@tuwien.ac.at

R. A. Agarwal
Department of Civil Engineering, Indian Institute of Technology Kanpur, Kanpur 208016, UP, India

J. Hrdlicka
Department of Energy Engineering, Czech Technical University in Prague, 166 07 Prague, Czech Republic

S. Varjani
Gujarat Pollution Control Board, Sector-10A, Gandhinagar 382010, Gujarat, India

F. Winter et al. (eds.), *CO_2 Separation, Purification and Conversion to Chemicals and Fuels*, Energy, Environment, and Sustainability,
https://doi.org/10.1007/978-981-13-3296-8_1

our climate. It is part of the United Nations Environment Programme (UNEP) and the World Meteorological Organization (WMO); see also their website www.ipcc.ch.

In nature, CO_2 is the most important carbon source and necessary to form together with water and sunlight sugar and oxygen, O_2, by photosynthesis which is the basis for our life on earth. Even if we are not yet able to perform the photosynthesis in industrial practice, CO_2 can be used in technical processes as the carbon source, e.g. taken from flue gas for storage but also for the production of valuable chemicals and fuels.

In Chap. 2, the sources of CO_2 emissions are illustrated and discussed. Besides the natural processes like respiration, decomposition of plants and vulcanic activities, anthropogenic sources such fossil fuel combustion, the industrial sector, the transportation sector as well as land use are the sources of CO_2 emission. The concentration of CO_2 in the atmosphere has been increased in the last few years and is expected to further increase at even faster rates. CO_2 is a strong greenhouse gas and therefore considered to contribute significantly to climate change and global warming. There exist different methods of carbon sequestration, and it can be an oceanic carbon sequestration or a geological or a biological carbon sequestration. These different processes are shown and illustrated.

In Chap. 3, the mitigation and utilization in composting of CO_2 are given, also considering the greenhouse gases CH_4 and N_2O. An overview of the different technologies is presented generating different products like biochar, compost, charcoal, phosphates, biogas. Biocatalytic CO_2 conservation looks very promising in composting and other waste management industries, also with a special focus on the hydrogen. However there is still much room for further practical improvement.

Chapter 4 gives an overview of the different CO_2 capture and storage processes focusing on post-combustion capture but also on CO_2 capture from the transportation sector, the cement and steel industry as well as marine technology. It is discussed that the technology deployment will need time even for well-tested processes like oxyfuel combustion, as well as chemical looping combustion (CLC) and calcium looping (CaL). The most established post-combustion carbon capture and storage (CCS) technology is amine scrubbing. It has been validated at the commercial scale for the treatment of flue gases from coal firing.

Chapter 5 goes into the details and focuses on oxyfuel combustion, especially using fluidized bed technology. In the oxyfuel combustion, the combustion air is replaced by oxygen, which requires an air separation unit (ASU). To maintain operating temperatures at acceptable levels and to provide a heat carrier, a high degree of flue gas recirculation (FGR) is essential.

The great advantage of using oxyfuel combustion is that the technology is not technically complicated and the resulting flue gas contains, besides trace pollutants, particularly CO_2 and water vapour, which can be easily separated, and then the CO_2 is ready for further utilization.

There is also a theoretical analysis provided in this chapter and effects on the operation of such units and real oxyfuel operation data provided. In addition, the formation and reduction of pollutants during oxyfuel combustion are elucidated like CO, NO_x and SO_2.

In Chap. 6, a very interesting synthesis route is shown and discussed in detail, the formation of methanol by the hydrogenation of CO_2. Methanol is a small but very important species in the chemical industry and a base material for further synthesis routes to larger molecules. However, on the other side, methanol can be used as an energy carrier and directly as an excellent fuel, e.g. for cars.

In this chapter, the heterogeneously catalysed synthesis of methanol is presented and new technologies are discussed. The utilization of specially designed catalysts using metal–organic frameworks (MOFs) with copper/zinc nanoparticles as catalysts is shown.

Ethylene is a very important gas significantly used in the chemical industry. Chapter 7 focuses on the production of ethylene from ethane with CO_2 in an oxidative dehydrogenation process where CO_2 is used as the reacting agent. There exist significant advantages of this process in relation to other production routes. Oxidative dehydrogenation can be operated at relatively low temperatures (350–600 °C) at very high conversion rates. Therefore, it is a significantly less energy-demanding production route.

However, catalysts are necessary for the process like alkali/earth alkali metal oxides and chlorides, or rare earth metal oxides or transition metal oxides. These different catalysts are discussed, and characterization methods and methods for their synthesis are demonstrated.

In Chap. 8, the electrochemical reduction of CO_2 into low carbon, hydrocarbon, oxygenated hydrocarbon chemicals and fuels, e.g. formic acid, formaldehyde, methanol, is discussed including promising combinations of methods like bio-electrochemical reduction, solar thermochemical reduction and photocatalytic processes.

A very important aspect is the selection of the electrodes and the electrolytes used. This together with temperature and pressure results in a wide range of options regarding operating conditions and materials.

The book finally concludes with Chap. 9 which contributes to the inorganic utilization of CO_2 in the process industry for soda ash (Na_2CO_3) and baking soda ($NaHCO_3$). The conventional production route to soda ash is the Solvay process which is not optimal in CO_2 utilization.

There exists a significant potential to reduce CO_2 consumption in new or modified process routes and not only in the soda industry, especially in combination with alkaline waste streams.

Chapter 2
Carbon Sequestration a Viable Option to Mitigate Climate Change

Sunita Varjani, Asha Humbal and Vijay Kumar Srivastava

Abstract Anthropogenic activity mainly burning of fossil fuels like coal, gas and oil is one of the major reasons which increase concentration of earth-warming gases. Chief among these gases is carbon dioxide. As per the data in last 250 years, CO_2 level increases from 250 to more than 280 parts per million (PPM). Major consequences of this rise in CO_2 level involve disturbance in climatic factors such as sea level rise; floods; droughts; changes in the amount, timing and distribution of rain; increased frequency and intensity of wildfires and disturbance of coastal marine and other ecosystems. That is why control over CO_2 production and reducing CO_2 level become important. One of the natural ways to CO_2 control involves CO_2 sequestration which involves removal of CO_2 from atmosphere or storage of CO_2 from emission sources to vegetation, soil and sediments. Biological carbon sequestration has opened up a new area of research towards enhancing rapid fixation of atmospheric carbon dioxide in present level to reduce and mitigate global warming and climate change. This chapter describes various sources of carbon dioxide with relation to increasing greenhouse gases. It also includes scientific basis for current understanding of climate change and the role of biological carbon sequestration like soil, grassland, peatland and forests for mitigating the increasing atmospheric CO_2 concentration.

Keywords Earth-warming gases · CO_2 · Biological sequestration
Climate change

S. Varjani (✉)
Gujarat Pollution Control Board, Sector-10A, Gandhinagar 382010, Gujarat, India
e-mail: drsvs18@gmail.com

A. Humbal
Central University of Gujarat, Gandhinagar 382010, Gujarat, India

V. K. Srivastava
Sankalchand Patel University, Sankalchand Patel Vidyadham,
Visnagar 384315, Gujarat, India

F. Winter et al. (eds.), *CO_2 Separation, Purification and Conversion to Chemicals and Fuels*, Energy, Environment, and Sustainability,
https://doi.org/10.1007/978-981-13-3296-8_2

2.1 Introduction

Change in the climatic condition is one of the biggest challenges to human society in the twenty-first century [1]. Increasing in various earth-warming gases as a result of various anthropogenic activities leads to change in current climatic conditions. Chief among these gases is carbon dioxide. Heat emitted from earth's surface is trap by greenhouse gases such as CO_2 which leads to earth to warm by trapping heat [2]. A small increase in amount of carbon dioxide has significant effect on climatic conditions. The concentration of CO_2 is increasing year on year as the increase in various human activities which are increasing the natural greenhouse effect and warms the planet [3]. Data show that over the last 200 years, CO_2 increases from 280 ppmv (parts per million by volume) to 400 ppmv [2]. As per the international energy agency, in 2016, 40% increase in CO_2 concentration observed than in the mid-1800. As per IPCC [4], during the twenty-first-century temperature will increase between 1.0 and 3.7 °C [1].

Before human-caused CO_2 emissions began, the level of CO_2 uptake and its atmospheric release was maintained through the global "carbon cycle". However, existing CO_2 uptake mechanisms are insufficient [5] as increasing in emission of carbon dioxide related to various anthropogenic activities like burning of fossil fuels such as gas, oil and coal which lead to enhancing the concentration of carbon dioxide (CO_2) in the atmosphere. Human-originated activity enhances the CO_2 concentration by more than a third since the Industrial Revolution began [6]. Human activities currently release over 30 billion tons of CO_2 into the atmosphere every year [7]. Increase in CO_2 level leads to various adverse effects such as sea level rise, changes in the amount, timing and distribution of rain, floods [5]. Therefore, it is essential to controlling the concentration of CO_2 for minimization of its dangerous impacts on the climatic condition. Reducing in concentration of carbon dioxide will require technically and economically feasible strategies. Carbon sequestration is the technology which removes the carbon dioxide from the atmosphere and diverted from emission sources and long-term storage of atmospheric carbon dioxide to mitigate global warming and to avoid dangerous impacts of climate change [8].

2.2 Sources of CO_2 Emission

The sources of CO_2 emission can be divided into two categories: natural sources and anthropogenic sources. Natural sources of CO_2 include respiration, decomposition and volcanic activity. Anthropogenic sources of CO_2 include fossil fuel combustion, industrial sector, land use changes and transportation sector (Fig. 2.1).

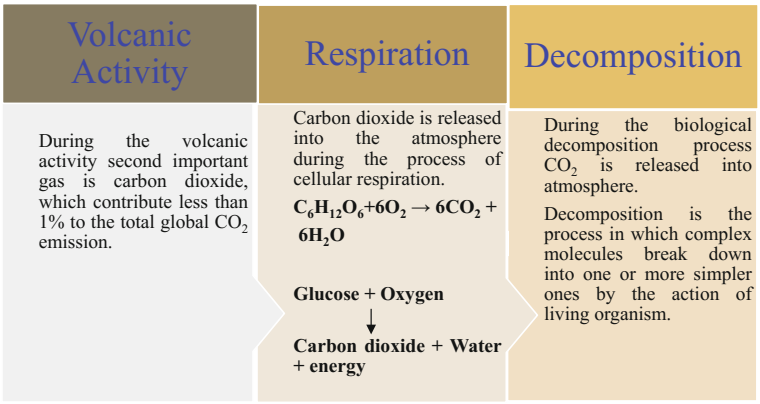

Fig. 2.1 Natural sources of CO_2 emission

2.2.1 *Fossil Fuel Combustion*

Fossil fuel power plants are considered as one of the largest sources of CO_2 emission. Worldwide more than one-third of the CO_2 release from the fossil-fuelled power plants [9]. Fossil fuel combustion produces 77% of total GWP–weighted emissions from all emission sources in 2015 [7]. 6–8 Gt/year of CO_2 release from 1000 MW pulverized coal-fired power plants, an oil-fired single cycle power plant about two-thirds of that and a natural gas combined cycle power plant about one-half of that [9].

2.2.2 *Industrial Sector*

There are multiple processes in industries which emit good amount of CO_2 into the atmosphere as by-product of various chemical processes. Metals production, chemicals production, cement production and petrochemical productions are the main four sources of CO_2 emission which approximately account for 4% of human CO_2 emission [10]. As per IPCC report 2014, industrial CO_2 emissions were 13.14 $GtCO_2$ in 2010. These emissions were comprised of 5.27 $GtCO_2$ direct energy-related emissions, 5.25 $GtCO_2$ indirect emissions from electricity and heat production.

2.2.3 Land Use Changes

Land use changes mainly include deforestation or afforestation, since trees act as carbon sink reduction in trees which result into reduction in CO_2 removal [11]. Land use and land use change account for 396–690 billion tons of carbon dioxide release to the atmosphere from 1850 to 2000 [12]. It is one of the extensive sources of carbon dioxide emissions globally, which accounts for 9% of human carbon dioxide emissions [10].

2.2.4 Transportation Sector

Transportation is one of the potential contributors to urban CO_2 emission. As per UN statistics, urban carbon accounts for 75% of total CO_2 emission and specifically transportation accounts for 17.5%. It is reported that in the year 2010, 22% of fossil fuel-related CO_2 emitted by transportation sector only.

2.3 What Is Carbon Sequestration?

Sequestration of carbon is processed in which atmospheric CO_2 is diverted or removed from emission source. It is the technology of prolong storage of CO_2 to minimize global warming and effect of climate change (Fig. 2.2).

2.3.1 Oceanic Carbon Sequestration

One strategy to minimize the concentration of atmospheric greenhouse gasses is oceanic carbon sequestration which includes capture carbon dioxide from large stationary sources and injects it into the deep ocean [13]. Ocean acts as the primary long-term sink for human-caused CO_2 emissions, and it uptakes about 2 gigaton of global net of carbon annually [5]. Due to the difference in partial pressure of CO_2

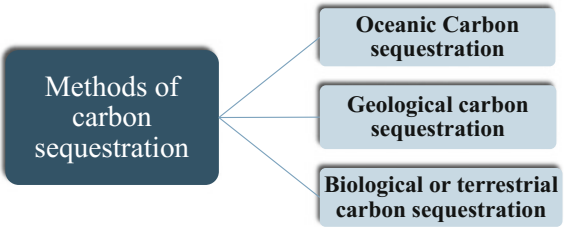

Fig. 2.2 Methods for carbon sequestration [5]

between atmosphere and ocean, CO_2 absorbed by ocean [14]. There is no practical limit to store the CO_2 because the ocean covers 70% of earth surface with an average depth of about 3800 m. However, the amount of CO_2 stored in the ocean depends on oceanic equilibration with the atmosphere (IPCC 2007). CO_2 is a weakly acidic gas, and mineral dissolved in sea water has created a mildly alkaline condition in ocean so that the oceans absorb large quantities of CO_2. Chemical balance between CO_2 and carbonic acid ($H_2CO_3^-$) in sea water determines the exchange of atmospheric CO_2 in ocean (IPCC 2007). The principal reaction of CO_2 is dissolved in sea water which is

$$CO_2 + H_2O + CO_3^{2-} \rightarrow 2HCO_3^-$$

$$CO_2 + H_2O + H \rightarrow HCO_3^- + 2H^+$$

The drawback of this method is that the ocean may become acidic when carbon dioxide dissolved into ocean water which leads to ocean acidification. Oceanic acidification directly affects the many coastal marine organisms and ecosystems [5] (Fig. 2.3).

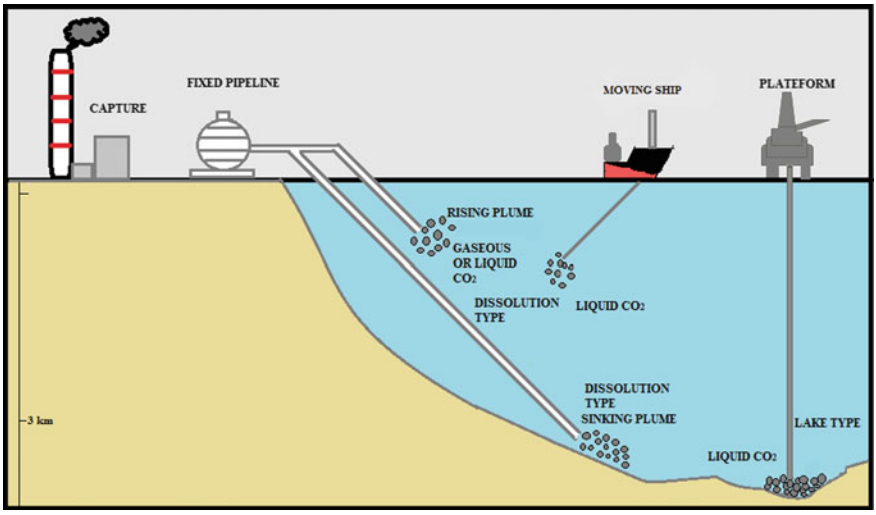

Fig. 2.3 Oceanic carbon sequestration [16]

2.3.2 Geological Carbon Sequestration

Geological carbon sequestration is a method of storing of CO_2 in deep geological formation to reduce the atmospheric CO_2 level and to avoid climate change [15]. Geological storage of CO_2 reduces emission of CO_2 into atmosphere by capturing CO_2 from major stationary sources, this capturing CO_2 transporting it by pipeline and injecting into porous rock formations [16]. This injected CO_2 will mix with water and enter into groundwater and retain CO_2 or certain trapped as carbonate [15]. There are various types of rock formations suitable for CO_2 storage includes depleted oil–gas reservoirs, deep saline formations and unmineable coal seams (Fig. 2.4) [16].

Geological storage potential in India accounts for 500–1000 $GtCO_2$, which includes 300–400 Gt of deep saline formations, 200–400 Gt of basalt formation traps, 5Gt of unmineable coal seam and 5–10 Gt of depleted oil and gas reservoirs (UNFCC Dec 2009). Disadvantages of this storage method are high economic cost and environmental risks such as seismic disturbances, contamination of potable water and adverse effects on ecosystems [5] (Fig. 2.5).

2.3.3 Biological Carbon Sequestration

Biological carbon sequestration refers as removal and storage of atmospheric carbon through soil, vegetation, woody products and wetlands. Biological carbon sequestration is also known as terrestrial carbon sequestration. Biological carbon sequestration can be effectively used to overcome the challenges of climate change [17]. Biological sequestration is natural way which is economically feasible

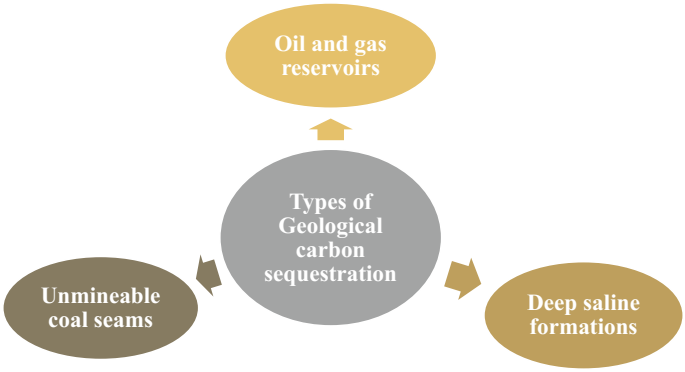

Fig. 2.4 Types of geological carbon sequestration [16]

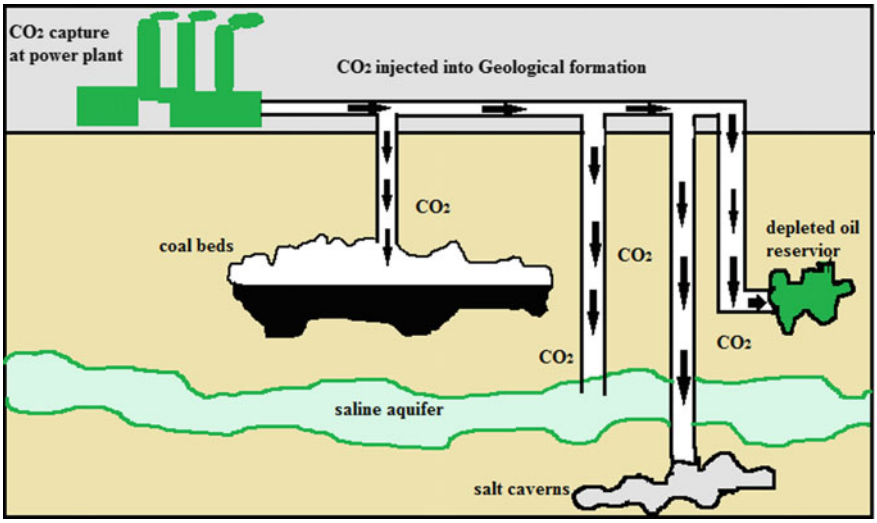

Fig. 2.5 Geological carbon sequestration [36]

strategies to reduce the atmospheric CO_2 concentration. Biological sequestration is mainly accomplished by natural; however, recently few artificial technologies are also developed for biological carbon sequestration [18]. The types of biological sequestration mainly include soil carbon sequestration and phytosequestration which further subdivides (Fig. 2.6).

2.3.3.1 Soil Carbon Sequestration

Soil carbon sequestration defines as the process by which the atmospheric CO_2 will be captured or stored into the soil [19]. This process mainly accomplished by plants through the process of photosynthesis [20]. Soil carbon storage is resulting from the interaction of various ecological processes [20]. Various types of soil carbon sequestration include (1) no-till farming; (2) biochar; (3) bioenergy crop; (4) wood burial; (5) nitrogen fixation; (6) various plant products.

(1) No-till farming

Till farming leads to the physical disturbance of upper soil as well as affects the soil organic matter [21]. The tillage practices increase the turnover of soil aggregates which result into loss of carbon content of soil [18] for the minimum physical disturbance of soils; nowadays, the farming does not use the till, which is known as zero till farming or also referred as no-till farming [21]. Practices of no-till farming improve carbon content of soil, and thereby, retention of earlier crop increases carbon content into soil [21]. This technology also helps to reduce soil erosion and improves infiltration as well as water retention capacity of the soil, and it also aids

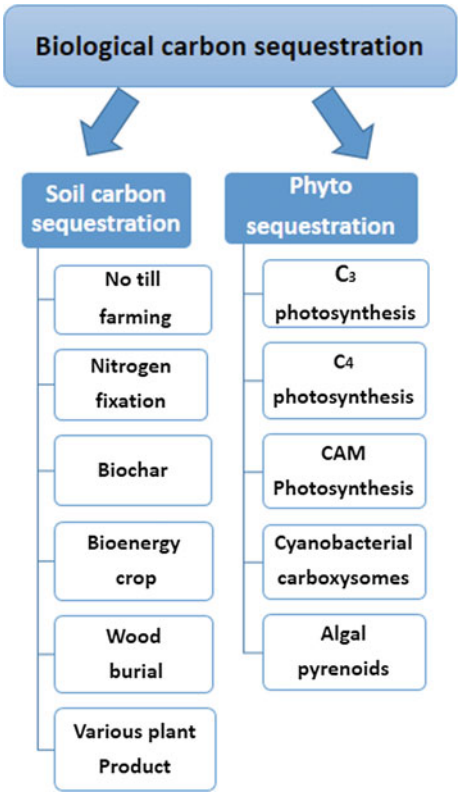

Fig. 2.6 Biological carbon sequestration [14]

the formation of soil aggregates [21]. Therefore, no-till practices enhance soil carbon sequestration.

(2) Biochar

The biochar is processed in which solid material was derived from thermochemical conversion of biomass in an oxygen challenging environment [22]. Production of biochar, in combination with its storage in soils, is one of the possible strategies to remove CO_2 from the atmosphere [23]. Biochar is chemically inert and more resistance towards the microbial decomposition so that the long-term storage of carbon [21]. Biochar is produced by biomass pyrolysis and persists in the soil for centuries to millennia [21]. Earlier it has been reported that biochar is process where biomass from forest and grassland fires is not fully burnt but is "carbonized" and deposited to the soil [24].

(3) Bioenergy crop

Converting the crop plant into bioenergy crop or as a renewable energy source decreases the carbon emission from fossil fuel as well as improve carbon sequestration into soil organic matter which ultimately contributes to mitigate the

concentration of atmospheric CO_2 [17, 21]. It is reported that bioenergy crops have the potential to sequester 317.5 $GtCO_2$ per year [17]. According to Wullschleger, the planting of bioenergy crop plant has the advantage of phosphate mine lands for carbon sequestration [25]. As per US DOE, few are species capable of alleviating energy constraints and deducing CO_2 levels [26]. Bioenergy crop can be used as an alternative source of energy production without increasing net CO_2 emissions and entrap atmospheric CO_2 by increasing biomass yield, and hence to contribute in mitigation of atmospheric carbon dioxide [26]. The potential of production of bioenergy and CO_2 sequestration is species-specific [26].

(4) Wood burial

Wood burial produced from dead or live trees which buried in topsoil area in anaerobic conditions. During this process, CO_2 will stay sequestrated instead of decomposition [18]. Zeng reported that wood burial has potential to long-term carbon sequestration which is 10 ± 5 GtC $year^{-1}$ and currently about 65 GtC is on the world's forest floors in the form of coarse woody debris suitable for burial [27].

(5) Nitrogen fixation

Nitrogen fixing trees accumulate carbon than non-nitrogen fixing trees [18]. 20–100% more soil carbon found in N fixers than non-N fixers [28]. Hence, nitrogen-fixing trees have a greater effect on soil organic matter [18]. The carbon input of soil increases if N fixing species increased, the rates of litterfall or fine root and mycorrhizal production [18]. Nitrogen fixer decreases the rate of decomposition of carbon and increases the carbon accumulation [29].

(6) Various plant products

Different types of plant product such as wood material are used as primary material for development of construction of building and houses that can store the carbon for long time. *Phytoliths* are type of plant derivatives that serve as soil carbon pool. *Phytoliths* produce after burning, breakdown and decaying of plant product [18]. Global potential of phytoliths as a carbon storage accounts for 1.5 Gt per year.

2.3.3.2 Phytosequestration

Plant acts as carbon sink for several centuries [30] by capturing atmospheric CO_2 by the process of photosynthesis. It could serve as carbon sink. Phytosequestration performed by several photosynthetic mechanisms such as C_3, C_4 and crassulacean acid metabolism (CAM) pathways found in plants, carboxysomes of cyanobacteria and algae [18]. Photosynthesis is a light-driven process in which inorganic carbon is converted into organic carbon; hence, atmospheric carbon is distributed in the various parts of the plants [18]. By this process, sequestration of global atmospheric carbon is performed.

(1) C_3, C_4 and CAM photosynthesis

In the C_3 plants, CO_2 enters into plant cell by the stomata to intracellular air spaces which arrive in the chloroplast [31]. CO_2 in the chloroplast fixed by the enzyme RUBISCO and converts it into the three carbon organic compounds (phosphoglyceric acid), hence, named as C_3 photosynthesis [31]. RUBISCO was bifunctional enzyme acting both as carboxylase and oxygenase (in low CO_2 environment). High concentration of O_2 decreases specificity of RUBISCO towards CO_2 [18]. Activity of RUBISCO to act as carboxylase or oxygenase depends on the CO_2/O_2 ratio [32]. C_4 photosynthesis represents modification of C_3 plant to enhancement of the RUBISCO carboxylase activity [32]. It has specific tissue arrangement called Kranz anatomy, which facilitates RUBISCO and CO_2 reaction for carbon fixation. In the C_4 photosynthetic pathway, CO_2 was uptake by phosphoenolpyruvate (PEP) enzyme, which forms the first product of four-carbon compound oxaloacetate (OAA); hence it called as C_4 plants [33]. Other than C_3 and C_4, there is another pathway found in CAM plants to cope up with the hot arid environment. In CAM photosynthetic pathway initially, CO_2 combines with PEP and forms OAA similar to the C_4 photosynthesis; however in CAM plants, carbon fixes at night and stores the OAA in large vacuoles within to avoid the waterless because of heat [33]. In this way, there is separation of two enzymes, PEP carboxylase and RUBISCO, which avoid risk of dehydration and use CO_2 for the Calvin cycle during the day.

(2) Cyanobacterial carboxysomes

Cyanobacteria possess unique kind of CO_2 concentrating mechanism (CCM) in order to enhance efficiency of RUBISCO, particularly under CO_2 limiting conditions [18, 34]. Carboxysomes are the micro-component within the cell which contains the RUBISCO of the cell together with carboxysomes carbonic anhydrase (CA). Accumulation of bicarbonate (HCO_3^-) and carbon dioxide (CO_2) within cell is done via transporters. CA is the enzyme which converts an accumulated cytosolic pool of HCO_3^- into CO_2 within the carboxysomes. The concentrated CO_2 was used by RUBISCO within the carboxysomes [34]. Therefore, in cyanobacterial carboxysomes are sites where CO_2 level remains high for capturing by RUBISCO for CO_2 fixation.

(3) Algal pyrenoids

CCM also found in algae with greater diversity in CCM than cyanobacteria. Carbon capturing structure in algae is known as pyrenoids. Pyrenoids are analogues to cyanobacterial carboxysomes, although found in chloroplast stroma and contain RUBISCO [35]. Pyrenoids help to concentrate CO_2 near RUBISCO and also inhibit the process of photorespiration [18].

2.4 Conclusion

The increase in various human activities leads to the increase in accumulation of greenhouse gases in the earth's atmosphere. As a result of this, there is rise in the air temperature and subsurface ocean temperature which can affect the precipitation weather events, forest fires and ultimately leads to change in whole climatic conditions. Thus, various strategies are required to reduce CO_2 concentration. To control the level of atmospheric CO_2, we need to identify novel approach(es) which combines decrease in CO_2 emission and increase in storage. Carbon sequestration is the technology which removes the carbon dioxide from the atmosphere and diverts from emission sources, and this technology also involves durable deposition of atmospheric CO_2 to mitigate global warming and its impact on climate change. There are mainly three methods of carbon sequestration: (a) oceanic carbon sequestration, (b) geological carbon sequestration and (c) biological carbon sequestration. Oceanic carbon sequestration and geological carbon sequestration have the large storage capacity. However, these methods are very costly and are not seen safe for long-term storage ability. Biological carbon sequestration is a novel and cost-effective approach to reduce the atmospheric CO_2. Biological carbon sequestration has opened up a new area of research towards enhancing rapid fixation of atmospheric carbon dioxide in the present level to reduce and mitigate global warming and climate change.

References

1. Fang J, Zhu J, Wang S, Yue C, Shen H (2011) Global warming, human-induced carbon emissions, and their uncertainties. Sci China Earth Sci 54(10):1458
2. Hertzberg M, Schreuder H (2016) Role of atmospheric carbon dioxide in climate change. Energy Environ 27(6–7):785–797
3. Anderson TR, Hawkins E, Jones PD (2016) CO_2, the greenhouse effect and global warming: from the pioneering work of Arrhenius and Callendar to today's earth system models. Endeavour 40(3):178–187
4. IPCC, Climate Change (2013) The physical science basis. Contribution of working group I to the fifth assessment report of the intergovernmental panel on climate change. Cambridge University Press, Cambridge (Warming is specified relative to the reference period, 1986–2005, and the figures represent ensemble-mean results of the ESMs)
5. Sundquist E, Burruss R, Faulkner S, Gleason R, Harden J, Kharaka Y, Waldrop M (2008) Carbon sequestration to mitigate climate change (No. 2008–3097). US Geological Survey
6. https://climate.nasa.gov/causes/. Last accessed 27 July 2018
7. EPA (2017) Inventory of U.S. greenhouse gas emissions and sinks 1990–2015. U.S. Environmental Protection Agency, Washington, D.C (EPA 430-P-17-001)
8. Dhanwantri K, Sharma P, Mehta S, Prakash P (2014) Carbon sequestration, its methods and significance. Environmental Sustainability: Concepts, Principles, Evidences and Innovations, p 151

9. Herzog H, Golomb D (2004) Carbon capture and storage from fossil fuel use. Encycl Energy 1(6562):277–287
10. Le Quéré C, Andres RJ, Boden T, Conway T, Houghton RA, House JI, Marland G, Peters GP, Van der Werf G, Ahlström A, Andrew RM (2012) The global carbon budget 1959–2011. Earth Syst Sci Data Discuss 5(2):1107–1157
11. Change C (2007) Working group III: mitigation of climate change. Executive summary: http://www.Ipcc.Ch/publicationsanddata/ar4/wg3/en/ch11s11-es.Html
12. Houghton RA (2010) How well do we know the flux of CO_2 from land-use change? Tellus B 62(5):337–351
13. Adams EE, Caldeira K (2008) Ocean storage of CO_2. Elements 4(5):319–324
14. Raghuvanshi SP, Chandra A, Raghav AK (2006) Carbon dioxide emissions from coal-based power generation in India. Energy Convers Manag 47(4):427–441
15. Duncan DW, Morrissey EA (2011) The concept of geologic carbon sequestration (No. 2010–3122). US Geological Survey
16. Benson S, Cook P, Metz B, Davidson O, De Coninck H, Loos M, Meyer L (2005) Underground geological storage, IPCC special report on carbon dioxide capture and storage, Chap. 5. Intergovernmental Panel on Climate Change
17. Sheikh AQ, Skinder BM, Ashok KP, Ganai BA (2014) Terrestrial carbon sequestration as a climate change mitigation activity. J Pollut Eff Control, pp 1–8
18. Nogia P, Sidhu GK, Mehrotra R, Mehrotra S (2016) Capturing atmospheric carbon: biological and nonbiological methods. Int J Low-Carbon Technol 11(2):266–274
19. Lal R, Negassa W, Lorenz K (2015) Carbon sequestration in soil. Curr Opin Environ Sustain 15:79–86
20. Ontl TA, Schulte LA (2012) Soil carbon storage. Nat Educ Knowl 3(10)
21. Paustian K, Six J, Elliott ET, Hunt HW (2000) Management options for reducing CO_2 emissions from agricultural soils. Biogeochemistry 48(1):147–163
22. Timmons D, Lema-Driscoll A, Uddin G (2017) The economics of Biochar carbon sequestration in Massachusetts
23. Schmidt MW, Noack AG (2000) Black carbon in soils and sediments: analysis, distribution, implications, and current challenges. Global Biogeochem Cycles 14(3):777–793
24. Lal R (2004) Soil carbon sequestration impacts on global climate change and food security. Science 304(5677):1623–1627
25. Wullschleger SD, Segrest SA, Rockwood D, Garten C Jr (2004, May) Enhancing soil carbon sequestration on phosphate mine lands in Florida by planting short-rotation bioenergy crops. In: Proceedings of the 3rd annual conference on carbon capture and sequestration
26. Lemus R, Lal R (2005) Bioenergy crops and carbon sequestration. Crit Rev Plant Sci 24(1):1–21
27. Zeng N (2008) Carbon sequestration via wood burial. Carbon Balance Manage 3(1):1
28. Resh SC, Binkley D, Parrotta JA (2002) Greater soil carbon sequestration under nitrogen-fixing trees compared with Eucalyptus species. Ecosystems 5(3):217–231
29. Binkley D (2005) How nitrogen-fixing trees change soil carbon. In: Tree species effects on soils: implications for global change. Springer, Dordrecht, pp 155–164
30. Jansson C, Wullschleger SD, Kalluri UC, Tuskan GA (2010) Phytosequestration: carbon biosequestration by plants and the prospects of genetic engineering. Bioscience 60(9):685–696
31. Yamori W (2016) Photosynthesis and respiration. In: Plant factory, pp 141–150
32. Ehleringer JR, Cerling TE (2002) C3 and C4 photosynthesis. Encycl Global Environ Change 2:186–190
33. Cseke LJ, Wullschleger SD, Sreedasyam A, Trivedi G, Larsen PE, Collart FR (2013) Carbon sequestration. In: Genomics and breeding for climate-resilient crops. Springer, Berlin, Heidelberg, pp 415–455

34. Price GD (2011) Inorganic carbon transporters of the cyanobacterial CO_2 concentrating mechanism. Photosynth Res 109(1–3):47–57
35. Raven JA, Cockell CS, De La Rocha CL (2008) The evolution of inorganic carbon concentrating mechanisms in photosynthesis. Philos Trans Royal Soc B: Biol Sci 363 (1504):2641–2650
36. https://energywatch-inc.com/carbon-capture-utilization-storage-pipe-dream-potential-solution/. Last accessed 27 July 2018

Chapter 3
Greenhouse Gases Emission Mitigation and Utilization in Composting and Waste Management Industry: Potentials and Challenges

Mukesh Kumar Awasthi, Yumin Duan, Junchao Zhao, Xiuna Ren, Sanjeev Kumar Awasthi, Tao Liu, Hongyu Chen, Ashok Pandey, Sunita Varjani and Zengqiang Zhang

Abstract The alleviation of greenhouse gas (GHG) emissions is a major provoke for waste management and composting industry in expect of the global warming regards. Carbon dioxide and GHG emission reduction during composting have been noticed as one of the important steps toward environmental engineering. To keep GHG below the standard limit, huge quantity CO_2 emissions' reduction through dissociation and exploitation will be necessary. In addition, CO_2 generation reduction will uprise an unique methods option when expanse of CO_2 emissions is considered to be enclosed in the waste collection, separation, and transportation price. This chapter with consideration the possible CO_2 reduction/fixation biotechnology and it's utilization via biochemical engineering as by-products in composting factory. Many CO_2 reduction and adsorption methods such as organic, inorganic and microbial adsorption and transformation to CO_2, oxidative dehydrogenation, hydrogenation, and polymerization are extensively considered. The methods' limitation and recent advancement and accomplished fact are also summarized.

M. K. Awasthi · Y. Duan · J. Zhao · X. Ren · S. K. Awasthi · T. Liu · H. Chen · Z. Zhang (✉)
College of Natural Resources and Environment, Northwest A&F University,
Yangling, Shaanxi, China
e-mail: zhangzq58@126.com

A. Pandey
CSIR-Indian Institute of Toxicology Research,
Vishvigyan Bhavan, Lucknow 266001, UP, India

S. Varjani
Gujarat Pollution Control Board Paryavaran Bhavan, Sector-10A,
Gandhinagar 382 010 Gujarat, India
e-mail: drsvs18@gmail.com

F. Winter et al. (eds.), *CO_2 Separation, Purification and Conversion to Chemicals and Fuels*, Energy, Environment, and Sustainability,
https://doi.org/10.1007/978-981-13-3296-8_3

Keywords Carbon dioxide · Biochemical engineering · Microbial adsorption
Biological transformation · Composting factory

3.1 Introduction

Global warming issues due to increasing huge quantity of greenhouse gases (GHGs) emissions have become worldwide long-term climate alteration problems. Carbon dioxide (CO_2), methane (CH_4), nitrous oxide (N_2O), and flue gases are the major GHGs on which CO_2 is gradually increasing up to a peak content with regard to its concentration existing in the global air (Fig. 3.1). According to the projection of Intergovernmental Panel on Climate Change (IPCC), by the year 2100, the earth environment may comprise more than 570 ppm of CO_2 and inducing a concentration of GHGs which has elevated significantly by the industrial counterrevolution (about 1750), and as a result, global CO_2 level has increased by 37%. Many previous studies anticipated that the risen of GHG level in atmosphere is interiorize by various anthropogenic activities like waste management and combustion of non-renewable fuel for power generation. GHG emissions are generated as the outcome of different non-energy-associated industrial practices.

The major element of GHG generation is CO_2 which corresponds to 63%, whereas CH_4 and N_2O to be 24% and 3%, respectively [32]. The maximum concentration of CO_2 generation (>30 Gt CO_2/year) directs to the greater proportion of CO_2 to global atmosphere issue. Consequently, the International Energy Agency (IEA) assumed that the entire CO_2 emissions functionally increased during the time of the year 1971–2007 from 14.1 to 29 Gt [34]. Normally, composting can biologically convert organic waste materials into or stable end product like compost,

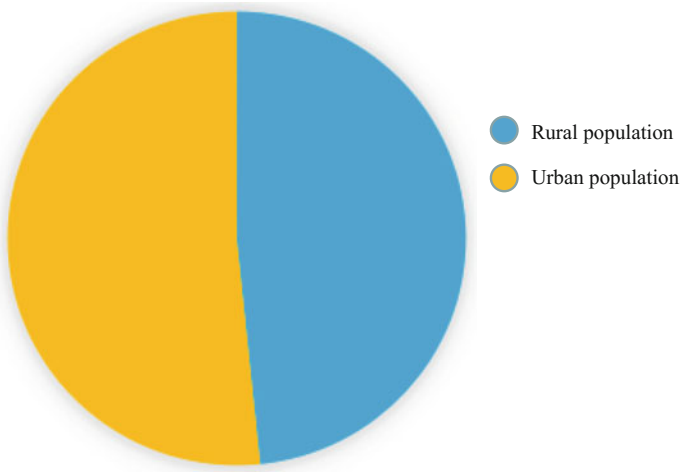

Fig. 3.1 Global population composition (area of residence)

which often under aerobic conditions releases GHGs in the form of CO_2, while under anaerobic conditions, it emitted CH_4 and N_2O. The organic matter degradation results in the emissions of huge quantities of CO_2. The composting and waste management industries account 5–8% of direct CO_2 emissions. The public revolves some of the climate variations due to the GHGs generation to atmosphere led to the United Nation Framework Convention on Climate Change (UNFCCC) in 1992. The main aim of this chapter was to address technology development for reduction of GHG property in the environment at a certain percentage that the human activities could not hinder with the atmosphere change.

Carbon dioxide fixation and adsorption (CDFA) can considerably mitigate CO_2 emissions sources as well as certain organic waste kinds such as manure and municipal solid waste generation as well as processing plant. CDFA technologies for waste recycling and energy-generated blabber included three steps: CO_2 fixation, conversion, and recycling. There are many kinds of composting industries that emit huge quantity of CO_2 with mixture of gases as a by-product. In composting industry, most of the organic wastes can be utilized as resources and recycled. Hence, the principal waste materials are H_2O and CO_2 because CO_2 is normally generated in composting with the bio-oxidation process with aeration. In fact, organic matter bio-oxidation processes generate CO_2 with superior cleanness as an end product. However, many of the CO_2 composting plants are generated in the form of mixture of gases as a consequence of transformation of organic matter and gradual conversion of stable end product. In this view, there are many important chapters published in various prospects of CO_2 fixation but in the area of organic waste composting and CO_2 conservation are still unclear. Due to the lack of a scientific knowledge on CO_2 sequestration and fixation in composting industry, the present chapter mainly described on this object.

3.2 MSW and GHG: A Global Overview

The proportion of GHGs has elevated considerably since the industrial development, and global CO_2 emission by manure management has 384.22 tons, Asia 41.9%, Europe 29.4%, Americas 21.3%, Africa 4.7%, Oceania 2.7% average by 1990–2016. In addition, manure that applied to soils has 211.00 tons, Asia 39.6%, Europe 32.6%, America 22.9%, Africa 4%, Oceania 0.9% average 1990–2016. Manure left on pasture has 936.77 tons, Asia 30.4%, Europe 6%, Americas 32.4%, Africa 25.1%, Oceania 6.1% average 1990–2016. Among them, Australia, Brazil, China, and India have significantly very high GHG emissions. For instance, about 35 million tons of food waste (FW) were directly disposed with municipal solid waste (MSW) in the USA, which correspond 21% of MSW in 2013. Agricultural activities, food processing, and other non-MSW industry produced 22 million tons of organic waste [25]. The quantity of food and other organic waste generation gradually increase with the MSW. The percentage of MSW generated in China approximately 191 million tons in 2015, which had rose 22% from 2005 (NBS

2016). Approximately 56% of the MSW is FW in China [47]. It reduces significantly the capacity of landfill. This MSW directly disposed in open filed which produce bulk of GHGs as correspond of spontaneous long-term mineralization of MSW and lead sever global warming context to the society and environment.

On account of the economic development and transformation of people's lifestyle, the requirement of meat and its by-products has considerably enhanced livestock and poultry industry. In 2016, the number of livestocks such as cattle, 96 pig, sheep, and chicken, in world was about 6331.6, 1474.88, 9817.97 and 97 1173.35, 2270.54, respectively. The rapid advancement and livestock production also transmit severe environmental trouble, which correspondingly cause health issues. Composting is efficient eco-friendly technology to recycle the organic waste and transformed to useful end product and can utilize for organic farming. It provides the alternative process to reduce the organic waste load in a landfill. However, the main generation of GHG is from composting, where complex organic materials into simple humified materials by the microbial activities under aerobic condition. The addition of bulking agent in composting feedstock is important to mitigate the considerable amount of the GHG emission by composting process. The GHG generation reduction process by composting can promote the practices of the physical addition, such as bulking agent, turning; organic additives such as biochar, compost, and charcoal; inorganic additives such as phosphogypsum, magnesium phosphate, zeolite, NaOH, lime, medical stone, bentonite, struvite salt, ceramic, and silica, respectively. Consequently, microbial additives such as aerobic, microbial consortium, substrate-specific microbes, fungal and bacterial consortium were also important role-play to decrease the GHG emissions during the composting.

3.3 GHG Environmental Effects

The effect of global warming can look on everywhere of environment such as glacier, ocean, agriculture, and biological ecosystem. It is well acknowledged that rising in temperature are promising to refresh weather perceptions and agricultural output. In addition, the environmental variation has major identified impact on the environment: gradual increasing in mean earth temperatures, melting ice glacier and polar ice caps, rising ocean water level, extra immoderate weather case, environ- ment changes, worldwide reduction of farm and residential lands, endangers of important species, and so on. Average CO_2 from coal and nuclear power plant and vehicle generation is the main GHGs. Other causative gases and pollutants are N_2O, ozone, CH_4, and chlorofluorocarbons. CO_2 is a major colorless gas as per the Environmental Health Center and makes up $\sim$0.037% of the atmosphere. Huge quantity of CO_2 is rhythm back and forth intermediate of the environment. Likewise, plants capture CO_2 from the air for photosynthesis but overgrazing another major concern.

Besides, SO_2 and N_2O_2 generation would produce the acid rain and GHGs impact on the atmosphere. Meanwhile, when the percentage of unsusceptible particle increases a positive level, it could adversely affect human health, etc. However,

the smoke from burning the agricultural residues and biochar manufacturing can reduce the CO_2 emission by certain range [44]. But N_2O is considered to be the major concern of ozone layer reduction in the twenty-first century, and its warming influence is 296 times higher that of CO_2 has a long residence time. It is indicated that N_2O in the atmosphere elevated linearly at a rate of 0.25% per year, and it is anticipated that by 2050 will rose up to 350 to 400 nL/L because N_2O reacts with the O atoms of the stratosphere to generate NO, which leads to the depletion of the ozone layer, thereby increasing the UV radiation reaching the earth's atmosphere; greatly maximizing the relative ratio of human skin cancer and other diseases, and can cause other health problems. The generation and chemical activity of NO_x and N_2O are closely correlated with major environmental issues such as the regeneration of acid rain, the alteration of photochemical smog circumstances, the demolition of the ozone layer, and the GHG impact. In addition, booming market demands for meat and milk products are impulsive a thriving livestock business. Internal digestion is a natural phenomenon that usually found in each livestock such as pig, cattle and sheep and produces huge quantity of GHGs by manure management. Humans impart to atmospheric methane intensity through operation that concentrates and amplifies biological mineralization. This cover landfilling of organic materials, breeding livestock, rice in paddies farming land and collecting domestic/industrial sludge for eco-friendly recycling and set up artificial wetlands.

3.4 General Challenge of GHG in the Composting Waste Management Industry

Greenhouse gases (GHG), including CH_4, N_2O, and CO_2, were produced by the microorganisms that consuming oxygen to decompose organic substances resulting due to the composting mass, anaerobic pocket forms and then anaerobic conditions created during the composting [14, 37]. However, according to the Fifth Assessment Report of the International Panel on Climate Change, CH_4 and N_2O have 25 and 296 times higher global warming potential than CO_2 but normally CO_2 emission is much more higher than CH_4 and N_2O generation because microbes transformed complex organic matter into stable manure by aerobic process and then huge quantity of heat produced in form of CO_2. Therefore, the CH_4 and N_2O are mostly responsible for the atmosphere pollution but the same time CO_2 emission much more greater role play to increase the global warming impact in to the environment.

The CO_2 emission effect has characteristics such as having a wide range of influence, complex constraints, and serious consequences [4]. Global climate change is a direct consequence of the greenhouse effect [10]. Therefore, the greenhouse effect is a major environmental problem faced by human beings. It has attracted the attention of most of the developed and developing countries governments and scientists and has become the key area of research [33]. The GHG effect on the ecological environment mainly includes the following aspects: (1) the greenhouse effect could cause sea level rise. It is estimated that the average global

sea level rise rate is about 6 cm every 10 years and the sea level will rise by 20 cm until 2030 [3]. This change in sea level will bring the following impacts and disasters to coastal areas; (2) the greenhouse effect has the negative effect on human health. Global warming could result in ozone concentrations decrease. Low-level ozone is a very dangerous pollutant which can damage lung tissue, trigger asthma, and other lung diseases as well as cancer; (3) the GHG has negative effect on the global climate change. As GHGs (CO_2, CH_4, and water vapor) enhance atmospheric counterradiation, the global temperature will generally rise, making it impossible for people to live in the tropics. Furthermore, climate anomalies can lead to droughts, floods, lightning, hurricanes, storm surges, sandstorms, frosts, snowstorms, and a series of severe weather. This has led to geological disasters such as mudslides and land subsidence.

The aforementioned examples indicated that GHG had negative effect on the global climate change. Hence, it is urgent to control the GHG emission during the composting and also challenge for the development of composting technology.

3.5 Source of GHG in the Composting Waste Management Industry

Composting is a biological process, which could transform degradable organic matter to stable humic-like end product through microorganism. The microorganism consumed more oxygen to decompose organic matter to supply energy for their own activity and multiplication, resulting in part-anaerobic condition, where could significant quantity of GHGs emitted in the form of CH_4, N_2O, and CO_2 [7, 19]. The GHG emissions could cause "greenhouse effect," which could have a negative effect on the air atmosphere, melting glaciers, and sea level rise. Therefore, finding some effective economical methods to control GHG emissions is urgent. For the aim of controlling the GHG emissions, it is necessary to solve out the source of CH_4, N_2O, and CO_2 emission. However, the process of CO_2 production in the compost buildup is a cyclic process [48]. The CO_2 emitted is derived from the CO_2 captured in the natural environment. Therefore, the CO_2 produced by the composting process is not considered as a contribution factor to global warming. Furthermore, according to the Fifth Assessment Report of the International Panel on Climate Change, CH_4 and N_2O have 25 and 296 times higher global warming potential than CO_2. Hence, we should pay attention on the source of CH_4 and N_2O.

3.5.1 The Source of CH_4

Due to the active decomposition and pulverization of composting mass could later on result in part-anaerobic condition [26]. The part-anaerobic condition has a positive effect on the methanogens, which cause the C loss through CH_4 emission

by 0.1–12.6%. CH_4 is a long-lived GHG, which could increase the long-wave radiation and then result in the rise of temperature [41]. It is supposed to understand the theory of CH_4 production. Reference to the previous study, the CH_4 production was divided into three steps including hydrolysis and fermentation stages, hydrogen production acetogenesis stage, and methane production stage. In the hydrolysis and fermentation stages, organic matter is decomposed into fatty acids and alcohols by the action of fermenting bacteria. In the second stage, hydrogen-producing acetogens convert propionic acid, butyric acid, and other fatty acids and ethanol into acetic acid, CO_2, and H_2. Afterward, acetic acid or $CO_2 + H_2$ convert into CH_4 through methanogens. And the specific schematic was shown in Fig. 3.1.

It is generally believed that during anaerobic biological treatment, about 70% of CH_4 in anaerobic biological treatment is derived from the decomposition of acetic acid, and the remaining CH_4 is produced from CO_2 and H_2 [2]. Methanogens are a very special type of archaea–bacteria, which synergize with hydrolyzed bacteria and acid-producing bacteria to make organics matter mechanized. The most important feature is that methanogenic bacteria can only use some simple substances in the substrate. Organic matter is dominated by simple carbon substances such as formic acid, methanol, methylamines. The methanogens could decompose two carbon substances such as acetic acid, but cannot decompose other fatty acids containing two or more carbons and alcohols other than methanol. And afterward, the "four-bacterial theory" of anaerobic digestion was proposed, which was on the basis of the above-mentioned three-stage theory [36]. Meanwhile, a variety of bacteria with the same type of acetogenic bacteria was added. Its main function is to convert CO_2/H_2 produced by hydrogen-producing acetogenic bacteria into acetic acid [40]. However, previous studies have shown that, the amount of acetic acid synthesized from CO_2/H_2 only accounts for only about 5% of the total acetic acid in the anaerobic system truly. The CH_4 emission principally strikes in the thermophilic phase due to the fast degradation of organic matter, which consumed oxygen to result in part-anaerobic condition to produce CH_4.

3.5.2 *The Source of N_2O*

According to the biochemical cycle, theory of nitrogen and metabolic biology of gas cycle biology, nitrification, and denitrification are two main processes to produce N_2O [11]. Under aerobic conditions, NH_4^+ is converted into NH_2OH by the action of bacteria and archaea. Afterward, the NH_2OH is oxidized to NO_2^- by the action of hydroxylamine oxidoreductase. Afterward, the NO_2^- is transformed to NO_3^- through nitrite oxidoreductase [17]. The transformation of NH_4^+ to NO_3^- is considered as nitrification. However, N_2O is a by-product of denitrification, and nitrification is one of the main ways of nitrogen conversion in the composting process. Therefore, it is main reason for the N_2O emission during the composting

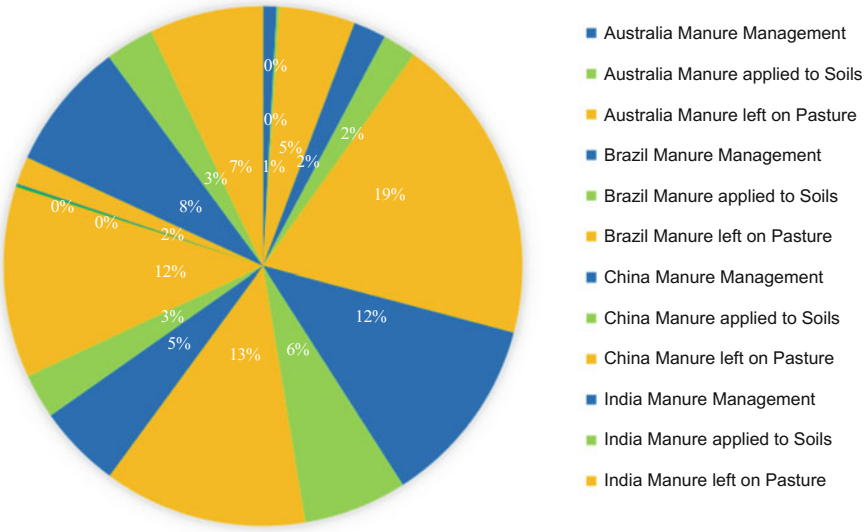

Fig. 3.2 Emissions by continent (CO_2 equivalent), average 1990–2016

process. NO_3^- are often converted into N_2 by denitrification or NO_3^- by alienation reduction through microorganisms respired under hypoxic conditions [16]. Consequently, N_2O is a by-product of denitrification, which is inhibited by the NO_3^- concentration and oxygen concentration. And the specific schematic diagram was as followed in Fig. 3.2.

There are many theories about N_2O emission. Some people think that it is impossible to produce N_2O in the initial phase of composting through denitrification due to the low concentration of NO_3^- and NO_2^-. But some people have different opinions, they think N_2O could be produced through nitrification in the initial stage. Moreover, some people have an opinion that NH_3 could be oxidized in high temperature by methanogens and then result in N_2O emission [13]. Besides, some people think that N_2O emission occurred at the compost surface in the initial phase, which is proper for the nitrobacteria due to the relatively lower temperature and enough oxygen. Consequently, though the theory about N_2O emission was different, it is important to control it to eliminate the effect on the atmosphere.

3.6 Current Research Trends and Gap Analysis

Greenhouse gas (GHG) has become a hot hit due to the negative effect on the global climate change. Besides, the GHG emission restricted the composting technology. In order to reduce the GHG emission during the composting, many researches had

been done in recent years. There are varieties of measures to control GHG emission as followed. Mitigation strategies to reduce greenhouse gas emissions during composting can comprise the application of bulking amendment, aeration systems, chemical or mature compost as a cover material. The choice of bulking agent is to depend on locally availability of agricultural organic waste such as sawdust [43], sawdust [29], corn stover [37], used mushrooms, and marshmallows [35]. The bulking agents' addition is designed to enhance the aeration within the compost and mitigate CH_4 emissions. In the process of composting kitchen waste, sawdust dust had the highest CH_4 and N_2O contents of >97.7 and 72.9%, comply by flowering mushrooms (97 and 28.8%), followed by corn stalks (93 and 46.6%) [43]. While this study did not show obvious remission in NH_3, in another compost fertilizer study, the combined use of pre-composting and vermicomposting significantly reduced CH_4 and N_2O emissions by 84.2 and 80.9% [37]. Jiang et al. [22] show that the efficiency of different aeration systems differs from the amount of air supply and the distribution of greenhouse gas emissions. For CH_4 emissions, constrained consecutive aeration with low aeration has the highest relieving at a maximum aeration which indicates at least a reduction. Contrary to NH_3, the highest ventilation rate results are considerably better than the lower aeration volume forced continuous aeration. N_2O intermittent aeration is improvised more than constrained or nonstop aeration. The suppression efficiency of the change of the gas along the pile height. Zhang et al. [45] show that the maximum reduction of CH_4 is related to the height of short piles but the highest efficiency is achieved in the case of N_2O, which reduces the pile to reach the maximum.

With mineral additives, such as medical stone [39], bentonite, biochar [1], phosphorus gypsum, could significantly reduce the GHG emission. According to the previous study, phosphorus gypsum is the main by-product of the production of phosphoric acid, which can effectively reduce CH4 during the fresh pig manure compost [28] and kitchen waste [42] by rising SO_4^{2-} concentration. Through the formation of struvite ($MgNH_4PO_4$, $6H_2O$), magnesium, and phosphate decreased NH_3 [46]. Besides, adding a nitrification inhibitor dicyandiamide ($C_2H_4N_4$) can reduce the emission of N_2O [28]. Luo et al. [27] noticed that compared manure alone composting, manure mixed with the mature compost together to reach the higher level of greenhouse gas emission reduction. Among all treatments to reduce the greenhouse gas, the bulking agent was supposed to study further due to the cheap price and wide distribution since the bulking agent could provide a better airflow to reduce CH_4 and N_2O. However, the above literature indicated that most of the investigations were restricted too small to in-vessel scale of composting and were usually performed in a closed reactor. Therefore, more investigation was required on the GHG mitigation during the composting of livestock manure and different kind of organic resources on various kinds of broadscale reactor and operation to extract more significant conclusions/recommendation for future research on the GHG reduction technologies.

3.7 GHG Mitigation Technological Advancement and Its Framework

Climate change is a global issue that is widely concerned by the international community nowadays. According to forecast, global temperature in 2025 will increase by 2 °C degrees compared with 100 years ago and it will increase by 4 °C in 2100. It is generally believed that the global greenhouse effect is attributed to several GHG, mainly including CO_2, CH_4, and N_2O, which contribute up to 80% of the greenhouse effect [18]. The massive emission of GHGs brings many hazards to the global ecological environment, such as increased pests and diseases in agricultural production, rising sea levels, increased natural disasters, desertification of land.

Composting is one of the practical and accepted approaches of organic solid waste management due to the easier operation process and smaller investment, which was also considered to be alternative mitigation strategies for GHG reduction. Composting process was performed under the aerobic environment that carbon and nitrogen elements in organic substances were transformed into stable, sanitary, and humic-like end product (compost). The main GHG emitted in this process was CO_2, which was produced through the respiration of microbial metabolism. While, due to the huge oxygen demand for the active growth of indigenous microorganisms and rapid decomposition, there were still some unavoidable partial anaerobic pockets formed in the composting mass, where more GHG are generated in the form of CH_4. Additionally, the N_2O was mostly produced through the incomplete nitrification and denitrification process, and thus the nitrous oxide can be detected in both aerobic and anaerobic environment [5]. Although the ammonia was not reported to be classified as GHG, its emissions during composting were also responsible for the acid rain and nitrogen loss. The importance of mitigation of GHG during composting process also attracted the attention of many researchers. The emissions-cutting measures undertaken from various considerations can be summarized as the compost raw materials and operational process performance [14].

3.7.1 Composting Raw Materials and Mixing Ratios

The emissions of different kinds of GHG were significantly affected by the composition of composting feedstock. For instance, the anaerobic conditions were easily formed in the cases of high moisture content and high bulking density of composting materials, which related to higher CH_4 emission [12]. The excess water and small porosity decreased the free airspace, which created an anaerobic condition for methanogens [30]. In summary, the proper bulking density and suitable moisture content not only related to the biodegradation of organic matter and the formation of humic-like substance during composting, but also ensured the mitigation of GHG emission. Another key factor of composting composition related to

the GHG emissions was the carbon to nitrogen ratio. Nutrients that provided energy for microbial life activities during composting process were significantly influenced by the C/N ratio [8]. More specifically, the C/N ratio used to evaluate GHG emissions should be based on the biodegradable content and the optimum range of C/N ratio was from 15 to 30, especially from 20 to 25 [15]. Different organic waste composting with a balanced C/N ratio, proper bulking density, and moisture content could have less GHG emissions.

3.7.2 Composting Operational Process

The composting operation process was different according to the composting systems. Generally, the composting systems can be divided into open system and closed system. The closed system had a higher operating costs compared to the other but it also had the advantages that the released gases could be easily collected by the gas recovery plant (Fig. 3.2), which reduced the environmental risk of GHG to some extent. Additionally, lots of researchers focus on improving the mitigation technologies such as aeration (turn frequency), employing additives, and bulking agent. Aeration was proved to be an important factor for gaseous emissions during composting, which was usually control by the air pump in both open system and closed system. Additionally, aeration in trough composting and window composting can also adjust by the turning frequency. It is considered that higher aeration provided more oxygen into compost system, and thus few of CH_4 emitted from anaerobic pockets; the concentration of GHG emission could be diluted thereafter. However, there were still some negative effects that higher aeration might increase the NH_3 and N_2O emission [21]. Chowdhury et al. [9] also noticed that low aeration decreased the ammonia emission and increased the methane generation (Figs. 3.3 and 3.4).

Furthermore, the high aeration also spent more energy. Thus, an overall impact evaluation should be considered to balance the proper aeration based on the total CO_2 equivalents [14]. Using chemical agent and mineral additives to mitigate GHG emission during composting has been reported by many researchers, which were

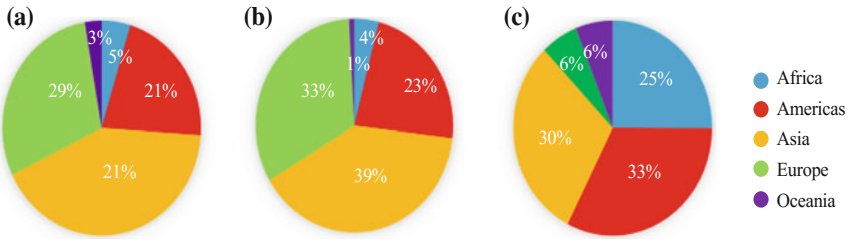

Fig. 3.3 Emissions by continent (CO_2 equivalent), manure management (**a**), manure applied to soils, (**b**) and manure left on pasture, (**c**) average from 1990 to 2016

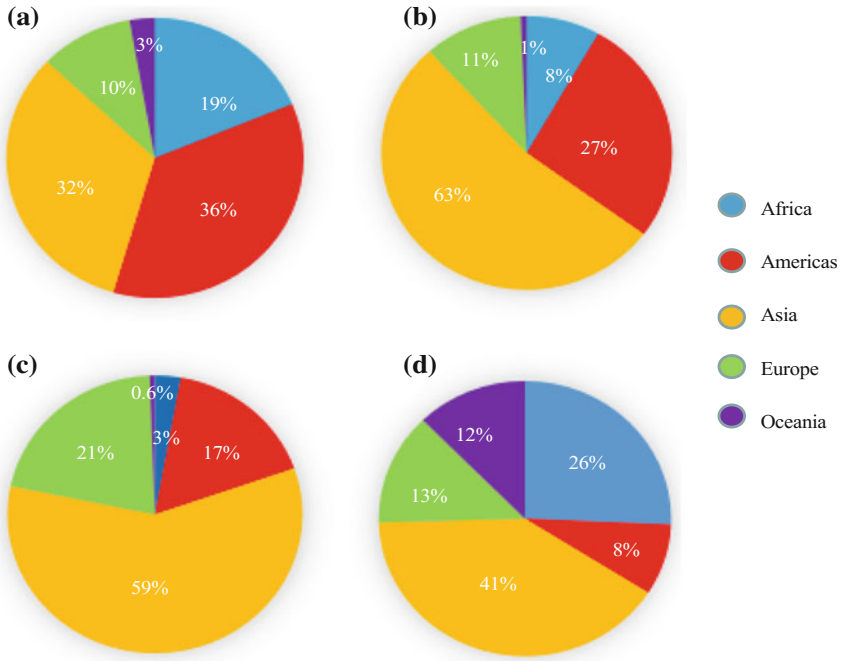

Fig. 3.4 Production share of cattle's (**a**), chickens (**b**), pigs (**c**), and sheep (**d**) by region average 1994–2016

easy operating and economical. Awasthi et al. [5, 6] reported that biochar, zeolite, and lime amendment could significantly reduce the GHG emission during sewage sludge while wood vinegar with the mixture of biochar and zeolite was also proved to be effect on GHG mitigation during pig manure [38]. Similarly, the addition of dicyandiamide and struvite during pig manure composting significantly reduces the N_2O emission [23, 24]. The common additives used in current research study for GHG mitigation are listed in Table 3.1.

The addition of bulking agents was usually selected by the local agricultural wastes such as wheat straw, cornstalk, wood chips, spent mushroom, and green waste. The aim of bulking agent was used to improve the porosity, balanced the oxygen supply, and adjusting the biodegradable carbon to nitrogen ratio. According to the study reported by Yang et al. [43], the use of sawdust was more effective than corn stalk and spent mushroom on the mitigation of CH_4 emission during kitchen waste composting. Additionally, the reed straw considerably mitigates the CH_4 and N_2O emission during duck manure composting [37]. The approach of bulking agent provided a better solution for CH_4 emission due to its improvement of aeration. When selecting emission reduction technologies, we must consider not only the mitigation of GHG during composting, but also the GHG emissions corresponding to these energies consumed during the implementation of the technology. As the

Table 3.1 Some of the additives used in current research study for GHG mitigation

Additives	Feedstock	Bulking agent	Mitigated gases	Reference
Biochar	Cattle manure	Straw	CH_4, NH_3	Chowdhury et al. [9]
Biochar	Poultry	Wheat straw	NH_3	Janczak et al. [20]
Biochar and lime	Sewage sludge	Wheat straw	CH_4, NH_3, N_2O	Awasthi et al. [6]
Medical stone	Pig manure	Wheat straw	NH_3, N_2O	Wang et al. [39]
Struvite	Broiler litter	Sawdust and hog fuel	NH_3	Zhang and Lau [46]
Struvite crystallization	Pig feces	Cornstalks	NH_3, N_2O	Jiang et al. [23]
Biochar, zeolite, and wood vinegar	Pig manure	Wheat straw	CO_2, CH_4, NH_3, N_2O	Wang et al. [38]
Zeolite and lime	Sewage sludge	Wheat straw	CH_4, NH_3, N_2O	Awasthi et al. [5]
Phosphogypsum and superphosphate	Kitchen waste	Cornstalks	CH_4, NH_3, N_2O	Yang et al. [42]
Phosphogypsum and dicyandiamide	Pig faces	Cornstalks	CH_4, NH_3, N_2O	Luo et al. [28]

mention above, every mitigation strategy has different effects on different GHGs (CO_2, CH_4, NH_3, and N_2O), and the assessment of these technologies should base on the global warming potential (total CO_2 equivalents).

3.8 Future Perspective and Opportunities in GHG Utilization

With the rapid advancement of economy and technology, a large number of GHG emissions have exacerbated the burden on the environment, and more effective measures will gradually be proposed in the future for better control of GHG emission. However, we should not only focus on the mitigation technologies another optional measures were finding the way for GHG utilization. GHG emissions were inevitable during composting and other industry activities. Thus, the technologies for collection, conversion, and utilization of GHG were more and more important at current situation. Some researchers found that catalytic conversion of the GHG to some environmentally product or efficient materials has bright market prospects, but the major challenges were the lack of effective methods. CH_4, one of the major components of GHG, has the possibility to be applied to the production of some fuels and chemical raw materials. For instance, some kinds of

chemical materials such as oxygenates, unsaturated C_2 hydrocarbons, and heavier hydrocarbons can be directly produced during many ways [25, 31]. Additionally, waste fermentation biogas project is a practical and effective method for renewable energy utilization and environmental protection (Figs. 3.5 and 3.6).

The main part of biogas during anaerobic fermentation, methane can be used as fuel or main feedstock during daily life and industrial production. Carbon dioxide, which is the highest part of GHG emitted worldwide, can significantly increase the oil recovery as a displacing agent during oil extraction. The technology of using CO_2 to enhance recovery has advantages such as large application scope, high oil

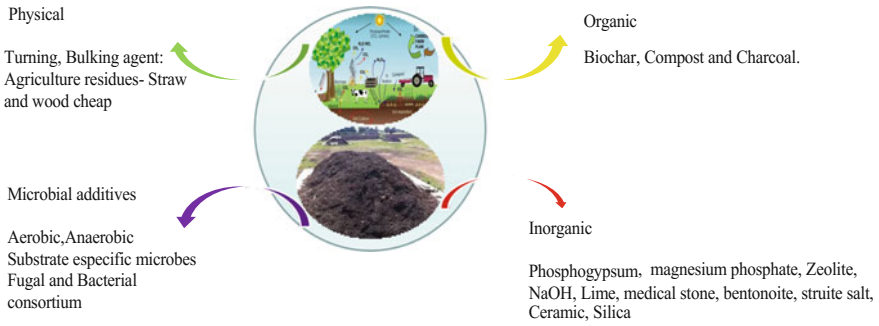

Fig. 3.5 Available technologies for composting

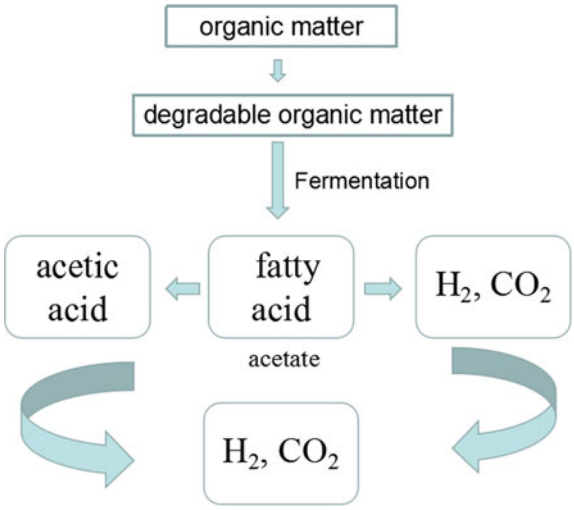

Fig. 3.6 Specific schematic of CH_4 production theory

displacement efficiency, and low cost. As a mature oil recovery technology in oil industry, it has been widely considered by many countries in the world. With the depletion of energy sources, more and more technologies are currently used to increase resource utilization and promote cleaner production. The utilization of GHG has also received attention from the current society. Many technologies have been able to convert GHG into energy, raw materials, and some materials for special uses and make a large amount of economic benefits. Furthermore, the utilization of GHG might be more acceptable for more enterprises due to its economic benefits compared with the GHG mitigation technologies (Figs. 3.7, 3.8, and 3.9).

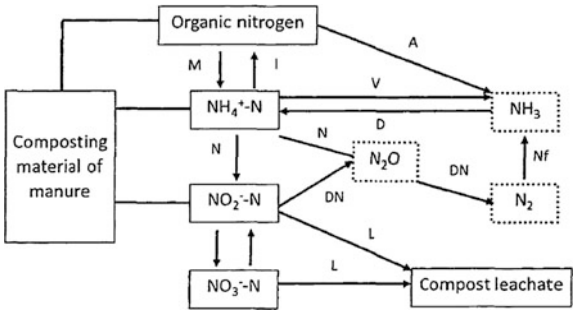

Fig. 3.7 Specific schematic diagram about nitrogen

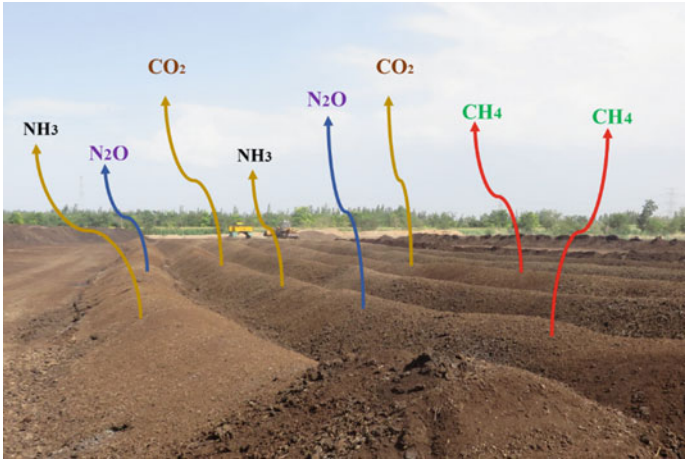

Fig. 3.8 Main gases emission during composting

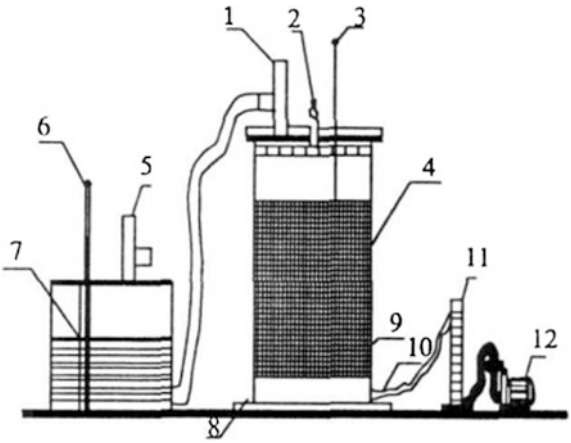

Fig. 3.9 Exhaust gas collection device under laboratory scale. 1—Air outlet of composting reactor; 2—Leachate refill port; 3—Thermometer; 4—Composting reactor; 5—Outlet of gas recovery plant; 6—Thermometer; 7—Gas recovery plant; 8—Leachate drain; 9—Air duct; 10—Intake pipe; 11—Flow meter; 12—Aeration pump

3.9 Conclusions

There are numerous possible derivatives for CO_2 fixation/mitigation from composting industry and its conservation as macronutrients in the feedstock for the manufacturing of stable/matured compost. Although, as the utilization and fixation of CO_2 by itself proscribed especial group of microbes and CO_2 provides no enthalpy subscription to the end product. Thus, the sum to net CO_2 emission could not be important unless more cost-efficient biotechnology and renewable energy derivation are accessible.. Subsequently, the end product quality and its demand, as well as total net loss of carbon by CO_2 and CH_4 emissions, have to be reconsidered for the discussion. Major influence of CO_2 fixation on CO_2 emissions during the composting could be accomplished only if mass of organic material is the object of transformation. However, many potential technologies are possible for CO_2 conservation in different industries during the composting or waste management sector still needs improvement. Based on the above consideration on CO_2 fixation technology improvement, it can be compiled that flue gas characteristics (primarily percentage of CO_2, temperature, and aeration) are the important impressive ingredients for determination of desirable process for CO_2 sequestration during the organic waste composting. Biocatalytic CO_2 conservation seems to have the great prospect for execution in composting and other waste management industries. Further, study is required on biochemical process and hydrogen source. Because electrochemical or photo-electrochemical CO_2 transition is auspicious, practical application for composting is still in its progress and needs major improvement.

Acknowledgements The authors are grateful for the financial support from a Research Fund for International Young Scientists from National Natural Science Foundation of China (Grant No. 31750110469), China, and The Introduction of Talent Research Start-up Fund (No. Z101021803), College of Natural Resources and Environment, Northwest A&F University, Yangling, Shaanxi Province 712100, China. We are also thankful to our all laboratory colleagues and research staff members for their constructive advice and help.

References

1. Agegnehu G, Bass AM, Nelson PN, Bird MI (2016) Benefits of biochar, compost and biochar-compost for soil quality, maize yield and greenhouse gas emissions in a tropical agricultural soil. Sci Total Environ 543:295–306
2. Amlinger F, Peyr S, Cuhls C (2008) Greenhouse gas emissions from composting and mechanical biological treatment. Waste Manage Res 26:47–60
3. Andersen JK, Boldrin A, Samuelsson J, Christensen TH, Scheutz C (2010) Quantification of greenhouse gas emissions from windrow composting of garden waste. J Environ Qual 39:713–724
4. Arriaga H, Viguria M, López DM, Merino P (2017) Ammonia and greenhouse gases losses from mechanically turned cattle manure windrows: a regional composting network. J Environ Manag 2017:557–563
5. Awasthi MK, Wang Q, Huang H, Li R, Shen F, Altaf HL, Wang P, Guo D, Guo Z, Jiang S, Zhang Z (2016) Effect of biochar amendment on greenhouse gas emission and bio-availability of heavy metals during sewage sludge co-composting. J Clean Prod 135:829–835
6. Awasthi MK, Wang Q, Huang H, Ren X, Lahori AH, Mahar A, Ali A, Shen F, Li R, Zhang Z (2016) Influence of zeolite and lime as additives on greenhouse gas emissions and maturity evolution during sewage sludge composting. Bioresour Technol 216:172–181
7. Beck-Friis B, Pell M, Sonesson U, Jönsson H, Kirchmann H (2000) Formation and emission of N_2O and CH_4 from compost heaps of organic household waste. Environ Monit Assess 62:317–331
8. Cayuela ML, Sánchez-Monedero MA, Roig A, Sinicco T, Mondini C (2012) Biochemical changes and GHG emissions during composting of lignocellulosic residues with different N-rich by- products. Chemosphere 88:196–203
9. Chowdhury MA, Neergaard A, Jensen SL (2014) Potential of aeration flow rate and bio-char addition to reduce greenhouse gas and ammonia emissions during manure composting. Chemosphere 97:16–25
10. Christensen TH, Gentil E, Boldrin A, Larsen AW, Weidema BP, Hauschild M (2009) C balance, carbon dioxide emissions and global warming potentials in LCA-modelling of waste management systems. Waste Manage 27(8):707–715
11. Čuček L, Klemeš JJ, Varbanov PS, Kravanja Z (2015) Significance of environmental footprints for evaluating sustainability and security of development. Clean Technol Environ Policy 17(8):2125–2141
12. de Guardia A, Petiot C, Rogeau D (2008) Influence of aeration rate and biodegradability fractionation on composting kinetics. Waste Manage 28:73–84
13. El Kader NA, Robin P, Paillat JM, Leterme P (2007) Turning, compacting and the addition of water as factors affecting gaseous emissions in farm manure composting. Bioresour Technol 98(14):2619–2628
14. Fillingham MA, Vanderzaag AC, Burtt S, Baldé H, Ngwabie NM, Smith W, Hakami A, Wagner-Riddle C, Bittman S, MacDonald D (2017) Greenhouse gas and ammonia emissions from production of compost bedding on a dairy farm. Waste Manage 70:45–52

15. Guo R, Li G, Jiang T, Schuchardt F, Chen T, Zhao Y, Shen Y (2012) Effect of aeration rate, C/N ratio and moisture content on the stability and maturity of compost. Bioresour Technol 112:171–178
16. Hao X, Chang C, Larney FJ (2004) Carbon, nitrogen balances and greenhouse gas emission during cattle feedlot manure composting. J Environ Qual 33(1):37–44
17. He Y, Inamori Y, Mizuochi M, Kong H, Norio I, Sun T (2001) Nitrous oxide emissions from aerated composting of organic waste. Environ Sci Technol 35(11):2347–2351
18. IPCC (2000) Special report on emissions scenarios, working group III, Intergovernmental Panel on Climate Change. Cambridge University Press, Britain
19. Jäckel U, Thummes K, Kämpfer P (2005) Thermophilic methane production and oxidation in compost. FEMS Microbiol Ecol 52:175–184
20. Janczak D, Malińska K, Czekała W, Cáceres R, Lewicki A, Dach J (2017) Biochar to reduce ammonia emissions in gaseous and liquid phase during composting of poultry manure with wheat straw. Waste Manage 66:36–45
21. Jiang T, Schuchardt F, Li G, Guo R, Zhao Y (2011) Effect of C/N ratio, aeration rate and moisture content on ammonia and greenhouse gas emission during the composting. J Environ Sci 23:1754–1760
22. Jiang T, Li G, Tang Q, Ma X, Wang G, Schuchardt F (2015) Effects of aeration method and aeration rate on greenhouse gas emissions during composting of pig faeces in pilot scale. J Environ Sci 31:124–132
23. Jiang T, Ma X, Tang Q, Yang J, Li G, Schuchardt F (2016) Combination use of nitrification inhibitor and struvite crystallization to reduce the NH_3 and N_2O emissions during composting. Bioresour Technol 217:210–218
24. Jiang T, Ma X, Yang J, Tang Q, Yi Z, Chen M, Li G (2016) Effect of different struvite crystallization methods on gaseous emission and the comprehensive comparison during the composting. Bioresour Technol 217:219–226
25. Le H, Lobban LL, Mallinson RG (2004) Plamsas for greenhouse gas utilization. ACS Division of Fuel Chemistry, Preprints, 49
26. Lou XF, Nair J (2009) The impact of landfilling and composting on greenhouse gas emissions —a review. Bioresour Technol 100(16):3792–3798
27. Luo WH, Yuan J, Luo YM, Li GX, Nghiem LD, Price WE (2014) Effects of mixing and covering with mature compost on gaseous emissions during composting. Chemosphere 117:14–19
28. Luo Y, Li G, Luo W, Schuchardt F, Jiang T, Xu D (2013) Effect of phosphogypsum and dicyandiamide as additives on NH_3, N_2O and CH_4 emissions during composting. J Environ Sci 25:1338–1345
29. Maulini-Duran C, Artola A, Font X, Sanchez A (2014) Gaseous emissions in municipal wastes composting: effect of the bulking agent. Bioresour Technol 172:260–268
30. McCartney D, Chen HT (2001) Using a biocell to measure effect of compressive settlement on free air space and microbial activity in windrow composting. Compost Sci Util 9:285–302
31. Pan C, Chávez O, Romero CE, Levy EK, Aguilar Corona A, Rubio-Maya C (2016) Heat mining assessment for geothermal reservoirs in Mexico using supercritical CO_2 injection. Energy 102:148–160
32. Parry ML, Canziani OF, Palutikof JP, van der Linden PJ, Hanson CE (2007) Climate change 2007: impacts, adaptation and vulnerability, Cambridge
33. Pereira RF, Cardoso EJBN, Oliveira FC, Estrada-Bonilla GA, Cerri CEP (2018) A novel way of assessing c dynamics during urban organic waste composting and greenhouse gas emissions in tropical region. Bioresour Technol. https://doi.org/10.1016/j.biteb.2018.02.002
34. Rossi F, Olguín EJ, Diels L, De Philippis R (2015) Microbial fixation of CO_2 in water bodies and in drylands to combat climate change, soil loss and desertification. N Biotechnol 32:109–120
35. Santos A, Bustamante MA, Tortosa G, Moral R, Bernal MP (2016) Gaseous emissions and process development during composting of pig slurry: the influence of the proportion of cotton gin waste. J Clean Prod 112:81–90

36. Turner DA, Williams ID, Kemp S (2015) Greenhouse gas emission factors for recycling of source-segregated waste materials. Resour Conserv Recycl 105:186–197
37. Wang J, Hu Z, Xu X, Jiang X, Zheng B, Liu X, Pan X, Kardol P (2014) Emissions of ammonia and greenhouse gases during combined pre-composting and vermicomposting of duck manure. Waste Manage 34:1546–1552
38. Wang Q, Awasthi MK, Ren X, Zhao J, Li R, Wang Z, Wang M, Chen H, Zhang Z (2018) Combining biochar, zeolite and wood vinegar for composting of pig manure: the effect on greenhouse gas emission and nitrogen conservation. Waste Manage 74:221–230
39. Wang Q, Wang Z, Awasthi MK, Jiang Y, Li R, Ren X, Zhao J, Shen F, Wang M, Zhang Z (2016) Evaluation of medical stone amendment for the reduction of nitrogen loss and bioavailability of heavy metals during pig manure composting. Bioresour Technol 220:297–304
40. Weitz KA, Thornelow SA, Nishtala SR, Yarkosky S, Zennes M (2002) The impact of municipal solid waste management on greenhouse gas emissions in the United States. J Air Waste Manage Assoc 52:1000–1011
41. Whalen SC, Reeburgh WS, Sandbeck KA (1990) Rapid methane oxidation in a landfill cover soil. Appl Environ Microbiol 56:3405–3411
42. Yang F, Li G, Shim H, Wang Y (2015) Effects of phosphogypsum and superphosphate on compost maturity and gaseous emissions during kitchen waste composting. Waste Manage 36:70–76
43. Yang F, Li GX, Yang QY, Luo WH (2013) Effect of bulking agents on maturity and gaseous emissions during kitchen waste composting. Chemosphere 93:1393–1399
44. Yu J, Dow A, Pingali S (2013) The energy efficiency of carbon dioxide fixation by a hydrogen-oxidizing bacterium. Int J Hydrogen Energy 38(21):8683–8690
45. Zhang H, Li C, Li G, Zang B, Yang Q (2012) Effect of Spent Air Reusing (SAR) on maturity and greenhouse gas emissions during municipal solid waste (MSW) composting-with different pile height. Proc Environ Sci 16:59–69
46. Zhang W, Lau A (2007) Reducing ammonia emission from poultry manure composting via struvite formation. J Chem Technol Biotechnol 82:598–602
47. Zhao W, Zhang B, Wang G, Guo H (2014) Methane formation route in the conversion of methanol to hydrocarbons. J Energy Chem 23:201–206
48. Zhu X, Burger M, Doane TA, Horwath WR (2013) Ammonia oxidation pathways and nitrifier denitrification are significant sources of N_2O and NO under low oxygen availability. Proc Natl Acad Sci USA 110:6328–6333

Chapter 4
Post-Combustion Carbon Capture and Storage in Industry

E. J. Anthony and P. T. Clough

Abstract Post-combustion CO_2 capture as a form of carbon capture and storage (CCS) is currently the most promising technology to reduce CO_2 emissions from the conversion of fossil fuels. Currently, in the form of amine scrubbing, it exists at the commercial scale; a number of other CCS technologies also exist at the commercial or near-commercial scale, in the form of pre-combustion capture from gasification processes, oxy-fuel combustion for CO_2 separation, and chemical and calcium looping. While the utility market is an evident focus of CCS technology, there are some doubts about whether or not this market will be largely dominated, in the next several decades, by renewable generation and the mass enrolment of energy storage devices, or if CCS technologies will be utilized to balance the supply–demand gap. However, there remain numerous opportunities in the industrial sector for CCS technology to contribute to reducing CO_2 emissions. These opportunities include well-known industries such as cement and steel as well as sectors like marine transport. This chapter will evaluate the available technologies and focus on the many opportunities that now exist in the industrial sector for CCS.

4.1 Introduction

The idea that anthropogenic production of CO_2 could significantly influence climate is well over 100 years old [1], and the recognition that coal and fossil fuel use are important contributors is similarly venerable [2]. For a more detailed discussion of the history of climate science and the modelling of climate change, the interested reader is referred elsewhere [3, 4], or to the book by Houghton [5].

Currently, the most firmly established post-combustion CCS technology is amine scrubbing, which has now been developed and validated at the commercial-scale for the treatment of flue gases from coal firing. Three projects in particular represent significant milestones at the demonstration stage. These include

E. J. Anthony · P. T. Clough (✉)
Cranfield University, Cranfield, UK
e-mail: p.t.clough@cranfield.ac.uk

F. Winter et al. (eds.), *CO_2 Separation, Purification and Conversion to Chemicals and Fuels*, Energy, Environment, and Sustainability,
https://doi.org/10.1007/978-981-13-3296-8_4

the 100 MWe SaskPower Project at Boundary Dam, Saskatchewan [6], and the 240 MWe Petra Nova facility in Houston, Texas [7], both of which are able to capture 90% of the CO_2 produced. The third large-scale (pre-combustion capture) demonstration project is the Japanese Tomakomai CCS demonstration project which sequesters 100,000 tonnes of CO_2 per year [8]. In addition, CCS technology has been widely used and developed for other industries for over 50 years [9]. Besides amine scrubbing, there are numerous other CCS technologies which are being explored including calcium looping (CaL), chemical looping combustion (CLC) and oxy-fuel combustion in both its pulverized fuel-fired manifestation and fluidized bed-fired manifestation [10].

Each technology has its associated problems; for amine scrubbing the issues are cost, volatilized amine loss, and significant efficiency penalty associated with the process due to the regeneration of the amine sorbent using steam. However, there remains no major barrier to its implementation besides the cost and efficiency penalty. For pre-combustion (often gasification) technologies, cost again represents a significant issue especially if the syngas produced has to be shifted to produce H_2 and, gasification has a persistent problem of failing to work well at the large commercial scale, when the fuel to be gasified is coal. The most recent major failure of this technology is that of the 582 MWe Kemper County project in Mississippi, whose price tag was around $7.1 billion [11]. For oxy-fuel combustion, the major issue is a lack of full-scale demonstration plants for what is otherwise a strongly established technology, albeit at the 20–30 MWth level [12].

For all other technologies, the issue is either their lack of demonstration plants, given that governments of all stripes throughout the world have effectively reduced or withdrawn their support for such projects, or more critically their lack of technical readiness. Thus for technologies like CaL and CLC, which in many cases, at best exist at the 1 or 2 MWth level, it seems exceedingly improbable that they will be fully commercial in the next decade [13–15]. To put this in perspective, it is important to realize that we are strongly likely to exceed the IEA 450 ppm CO_2 goal in the next 20 years [16], with CO_2 levels increasing at a rate of between 1.6 and 3 ppm per year [17]. By contrast, major energy technologies can take 20–30 years to fully commercialize and up to 10 years to build—see Fig. 4.1 [18]. This means that the relatively unpalatable conclusion is that many of the newer CCS technologies are unlikely to be commercially available within the desired time frame.

It can be argued for the utility sector, and this is not necessarily a bad thing, that renewables have been and can be expected to make increasing inroads. While this argument has a good deal of validity, it remains true that intermittency and the need for flexible generation or additional energy storage are the Achilles' heel of most renewable technologies, with the possible exception of tidal power, geothermal and perhaps biomass for which geographical/environmental constraints also restrict deployment.

As the utility market becomes increasingly dominated by renewables, the need for dispatchable power will grow and constrain further investment of renewables in the energy market, unless one is in the favourable position of having ample supplies

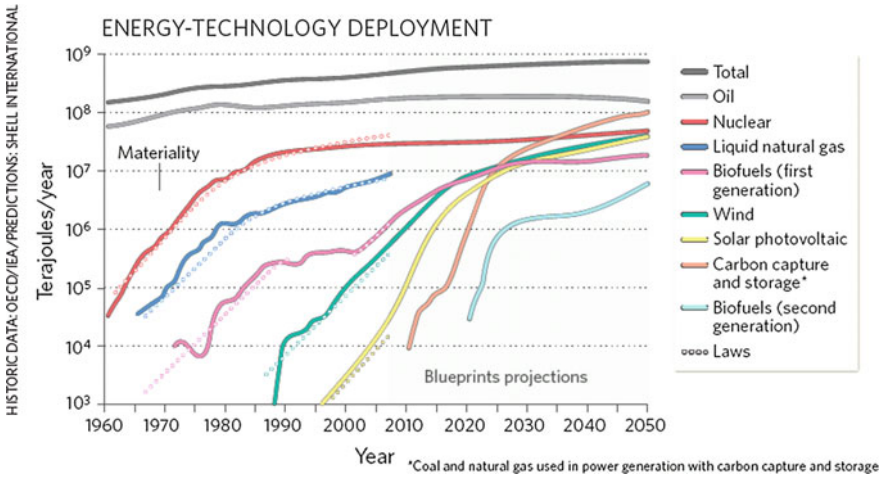

Fig. 4.1 Global production of primary energy sources. When a technology produces 1000 terajoules a year (equivalent to 500 barrels of oil a day), the technology is 'available'. It can take 30 years to reach materiality (1% of work energy mix) [18]

of biomass, tidal or geothermal power. This realization can be regarded as a techno-economic equivalent of Le Chatelier's principle, something which was recognized over 70 years ago by the Nobel Prize-winning economist Paul Samuelson [19]. The fact is that the levelized cost of electricity from renewables has been consistently falling and may not mean a power sector totally dominated by renewables, as there is a need for demand, intermittency and frequency response to be included in future analysis of energy economics. For instance, in addition to the intermittency problem, if a particular element is critical to a technology, e.g. Ni or Pd for enhanced reforming to produce H_2 [20], Li for batteries, or rare earth for magnets in wind turbines, the question must be asked at what point does demand for that element exceed potential supply or influence the pricing significantly. Without these kinds of considerations, simple evaluations based on the steady improvements in renewable energy technologies and a fall in the levelized cost of electricity available from renewable energy sources are likely to be misleading.

In the short term, however, it is more likely that many economies will simply switch to natural gas over coal given low oil and gas prices and the public pressure to improve air quality. In this connection, it is instructive to note that SaskPower has decided to go ahead with the future construction of a natural gas power plant along with further solar and wind power, rather than pursuing more back-end CCS technology with amine scrubbing [6]. In the absence of significant carbon prices, a new dash to gas is likely to be the response of most large energy markets worldwide [21]. However, without also including CCS with gas-fired plants, the reality is that anthropogenic CO_2 emissions will continue to rise and we will still exceed 450 ppm of CO_2 and continue on towards levels of 500–600 ppm before the end of the century. Ultimately, it is likely that the steady change from coal thermal power to a

mixture of dispatchable, unabated gas power with a lesser amount of nuclear and renewables will continue worldwide, notwithstanding some attempts to maintain the position of coal in some markets. Both for the coal-fired plants and the gas plants, it is imperative that CCS be used to prevent CO_2 concentrations moving towards the 500–600 ppm range, as it seems extremely unlikely that the current target of 450 ppm will be met. Instead, the most promising option may well be to establish the principle that for every tonne of CO_2 produced the same amount is stored, sequestered or used providing that use does not constitute a short-term route for reintroducing the CO_2 back into the atmosphere.

4.2 Industrial CCS

The next question to be asked is whether there are other sectors where it would make economic sense to control CO_2 emissions, and where amine scrubbing might not be the obvious solution. Here there are evidently a number of major contenders, namely transportation, the cement industry, the steel industry and marine transportation. While these sectors are responsible for perhaps 20% or so of the global CO_2 production [22], it seems unlikely that the strategies used for the power generation sector will be appropriate due to the composition and quality of the flue gas to be processed, and here there may be an opportunity for some of the newer post-combustion CCS technologies to make a large impact, especially if the production of products or other benefits accrue so as to reduce the overall cost of CO_2 avoided. Furthermore, due to the general centralization of industrial activities there is a significant advantage to CCS integration in the form of CCS 'clusters' or 'hubs'; note Fig. 4.2 showing the proposed Teesside Collective CCS cluster network in the north-east of England.

4.3 Transportation

In the case of transportation, simple considerations of weight mean that CCS applications are unlikely to be a feasible economic solution. Instead, the use of batteries, especially advanced Li batteries, hybrid technology, and possibly hydrogen in conjunction with fuel cells [20] remain the most viable options. Perhaps the only problematic area is aviation, where the use of hydrogen and batteries are likely to be precluded by safety and weight issues, respectively. Instead, it might be possible to resolve these issues by capturing an equivalent amount of CO_2 from the atmosphere, following the so-called air-capture route [24]. While this has normally been rejected on economic grounds, more recent work by proponents of this technology have suggested that the levelized cost per ton CO_2

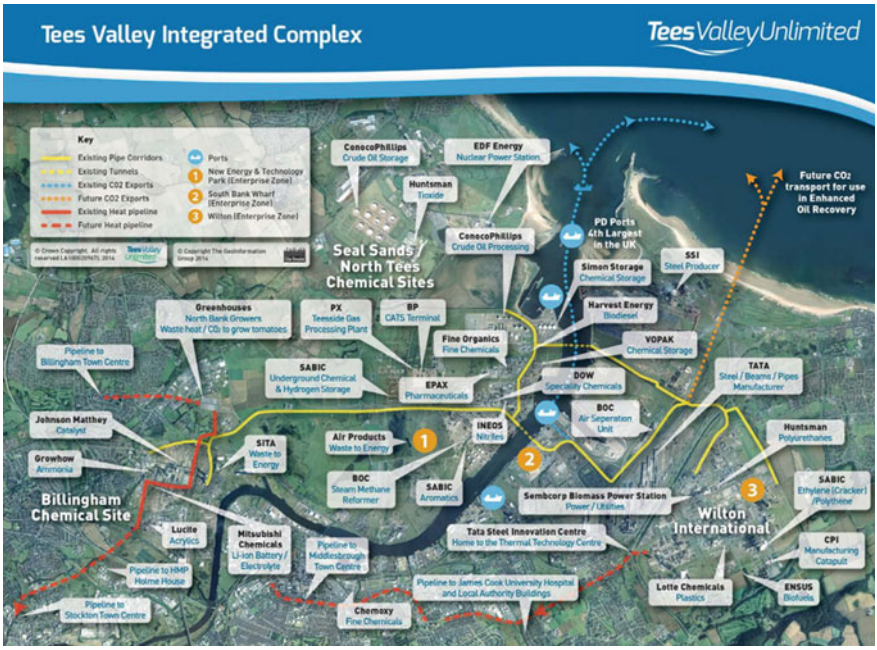

Fig. 4.2 Teeside collective complex showing the potential for an integrated CCS network in the north-east of England [23]

captured from the atmosphere ranges from 94 to 232 $/t-$CO_2$ [24], which is substantially better by almost an order of magnitude than figures developed earlier by the American Physical Society [25], where costs of up to 1000 $/t-$CO_2$ were suggested. Ultimately, such negative emissions technologies may be needed, and in which case they would require some form of CCS. However, it should be noted that this subject is outside of the main focus of this chapter and there is also a vigorous and heated discussion about the potential of negative emissions, and its capacity to significantly affect the anthropogenic CO_2 production [26, 27]. Recently, this option has been characterized by Anders and Peters in the following words 'Negative Emission Technology is not an insurance policy but rather an unjust and high-stakes gamble' [26]. However, the proposition that negative emissions might be able to displace fossil fuels in one sector, namely that of aviation, seems more modest and more achievable. Alternative technologies may also come to the fore such as using enhanced weathering of minerals; however, what is clear is that all such technical options are in their infancy and cannot be depended on to provide workable solutions without significantly more research and potentially massive investment [28], and so they are unlikely to preclude the need for CCS and most definitely should not be used as a 'get out of jail free' card for technical solutions to global warming.

4.4 Cement Production and Calcium Looping Technology

The global emissions of CO_2 from cement production were estimated as 1.45 ± 0.2 Gt CO_2 in 2018 [29]; of that ~50% of the emissions come from calcining limestone [30]. The cement industry is, therefore, one which has drawn increasing attention as a potential area where CCS could be applied. What choice of technology that could be used depends on a number of factors including plant size and location, but it is clear that amine scrubbing could be used effectively with this industry to minimize emissions, with estimated costs in the range of 90–100 euros/t of avoided CO_2 [31].

Calcium looping is the continuous temperature swing cycling of a Ca-based CO_2 sorbent between two reactors, a calciner and carbonator, where CO_2 is released and absorbed, respectively. Like all CCS technologies, one of the major issues for CaL is cost and the likely energy penalty imposed by the technology. In terms of cost, seven studies produced costs ranging from 16 to 38 $\$_{2011}$/t of CO_2 avoided, with an average of 26 ± 10 \$/t of CO_2; furthermore the cost reductions with efficiency improvements are approaching the realm of diminishing returns [32, 33]. More recently there has been an attempt to take into account the uncertainty associated with the various input parameters, and ultimately this may offer a more reliable way of estimating realistic costs [34]. Similarly, a recent study which used a probability analysis suggests that the probable efficiency penalties are 9.5 and 11.5% for CaL and MEA retrofits [35]. What can probably be said is that even with all of the uncertainties in estimating costs and efficiencies, in the absence of full-scale demonstration units, CaL technology is cost competitive with amine scrubbing and offers a lower energy penalty than amine scrubbing. More recently, cement manufacture from wastes from the Ca looping process has been demonstrated at the kilogram level [36], and interestingly a near-100% O_2 firing has been demonstrated at the pilot scale, and these results have been confirmed by tests with 80% oxygen firing in the calciner of a 1.7 MWth pilot plant unit [37]. This result suggests that a reduction in capital costs of about 21.7% might be possible, in terms of capital costs, with a 14.3 and 27.4% reduction in the levelized cost of electricity and cost of CO_2 avoided, respectively [38], which would make the technology even more attractive.

A typical schematic of how a CaL system that was integrated into a cement plant would look is provided in Fig. 4.3 and here the authors of this particular scheme estimated an avoided cost of 23\$ t/CO_2 with 99% capture of the total CO_2 from the plant.

In the UNIDO road map, about 495 CCS projects are required for the cement sector by 2050 [40]. Regardless of whether or not CaL is incorporated directly into a cement plant, the possibility of using the spent lime as a marketable industrial product has the clear potential to make the technology an extremely attractive one. There remains a clear need to demonstrate the technology at a larger scale. Further to this, the European Commission has recently provided €12 million to a €21 million pilot plant project (LEILAC—Low Emissions Intensity Lime and Cement)

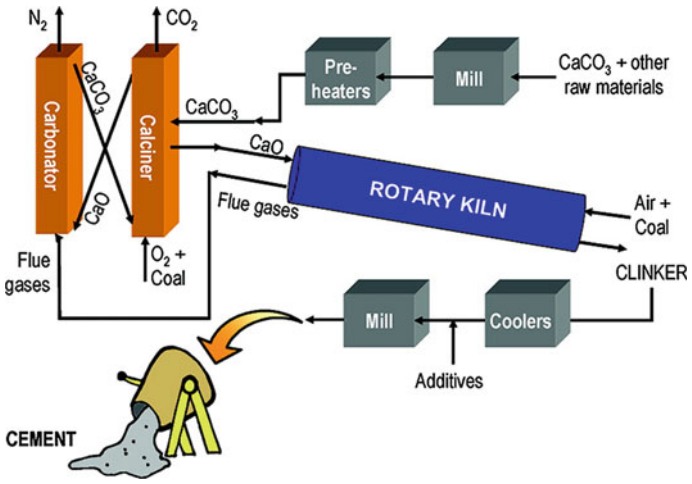

Fig. 4.3 CO_2 capture from cement plants using oxy-fired pre-calcination and/or calcium looping [39]

to design, construct and test an innovative calciner (seen in Fig. 4.4) that is indirectly heated (operating at >1000 °C) [41].

4.5 The Steel Industry and CCS Technology

The steel industry is another major producer of CO_2, generating about 8% of the anthropogenic CO_2 emissions [42]. Typically, a modern steel-making plant will produce more than 1 tonne of CO_2 per tonne of steel (a recent paper suggests that this figure could be as high as 1.8 tonnes/1 tonne of steel [43]).

Decarbonization of the steel industry is critical to meeting the targets set out in the Paris agreement and other national ambitions and Table 4.1 and Fig. 4.5 identify where CO_2 is mostly produced from in a steel plant. Blast furnaces are, therefore, a key target for decarbonizing first, and one choice is to apply post-combustion CCS, for example, calcium looping—its potential integration is shown in Fig. 4.6.

This view is supported by Arasto et al. [47], who modelled a steel plant with CCS and came to the conclusion that it would be feasible to reduce CO_2 emissions in the range of 50–75% using a CCS process, but that higher levels of removal would be challenging because of the different sources, qualities and conditions of CO_2 emissions in a modern steel mill. It is the conclusion of Ho et al. [48], that the cheapest approaches involve membrane technology rather than the more traditional use of amines, and that a base cost was approximately $85 ton of CO_2 avoided. Interestingly, amine capture from the lime kiln appeared to cost $110/ton and so would offer an opportunity for significant savings and simple integration with calcium looping

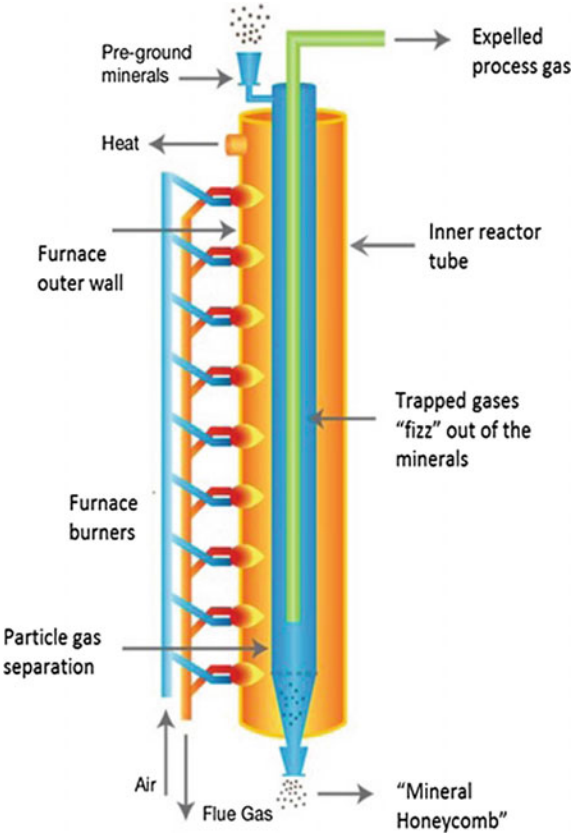

Fig. 4.4 Schematic design of an indirectly heated calciner from the Low Emissions Intensity Lime and Cement (LEILAC) project [41]

Table 4.1 Principal sources of CO_2 from a steel plant, per tonne of liquid steel [45]

Sources of CO_2 in a steel plant	t-CO_2/t-liquid steel
Coking plant	0.06–0.07
Sinter plant	0.10–0.11
Blast furnace	1.14–1.40
Rolling and finishing	0.20–0.29
Oxygen plant and power plant	0.12–0.21

technology. Other technologies that are possible options include amine scrubbing, perhaps with new and improved absorbents, and membrane separation processes. A representation of a blast furnace with CCS is provided in Fig. 4.7.

Besides calcium looping, other more complicated routes relevant to the steel industry are also being explored. For instance, a scheme has been developed for the design of a Ca–Cu chemical looping process for hydrogen production in the steel industry and might offer a route for the decarbonization of blast furnace gas using a sorption sorption-enhanced water-gas shift reaction [49]. Moreover, better joint

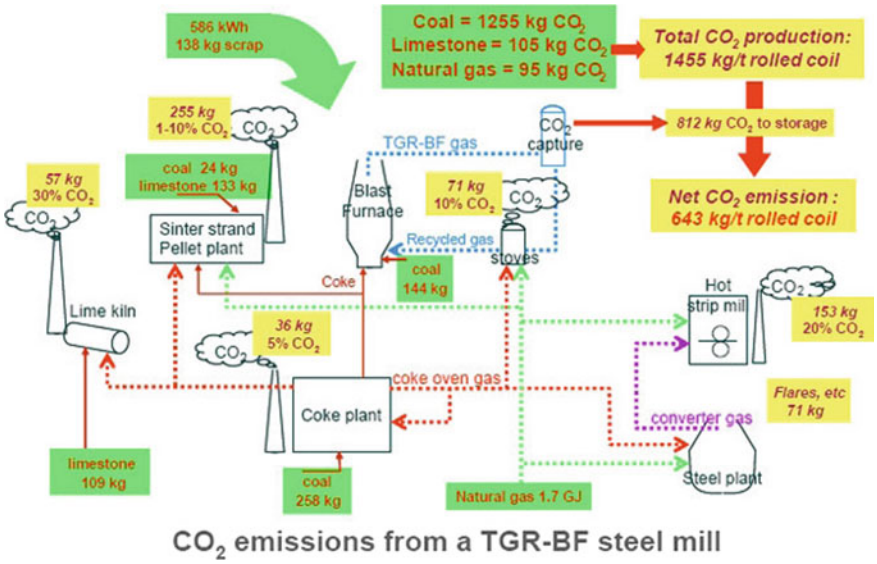

Fig. 4.5 Simplified flow sheet of an integrated steel mill operating with a top gas recycling-blast furnace (TGR-BF) showing carbon-bearing material input (green boxes), CO_2 emissions, expressed in volume (kg/t of hot-rolled coil) and concentration in the flue gas (%) [44]

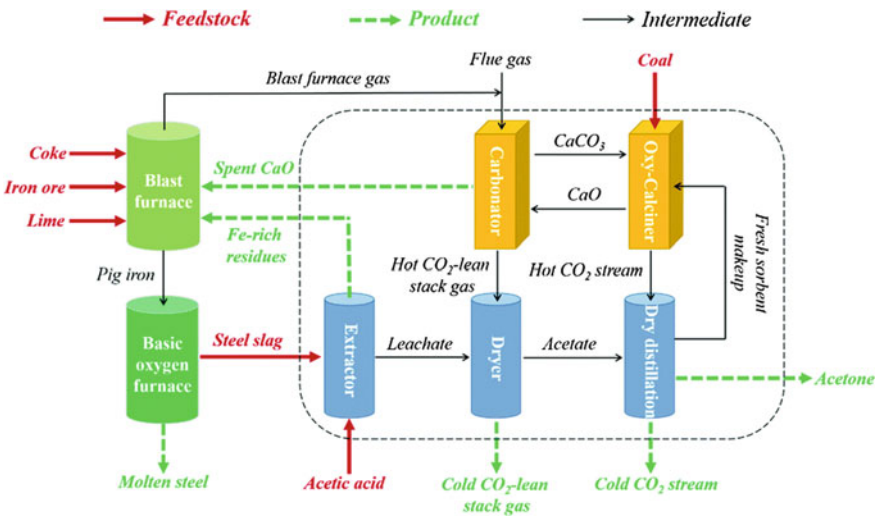

Fig. 4.6 General schematic of integrated CO_2 capture and steel slag valorization process proposed for use in iron and steel industry [46]

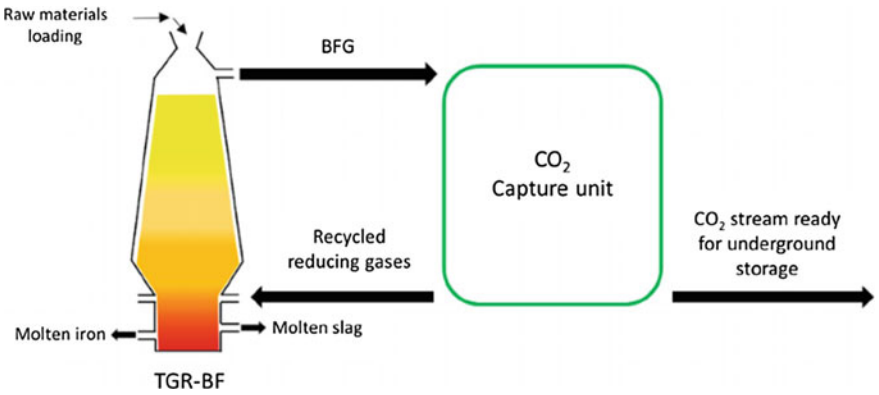

Fig. 4.7 Representation of a blast furnace with top gas recycling (TGR-BF), BFG is sent to a CO_2 Capture unit for separation into a reducing stream for recycling back to the furnace, with a concentrated CO_2 stream for storage [43]

CaL–CLC materials are also being developed which appear to offer substantial improvements over previous efforts to marry the CaL and CLC processes [50]. However, two things are clear at this moment, namely that efforts to develop suitable CCS processes are still in the development stage and there is no clear winning technology. It should also be noted that if waste materials can be used, or the lime product from CaL can be fed into the steel making process, then considerable economies may be made [51]. For wastes, however, the normal limitation will be that there is insufficient material to make a major difference on a global scale.

4.6 Marine Technology

International Maritime has set a goal of 30% CO_2 reduction from shipping by 2020 [52]. Evidently, the major difference between shipping and other transportation technologies is the relative size and space provided by large marine vessels. Given that large amounts of cryogenic products such as liquefied natural gas are currently shipped, there seems no essential problem in capturing and storing CO_2 on board, to be discharged at port, or to a dedicated pipeline system. One problem is that the current dominant traditional marine fuel, heavy oil, is high in sulphur and so any technology used must be able to deal with high levels of SO_2 in the flue gas, if on-board capture is considered.

Another marine option to enhance the flexibility of CCS is to actually build marine transportation to ship CO_2 in carriers. Here, a recent study has suggested that LNG could be used as a marine fuel for CO_2 carriers as compared to marine gas oil [53].

4.7 Storage of CO_2

Arguably, technological advances and improvements for any CO_2 capture process can only have very limited impact without the potential for storage being appropriate for the scale of injection, accessible by pipeline and monitored for long-term security. Saline aquifers, operational and exhausted oil and gas reservoirs, and other unique geological formations are all potential options for storing CO_2. The availability and location of these storage options are not always ideal; for example, the ~1 Mtpa of CO_2 captured from the Boundary Dam Project is piped up to 66 km away to a geological storage site for enhanced oil recovery (EOR) [6].

Recently, much of the work on the storage aspect of CCS has focussed on the location and suitability of each individual storage site. Within the UK, surveys of CO_2 storage potential have found upwards of 70 Gt, most of which is in the form of saline aquifers (which are often highly variable and can be challenging to implement as a storage site); nevertheless, they note that by just considering the top three storage sites around the UK, there is the potential to store a quarter of all the UK's power and industrial emissions (2014) for 30 years [54, 55]. China, USA and India (the world's largest CO_2 emitters) have also made similar assessments of their CO_2 storage potential, each noting that in general, CO_2 storage sites are quite distant (some up to 250 km) from the CO_2 production sites, but not necessarily that there is a lack of storage volume [56–58]. This issue was noted recently for the UK's cement and lime producers, where only a small fraction is currently close enough to a CO_2 corridor such that they can be decarbonized economically [59]. It is, therefore, crucial for all new CO_2 point sources (power plants and industrial facilities) to be located close to either a CO_2 transportation corridor of piping or a storage site [10]. It is deemed unlikely that the large-scale deployment of CO_2 storage can be achieved by single companies or clusters of companies alone, as the costs and investment risks are too great; therefore, government-level action is required in a top-down approach, whereby long-term policies, financial backing and carbon pricing are guaranteed.

The potential impact that CCS can have on global CO_2 emissions could be significant, and even CO_2 sequestration by EOR can make a sizeable dent in CO_2 emissions (accounting for the additional CO_2 that is released through the processing and use of the extra oil recovered), see Fig. 4.8. What can also be noted from Fig. 4.8 is that if CO_2 capture technologies are to tackle the expected 14–20% of ~35.5 Gt of anthropogenic CO_2 produced each year, then CCU alone will simply not make a big enough difference to CO_2 emissions to minimize climate change risks [60].

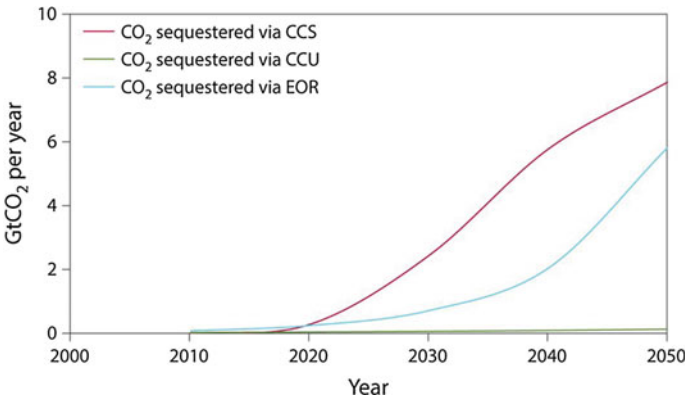

Fig. 4.8 Potential CO_2 sequestration impact of CCS, CCU and EOR [60]

4.8 Conclusions

This chapter attempts to make the case that CCS options are required, regardless of developments in renewable energy in the utility sector, if only to maintain flexibility and deal with the problem of intermittency, which would make 100% renewables in this sector ruinously expensive. Here at least it seems likely that the dominant technology will be amine scrubbing, although oxy-fuel combustion does represent another possible option if and when suitable demonstration plants are built. There is also a major need to decarbonize gas-fired plants, if we are to meet any of our CO_2 emissions targets, and here again it seems likely that some form of amine scrubbing will represent the optimum solution.

For the industrial sector, the situation is much less clear as there are simply so many possible industrial processes to consider. For the two largest, cement manufacture and steel manufacture, it is clear that CCS options are required. For the cement industry, it appears that some combination with CaL would represent an excellent solution, while for the steel industry there are no clear technical winners on offer at this time. However, again both industries will require some form of CCS.

Acknowledgements The authors would like to acknowledge Professor V. Manovic (Cranfield University, UK) for a number of valuable discussions regarding CCS and its fuel flexibility, economics and applications in the steel industry.

References

1. Arrhenius S (1896) On the influence of carbonic acid in the air upon the temperature of the ground. Philos Mag Ser 5. https://doi.org/10.1080/14786449608620846
2. Arrhenius S (2017) Worlds in the making; the evolution of the universe. Independently Published

3. Treut L et al (2007) Historical overview of climate change science. Earth. https://doi.org/10.1016/j.soilbio.2010.04.001
4. Edwards PNA (2010) Vast machine: computer models, climate data, and the politics of global warming. MIT Press
5. Houghton J (2005) Global warming. Reports Prog Phys. https://doi.org/10.1088/0034-4885/68/6/r02
6. SaskPower. Boundary Dam Project (2018) Available at: https://www.saskpower.com/our-power-future/infrastructure-projects/carbon-capture-and-storage/boundary-dam-carbon-capture-project. Accessed on 26th July 2018
7. NRG Energy. Petra Nova facility (2018) Available at: https://www.nrg.com/case-studies/petra-nova.html. Accessed 26th July 2018
8. Japan CCS Co. Ltd. Tomakomai CCS Demonstration Project. 2017
9. Rochelle GT Amine Scrubbing for CO_2 Capture. Sci Am Assoc Adv Sci 325:1652–1653
10. Bui M et al (2018) Carbon capture and storage (CCS): the way forward. Energy Environ Sci. https://doi.org/10.1039/c7ee02342a
11. IEEE. Kemper County Project. Available at: https://spectrum.ieee.org/energywise/energy/fossil-fuels/the-three-factors-that-doomed-kemper-county-igcc. Accessed 26th July 2018
12. Zheng L (2011) Overview of oxy-fuel combustion technology for carbon dioxide (CO_2) capture. In Zheng LBTOFC. for P. G. and C. D. (CO_2) C (ed) Woodhead Publishing Series in Energy, pp 1–13. Woodhead Publishing. https://doi.org/10.1533/9780857090980.1
13. US DoE (2014) Technology readiness assessment. DOE/NETL-2015/1710
14. Hills T, Leeson D, Florin N, Fennell P (2016) Carbon capture in the cement industry: technologies, progress, and retrofitting. Environ Sci Technol. https://doi.org/10.1021/acs.est.5b03508
15. Jarvis SM, Samsatli S (2018) Technologies and infrastructures underpinning future CO_2 value chains: a comprehensive review and comparative analysis. Renew Sustain Energy Rev. https://doi.org/10.1016/j.rser.2018.01.007
16. Moriarty Damon P Energy policy and economics under climate change. AIMS Energy 6:272–290
17. NOAHH (2018) Current CO_2 concentrations in the atmosphere. Available at: https://www.esrl.noaa.gov/gmd/ccgg/trends/gr.html. Accessed 26th July 2018
18. Kramer GJ, Haigh M (2009) No quick switch to low-carbon energy. Nature. https://doi.org/10.1038/462568a
19. Samuelson P (1948) Consumption theory in terms of revealed preference. Economica. https://doi.org/10.2307/2549561
20. Ji G et al (2018) Enhanced hydrogen production from thermochemical processes. Energy Environ Sci. https://doi.org/10.1039/c8ee01393d
21. Ward A (2017) Big oil bets on a dash for gas. Financial Times. Published 7th September 2017
22. IEA (2016) CO_2 emissions from fuel combustion. OECD/IEA. https://doi.org/10.1787/co2_fuel-2016-en
23. Tennison S (2015) Developing an industrial CCS network in Teesside. In CCS in process industries—state-of-the-art and future opportunities (IEA GHG and IEA IETS)
24. Keith DW, Holmes G, St. Angelo D, Heidel K (2018) A process for capturing CO_2 from the atmosphere. Joule. https://doi.org/10.1016/j.joule.2018.05.006
25. Socolow R et al (2011) Direct air capture of CO_2 with chemicals: a technology assessment for the APS panel on public affairs. APS Physics
26. Anderson K, Peters G (2016) The trouble with negative emissions. Science. https://doi.org/10.1126/science.aah4567
27. Lackner KS (2016) The promise of negative emissions. Science. https://doi.org/10.1126/science.aal2432
28. Beerling DJ et al (2018) Publisher correction: farming with crops and rocks to address global climate, food and soil security. Nature Plants. https://doi.org/10.1038/s41477-018-0162-5
29. Andrew RM (2018) Global CO_2 emissions from cement production. Earth Syst Sci Data 10:195–217

30. Blamey J, Anthony EJ (2015) End use of lime-based sorbents from calcium looping systems. In Fennell P, Anthony B (eds) Calcium and chemical looping technology for power generation and carbon dioxide (CO_2) capture, pp 153–169. Woodhead Publishing. http://dx.doi.org/10.1016/B978-0-85709-243-4.00008-2
31. Garðarsdóttir SÓ, Normann F, Skagestad R, Johnsson F (2018) Investment costs and CO_2 reduction potential of carbon capture from industrial plants—a Swedish case study. Int J Greenh Gas Control 76:111–124
32. Lee JSM et al (2016) CCS—a technology for now: general discussion. Faraday Discuss 192:125–151
33. Fennell P (2015) Economics of chemical and calcium looping. In Fennell P, Anthony B (eds) Calcium and chemical looping technology for power generation and carbon dioxide (CO_2) capture, pp 39–48. Woodhead Publishing. http://dx.doi.org/10.1016/B978-0-85709-243-4.00003-3
34. Hanak DP, Manovic V (2017) Economic feasibility of calcium looping under uncertainty. Appl Energy. https://doi.org/10.1016/j.apenergy.2017.09.078
35. Hanak DP, Kolios AJ, Manovic V (2016) Comparison of probabilistic performance of calcium looping and chemical solvent scrubbing retrofits for CO_2 capture from coal-fired power plant. Appl Energy. https://doi.org/10.1016/j.apenergy.2016.03.102
36. Erans M et al (2018) Pilot testing of enhanced sorbents for calcium looping with cement production. Appl Energy. https://doi.org/10.1016/j.apenergy.2018.05.039
37. Arias B, Diego ME, Méndez A, Alonso M, Abanades JC (2018) Calcium looping performance under extreme oxy-fuel combustion conditions in the calciner. Fuel. https://doi.org/10.1016/j.fuel.2018.02.163
38. Hanak DP, Anthony EJ, Manovic V (2015) A review of developments in pilot-plant testing and modelling of calcium looping process for CO_2 capture from power generation systems. Energy Environ Sci. https://doi.org/10.1039/c5ee01228g
39. Rodríguez N, Murillo R, Abanades JC (2012) CO_2 capture from cement plants using oxyfired precalcination and/or calcium looping. Environ Sci Technol. https://doi.org/10.1021/es2030593
40. OECD and IEA and UNIDO (2011) Technology roadmap: carbon capture and storage in industrial applications
41. Hills TP, Sceats M, Rennie D, Fennell P (2017) LEILAC: low cost CO_2 capture for the cement and lime industries. Energy Procedia. https://doi.org/10.1016/j.egypro.2017.03.1753
42. Worldsteel. Steel Statistical Yearbook 2016 (2016) World Steel Assoc. Statistics Denmark
43. Ramírez-Santos ÁA, Castel C, Favre E (2018) A review of gas separation technologies within emission reduction programs in the iron and steel sector: current application and development perspectives. Sep Purif Techn. https://doi.org/10.1016/j.seppur.2017.11.063
44. Global CCS Institute (2010) Global technology roadmap for CCS in industry—steel sectorial report
45. De Beer J, Harnisch J, Kerssemeeckers M (2000) Greenhouse gas emissions from major industrial sources—III iron and steel production report number PH3/30 September 2000. PH3/30
46. Tian S et al (2016) Highly efficient CO_2 capture with simultaneous iron and CaO recycling for the iron and steel industry. Green Chem. https://doi.org/10.1039/c6gc00400h
47. Arasto A, Tsupari E, Kärki J, Pisilä E, Sorsamäki L (2013) Post-combustion capture of CO_2 at an integrated steel mill—part I: technical concept analysis. Int J Greenh Gas Control. https://doi.org/10.1016/j.ijggc.2012.08.018
48. Ho MT, Bustamante A, Wiley DE (2013) Comparison of CO_2 capture economics for iron and steel mills. Int J Greenh Gas Control. https://doi.org/10.1016/j.ijggc.2013.08.003
49. Fernández JR, Martínez I, Abanades JC, Romano MC (2017) Conceptual design of a Ca–Cu chemical looping process for hydrogen production in integrated steelworks. Int J Hydrogen Energy. https://doi.org/10.1016/j.ijhydene.2017.02.141
50. Chen J et al (2018) Self-activated, nanostructured composite for improved CaL–CLC technology. Chem Eng J 351:1038–1046

51. Su C, Duan L, Donat F, Anthony EJ (2018) From waste to high value utilization of spent bleaching clay in synthesizing high-performance calcium-based sorbent for CO_2 capture. Appl Energy. https://doi.org/10.1016/j.apenergy.2017.10.104
52. Wang H, Zhou P, Wang Z (2017) Reviews on current carbon emission reduction technologies and projects and their feasibilities on ships. J Mar Sci Appl. https://doi.org/10.1007/s11804-017-1413-y
53. Yoo BY (2017) Economic assessment of liquefied natural gas (LNG) as a marine fuel for CO_2 carriers compared to marine gas oil (MGO). Energy. https://doi.org/10.1016/j.energy.2017.01.061
54. Gammer D (2017) Taking stock of UK CO_2 storage. Energy technologies institute
55. Senior (Senior CCS Solutions Ltd), B (2010) CO_2 storage in the UK—industry potential
56. International Energy Agency (2016) The potential for equipping China's existing coal fleet with carbon capture and storage
57. Holloway S et al (2007) A regional assessment of the potential for CO_2 storage in the Indian subcontinent. IEA Greenhouse Gas R&D Programme (IEAGHG).
58. National Energy Technology Laboratory (NETL) (2015) Carbon storage Atlas (V). Available at: https://www.netl.doe.gov/research/coal/carbon-storage/natcarb-atlas. Accessed 26th July 2018
59. Hills T, Florin N, Fennell PS (2016) Decarbonising the cement sector: a bottom-up model for optimising carbon capture application in the UK. J Clean Prod 139:1351–1361
60. Mac Dowell N, Fennell PS, Shah N, Maitland GC (2017) The role of CO_2 capture and utilization in mitigating climate change. Nat Clim Chang 7:243

Chapter 5
CO_2 Capture by Oxyfuel Combustion

Jan Hrdlicka, Matěj Vodička, Pavel Skopec, František Hrdlička and Tomáš Dlouhý

Abstract This chapter presents detailed description of oxyfuel combustion plant configuration, discusses specific features and differences between oxyfuel combustion and air combustion, and shows detailed numerical approach for establishing material balance of the oxyfuel combustion process. This numerical approach includes calculation of fluidization medium flow for the case of fluidized bed combustor. Based on experimental data, validation of the model is provided. The text discusses oxyfuel combustion in a fluidized bed, which is generally more complicated, especially by the need to maintain proper fluidization conditions. A practical example of a change of the operation mode from air to oxyfuel in a fluidized bed combustor is presented. Last part of the chapter is dedicated to discussing the formation discussion of particular pollutants that need to be removed from the off-gas before the condensation of water vapor to obtain the final CO_2 can be performed. The discussion concerns differences in processes of formation and possibilities of reduction of carbon monoxide, sulfur, and nitrogen oxides that must be absent in the final CO_2 due to the risk of liquid acids formation which can take place under high pressure.

Keywords CCS · Oxyfuel combustion · CO_2 capture

J. Hrdlička (✉) · M. Vodička · P. Skopec · F. Hrdlička · T. Dlouhý
Department of Energy Engineering, Faculty of Mechanical Engineering, Czech Technical University, Technická 4, 166 07 Praha 6, Czech Republic
e-mail: jan.hrdlicka@fs.cvut.cz

M. Vodička
e-mail: matej.vodicka@fs.cvut.cz

P. Skopec
e-mail: p.skopec@fs.cvut.cz

F. Hrdlicka
e-mail: frantisek.hrdlicka@fs.cvut.cz

T. Dlouhý
e-mail: tomas.dlouhy@fs.cvut.cz

F. Winter et al. (eds.), *CO_2 Separation, Purification and Conversion to Chemicals and Fuels*, Energy, Environment, and Sustainability,
https://doi.org/10.1007/978-981-13-3296-8_5

List of Symbols

C Fraction of carbon in fuel [kg/kg]
H Fraction of hydrogen in fuel [kg/kg]
N Fraction of nitrogen in fuel [kg/kg]
O Fraction of oxygen in fuel [kg/kg]
S Fraction of combustible sulfur in fuel [kg/kg]
V Specific volume [Nm^3/kg]
c concentration [Nm^3/Nm^3]
r Recirculation coefficient [-]

Greek symbols

α Excess of oxidizer [-]
κ Volumetric compensation factor [-]
ω Concentration [Nm^3/Nm^3]

Upper indexes

daf Dry ash free
r As received

Lower indexes

D Dry
FG Flue gas
FGR Flue gas recirculation
O Oxidizer
W Wet
i Flue gas component (O_2, CO_2, H_2O, SO_2, N_2, Ar)
min Minimal, stoichiometric

5.1 Introduction

The term "oxyfuel combustion" describes in technical practice such a combustion system, where the concentration of gaseous oxygen in the oxidizer for fuel combustion is higher than approximately 21%, which is the oxygen concentration in the air. The oxygen concentration can be as high as 100%; this case then refers to full oxyfuel conditions. However, the oxygen concentration can range within the interval of 21–100% as well; in this case, we refer to an oxygen-enhanced combustion system. In real cases, we can hardly reach truly 100% oxygen concentration in the combustion oxidizer, at least for the reason that for the industrial scale it

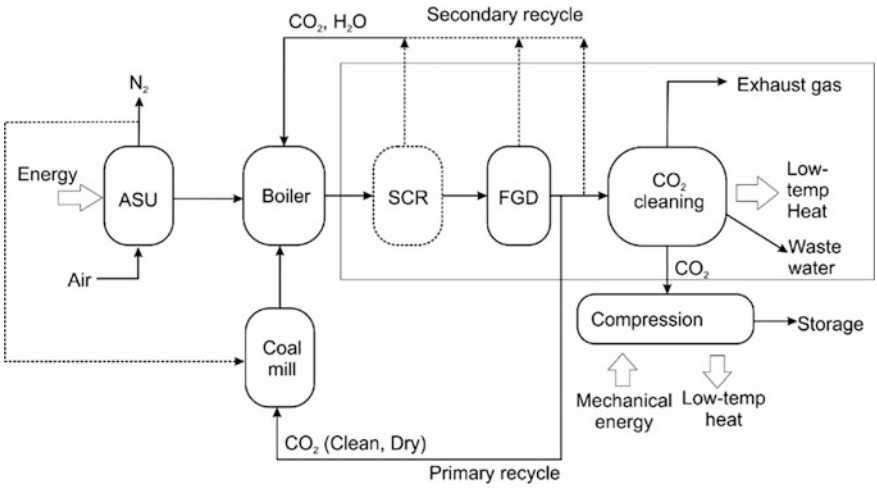

Fig. 5.1 Configuration of an oxyfuel combustion plant, reproduced from [2]

would not be economically feasible to produce and use a high-purity oxygen. Therefore, there is always impurity in the oxygen, typically N_2 and Ar from air separation. The real concentration of oxygen in practical applications is around 95–97% [1, 2].

The concept of oxyfuel combustion was first adopted in various industrial applications like cement or glass production. The oxyfuel combustion was proposed already in 1980s in the context of providing CO_2-rich flue gas for enhanced crude oil recovery (EOR). Recently, the use of oxyfuel combustion is mainly expected as one of the CCS technologies for solid fuel fired power plants, and so most of the following information, conditions, and rules in this chapter is related to this application.

Using oxygen in a combustion process eliminates nitrogen as the major flue gas component in an air-fired mode. The flue gas is then composed particularly of CO_2, water vapor, and remaining excess oxygen. Typical scheme of the oxyfuel combustion setup is shown in Fig. 5.1.

5.2 Principles of the Oxyfuel Combustion

From the conventional air combustion, the oxyfuel combustion process differs in three main points: use of an air separation unit (ASU), use of a gas processing unit, and use of extensive flue gas recirculation (FGR).

- Air separation unit and oxygen supply into the combustor

The air separation unit provides oxygen to the combustion process, and it is the greatest energy penalty for the oxyfuel technology—in relation to electricity

generation—it decreases the net power plant efficiency by 7–9%. Nowadays the best possibility of the oxygen supply for the industrial oxyfuel combustor is by a cryogenic distillation unit. No other technologies exist in such sizing to be able to produce sufficient amount of oxygen for typical industrial consumptions in range of tens or hundreds of tons of oxygen per hour, even when new developments on membrane separation are recently ongoing.

The point of the oxygen input is important in the oxyfuel combustor design, particularly due to safety reasons. Oxygen should not be used to support solid fuel transport to furnace similarly as combustion air is utilized in air-fired boilers. It cannot be even supplied to the FGR stream before coal mill for the case of pulverized combustion, or before grinders in the case of FB combustion. Although CO_2 has inhibitory effect on explosions and it could be possible to raise the O_2 level in the mixture above 21%, possible cases of equipment failures in control valves, recycle fans, etc. are considered as security risks. In the case of PC boilers, the method of oxygen injection and mixing is a question of the optimal burner design, taking into consideration satisfactory ignition, flame stabilization or optimization on NO_x formation. In the case of FB boilers, the oxygen is supplied always into the primary fluidizing medium stream, which is particularly composed of recirculated flue gas.

- Flue gas recirculation (FGR)

The FGR is essential for reducing temperature and supplying sufficient amount of heat carrier in order to carry away the heat released by oxygen combustion of fuel, since the amount of flue gas is about 80% lower compared to conventional air combustion (see further in Table 5.2). There are two main FGR supply options—dry and wet FGR. Dry FGR refers to a case where the flue gas is cooled down below the dew point and the water vapor is condensed. Wet FGR refers to keeping the flue gas temperature all the time from extraction to supply point above its dew point, thus the water vapor remains in the gas. The wet FGR line must be thermally insulated to prevent unwanted condensation, especially under partial loads of the boiler. Applying dry FGR is usually necessary in case of pre-drying or pneumatic transport of the fuel. In this case, the volumetric flow of the FGR reduces accordingly to its actual temperature, determined by the water vapor saturation pressure.

- CO_2 processing

The oxyfuel system employs all typical measures for reducing concentrations of pollutants, e.g., sulfur and nitrogen oxides. In an ideal case, the final CO_2 contains only water vapor and residual oxygen. As a next stage, compression and dehydration of the CO_2 stream take place. Compression of the gases is highly energy demanding, and it is another important energy penalty, decreasing the electrical efficiency by 2–3% [2–4]. The possible process scheme for CO_2 processing is shown in Fig. 5.2.

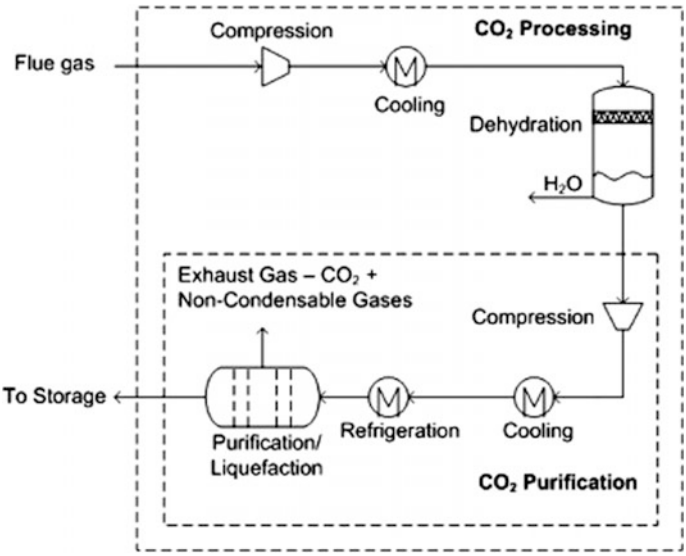

Fig. 5.2 Configuration of a CO_2 processing technology [2]

5.3 Theoretical Analysis and Operation Data

The analysis of oxyfuel combustion process is based on input data of fuel analysis (for solid fuel fractions of C, H, N, S, O elements as received) and provide complete balance of respective gas streams and species, all related to 1 kg of burned fuel. Complete set of equations [5] is shown in Table 5.1. The equations presume complete combustion, which means that all carbon in the fuel is completely oxidized to CO_2. Table 5.1 provides calculation of volumes of oxygen, carbon dioxide, nitrogen, sulfur dioxide, and noble gases (represented as argon) in the flue gas as well as in the required volume of oxidizing medium that is composed of flue gas from FGR and fresh oxygen.

In Table 5.1, the value "r" is the ratio of recirculated flue gas and is defined as follows:

$$r = \frac{V_{FGR,W}}{V_{FG,W}}$$

The symbol κ in Table 5.1, row 9, is a volumetric compensation factor for wet oxidizing medium. It is normally used for air combustion mode and defines an increase of specific volume of air, when it contains moisture. For 20 °C and 70% relative humidity, the κ is equal to approximately 1.016. In the case of oxyfuel mode, it can be presumed that the fresh oxygen is free of any moisture, thus the value of κ equals to one.

Table 5.1 Set of equations for calculation of gas streams in oxyfuel combustion

	Volume of oxidizer	Volume of flue gas	FGR	Volume of primary mixture
O_2	$\alpha \cdot 22.39 \cdot \left(\frac{C^r}{12.01} + \frac{H^r}{4.032} + \frac{S^r}{32.06} - \frac{O^r}{32} \right)$	$\frac{\alpha-1}{\alpha} \cdot \omega_{O_2} \cdot V_{O,D}$	$r \cdot V_{FG,O_2}$	$V_{O,O_2} + V_{FGR,O_2}$
N_2	$\alpha \cdot \omega_{N_2} \cdot V_{O,D,min}$	$\frac{22.4}{28.016} \cdot N^r + V_{O,N_2}$	$r \cdot V_{FG,N_2}$	$V_{O,N_2} + V_{FGR,N_2}$
CO_2	$\alpha \cdot \omega_{CO_2} \cdot V_{O,D,min}$	$\frac{22.26}{12.01} \cdot C^r + V_{O,CO_2}$	$r \cdot V_{FG,CO_2}$	$V_{O,CO_2} + V_{FGR,CO_2}$
Ar	$\alpha \cdot \omega_{Ar} \cdot V_{O,D,min}$	$V_{O,Ar}$	$r \cdot V_{FG,Ar}$	$V_{O,Ar} + V_{FGR,Ar}$
SO_2	$\alpha \cdot \omega_{SO_2} \cdot V_{O,D,min}$	$\frac{21.89}{32.06} \cdot S^r + V_{O,SO_2}$	$r \cdot V_{FG,SO_2}$	$V_{O,SO_2} + V_{FGR,SO_2}$
Volume of dry gas $V_{...,D}$	$\sum_i V_{O,i}$	$\sum_i V_{FG,i}$	$\sum_i V_{FGR,i}$	$\sum_i V_{FM,i}$
H_2O	$V_{O,W} - V_{O,D}$	$V_{FUEL\ H_2O} + V_{O,H_2O} - C$	$V_{FGR,W} - V_{FGR,D}$	$V_{O,H_2O} + V_{FGR,H_2O}$
Volume of wet gas $V_{...,W}$	$\kappa \cdot V_{O,D}$	$V_{FG,D} + V_{FG,H_2O}$	$\frac{V_{FGR,D}}{1-\omega''_{H_2O}}$	$V_{FM,D} + V_{FM,H_2O}$
Stoichiometric volume of oxidizer	$V_{O,D,min} = \frac{V_{O,O_2}}{\omega_{O_2}} = \frac{22.39 \cdot \left(\frac{C^r}{12.01} + \frac{H^r}{4.032} + \frac{S^r}{32.06} - \frac{O^r}{32} \right)}{\omega_{O_2}}$			
Volume of water vapor in flue gas	$V_{FG,H_2O} = \frac{44.8}{4.032} \cdot H^r + \frac{22.4}{18.016} \cdot W^r + V_{O,H_2O}$			
Volume of water vapor in FGR without condensation	$V_{REC,H_2O} = r \cdot V_{FG,H_2O}$			
Volumetric correction for condensation C	$\frac{r \cdot \left(V_{FUEL,H_2O} + V_{O,H_2O} - \frac{\omega''_{H_2O} \cdot V_{FG,D}}{1-\omega''_{H_2O}} \right)}{r+1}$			
Indexes i	O_2, N_2, CO_2, Ar, SO_2			

The symbol α in the equation set defines the excess of oxidizer (i.e., either air or oxygen) in the balance. Exact stoichiometric supply of oxygen per 1 kg of fuel never leads to complete combustion, thus certain excess of oxygen must be used. The value of α is then defined as follows:

$$\alpha = \frac{V_{O,D}}{V_{O,D,\min}}$$

and the $V_{O,D,\min}$, which equals to stoichiometric (thus "minimal") amount, is obtained from the V_{O2} with $\alpha = 1$ and using the input elemental composition of fuel in "as received" conditions, by the following equation:

$$V_{O,D,\min} = \frac{V_{O_2,D}}{c_{O_2,D}}$$

where c_{O2} is volumetric (or molar) fraction of oxygen in the oxidizer. The value equals to 0.21 for the case of air mode and equals roughly—depending on oxygen purity—to 1 for the oxyfuel mode.

Using the set of equations in Table 5.1, comparison between air and oxyfuel mode balance can be obtained, as shown in Table 5.2, which shows differences in specific volumes of gas flows between air and oxyfuel combustion modes. The volumes are expressed in normal cubic meters and are related to 1 kg of burned fuel. The values in Table 5.2 were obtained based on mass fractions of elements in a sample of lignite coal, and presume purity of oxygen for the oxyfuel mode of 95% (the balance is nitrogen).

Table 5.2 Flue gas from air and oxyfuel combustion, 20% oxygen excess, lignite coal

	Air mode	Oxyfuel mode	Unit
O_2 in flue gas	3.6	18.2	vol%
Specific volumes			
O_{2min}	1.032	1.032	Nm^3/kg
Oxidizer dry, min	4.916	1.032	Nm^3/kg
Oxidizer wet, min	4.995	–	Nm^3/kg
Oxidizer total, dry	5.900	1.239	Nm^3/kg
Flue gas dry	5.793	1.133	Nm^3/kg
Flue gas wet	6.557	1.596	Nm^3/kg
Concentrations of flue gas components, wet/dry, normal conditions			
CO_2	14.0/15.9	50.9/80.9	vol%
H_2O	11.6/0.0	37.1/0.0	vol%
N_2	70.3/79.6	0.3/0.4	vol%
SO_2	0.08/0.09	0.3/0.4	vol%
O_2	3.1/3.6	11.5/18.2	vol%
Noble gases	0.8/0.9	0.0/0.0	vol%

Table 5.2 shows that the volume of flue gas is about 80% lower in oxyfuel mode compared to air mode. Accordingly, this corresponds to a change of adiabatic flame temperature for this coal from about 1500–3100 °C. Material reasons then imply the necessity of high degree FGR as a heat carrier, as mentioned already above.

In this model example, the CO_2 concentration in dry flue gas reaches up to 90%. Real concentration in the wet flue gas is about 48%, however. The example also shows that the second major component in the flue gas in oxyfuel mode is oxygen from the oxygen excess. If we consider 20% oxygen excess, which is a reasonably low value for operation of a boiler, ensuring (nearly) complete carbon burnout, the oxygen concentration in dry flue gas in air mode reaches to about 3.5%; however, the same setup in oxyfuel mode results into about 10% oxygen dry concentration. It means that in real practice, it is not possible to reach more than roughly 90% CO_2 dry on the outgoing flue gas.

The oxyfuel combustors are highly sensitive toward ingress of air. Generally, boilers are operated in underpressure in order to avoid leaking flue gases from inside to the boiler room. However, this cannot fully apply to oxyfuel boilers, since any unsealed or leaking point in the boiler body causes ingress of air that dilutes the CO_2. The following Fig. 5.3 shows correlation between CO_2 concentration in oxyfuel mode, considering the same lignite coal as above, and the degree of air ingress, expressed against two parameters. The first parameter is the degree of air ingress as a percentage of fresh oxygen flow. The second parameter is specific for oxyfuel fluidized bed combustion, and it is a percentage of oxidizer flow. Specifics of FB oxyfuel combustion are discussed in the next chapter.

Figure 5.3 clearly shows that, for example, if we replace 10% of fresh oxygen flow by oxygen from air ingress, the CO_2 concentration drops to about 85 vol%. The same situation can present as an intake of 2% air into the combustor. If the air ingress reaches 10%, the outlet CO_2 concentration is as low as 60 vol%. Real air-fired boilers can typically reach this value as a normal operating condition. It, therefore, means that the air ingress is really an important problem that can significantly decrease the CO_2 concentration and must be considered seriously.

5.3.1 Concentrations of Components and Emission Factors

Table 5.2 gives a good overview of major flue gas components and their relative concentration in the off-gas. As an example, absolute amount of water vapor from combustion of the coal used for data in Table 5.2 is always about 0.7 Nm^3/kg of burned fuel (or 0.78 Nm^3/kg, including the moisture from air in air-fired mode). However, if we calculate its relative concentration, related to 1 Nm^3 of the off-gas wet, we get 14% for air-fired mode and 46% for oxyfuel mode. The same applies to the concentrations of all other species in the off-gas. In order to be able to compare them, typically emissions of pollutants, volumetric or mass concentrations cannot be used, since they are referenced to different specific volumes of the off-gas in air and oxyfuel modes. Instead, emission factor must be used, referencing the mass of a

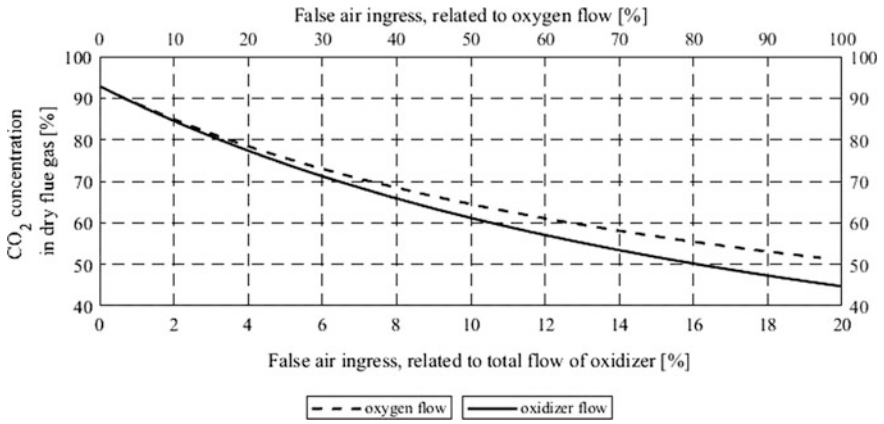

Fig. 5.3 Effect of air ingress on CO_2 concentration

specie to a parameter that does not change among air and oxyfuel combustion mode. Such a parameter can be lower heating value of the burned fuel. For this case, the emission factor is obtained as follows:

- measured volume concentration (e.g., in ppmv) is recalculated to mass concentration at normal thermodynamic conditions, using ideal gas equation of state;
- the emission factor is obtained by the equation

$$\varepsilon = \frac{\rho_{i,W} V_{\mathrm{fg},W}}{\mathrm{LHV}^{\mathrm{r}}} = \frac{\rho_{i,D} V_{\mathrm{fg},D}}{\mathrm{LHV}^{\mathrm{r}}}$$

where ρ_i is the mass concentration of the specie, $V_{\mathrm{fg},}$ is the specific volume of the off-gas, calculated according to Table 5.1, and $\mathrm{LHV}^{\mathrm{r}}$ is the lower heating value of the burned fuel in as-received conditions. The equation must be consistent—if a concentration in dry gas is used, the volume of the flue gas must be in dry conditions as well, and vice versa. The emission factor ε is typically represented in mg/MJ. More details on the emission factors can be found elsewhere [6].

5.3.2 *Specifics for Fluidized Bed Combustion*

Additionally to the facts above, the fluidized bed combustion in oxyfuel mode has particularly the following specific features:

- sufficient flue gas recirculation (FGR) must be kept not only for supplying enough heat carrier to maintain acceptable combustion temperature, but also to

sustain the fluidization. Fluidization is determined particularly by minimum fluidization velocity and terminal particle velocity (details on the characteristic velocities can be found elsewhere [7]);

- properties of the fluidization medium significantly change, since it is formed by recirculated flue gas and oxygen. Changed material properties, therefore, have significant impact on fluidization regime. The minimum fluidization velocity increases by approximately 8.5% and terminal velocity by 4–6% compared to air-fired mode;
- in the oxyfuel mode, it is not possible to reach similar thermal and flow conditions at the same time as in the air-fired mode.

The last point is illustrated in Figs. 5.4 and 5.5. Figure 5.4 represents a case of wet FGR; i.e., it means that the recirculated flue gas does not condense. Figure 5.5 illustrates the case of dry FGR; i.e., the water vapor in the FGR condenses and some of the mass flow for fluidization is, therefore, lost. Generally, there should be a balance between the thermal conditions in the fluidized bed (determined by adiabatic flame temperature T_{AD}) and the fluidization regime, determined here by the total volume of the fluidization medium V_{fm}. Figures 5.4 and 5.5 also show normalized values. This means that value of T_{AD} and V_{fm} equal to one represents a case, when these parameters are equal in air and oxyfuel combustion mode. The dotted line highlights the value of one of these parameters.

The dashed line, showing the equal conditions in air and oxyfuel modes, represents a situation that is impossible to happen, however. Keeping equal T_{AD} (at FGR ratio = 3.6) in air and in oxyfuel modes causes significant decrease in the volume of fluidization medium V_{fm} in the oxyfuel mode. Alternatively, by increasing FGR up to FGR ratio around 4.7, the point of the equal volume of fluidization medium in oxyfuel and air modes is reached. However, this point corresponds to a lower T_{AD}, which means a lower temperature in the fluidized bed in the oxyfuel mode. This situation is even more important in the case of using dry

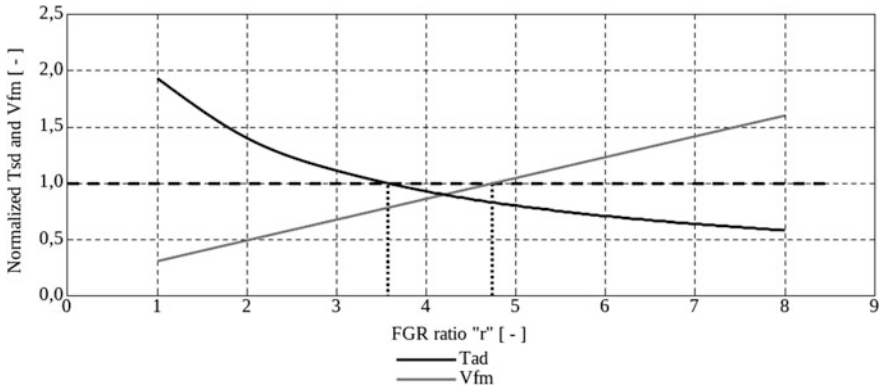

Fig. 5.4 Adiabatic temperature and volume of fluidization medium correlated with FGR ratio—wet FGR

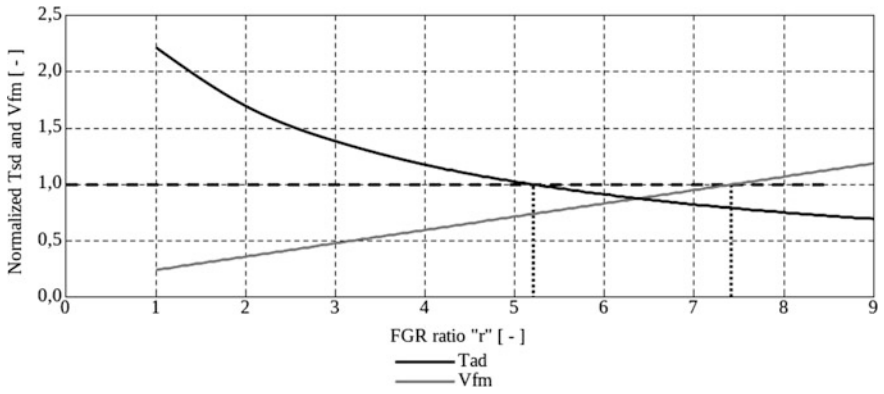

Fig. 5.5 Adiabatic temperature and volume of fluidization medium correlated with FGR ratio—dry FGR

FGR, as shown in Fig. 5.5, since there is missing certain volume of fluidization medium due to water condensation and subsequent volume flow reduction, determined by the *C* coefficient in Table 5.1. The graphs in Figs. 5.4 and 5.5, therefore, show important constraints and specifics of the fluidized bed combustion in oxyfuel mode:

- keeping constant T_{AD} (and the bed temperature as a result) is a trade-off by a decrease of fluidization velocity of about 30–40%;
- it must be, therefore, ensured that the fluidization velocity does not drop below minimum fluidization velocity;
- the high degree of FGR is essential in order to keep the required fluidization;
- there is no risk of exceeding the terminal particle velocity when changing from air to oxyfuel mode;
- bubbling fluidized bed combustor in oxyfuel mode ought to be operated at elevated bed temperatures to prevent defluidization, especially when switching from air to oxyfuel operation mode.

5.3.3 Real Oxyfuel Operation Data

The theoretical analysis is supported by examples of experimental data that were obtained in two oxyfuel bubbling fluidized bed combustors, one in laboratory scale (power load approximately 30 kW) and the second in pilot scale (approximately 0.5 MW power load). The 30 kW facility is described in [8], the 0.5 MW facility is a pilot scale BFB hot water boiler that is able to operate in both, air and oxyfuel mode. As a representative example, data from combustion of a lignite coal at 880 °C bed temperature, 6–8% oxygen concentration in the flue gas and various CO_2/O_2 ratios in the fluidization medium are used—see Tables 5.3 and 5.4. These tables

Table 5.3 Oxyfuel experimental data, 30 kW BFB

Parameter	Experiment 30A	Experiment 30B	Experiment 30C
CO_2/O_2 (vol%)	64/36	69/31	74/26
Bed temperature (°C)^M	880	880	900
O_2 dry flue gas (%)^M	8.5	6.6	8.3
CO_2 dry flue gas (%)^M	87.0	90.8	84.0
Fuel feeding (kg/h)^M	4.2	4.3	4.1
FGR temperature (°C)^M	76	89	56
Fluidization velocity (m/s)	0.94	1.12	1.18
Recirculation coefficient r (-)	2.63	3.29	4.78
Measured oxygen flow $\left(m_N^3/h\right)^M$	5.2	5.1	5.0
Calculated oxygen flow $\left(m_N^3/h\right)$	5.0	5.0	4.8
Relative deviation measured-calculated oxygen flow (%)	+5.2	+1.4	+2.7
Index^M indicates a measured value			

Table 5.4 Oxyfuel experimental data, 500 kW BFB

Parameter	Experiment 500A	Experiment 500B	Experiment 500C
CO_2/O_2 (vol%)	67/33	70/30	72/28
Bed temperature (°C)^M	883	881	883
O_2 dry flue gas (%)^M	7	5	3.3
CO_2 dry flue gas (%)^M	80	76.2	85.2
Fuel feeding (kg/h)^M	52	39.1	44
FGR temperature (°C)^M	200	136	138
Fluidization velocity (m/s)	1.44	1.07	1.18
Recirculation coefficient r (−)	3.17	3.28	3.45
Measured oxygen flow $\left(m_N^3/h\right)^M$	57.6	44.9	49.5
Calculated oxygen flow $\left(m_N^3/h\right)$	57.4	38.8	42.9
Relative deviation measured-calculated oxygen flow (%)	+0.5	+13.5	+13.2
Index^M indicates a measured value			

show the most important measured operation parameters, characterizing the oxyfuel combustion mode. As a measure of correlation of model and measurement, the value of oxygen consumption is used.

Firstly, the numerical model presented in Table 5.1 fits very well for the laboratory scale, but gives generally less satisfactory results for the pilot scale facility. One can also identify the dry FGR, used in the 30 kW combustor, and wet FGR used in the larger facility, given by the FGR temperature. Secondly, there is

significant difference in the CO_2 concentration at the outlet from the combustor. In the 30 kW combustor's best case, about 91% CO_2 in dry flue gas was reached. Adding the oxygen share from oxygen excess results in about 3% of residual components that are particularly nitrogen or noble gases—either from oxygen impurity, or air ingress. This is very satisfactory result. However, the pilot scale boiler shows worse performance. Even if operated at about +10 Pa overpressure at the flue gas outlet, the CO_2 concentration does not exceed approximately 80–85%. This is associated with the issue of air intake, discussed above.

Tables 5.3 and 5.4 also show different options how to control the fluidized bed temperature. This was approximately 880 °C in all presented cases; however, all other parameters were changing. For instance, when the CO_2/O_2 ratio grows, which means less oxygen in the oxidizer, growing recirculation coefficient can observe. This is due to the necessity to supply a constant amount of oxygen in lower concentration to keep the bed temperature constant, which results in a higher FGR flow to keep the mass flow of the oxygen constant as well. Associated effect is a growing fluidization velocity.

5.4 Formation Principles and Reduction Possibilities of Gaseous Pollutants

This part of the chapter deals with oxyfuel-specific formation of three fundamental pollutants that are always in the close focus and that are unwanted in the output CO_2 from the process—carbon monoxide, sulfur dioxide/trioxide, and nitrogen oxides.

5.5 Carbon Monoxide

Carbon monoxide is referred to as a product of incomplete oxidation of hydrocarbons in fuel. However, at high concentrations of CO_2 in the gas phase, which is typical for oxyfuel combustion, CO can be also produced by dissociation of CO_2:

$$2CO_2 \leftrightarrow 2CO + O_2$$

This reaction is strongly endothermic and therefore can take place in the flame zone or in the nearly stoichiometric conditions. Typically, in a pulverized combustion, it is the primary mixture zone. In a fluidized bed combustion, it is in the dense part of the fluidized bed. Another important pathway leading to the increase of CO concentration in the flame zone of oxyfuel flames, where the reaction between CO_2 and H radical can take place.

$$CO_2 + H^{\cdot} \leftrightarrow CO + OH^{\cdot}$$

The last important source of CO in oxyfuel combustion is the Boudouard reaction:

$$C + CO_2 \leftrightarrow 2CO$$

The Boudouard reaction is strongly endothermic as well. All the specified reactions are promoted by elevated CO_2 concentration and high temperature [2]. The Boudouard reaction, typically known from gasification, is further supported by a higher presence of unburned carbon particles.

The burnout of CO is affected, similarly to the air combustion, particularly by temperature and availability of oxygen [9]. Figures 5.6 and 5.7 show the correlation of CO emission factors in air and oxyfuel combustion modes in both 30 and 500 kW BFB combustors with actual oxygen concentration, measured at the outlet from the combustors, and with the same parameter recalculated to the stoichiometry of the oxidizer—air and oxygen for the respective combustion modes—as described in Chap. 3. The lines marked as "30" refer to the 30 kW facility and "500" to the 500 kW facility.

From Figs. 5.6 and 5.7, it is obvious that the same oxygen concentration in the flue gas is completely different from oxygen excess ratio (calculated as specific volume of total oxygen used to its stoichiometric volume) between air and oxyfuel modes. Figure 5.7 clearly shows that at low stoichiometry CO levels are significantly higher in oxyfuel mode, and quickly drop as long as there is enough oxygen to burn out the solid carbon residue, which supports the Boudouard reaction. At oxygen excess ratio 1.20 (i.e., oxygen excess 20%, as calculated in Table 5.2) the CO emission factors are significantly lower, compared to air-fired mode, by about a

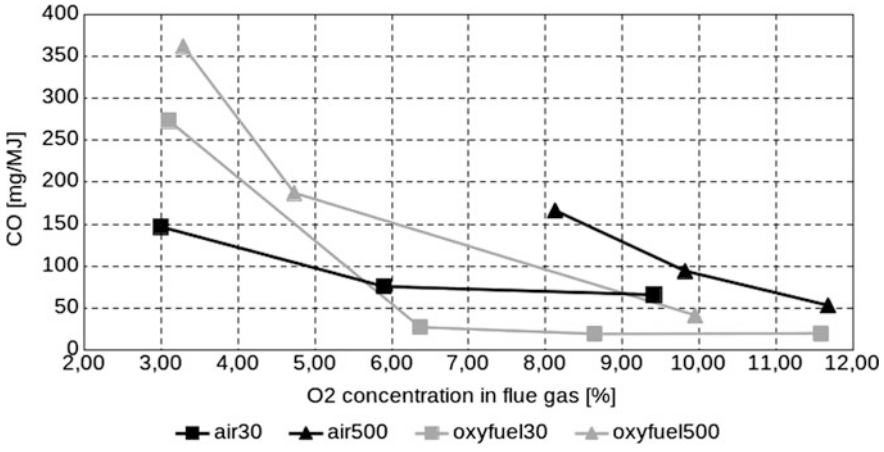

Fig. 5.6 CO emission factor correlated with oxygen concentration

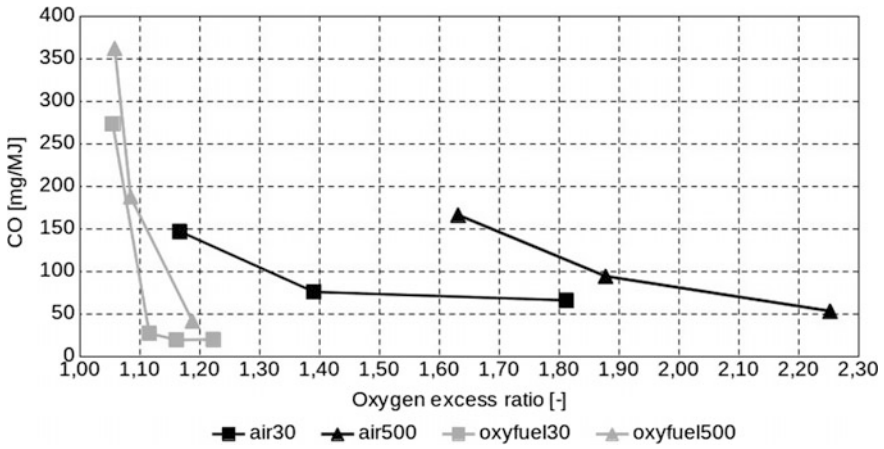

Fig. 5.7 CO emission factor correlated with oxygen excess ratio

factor of two. From this point of view, 20% oxygen excess is fully satisfactory for the oxyfuel combustion to keep the CO levels at acceptable low values. For the same case in air mode, the CO levels are 3–4 times higher and drop to the factor of two at oxygen excess ratio of about 1.80.

5.5.1 Nitrogen Oxides

Three known pathways of formation are generally accepted for NO_x—thermal (Zeldovich), prompt (Fenimore), and fuel-N oxidation. Significance of these pathways differs according to the type of the combustion system. In the air-fired pulverized coal combustion, about 20% of NO_x is formed through the thermal mechanism and the rest is formed from fuel-N while the prompt mechanism is negligible. In the air-fired fluidized bed combustion, almost 100% of NO_x is formed from fuel-N and the other mechanisms have negligible significance due to generally lower combustion temperatures. Schematic diagram of the pathways of oxidation of the fuel-N is shown in Fig. 5.8.

Generally, a lack of nitrogen in the oxyfuel combustion mode prevents the thermal and prompt pathway of NO_x formation that are both associated with reactions of nitrogen molecule from the air. In addition, the equilibrium of the Zeldovich reaction in the thermal mechanism can be negatively affected by excessive NO concentration compared to N_2 concentration—in the oxyfuel mode, there is practically no nitrogen as an input molecule to the Zeldovich reaction, but there is significantly higher relative concentration of NO compared to air-fired mode. Therefore, the Zeldovich reaction is supposed to be reversed to reduce NO to N_2. In the oxidation scheme of the fuel-N in Fig. 5.8, it can be particularly seen as

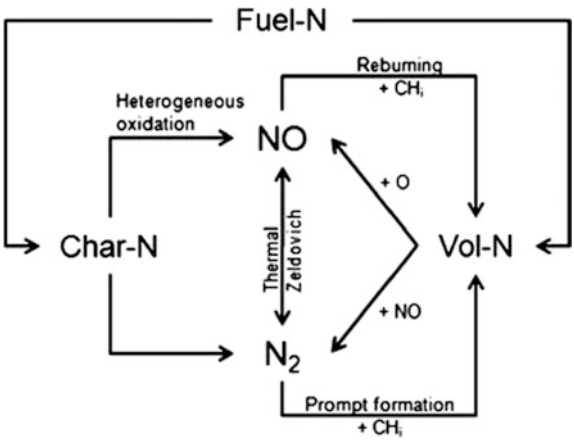

Fig. 5.8 Scheme of the fuel-N oxidation [2]

the nitrogen in volatile matter is moving the equilibrium NO toward nitrogen. To benefit from this reduction, it is important to keep nearly stoichiometric conditions in the primary combustion zone, and ingress of air must be prevented. An important additional reduction factor for the NO_x emissions is the flue gas recirculation that causes the NO_x to pass through the fuel-rich regions and undergo reduction reactions to N_2 [2, 3, 10].

The formation of NO_x in the oxyfuel mode depends, therefore, particularly on the availability of oxygen for oxidation of the fuel nitrogen. Figures 5.9 and 5.10 show the correlation of NO_x with oxygen concentration in off-gas and oxygen excess ratio for air and oxyfuel combustion modes. The data originate from experiments carried out in the 30 and 500 kW combustors mentioned above.

From Fig. 5.9, one could draw a conclusion that the real NO_x emissions are significantly lower in oxyfuel combustion, compared to air mode, by at least the

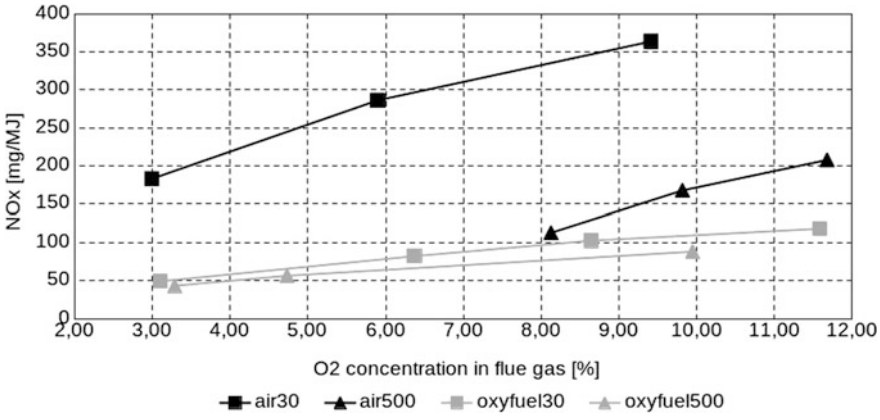

Fig. 5.9 NO_x as sum of NO + NO_2 emission factors correlated with oxygen concentration

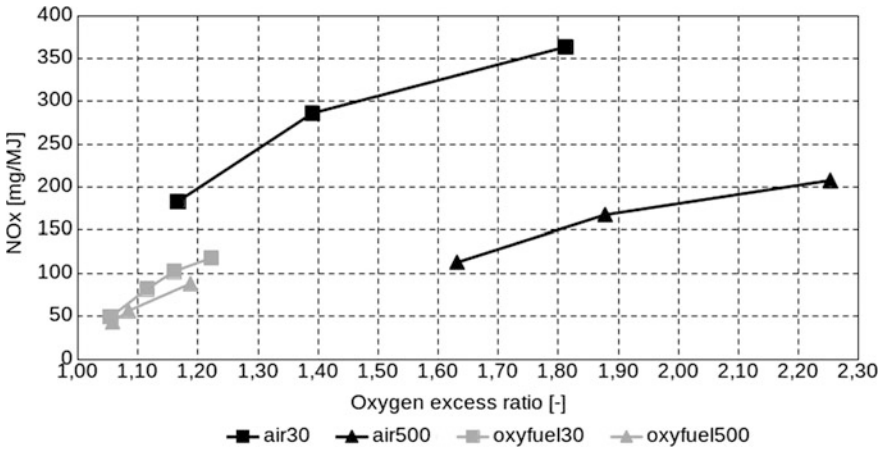

Fig. 5.10 NO_x as sum of NO + NO_2 emission factors correlated with oxygen excess ratio

factor of two. That would be generally true in combustion systems, where the nitrogen oxides originate from atmospheric nitrogen, formed by prompt and thermal mechanism. In this specific case of fluidized bed, just the fuel-N oxidation is the relevant mechanism. The chart in Fig. 5.10 shows that it is merely about the correlation of oxygen stoichiometry and correct plotting of the correlation curves, since fuel-N oxidation depends practically only on oxygen availability. This figure shows that regardless of the principle of combustion (air/oxyfuel) the correlation is much alike and the real benefit of the oxyfuel mode is that the oxygen stoichiometry is much closer to one compared to air mode. However, since combustors in oxyfuel mode can operate satisfactorily at lower oxygen stoichiometry for CO burnout (see Fig. 5.7), the NO_x production can be considered as truly lower compared to air mode. It is also interesting to see that there is no significant difference in NO_x production between the combustor sizes in oxyfuel, as it is in air mode.

Figure 5.11 shows correlation of NO_x emission factor with temperature. The temperature range in this experimental example is restricted into the range from approximately 800 to 960 °C, which applies to the fluidized bed combustors. The experimental data plotted in Fig. 5.11 are all for 6% oxygen concentration in the off-gas, which means, as already mentioned above, oxygen excess ratio of about 1.40 for air mode and about 1.12 for oxyfuel mode, see also, e.g., Fig 5.7 or 5.10. This is the reason why the emission factors of NO_x are higher for the air mode. Otherwise, the experimental data shows that the temperature correlation of NO_x in oxyfuel mode is quite weak and in this specific range, the temperature does not have any significant effect on NO_x formation. In comparison, a stronger correlation can be seen for the air combustion mode, but always with keeping in mind the different oxygen stoichiometry. Other oxyfuel combustion systems, like pulverized coal combustion, operating at higher temperature, can show stronger correlation at higher temperatures, according to the equilibria and kinetic shift in the fuel nitrogen release and oxidation/reduction reaction system.

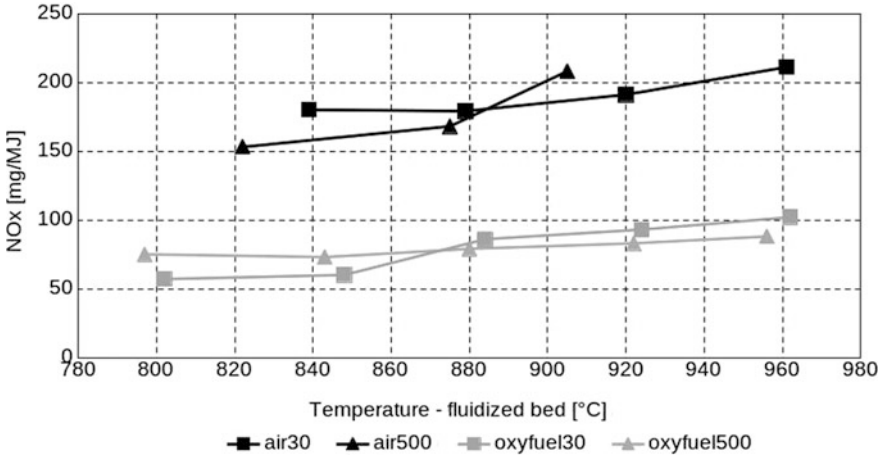

Fig. 5.11 NO_x emission factors correlated with temperature—fluidized bed combustion specific

5.5.2 Sulfur Dioxide

Sulfur in fuels is present generally in forms of pyrite, sulfates, organic bonds, and elemental S. Its share and amount depend on the type of fuel, and all sulfur that can be oxidized is converted at combustion temperatures to SO_2 or SO_3. In typical air combustion, the predominant product is SO_2. The SO_3 forms only about 1% of the SO_2 amount, but in oxyfuel combustion, the share of SO_3 can be increased up to about 5% [3, 11, 12]. The importance of the SO_3 is particularly in its subsequent reaction with water vapor to form sulfuric acid. This conversion starts at the temperature of about 400 °C and is nearly completed at about 200 °C, which thus makes a significant corrosion risk in the oxyfuel combustion mode, typically at locally cold surfaces, e.g., water or air preheaters [13, 14].

Approaches for reducing SO_2 (and SO_3 in parallel) concentration in the off-gas either rely on "post-combustion" methods, based on treatment of the final off-gas, or on in situ SO_2 capture directly in the combustion process. Among the post-combustion methods typically belong wet or semi-dry flue gas desulfurization (FGD) technologies [15], both using a scrubbing process of the off-gas. As to the recent knowledge, converting the combustion mode from air to oxyfuel does not negatively affect either attainability of high SO_2 capture ratio or quality of the final product by the elevated CO_2 partial pressure [16].

The direct in situ capture is advantageous due to its technological simplicity, low investment, and operation costs. In principle, an additive, typically calcium or magnesium carbonate, is either directly fed by pneumatic transport into the combustion zone or it can be premixed with fuel prior to combustion. However, its performance is strongly affected by several process parameters, like heat and mass transfer rates, temperature or composition of gas phase, and by material properties

of the additive, typically porosity, reactivity, and particle size. These circumstances restrict its applicability to the fluidized bed combustion technologies, where the most satisfactory conditions can be met. The reaction mechanism is in principle either a calcination of the carbonate-based sorbent (typically limestone $CaCO_3$) with subsequent reaction with SO_2/SO_3, or direct sulfation. In both cases, the final product is calcium sulfate, but the reaction pathways significantly differ in reaction rate and conversion degree. Generally, more favorable (i.e., reaching higher SO_2 capture ratio) is the calcination-based mechanism, but performance of this scheme is limited by partial pressure of CO_2 in the gas phase [9, 17–19]. In oxyfuel combustion mode, the partial pressure of CO_2 is significantly higher than in air mode. Figure 5.12 shows the calcination equilibrium curve, calculated from [20].

Figure 5.12 depicts typical operation regions of air and oxyfuel combustion in terms of CO_2 partial pressure (or concentration, when considering an ideal gas behavior) and temperature. The left-hand side of the equilibrium curve means that the direct SO_2 capture proceeds as direct sulfation; therefore, lower capture ratio and slower reaction rate can be expected. In practice, it means a higher consumption of the sorbent to reach the required capture ratio. According to Fig. 5.12, the reaction mechanism is always calcination in air combustion mode. In oxyfuel mode, the CO_2 partial pressure reaches about 0.5 bar—see also Table 5.2. At this concentration, the turning point temperature is about 855 °C, which must be exceeded, if the calcination pathway is required. In the fluidized bed combustor, it is a key question of operation, since the FB combustors are typically operated in temperature range of 800–900 °C [9, 21].

The following figures illustrate in details differences and specifics of the direct SO_2 capture in fluidized bed between air and oxyfuel combustion modes. All data shown are from experiments using the same experimental facilities as mentioned above and a fuel—lignite coal of combustible sulfur content S^{daf} = 1.33% wt. The stoichiometry of the sorbent addition is expressed as mole of added calcium carbonate to mole of sulfur in the coal and is denoted as Ca/S ratio.

First, measuring the SO_2 emission factor without any sorbent addition is presented. One can evaluate the so-called sulfur self-retention, which is an ability of

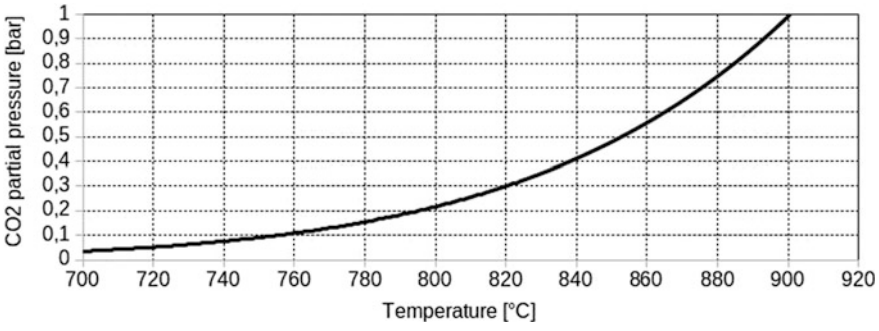

Fig. 5.12 Equilibrium of the calcination reaction in SO_2 direct capture

the carbonates in fuel ash to react with SO_2 (SO_3) from sulfur oxidation by exactly the same mechanism. For air combustion mode at 880 °C and the same oxygen stoichiometry, the measured value is about 700 mg/MJ, whereas for oxyfuel mode it is about 550 mg/MJ. Detailed example of sulfur retention correlated with temperature, measured in the 30 kW combustor, is shown in Fig. 5.13.

The sulfur self-retention is more than double in the oxyfuel mode compared to air mode. There is only weak correlation with temperature in air mode and one can observe an optimum of about 880 °C in oxyfuel mode.

Figure 5.14 shows the correlation of the SO_2 capture with stoichiometry of the added sorbent—the Ca/S ratio—in both air and oxyfuel modes.

The desulfurization performance, evaluated on the basis of SO_2 emissions factors, is significantly higher in the oxyfuel mode. The behavior in oxyfuel mode was nearly the same in both used combustors, so the full gray curve is shown on secondary "*y*" axis of different scale 20–100%. The better performance in oxyfuel mode can be possibly attributed to two factors—higher water vapor concentration (see Table 5.2) enabling formation of $Ca(OH)_2$ from the calcined sorbent, and higher relative concentration of SO_2 in the gas phase, shifting the reaction equilibria toward the products.

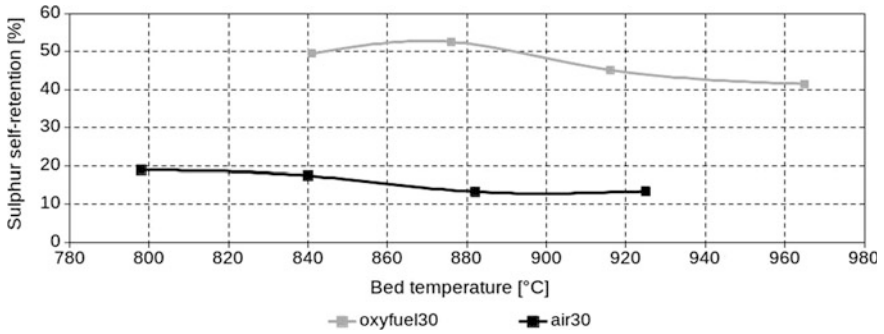

Fig. 5.13 Sulfur self-retention air and oxyfuel combustion mode

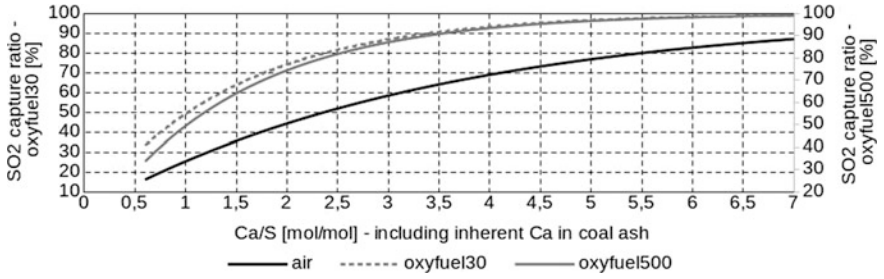

Fig. 5.14 Sulfur capture correlated with sorbent stoichiometry in air and oxyfuel combustion mode

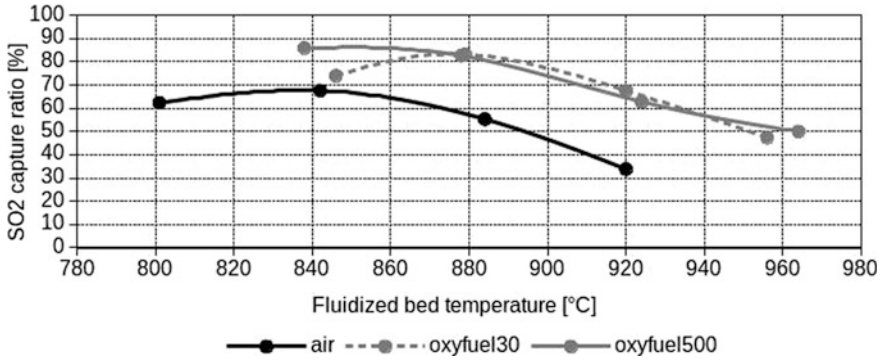

Fig. 5.15 Direct SO_2 capture—correlation with temperature at Ca/S = 3 mol/mol

Besides the different behavior of Ca/S correlation, there is a difference in temperature optimum between air and oxyfuel modes. This is shown in Fig. 5.15, which plots SO_2 capture with bed temperature, all at the same sorbent stoichiometry Ca/S = 3 mol/mol. For this model example, data from experiments using a high purity (>99% $CaCO_3$) geologically old limestone are used.

Figure 5.15 clearly shows that the temperature profile has shifted optimum toward higher temperature in the oxyfuel mode. For the air mode it is about 840 °C, whereas for oxyfuel mode about 880 °C, well corresponding with the theoretical considerations. Particularly, the 840 °C point in oxyfuel mode lays in the region of direct sulfation of Fig. 5.12, whereas all points of the air-mode curve lay in the calcination region. When comparing optimal temperature for air and oxyfuel modes, the SO_2 capture is about 15 percent points higher in oxyfuel mode. Results from both combustors in oxyfuel mode are well coherent and do not show significant differences.

Certain role plays the concentration of oxygen in the gas phase. First, oxygen is needed in the reaction mechanism to oxidized intermediate product to final calcium sulfate. Second, the oxygen concentration is a measure of oxidizer excess and is closely related to CO_2 concentration—simply, more oxygen in the gas phase means lower concentration (partial pressure) of CO_2 with positive effect on equilibria of the reaction mechanism toward desired products. Figure 5.16 depicts the SO_2 capture with oxygen concentration in the gas phase.

Figure 5.16 shows that the effect of oxygen concentration is quite weak and its change within the tested range does not bring any significant changes in the SO_2 capture ratio.

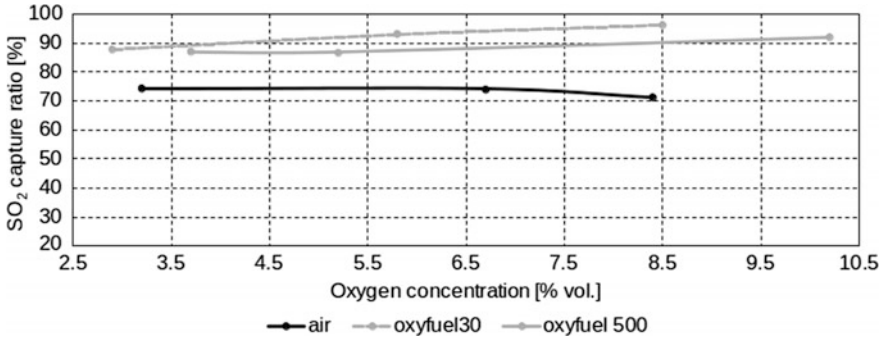

Fig. 5.16 Direct SO_2 capture—correlation with oxygen concentration at Ca/S = 3 mol/mol

5.6 Summary

This chapter aims to give a comprehensive overview of the important aspects of oxyfuel combustion compared to conventional air combustion. Differences in these aspects are most of all determined by change of oxidizer from air to oxygen of technical purity. The result is a fundamental change in composition of the off-gas that mostly comprises of CO_2 and water vapor, as well as the change of specific volume of this off-gas that is about 80% lower. Different composition is reflected in different material properties, like density, viscosity or specific heat capacity and in different chemistry in formation and reduction of unwanted components—pollutants. Lower specific volume of the off-gas is reflected in a need of high degree of flue gas recirculation, necessary for providing the heat carrier in order to decrease adiabatic flame temperature back to values that are typical for air combustion. Additionally for fluidized bed combustion, change to oxyfuel combustion mode is associated with parallel need of maintaining sufficient fluidization conditions. As so, it is not possible to reach flow and thermal conditions identical to air combustion mode at once.

Concentrations of species in the off-gas in oxyfuel mode are completely different from air conditions and an emission factor must be used in order to compare their amount. The different specific volume of the off-gas that is used as concentration reference gives this necessity. Carbon dioxide, which is the required output of the oxyfuel combustion, has, in an ideal practical case, usually a share of no more than 50% in wet off-gas. However, this value depends particularly on water content in the fuel, and on the type of FGR (wet/dry). The remaining major species are water vapor and oxygen from oxidizer excess. Comparing the stoichiometric conditions of the combustion process by using oxygen concentration, the oxyfuel mode runs in far lower stoichiometry (excess of oxygen) than the air-fired process. The real operating conditions of the oxyfuel combustor mean, most of all, further decrease of the output of CO_2 concentration by diluting it by air that is taken in by leakages and

unsealed elements of the combustor. Real CO_2 concentrations usually do not exceed 80–85 vol%, dry gas.

The CO_2 must be free of particularly all condensable or acid-forming substances prior to further water vapor condensation, compression, and transport. In the oxyfuel combustion technology, it means the necessity of removal of all main gas-phase pollutants. This chapter focused on the three most important—carbon monoxide, nitrogen oxides, and sulfur oxides; however, trace pollutants are of high importance as well. Due to different process conditions, formation and removal processes are affected. Carbon monoxide formation is enhanced by reactions that are not important in air-fired combustor, for example, char gasification. In NO_x chemistry, thermal and prompt ways of formation are practically impossible due to a lack of atmospheric nitrogen. This benefit is not relevant for a fluidized bed oxyfuel combustion, where are the NO_x formed by fuel nitrogen oxidation. Generally, NO_x emission factors are lower compared to air mode, but it must be noticed that at different oxygen stoichiometry. Removal of sulfur oxides is essential and can be done by technologies in similar way as in conventional air combustion. The post-combustion methods, like wet FGD, are not affected in principle and can keep their high capture degree and quality of by-products. Performance of the in situ method, used for fluidized bed technology, is enhanced compared to air combustion, even if the optimal working conditions are slightly different.

The oxyfuel combustion undoubtedly belongs to the recently most developed capture part of CCS/U technologies, which is confirmed by the number of pilot scale and demonstration facilities in different scales worldwide. It benefits mostly from the relative technology robustness and simplicity and technological maturity of the key components from the hundred-years combustion technology development, but it suffers predominantly from energy penalty and low flexibility of oxygen production. If the oxyfuel combustion technology should be introduced into industrial and commercial practice in the future, there are several aspects to focus on. The first is the oxygen production that need to be flexible and less energy demanding. Second is the fuel—in Europe— there is a significant trend in declining combustion of fossil fuels, including coal, and it cannot be reasonably expected that a number of large-scale coal-fired boilers would be ever built here in the future. Besides retrofitting recent combustors, the technology will, therefore, need to be effectively scaled down for application at the district level and in this smaller scale be able to work in multi-fuel modes, combining locally available fuels concerning biomass, alternative or refuse-derived fuels.

References

1. Stanger R et al (2015) Oxyfuel combustion for CO_2 capture in power plants. Int J Greenhouse Gas Control 40:55–125
2. Toftegaard MB et al (2010) Oxy-fuel combustion of solid fuels. Prog Energy Combust Sci 36:581–625

3. Scheffknecht G et al (2011) Oxy-fuel coal combustion—a review of the current state-of-the-art. Int J Greenhouse Gas Control 5S:S16–S35
4. Wall TF (2007) Combustion processes for carbon capture. Proc Combust Inst 31:31–47
5. Skopec P, Hrdlicka J (2016) Specific features of the oxyfuel combustion conditions and a bubbling fluidized bed. Acta Polytechnica 56:336–343
6. Hrdlicka J et al (2016) Emission factors of gaseous pollutants from small scale combustion of biofuels. Fuel 165:68–74
7. Kunii D, Levenspiel O (1991) Fluidization engineering. Butterworth-Heinemann, Stoneham. ISBN 0-409-90233-0
8. Hrdlicka J et al (2016) Oxyfuel combustion in a bubbling fluidized bed combustor. Energy Procedia 86:116–123
9. Tomeczek J (1994) Coal combustion. Krieger publishing company, Malabar. ISBN 0-89464-651-6
10. Lackner M, Winter F, Agarwal AK (2010) Handbook of combustion. Wiley-VCH Verlag GmbH, Weinheim. ISBN 978-3-527-32449-1
11. Schenk PW, Steudel R (1968) Oxides of sulphur. In: Nickless G (ed) Inorganic sulphur chemistry. Elsevier, Amsterdam
12. Müller M, Schnell U, Scheffknecht G (2013) Modelling the fate of sulphur during pulverized coal combustion under conventional and oxy-fuel conditions. Energy Procedia 37:1377–1388
13. Spörl R, Maier J, Scheffknecht G (2013) Sulphur oxide emissions from dust-fired oxy-fuel combustion of coal. Energy Procedia 37:1435–1447
14. Pavlík V et al (2007) Degradation of concrete by flue gases from coal combustion. Cem Concr Res 37:1085–1095
15. Vejvoda J, Machač P, Buryan P (2003) Technologie ochrany ovzduší a čištění odpadních plynů. VŠCHT v Praze, Praha. ISBN 80-7080-517-X
16. Faber R et al (2011) Flue gas desulphurization for hot recycle Oxyfuel combustion: experiences from the 30MWth Oxyfuel pilot plant in Schwarze Pumpe. Int J Greenhouse Gas Control 5S:S210–S223
17. Hu G et al (2006) Review of the direct sulfation reaction of limestone. Prog Energy Combust Sci 32:386–407
18. Anthony EJ, Granatstein DL (2001) Sulfation phenomena in fluidized bed combustion systems. Prog Energy Combust Sci 27:215–236
19. Wang C et al (2010) The effect of water on the sulphation of limestone. Fuel 89:2628–2632
20. Baker EH (1962) The calcium oxide-carbon dioxide system in the pressure range 1–300 atmospheres. J Chem Soc 464–470
21. Miller B, Tillmann D (2008) Combustion engineering issues for solid fuel systems. Elsevier, London. ISBN 978-0-12-373611-6

Chapter 6
Methanol Synthesis from CO_2 Hydrogenation Using Metal–Organic Frameworks

Rashmi A. Agarwal

Abstract Increasing level of CO_2 in the atmosphere is a serious concern. Converting CO_2 waste to a potentially clean fuel methanol, by catalytic hydrogenation, will be highly demanding in the perspective of economy and sustainability. Traditionally, it is produced from syngas at high temperature and pressure by utilizing catalyst ($Cu/ZnO/Al_2O_3$). For methanol synthesis, cheap CO_2 sources are available at industrial scale through CCS technology but options for low-cost hydrogen are limited. Despite it Cu nanoparticles in the catalyst are initially discrete and well dispersed but slowly they aggregate and separate out from the ZnO_x interface diminishing the catalytic activity over time ascribed to less number of active sites. To maintain high catalytic activity and selectivity of this catalyst, its stabilization is very crucial. This problem can be resolved by metal–organic frameworks (MOFs) consisting of pores which anchor Cu/ZnO_x nanoparticles in their channels preventing their aggregation as well as their phase separation between Cu and ZnO_x interface. Due to strong metal-supported interactions and confinement effects within the MOF lead to more dispersed and ultrasmall nanoparticles for CO_2 hydrogenation.

Keywords Hydrogenation · CO_2 · Methanol · Cu NPs · Zn NPs Zr · Metal–organic framework (MOF)

Nomenclature

Zn NPs	Zinc nanoparticles
Cu NPs	Copper nanoparticles
CO	Carbon monoxide
CO_2	Carbon dioxide
MOF	Metal organic framework
Zr	Zirconium

R. A. Agarwal (✉)
Department of Civil Engineering, Indian Institute of Technology Kanpur, Kanpur 208016, UP, India
e-mail: raga@iitk.ac.in

F. Winter et al. (eds.), *CO_2 Separation, Purification and Conversion to Chemicals and Fuels*, Energy, Environment, and Sustainability,
https://doi.org/10.1007/978-981-13-3296-8_6

ZnO_x	Zinc oxide
Al_2O_3	Aluminum oxide
CCS	Carbon capture and sequestration
KIT-6	(KAIST: Korean Advanced Institute of Science and Technology) mesoporous silica $(SiO_2)_n$ consisting of interconnected cage type pores (>5 nm) with highly ordered body centered cubic symmetry
aZ	Amorphous ZrO_2 (zirconium oxide)
mZ	Monoclinic ZrO_2
tZ	Tetragonal ZrO_2
PNP	N,N′-bis(diphenylphosphine)-2,6-diaminopyridine
acac	Acetyl acetone
$NHMe_2$	Dimethyl amine
K_3PO_4	Potassium Phosphate
$HNTf_2$	Bis(trifluoromethanesulfonyl)amine
DMF	N,N-Dimethyl formamide
DMFA	Dimethylammonium formate
Cu(100)	Copper surface having 100 plane
Cu(111)	Copper surface having 111 plane
Triphos	Name for organophosphorus tridentate ligands
Cu ⊂ UiO-66	Cu nanocrystals within the UiO-66 metal organic framework

6.1 Introduction

Increasing level of CO_2 on the earth has forced researchers to work actively in this field since it has concluded that the fossil fuel burning and deforestation are mainly responsible for immensely high contribution of CO_2 in the atmosphere endorsed by the Intergovernmental Panel on Climate Change (IPCC) [1]. Solar radiations heat the earth surface without any interruptions and re-emitted lower energy infrared radiations get absorbed by CO_2 which is present in excess leading to global warming. Environmental pollution and CO_2 emissions are also due to the industrial revolution and civilization which give a comfort zone to human life since these provide new technologies to utilize them [2]. That is why conversion of CO_2 into a valuable product is essential to prevent global warming and to stop fossil fuel burning. As it is well known that methanol is not only a cleanest burning fuel but also a reactant to produce olefin and other significant chemicals [3], hence conversion of CO_2 into methanol is an effective way to utilize CO_2 due to environmental problems. But significant challenges are faced due to chemically inert nature of CO_2 which makes it thermodynamically stable. Methanol is an excellent alternative fuel and can be blended with gasoline [4]. At industrial scale, methanol is produced from syngas (synthesis gas or met gas is a mixture of CO, CO_2, and H_2) by employing a variety of catalysts based on $Cu/ZnO/Al_2O_3$ [5]. A number of

review papers have already discussed the catalytic activity of the mentioned catalyst for the CO_2 hydrogenation reaction [6–8].

6.2 Discussion on Heterogeneous and Homogeneous Catalysts

Generally, higher temperature (>200 °C) is required for these systems to work but it restricts the CO_2 reduction reaction which is entropically not favorable [9]. Additionally, it remained challenging at that time to rationally tune the reactivity and selectivity of such heterogeneous catalysts. Therefore, homogeneous catalysts which were selectively capable of converting CO_2 and H_2 to CH_3OH had been tried. Three homogeneous catalysts have been used by Sanford et al. to convert CO_2 into methanol via the intermediates formic acid, methyl formate formation, respectively [10]. Later it was evidenced by Leitner that ruthenium complex along with $NHTf_2$ converts CO_2 into methanol via formic acid or methyl formate formation [11, 12]. Basic media was required for CO_2 capture but mentioned homogeneous catalysts start their working in acidic conditions, that is why these catalysts were unsuitable for this purpose [13]. To overcome this problem, a combination of homogeneous Ru-PNP (PNP: electron-rich and bulky tridentate ligand) pincer complex, $NHMe_2$, and K_3PO_4 were utilized by Rezayee et al. to produce methanol, DMF, and DMFA [14]. But the catalyst was not stable at 155 °C, hence comparatively mild temperature (125–165 °C) reaction conditions were required. Kothandaraman et al. demonstrated by employing pentaethylenehexamine (PEHA) and a Ru-PNP complex for CO_2 reduction CH_3OH could be separated through distillation from the reaction mixture and more CH_3OH was produced. From, Methanol economy point of view, for the first time CH_3OH synthesis has been carried out by directly capturing CO_2 from the air [15]. Due to high boiling point and high nitrogen content (high basicity) of amines, a large amount of CO_2 adsorption takes place which leads to high subsequent reduction to methanol. By employing homogeneous iridium catalyst, Laurenczy and co-workers demonstrated that methanol can be produced from CO_2 at room temperature by utilizing formic acid [16]. But all these methods require very costly noble metals, so these metals should be replaced with the non-precious metals such as iron, cobalt, or copper which are found abundantly. First, homogeneous catalyst with non-noble metal has been formed in situ at 100 °C from $[Co(acac)_3]$, Triphos, and $HNTf_2$ [17].

In comparison between heterogeneous and homogeneous catalysis, heterogeneous catalysis is more advantageous, simple, and cheaper because the catalyst can be easily recollected from the mixed chemical environment of the products and catalyst without making any effort. Main problem which was being faced for heterogeneous catalysis was high temperature of the reaction. Since the reaction of CO_2 hydrogenation is an exothermic process liberating high amount of energy. Due to this liberated energy at high temperature, the endothermic reverse water gas shift

(RWGS) reaction takes place transforming CO_2 into CO as shown in Eqs. 1 and 2. This problem was resolved to some extent (250 °C and 6 bar) in recently discovered catalyst "MnOx"/mesoporous Co_3O_4, but having lower selectivity for methanol synthesis owing to the byproduct (hydrocarbon and/or CO) formation [18].

$$CO_2 + 3H_2 \rightleftarrows CH_3OH + H_2O, \quad \Delta H_{(298K)} = -49\,\text{kJ mol}^{-1} \tag{1}$$

$$CO_2 + H_2 \rightleftarrows CO + H_2O, \quad \Delta H_{(298K)} = 42\,\text{kJ mol}^{-1} \tag{2}$$

Most recently, Rungtaweevoranit et al. and Win et al. have reported CO_2 hydrogenation in the metal–organic framework (MOF) by encapsulating Cu and Cu/ZnO NPs, respectively, within the cavities of MOF at low temperatures [19, 20]. MOFs are the repeating structures (1D, 2D, or 3D) of the combination of metal ion or metal-ion cluster with the organic linker which are linked through the coordination bond leading to permanent porosity [21–25]. Palomino et al. demonstrated that ZnO NPs deposition on Cu(100) and Cu(111) surfaces produces highly active catalysts [26]. The structure of the copper substrate influences the catalytic performance of a ZnO–copper interface. Efficient interactions or mixing effects between Cu and ZnO NPs are considered for the high catalytic activity of Cu–ZnO [27–30]. Very recently, CO_2-to-methanol hydrogenation was investigated by Tada et al. observing the effect of the ZrO_2 phase on Cu species formation of Cu/ZrO_2-based catalysts [31]. In this chapter, detailed study will be discussed about Cu/ZnO_x NPs encapsulation within the cavities of MOF for CO_2 hydrogenation to methanol. It will lead to the persistent stability of the catalyst due to efficient mixing between these two species (Cu and ZnO_x) as well as low temperature which is required for the reduction.

6.3 Advantages of Converting CO_2 into Methanol

Potential uses of converting CO_2 into methanol have been mainly discussed by Olah et al. [32–35]. There will be no need for any other alternate energy source if captured CO_2 is converted into clean liquid fuel methanol using the hydrogen from renewable energy source [36–38]. Methanol not only has higher energy density but also easily stored and used. It is due to the currently used liquid fuels (diesel, gasoline) have high emission of greenhouse gases which is unacceptable for long-term use. High volatile methanol is an excellent blending component in gasoline due to its high octane rating in internal combustion engines (ICE). Direct-methanol fuel cells can be run by the methanol fuel. Bromberg et al. have already discussed that methanol can be used very efficiently in modified diesel engines as well [39, 40]. Vehicles running from methanol fuel will have clean combustion with no harmful emissions. Environment will be more cleaner

consisting of minimum pollutants leading to reduced health-related problems. To arrest global warming, CO_2 hydrogenation to methanol will be helpful due to less CO_2 content in the ambient air.

6.4 Thermodynamic Analysis of CO_2 Hydrogenation to Methanol

Methanol synthesis via CO_2 hydrogenation from syngas is an exothermic reaction; on the other hand, due to chemically inert nature of CO_2, it demands for higher activation energy to produce methanol. That is why higher temperature (>240 °C) is required for the reaction to make it reactive but at the same time at higher temperature reverse water gas shift reaction (RWGS) takes place producing CO from CO_2 and decreasing methanol production yield. It is attributed to the endothermic nature of the RWGS reaction. To control RWGS reaction lower temperature and higher pressure is required.

Water also plays an important role to inhibit the rate of reaction of methanol synthesis by CO_2 reduction [41]. First of all, in situ water sorption was reported by Iliuta et al. for CO_2 hydrogenation [42]. To alleviate thermodynamic barriers recently it was observed that methanol yield is 130% higher for water sorption enhanced hydrogenation in comparison with conventional hydrogenation of CO_2 between temperature range 220–270 °C. But water sorption at higher temperatures leads to a decrease in methanol selectivity due to more prominent RWGS reaction leading to CO formation because equilibrium is affected to a great extent. Same thing happens at higher pressures, methanol selectivity increases with pressure variations but due to more dominating RWGS reaction methanol selectivity decreases because equilibrium is affected [43].

More recently, it was concluded that CO_2 hydrogenation reaction can be improved via product (methanol) condensation as shown in Eq. 3, at lower temperatures and certain pressure with the addition of water leading to significant enhancement in CO_2 conversion [44], because reverse water gas shift equilibrium is controlled.

$$[CH_3OH + CH_3OH \rightleftarrows CH_3OCH_3 + H_2O] \tag{3}$$

6.5 Challenges in Reduction of CO_2 to Methanol

Since CO_2 is an inert molecule due to the presence of two double bonds between carbon and oxygen atoms. That is why higher energy is needed for reduction of CO_2 to produce methanol. It is well known that reduction of CO_2 into CO is possible at metal surfaces of the catalytic systems which is a primary step for all

conversion reactions [45, 46]. A good catalyst which is highly stable is required for hydrogenation of CO_2 to convert it into value-added products [47]. Synthesized water after CO_2 reduction reaction facilitates rapid sintering and deactivation of the commonly used Cu/ZnO catalyst [48]. If CO_2 hydrogenation occurs at higher temperature, then the problem occurs through RWGS endothermic reaction converting CO_2 into CO and H_2O. If temperature is low, then catalytic activity will be slow. It is a big challenge that temperature should be less for the CO_2 reduction reaction and catalytic activity of the catalyst should be intact throughout the reaction.

6.6 Recent Advancements

All important points keeping in mind from the above discussion for CO_2 hydrogenation method have to be selected consisting low temperature and stable catalytic system. In this section, latest advancements will be discussed in detail for CO_2 hydrogenation to methanol which were briefly described in the introduction section.

As it was mentioned by Palomino et al. that the binding and conversion of CO_2 into a formate intermediate (stable up to >500 K) are supported by the formation of a ZnO–Cu interface [26]. For methanol synthesis, ZnO/Cu(100) is a much better catalyst. If the pressure of CO_2 is high or the sample temperature is higher, the transformation will be faster from Zn → ZnO during CO_2 hydrogenation, increasing its stability over the Cu surface. Thus, the catalytic efficiency of a ZnO–Cu interface is affected by the structure of the copper substrate because chemical and catalytic properties of the oxide are influenced by the size and metal-oxide interactions.

A series of ZrO_2/KIT-6 [Cu/a-ZrO_2 (a-ZrO_2: amorphous ZrO_2) or C/aZ, Cu/m-ZrO_2 (m-ZrO_2: monoclinic ZrO_2) or C/mZ, Cu/a-ZrO_2/KIT-6 or C/aZ/K, and Cu/t-ZrO_2/KIT-6 (t-ZrO_2: tetragonal ZrO_2) or C/tZ/K] have been prepared using an incipient wetness impregnation method [49] by Tada et al. [31] (Scheme 6.1). Because of the insertion of the ZrO_2 (43–47%) into the pores of KIT-6 (acts like a spacer) decreased the specific surface area of KIT-6 from 987 to 298–435 $m^2\ g^{-1}$, on the other hand, Cu loading was in between 9 and 16%. Particularly, C/Z/K(400) and C/aZ had excellent selectivity for CO_2-to-methanol reduction reaction due to the formation of well-dispersed Cu NPs (<10 nm) or Cu active sites on the catalyst due to the amorphous nature of a-ZrO_2 was thought to affect the nanoparticle formation of the Cu species. Deposition of large amount of Cu species (40–50 nm) on KIT-6 shows less reactivity of C/Z/K(800) and C/Z/K(600) at this high temperature.

Previous reports show that Cu+ species which is well known to be an active species in CO_2-to-methanol hydrogenation was possibly stabilized due to the presence of SiO_2 in Cu/ZrO_2/SiO_2 catalysts [50–52]. CO_2 hydrogenation/reduction reaction takes place in steps; at first, CO_2-to-methanol hydrogenation occurs which

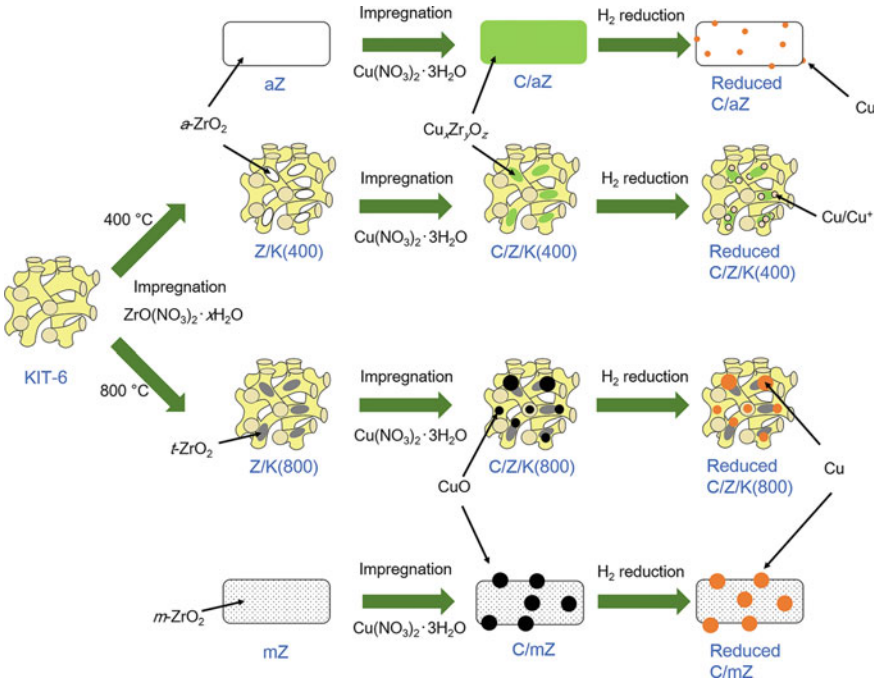

Scheme 6.1 Schematic image of the catalyst preparation of C/aZ, C/Z/K(400), C/Z/K(800), and C/mZ

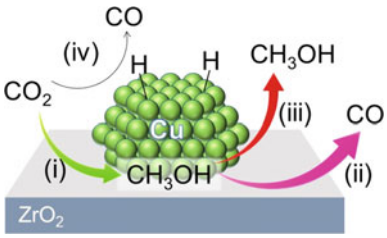

Scheme 6.2 Proposed mechanism of CO_2-to-methanol hydrogenation of Cu nanoparticles on ZrO_2; (i) CO_2 is hydrogenated to methanol at the interface between Cu and ZrO_2; (ii) When methanol strongly adsorbs on the ZrO_2 surface, methanol is decomposed to CO; (iii) When methanol weakly adsorbs on the ZrO_2 surface, methanol easily desorbs from the surface, resulting in the suppression of methanol decomposition; and (iv) CO_2 is converted to CO via RWGS reaction on the metallic Cu surface

is followed by subsequent methanol decomposition over ZrO_2-supported Cu catalysts (Scheme 6.2). Weak adsorption of methanol molecules occurs on the aZ surface inhibiting undesirable decomposition of methanol compared to the mZ surface leading to high methanol selectivity.

Recently, Rungtaweevoranit et al. reported 100% selectivity for methanol by using Cu ⊂ UiO-66 (Cu nanocrystals within the UiO-66 MOF) which was acquired from pre-synthesized Cu NCs (18 nm) capped with polyvinylpyrrolidone (PVP) which were immersed in a solution of Zr-based MOF, $Zr_6O_4(OH)_4(BDC)_6$ (BDC = 1,4-benzenedicarboxylate), (UiO-66) precursors [19]. In this way, Cu NCs were encapsulated inside the framework. This catalyst was compared with the other catalyst (Cu on UiO-66) which was obtained from mixing Cu NCs and pre-synthesized MOF (UiO-66) in a colloidal solution. wt% of copper still is higher in the second catalyst, but methanol selectivity is greater for Cu ⊂ UiO-66 at 175 °C. This is attributed to the more number of high interfacial contact points or strong interactions between nanosized Zr oxide SBUs (work like ZrO_2 or even better than any Cu catalyst) and Cu NCs, creating active Cu sites (Figs. 6.1 and 6.2) for CO_2 hydrogenation to methanol [53].

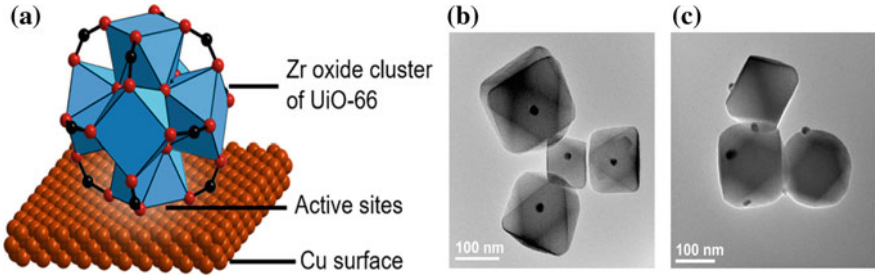

Fig. 6.1 Crystal structure and TEM images of Cu NC-UiO-66. **a** Illustration of active site of Cu NC-UiO-66 catalyst. One Zr oxide SBU $[Zr_6O_4(OH)_4(-CO_2)_{12}]$ is used as a representative of ordered array of SBUs. Atom labeling scheme: Cu, brown; C, black; O, red; Zr, blue polyhedra. H atoms are omitted for clarity, **b** Cu ⊂ UiO-66 (single Cu NC inside UiO-66), **c** Cu on UiO-66

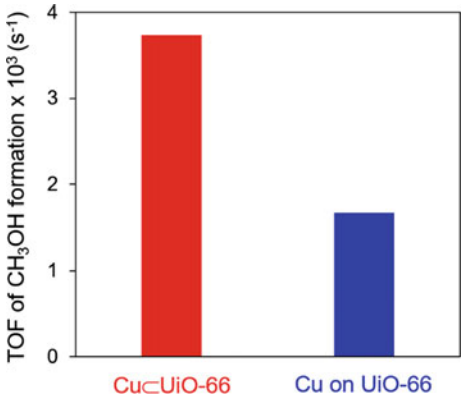

Fig. 6.2 Initial turnover frequencies (TOFs) of methanol formation over Cu ⊂ UiO-66 and Cu on UiO-66. The reaction rates were measured after 1 h. Reaction conditions: 7 sccm (Standard Cubic Centimeters per Minute) of CO_2, 21 sccm of H_2, 10 bar, and 175 °C

Most recently, Lin et al. used thermally stable UiO-bpy MOF consisting $Zr_6(\mu_3\text{-}O)_4(\mu_3\text{-}OH)_4$ secondary building units (SBUs) to anchor Cu and ZnO_x NPs which act as a catalyst [20]. This was done through post-synthetic modification by inserting Cu^{2+} ions followed by introduction of Zn^{2+} ions. Cu/ZnO_x NPs smaller than 1 nm were synthesized in situ at 250 °C in the presence of H_2 as a reducing agent (Scheme 6.3) to have Cu/ZnO_x@MOF with high activity and selectivity. Formation of ultrasmall NPs has been characterized by temperature-programmed

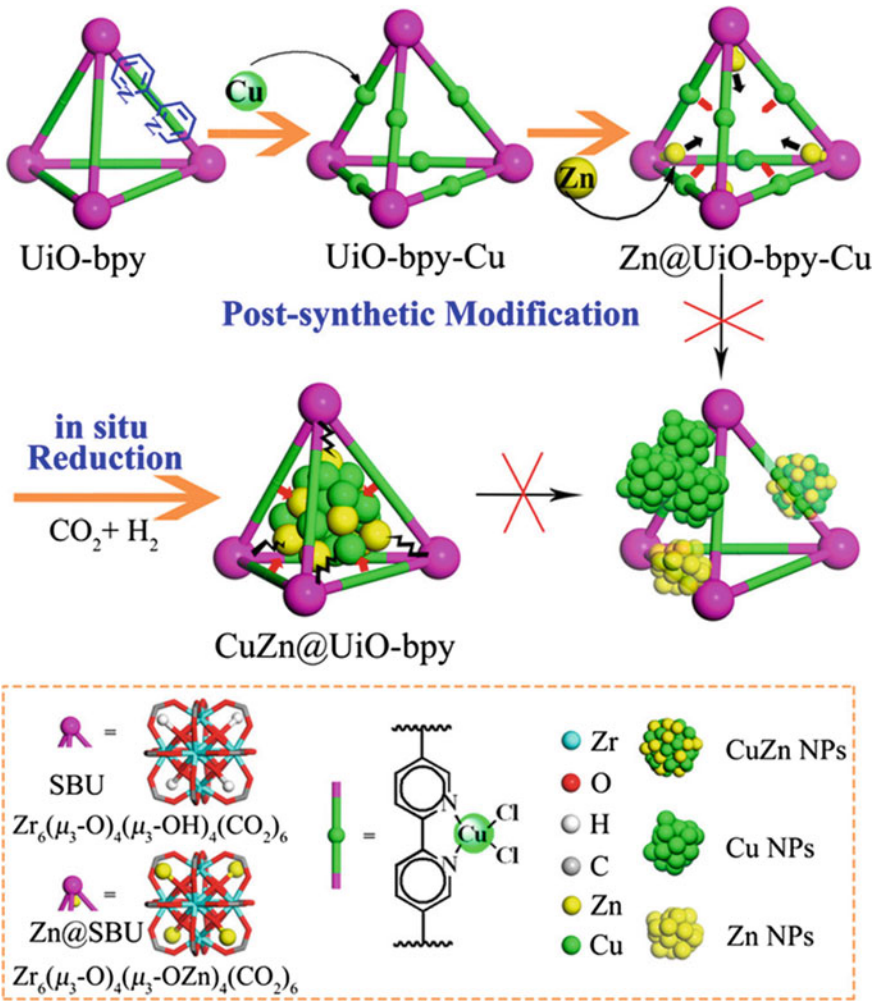

Scheme 6.3 Preparation of CuZn@UiO-bpy via in situ reduction of post-synthetically metalated UiO-bpy (Cu^{2+} ions were coordinated to the bpy groups, while Zn^{2+} ions were attached to the SBUs)

reduction (TPR) with hydrogen (H_2-TPR), X-ray photoelectron spectroscopy (XPS), Di use reflectance UV−vis−NIR spectroscopy. There is no phase separation between Cu and Zn NPs, and they are very well mixed examined by energy-dispersive X-ray spectroscopy (EDX) as well as from scanning transmission electron microscopy-high angle annular dark-field (STEM-HAADF) images. Cu/ZnO_x@MOF showed 100% methanol selectivity at 200–250 °C temperature with a gas hourly space velocity (GHSV) 18,000 h^{-1}. In this case, no RWGS reaction takes place because there is no phase separation between Cu and ZnO NPs or catalytic activity of Cu/ZnO_x is maintained. MOF was highly intact after the catalytic reaction as shown by PXRD, TEM, SEM, and EDX mapping data there exists homogeneous distribution of Cu and Zn NPs within the MOF. It was stable for CO_2 hydrogenation reaction for 100 h exhibiting 100% selectivity for methanol. Selectivity of the Cu@UiO-bpy without Zn NPs was 51.9% showing that Zn plays an important role in catalysis.

CO_2 hydrogenation to methanol was comparatively less selective with DSM-CuZn@UiO-bpy than CuZn@UiO-bpy due to large size of Cu/ZnO_x NPs which were synthesized by ex situ double solvent method (DSM) leading to less efficient mixing between both the NPs. Mostly, Zn(0) species is more pronounced in XPS spectra of CuZn@UiO-bpy than reported in the literature [54] which is due to the efficient mixing or alloying of Zn into metallic Cu [55, 56]. Finally, it can be said that this catalyst is an excellent candidate for CO_2 hydrogenation reaction where adsorption and activation of H_2 and CO_2 occur via interface sites of Cu, ZnO_x, and Zr_6 SBUs which are efficiently mixed (Fig. 6.3).

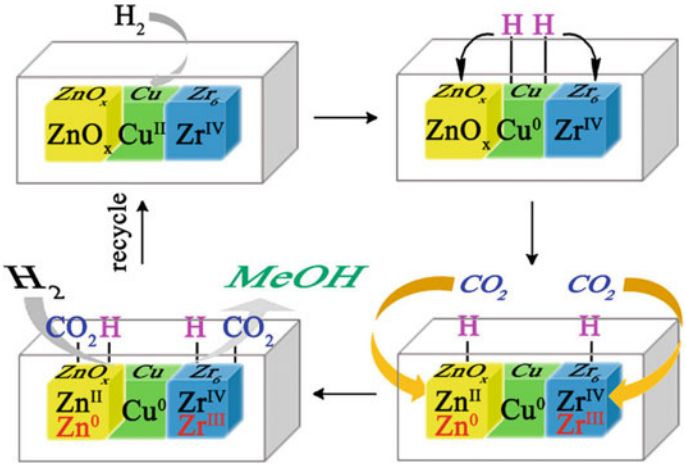

Fig. 6.3 Schematic showing the encapsulated active sites in MOFs and the functions of the various surface sites in catalytic CO_2 hydrogenation

6.7 Conclusions and Future Scope

In summary, it can be concluded that heterogeneous catalysts are the best solution for CO_2 reduction reaction to methanol due to simple and cheap method as well as easy recollection of the catalyst than homogeneous catalysts separation is very difficult. Excellent heterogeneous catalyst for CO_2 hydrogenation to methanol involves ultrasmall nanoparticles (NPs) of Cu or Cu/ZnO_x which are encapsulated within the Zr-based metal–organic frameworks (MOFs) through strong metal-support interactions which are created by the moieties of the MOF like bipyridine (bpy) and secondary building units (SBUs) those stabilize Cu NPs or preventing its agglomeration and phase separation between Cu and ZnO_x at reasonable 175–250 °C temperature conditions. This temperature is very much suitable for the Cu/ZnO_x catalyst which makes the catalyst highly stable for catalytic hydrogenation reaction. In this case, no sintering of the catalyst occurs that shows its intact nature. As well as reverse water gas shift reaction does not take place due to no phase separation between Cu and ZnO NPs or catalytic activity of Cu/ZnO_x is maintained throughout the CO_2 reduction reactions.

For future perspective view, metal–organic frameworks can be suitably designed from their interior according to the requirement for specific purpose. These structures other than Zr moiety should be designed with their chemical selectivity, stability, and tunability. Because there is a good scope to synthesize higher yield of methanol with high selectivity because of the catalytic stability throughout the reactions.

References

1. Gupta M, Coyle I, Thambimuthu K (2003) CO_2 capture technologies and opportunities in Canada. In: First Canadian CC&S technology roadmap workshop
2. Tans P (2009) Trends in carbon dioxide. NOAA/ESRL; http://www.esrl.noaa.gov/gmd/ccgg/trends/S
3. Porosoff MD, Yan BH, Chen JG (2016) Catalytic reduction of CO_2 by H_2 for synthesis of CO, methanol and hydrocarbons: challenges and opportunities. Energy Environ Sci 9:62–73
4. Olah GA (2005) Beyond oil and gas: the methanol economy. Angew Chem Int Ed 44:2636–2639
5. Ali KA, Abdullah AZ, Mohamed AR (2015) Recent development in catalytic technologies for methanol synthesis from renewable sources: a critical review. Renew Sustain Energy Rev 44:505–518
6. Ganesh I (2014) Conversion of carbon dioxide into methanol—a potential liquid fuel: fundamental challenges and opportunities (a review). Renew Sustain Energy Rev 31:221–257
7. Jadhav SG, Vaidya PD, Bhanage BM, Joshi JB (2014) Catalytic carbon dioxide hydrogenation to methanol: a review of recent studies. Chem Eng Res Des 92:2557–2567
8. Goeppert A, Czaun M, Jones J-P, Surya Prakash GK, Olah GA (2014) Recycling of carbon dioxide to methanol and derived products—closing the loop. Chem Soc Rev 43:7995–8048
9. Martino G, Courty P, Marcilly C, Kochloefl K, Lunsford JH (1997) Handbook of heterogeneous catalysis. Wiley-VCH, Weinheim, pp 1801–1818

10. Huff CA, Sanford MS (2011) Cascade catalysis for the homogeneous hydrogenation of CO_2 to methanol. J Am Chem Soc 133:18122–18125
11. Wesselbaum S, vom Stein T, Klankermeyer J, Leitner W (2012) Hydrogenation of carbon dioxide to methanol by using a homogeneous ruthenium-phosphine catalyst. Angew Chem Int Ed 51:7499–7502
12. Wesselbaum S, Moha V, Meuresch M, Brosinski S, Thenert KM, Kothe J, Stein T, Englert U, Hölscher M, Klankermayer J, Leitner W (2015) Hydrogenation of carbon dioxide to methanol using a homogeneous ruthenium–Triphos catalyst: from mechanistic investigations to multiphase catalysis. Chem Sci 6:693–704
13. Macdowell N, Florin N, Buchard A, Hallett J, Galindo A, Jackson G, Adjiman CS, Williams CK, Shah N, Fennell P (2010) An overview of CO_2 capture technologies. Energy Environ Sci 3:1645–1669
14. Rezayee NM, Huff CA, Sanford MS (2015) Tandem amine and ruthenium-catalyzed hydrogenation of CO_2 to methanol. J Am Chem Soc 137:1028–1031
15. Kothandaraman J, Goeppert A, Czaun M, Olah GA, Prakash GK (2016) Conversion of CO_2 from air into methanol using a polyamine and a homogeneous ruthenium catalyst. J Am Chem Soc 138:778–781
16. Sordakis K, Tsurusaki A, Iguchi M, Kawanami H, Himeda Y, Laurenczy G (2016) Carbon dioxide to methanol: the aqueous catalytic way at room temperature. Chem Eur J 22:15605–15608
17. Schneidewind J, Adam R, Baumann W, Jackstell R, Beller M (2017) Low-temperature hydrogenation of carbon dioxide to methanol with a homogeneous cobalt catalyst. Angew Chem 129:1916–1919
18. Li C-S, Melaet G, Ralston WT, An K, Brooks C, Ye Y, Liu Y-S, Zhu J, Guo J, Alayoglu S, Somorjai GA (2015) High-performance hybrid oxide catalyst of manganese and cobalt for low-pressure methanol synthesis. Nat Commun 6:6538–6342
19. Rungtaweevoranit B, Baek J, Araujo JR, Archanjo BS, Choi KM, Yaghi OM, Somorjai GA (2016) Copper nanocrystals encapsulated in Zr-based metal-organic frameworks for highly selective CO_2 hydrogenation to methanol. Nano Lett 16:7645–7649
20. An B, Zhang J, Cheng K, Ji P, Wang C, Lin W (2017) Confinement of ultrasmall Cu/ZnO_x nanoparticles in metal-organic frameworks for selective methanol synthesis from catalytic hydrogenation of CO_2. J Am Chem Soc 139:3834–3840
21. Zhou H-C, Long JR, Yaghi OM (2012) Introduction to metal-organic frameworks. Chem Rev 112(2):673–674
22. Zhou HC, Kitagawa S (2014) Metal-organic frameworks (MOFs). Chem Soc Rev 43:5415–5418
23. Li B, Chrzanowski M, Zhang Y, Ma S (2016) Applications of metal-organic frameworks featuring multi-functional sites. Coord Chem Rev 307:106–129
24. Seoane B, Castellanos S, Dikhtiarenko A, Kapteijn F, Gascon J (2016) Multi-scale crystal engineering of metal organic frameworks. Coord Chem Rev 307:147–187
25. Yuan S, Feng L, Wang K, Pang J, Bosch M, Lollar C, Sun Y, Qin J, Yang X, Zhang P, Wang Q, Zou L, Zhang Y, Zhang L, Fang Y, Li J, Zhou HC (2018) Stable metal–organic frameworks: design, synthesis, and applications. Adv Mater
26. Palomino RM, Ramírez PJ, Liu Z, Hamlyn R, Waluyo I, Mahapatra M, Orozco I, Hunt A, Simonovis JP, Senanayake SD, Rodriguez JA (2018) Hydrogenation of CO_2 on ZnO/Cu(100) and ZnO/Cu(111) catalysts: role of copper structure and metal-oxide interface in methanol synthesis. J Phys Chem B 122:794–800
27. Lunkenbein T, Schumann J, Behrens M, Schlögl R, Willinger MG (2015) Formation of a ZnO overlayer in industrial $Cu/ZnO/Al_2O_3$ catalysts induced by strong metal–support interactions. Angew Chem Int Ed 54:4544–4548
28. Schumann J, Eichelbaum M, Lunkenbein T, Thomas N, Álvárez-Galvan MC, Schlögl R, Behrens M (2015) Promoting strong metal support interaction: doping ZnO for enhanced activity of Cu/ ZnO: M (M = Al, Ga, Mg) catalysts. ACS Catal 5:3260–3270

29. Kandemir T, Kasatkin I, Girgsdies F, Zander S, Kühl S, Tovar M, Schlögl R, Behrens M (2014) Microstructural and defect analysis of metal nanoparticles in functional catalysts by diffraction and electron microscopy: the Cu/ZnO catalyst for methanol synthesis. Top Catal 57:188–206
30. Kattel S, Ramírez PJ, Chen JG, Rodriguez JA, Liu P (2017) Active sites for CO_2 hydrogenation to methanol on Cu/ZnO catalysts. Science 355:1296–1299
31. Tada S, Katagiri A, Kiyota K, Honma T, Kamei H, Nariyuki A, Uchida S, Satokawa S (2018) Cu species incorporated into amorphous ZrO_2 with high activity and selectivity in CO_2-to-methanol hydrogenation. J Phys Chem C 122:5430–5442
32. Olah GA, Goeppert A, Prakash GKS (2006) Beyond oil and gas: the methanol economy. Wiley-VCH, Weinheim
33. Olah GA, Geoppert A, Prakash GKS (2009) Chemical recycling of carbon dioxide to methanol and dimethylether: from greenhouse gas to renewable, environmentally carbon neutral fuels and synthetic hydrocarbons. J Org Chem 74(2):487–498
34. Olah GA (2005) Beyond oil and gas: the methanol economy. Angew Chem Int Ed 44:2636–2639
35. Olah GA, Toeroek B, Joschek JP, Bucsi I, Esteves PM, Rasul G, Prakash GKS (2002) Efficient chemoselective carboxylation of aromatics to arylcarboxylic acids with a superelectrophilically activated carbon dioxide–Al_2Cl_6/Al system. J Am Chem Soc 124:11379–11391
36. Centi G, Perathoner S (2011) CO_2-based energy vectors for the storage of solar energy. Greenhouse Gases Sci Technol 1:21–35
37. Bockris JOM (2008) Hydrogen no longer a high cost solution to global warming: new ideas. Int J Hydrogen Energy 33:2129–2131
38. Nowotny J, Sheppard LR (2007) Solar-hydrogen. Int J Hydrogen Energy 32:2607–2608
39. Bromberg L, Cohn DR (2009) Alcohol fueled heavy duty vehicles using clean, high efficiency engines. PSFC/JA-09-31. MIT, Cambridge
40. Bromberg L, Cohn DR (2010) Heavy duty vehicles using clean, high efficiency alcohol engines, PSFC/JA-10-43. MIT, Cambridge
41. Saito M, Fujitani T, Takeuchi M, Watanabe T (1996) Development of copper/zinc oxide-based multicomponent catalysts for methanol synthesis from carbon dioxide and hydrogen. Appl Catal A 138:311–318
42. Iliuta I, Iliuta MC, Larachi F (2011) Sorption-enhanced dimethyl ether synthesis—multiscale reactor modeling. Chem Eng Sci 66:2241–2251
43. Zachopoulos A, Heracleous E (2017) Overcoming the equilibrium barriers of CO_2 hydrogenation to methanol via water sorption: a thermodynamic analysis. J CO_2 Utilization 21:360–367
44. Stangeland K, Li H, Yu Z (2018) Thermodynamic analysis of chemical and phase equilibria in CO_2 hydrogenation to methanol, dimethyl ether, and higher alcohols. Ind Eng Chem Res 57:4081–4094
45. Centi G, Perathoner S (2009) Opportunities and prospects in the chemical recycling of carbon dioxide to fuels. Catal Today 148:191–205
46. Pan X, Fan Z, Chen W, Ding Y, Luo H, Bao X (2007) Enhanced ethanol production inside carbon-nanotube reactors containing catalytic particles. Nat Mater 6(7):507–511
47. Centi G, Perathoner S (2009) The role of nanostructure in improving the performance of electrodes for energy storage and conversion. Eur J Inorg Chem 2009(26):3851–3878
48. Wu JG, Saito M, Takeuchi M, Watanabe T (2001) The stability of Cu/ZnO-based catalysts in methanol synthesis from a CO_2-rich feed and from a CO-rich feed. Appl Catal A 218:235–240
49. Shimoda N, Nakayama K, Kiyota K, Satokawa S (2017) Synthesis of tetragonal zirconia in mesoporous silica and its catalytic property for methanol oxidative decomposition. RSC Adv 7:55819–55829

50. Arena F, Italiano G, Barbera K, Bordiga S, Bonura G, Spadaro L, Frusteri F (2008) Solid-state interactions, adsorption sites and functionality of Cu-ZnO/ZrO_2 catalysts in the CO_2 hydrogenation to CH_3OH. Appl Catal A 350:16–23
51. Samson K, Śliwa M, Socha RP, Góra-Marek K, Mucha D, Rutkowska-Zbik D, Paul JF, Ruggiero-Mikołajczyk M, Grabowski R, Słoczyński J (2014) Influence of ZrO_2 structure and copper electronic state on activity of Cu/ZrO_2 catalysts in methanol synthesis from CO_2. ACS Catal 4:3730–3741
52. Toyir J, de la Piscina PR, Fierro JLG, Homs N (2001) Catalytic performance for CO_2 conversion to methanol of gallium-promoted copper-based catalysts: influence of metallic precursors. Appl Catal B 34:255–266
53. Joo SH, Park JY, Tsung C-K, Yamada Y, Yang P, Somorjai GA (2009) Thermally stable Pt/mesoporous silica core-shell nanocatalysts for high-temperature reactions. Nat Mater 8:126–131
54. Liao F, Huang Y, Ge J, Zheng W, Tedsree K, Collier P, Hong X, Tsang SC (2011) Morphology-dependent interactions of ZnO with Cu nanoparticles at the materials' interface in selective hydrogenation of CO_2 to CH_3OH*. Angew Chem Int Ed 50:2162–2165
55. Ullah Awan S, Hasanain K, Bertino MF, Hassnain Jaffari G (2012) Ferromagnetism in Li doped ZnO nanoparticles: the role of interstitial Li. J Appl Phys 112:103924–103932
56. Schott V, Oberhofer H, Birkner A, Xu M, Wang Y, Muhler M, Reuter K, Wöll C (2013) Chemical activity of thin oxide layers: strong interactions with the support yield a new thin-film phase of ZnO. Angew Chem Int Ed 52:11925–11929

Chapter 7
Oxidative Dehydrogenation of Ethane to Ethylene Over Metal Oxide Catalysts Using Carbon Dioxide

P. Thirumala Bai, K. S. Rajmohan, P. S. Sai Prasad and S. Srinath

Abstract Ethylene is the most significant product that is being used in different sectors. The demand for ethylene is increasing year by year as it is the preferred raw material in the production of various industrially important products such as HDPE, LDPE, PVC, ethylene glycol, styrene, and ethylene dichloride. Carbon dioxide is a promising oxidant for the dehydrogenation of ethane. The global consumption of ethylene has increased to approx. 160 million ton per year with an annual growth rate of 4%. A significant amount of ethylene is produced by pyrolysis of various hydrocarbon stocks using steam, which is a highly energy-intensive process. Oxidative dehydrogenation of ethane using carbon dioxide is considered as one of the alternative methods for obtaining ethylene with higher yield. This chapter explores the effectiveness of metal oxide catalysts, with a particular interest in achieving higher selectivity to ethylene and better conversion of ethane and carbon dioxide. Various methods of preparation and physicochemical characterization techniques of catalysts were analyzed in detail. Performances of metal oxides and metal oxide-supported Cr_2O_3 catalysts were evaluated in a fixed-bed quartz reactor at 550–675 °C. Cr_2O_3 on metal oxide catalysts is suitable for oxidative dehydrogenation of ethane in the presence of CO_2. CO_2 which acts as a diluent for enhancing the equilibrium conversion of light alkanes and as an agent for the removal of coke formed on the catalyst thus acquires enormous importance.

Keywords Oxidative dehydrogenation · Ethane · Ethylene · Carbon dioxide Metal oxides

P. T. Bai · K. S. Rajmohan · S. Srinath (✉)
Department of Chemical Engineering, National Institute of Technology Warangal, Warangal, Telangana, India
e-mail: srinath@nitw.ac.in

P. S.S. Prasad
Indian Institute of Chemical Technology, Hyderabad, India

F. Winter et al. (eds.), *CO_2 Separation, Purification and Conversion to Chemicals and Fuels*, Energy, Environment, and Sustainability,
https://doi.org/10.1007/978-981-13-3296-8_7

7.1 Introduction

In the present decade, the mitigation of CO_2, one of the greenhouse gases responsible for the global and climatic change, is a widely discussed topic. In addition, the application of carbon dioxide for the production of various value-added chemicals is a viable option to reduce the effect of CO_2 emissions [1]. The use of carbon dioxide as a soft oxidant can also be considered as another option to reduce CO_2 emissions. Ethylene is the most preferred raw material in the production of various important products such as HDPE, LDPE, PVC, ethylene glycol, styrene, and ethylene dichloride [2]. The global consumption of ethylene has increased to approximately 160 million ton per year with an annual growth rate of 4%. Most of the industries in the world use steam cracking of hydrocarbon feedstock like natural gas and naphtha for commercial production of ethylene. Catalytic oxidative dehydrogenation (ODH) of ethane using carbon dioxide has emerged as a highly attractive alternative. In comparison to steam cracking route ODH of CO_2 to ethylene can be an important option, mainly due to the decrease in coke formation, less energy requirement and there is no equilibrium constraint on ethane conversion. The current statistics reveal that steam cracking is the source for producing more than 30% of ethylene from ethane. Thus, the ODH of ethane using redox catalysts is considered as an attractive choice when compared to the current steam cracking processes. ODH can be operated at a fairly low temperature (350–650 °C), resulting in reducing the energy input. Various catalysts including V and Mo oxides and their mixed oxides using the ammonium salts of V and Mo, Cr–V–O oxide, Cr–O are being employed for ODH of ethane using mild carbon dioxide. These are found to be active for this ODH reaction.

The present chapter discusses the different technologies utilizing the CO_2 as a promoter and soft oxidant for the production of ethylene. The aim of this chapter is to trace the emergence, application, and understanding of these systems, which clearly represent the importance of CO_2 as an activator [3]. Preparation and physicochemical characterization of metal oxide catalysts with different supports are discussed for ODH of ethane using CO_2 as a soft oxidant.

7.2 CO_2 Mitigation

Over the past decades, much attention has been paid to limiting the emissions of carbon dioxide into the atmosphere as it is a greenhouse gas and is recognized as a major culprit for global warming. The carbon dioxide concentration in the atmosphere is increasing rapidly since 1950 due to human activities. The carbon dioxide concentration in the earth's atmosphere is rising by about 2 parts per million by volume per year. Before the industrial revolution began, i.e., 1750, the carbon dioxide concentration was about 280 ppmv when compared to 358 ppmv by 1994. If the emission of CO_2 continued as per the rate observed in 1994, the concentration

of carbon dioxide will be doubled by the end of the twenty-first century. It was about 0.6 °C rise in the standard temperature in the twentieth century according to recent projections of the Climate Change Committee, the temperature could rise to 5.8 °C above the 1990 average by 2100. According to Climate Change Committee (IPCC), multi-model averages show that the temperature increases may range from 1.1 to 6.4 °C and sea level rise from 0.18 to 0.59 m. This could lead to the impact on the availability of freshwater, oceanic acidification, food production, flooding of coastal areas, and increased ailments associated with extreme weather events. Because of these huge detriments, most of the researchers have been working for the development of technologies which can reduce the production of major greenhouse gas (CO_2) and the CO_2 in the atmosphere can be reduced by CO_2 fixation, i.e., CO_2 separation and recovery, utilization, dissolution, and disposal.

The effect of CO_2 mitigation on global warming can be seen in Fig. 7.1. The reduction in temperature around 6 °C can be observed with the mitigation of CO_2 in near future, which indicates the importance of mitigation with respect to global warming. Several technologies are available for improving the energy efficiency, energy conversion, and exploitation of CO_2. The carbon dioxide recovered can be utilized to manufacture chemicals, fuels, and other products.

There are several advantages of utilizing CO_2 in the manufacture of fuels and chemicals.

(1) Carbon dioxide is an inexpensive, nonhazardous feedstock which can replace toxic chemicals like phosgene or isocyanides.
(2) Carbon dioxide is a renewable feedstock when compared to oil or coal.
(3) Carbon dioxide can be used to produce chemicals, new materials like polymers.
(4) Utilization of carbon dioxide can lead to new routes for existing chemical intermediates and products which could be more efficient and economical than existing methods.
(5) Manufacture of chemicals from carbon dioxide could have a small but significant positive impact on the global carbon balance.

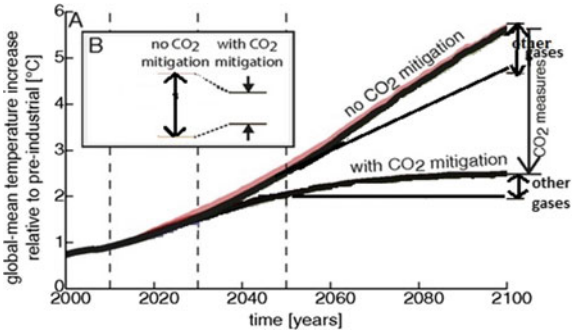

Fig. 7.1 Effect of CO_2 mitigation on global temperature [39]

7.2.1 Carbon Dioxide as a Soft Oxidant in Catalysis

Consumption of CO_2 depends on the utilization of high energy starting materials, or low-energy synthetic targets or a shift of the equilibrium by removal of the products [4]. Though considerably advanced technologies are available in the field of CO_2, there are still inherent drawbacks, like the hydrogen economy, more energy consumption. In view of the above constraints, alternative technologies are required for utilization of CO_2. Hence, presently carbon dioxide-assisted oxidative dehydrogenation of alkenes has been paid more attention because of the technical and environmental benefits [1]. Carbon dioxide can be used as a promoter and mild oxidant in catalytic conversions [3]. The reactivity series of the various gases in the gasification of coke are arranged to be $O_2 > H_2O > CO_2 > H_2$, which indicates that the CO_2 is less reactive when compared to the molecules of water and oxygen but shows high oxidizing ability. The highest heat capacity of CO_2 when compared to typical gases reduces the hot spot phenomenon. Carbon dioxide acts as a diluent in oxidative dehydrogenation reaction and also serves as an oxidant, which shows the numerous valuable properties when compared with oxygen and other oxidants.

CO_2 plays a major role as a mild oxidant in alkanes to olefins through the catalytic activation of CO_2 which lead to the formation of oxygen and carbon monoxide components. Carbon dioxide accelerates the rate of reaction by altering the dehydrogenation mechanism in an oxidative approach to enhance the selectivity. CO_2 also modifies the chemical equilibrium in oxidative dehydrogenation by removal of hydrogen in combination with a reverse water gas shift reaction forming CO and H_2O:

$$H_2 + CO_2 \rightarrow CO + H_2O \tag{1}$$

Removal of hydrogen can surmount the equilibrium and enhance the catalytic activity. The carbon dioxide restrains undesirable products of total oxidation owing to its poor oxidizing ability and improves the selectivity by modifying the non-selective sites of the catalysts [3].

7.3 Conventional Ethylene Production Processes

Depending upon the operating temperature, the technologies for ethylene production are broadly classified into two categories.

(i) **High-temperature process**: steam and thermal cracking.
(ii) **Low-temperature process**: oxidative dehydrogenation of ethane (ODHE).

7.3.1 Thermal Cracking

Thermal cracking processes operate at 370–400 °C and a pressure range of 6–12 atmospheres Burton process [5]. Presently, moderate temperatures (450–750 °C) [6] and high pressure (70 atm) are applied to crack the hydrocarbon molecules. To obtain high-degree conversions, it is required to operate thermal dehydrogenation process at high temperatures due to endothermic nature of the process. To attain the cracking temperature, the feed oil is sent through the heating tubes of the cracking furnace [6]. As a result, high costs are required to maintain the high reaction temperatures [7]. Thermal cracking proceeds in two ways; in one of them, cracking occurs in the heating tubes of the cracking furnace and partly in the pipelines which lead to the process steps following cracking. In this cracking procedure, the delay is relatively short in the order of one minute. The pressure in the furnace varies greatly along the length of the furnace.

In the other method, first, the hydrocarbon feed is heated to a desired reaction temperature in cracking furnace, while the main cracking reaction occurs in the reaction zone, in which the time delay is very high when compared to the previous method, i.e., in the order of 10–30 min. The reaction zone falls in an upright, cylindrical pressure vessel, at one end of which the oil feed heated in the cracking furnace is introduced, while the extraction of the mixture takes place at the other end. For distillation, the mixture passes through several refining steps. The flow direction in the reaction zone is either downward from above or upward from below.

7.3.1.1 Disadvantages in Thermal Cracking

- The reaction is highly endothermic (143 kJ/mol).
- High pressure (around 70 atm).

This method leads to high amounts of solid, undesirable coke.

7.3.2 Steam Cracking

The large amount of commercial ethylene production is based on pyrolysis generally called as steam cracking. Steam cracking leads to break down of saturated hydrocarbons into smaller/unsaturated hydrocarbons. For lighter alkenes (ethylene and propylene), it is the major industrial method for production. Hydrocarbon feed stream is heated to cracking temperature, i.e., 500–680 °C, with flue gas which is mixed with steam in the convection section. Further feed steam is heated under

controlled residence time to cracking temperature 750–875 °C for 0.1–0.5 s in a fired tubular reactor, where hydrocarbons in the feedstock are cracked into smaller molecules during this short reaction time. It requires high energy for the conversion of saturated hydrocarbons to olefins in the radiant tube which is highly endothermic in nature. The products of the reaction leaving at 800–850 °C from the radiant tube are cooled to 550–650 °C within very short time, i.e., 0.02–0.1 s to prevent degradation by secondary reactions. Further the cracked gas can be cooled by vaporization of high-pressure boiler feed water.

7.3.2.1 Disadvantages of Steam Cracking

The following challenges are associated with steam reforming.

a. The dehydrogenation reaction is highly endothermic;
b. Very short residence time;
c. Coking;
d. Decrease catalyst activity;
e. Reduction in product yields;
f. High energy requirement and reduction in coil service life;
g. More the feedstock more are the undesired products.

7.4 Necessity for Alternative Methods

The conventional processes have several disadvantages. One of the essential shortcomings is endothermic nature of the alkane dehydrogenation reaction. As per Le Chatlier's principle, high temperature is required for higher conversions. The temperatures for 50% conversion of alkane to corresponding alkenes are in the range of about 720 °C. High-temperature cracking processes may lead to the formation of undesirable products and high rates of deactivation of the catalyst by coking [8]. Finally, as the dehydrogenation is highly endothermic it is required to add heat to maintain the reaction, which adds considerably to the cost of the process.

Latest developments in oxidation technology are as follows:

(a) The use of new raw materials: alkanes and alkenes as raw materials;
(b) The development of new catalysts and processes: heterogeneous catalysts (i.e., silica-based, metal oxides).

7.4.1 Oxidative Dehydrogenation

Ethane oxidative dehydrogenation has the following advantages.

(1) Eliminates thermodynamic limitations in the ethane conversion;
(2) It is an exothermic reaction and economically feasible;
(3) Relatively operates at low reaction temperatures (350–600 °C);
(4) Catalyst regeneration;
(5) It enables one to achieve total conversion at much lower temperatures.

7.5 Catalysts for Oxidative Dehydrogenation of Ethane

The catalytic system for ODH of ethane can be classified into three groups:

- Catalytic systems based on oxides and ions of group I A and II A metals dispersed on inactive supports (e.g., Li, Na/MgO or Li/metal chlorides);
- Rare earth metals oxides (La_2O_3, Sm_2O_3, CeO_2);
- Transition metal oxides, containing Mo, Cr, Ga, and V.

The catalytic performances of various systems in ODH of ethane are presented in Table 7.1. The metal catalysts from groups I A and II A are usually active at temperatures higher than 600 °C. They were found earlier as active for the reaction of oxidative coupling of methane, OCM [9]. The mechanism of ethane molecule activation on these catalysts is like that of methane activation. The activation

Table 7.1 Oxides of group I A and II A metals

Catalyst	Temp. [°C]	Conversion C_2H_6	Selectivity C_2H_4	Yield C_2H_4	References
Li–Mg	580	38	80	30.4	[11]
Li–Na–Mg–O	650	38	85	32.3	[11]
Li–Cl–Mg	620	75	77	58.0	[12]
BaF_2–LaOF	660	55	74	40.7	[13]
BaF_2/Sm_2O_3–LaF_3	680	42	84	35.3	[14]
$BaCl_2/Ho_2O_3$	640	57	68	38.8	[15]
Fe_2O_3–Al_2O_3–La_2O_3	550	87	96	83.5	[16]
La–Ba–Mn–Cu–O–F	680	38	49	18.6	[17]
a–Ba–Mn–Cu–O–Cl	680	63	63	39.7	[17]
$NiMoO_4$	560	11	65	7.2	[18]

consists of abstraction of a hydrogen atom from an ethane molecule by an anion radical O– generated on a catalyst surface on a Li^+–O– centre. The role of metal catalyst is initiating the gas-phase reaction.

The activity of the catalyst can be extensively enhanced by the addition of small amounts of chlorine or chlorine-containing compounds (e.g., tetrachloromethane or HCl), or halides directly added to the catalyst in the initial stage of preparation [10]. It is suggested that chlorine radicals are responsible for the decomposition of the ethyl radical to ethene. Among all these catalysts, the most successful one is the Cl–Li/MgO. The yield of ethane is found to be in the range of 30–40%, while the ethylene selectivity is of 70–80% at ∼40–60% conversions [11, 12].

The second group of catalysts for ODH of ethane comprises oxides of rare earth metals (La_2O_3, Sm_2O_3, CeO_2, and Pr6O11). The rare earth metal oxides are active and stable even at high temperature, i.e., 500–700 °C. The mechanism of these catalysts is similar to first group catalysts, i.e., group I A and II A metals. The good catalytic performances in ODH of ethane have been obtained with La_2O_3 and Sm_2O_3; however, the best system contained La_2O_3 in a mixture with Fe_2O_3 supported on a-Al_2O_3. The yields 40–80% with selectivity between 70 and 90% conversions were reported [13–18].

The third class of catalysts is based on oxides of transition metals, containing in particular Mo and V. They can activate ethane at temperatures usually 400–550 °C and operate most probably by a redox mechanism. Among them, Mo–V–O system promoted with Sb, Nb, active at relatively low temperatures ∼400 °C gives a yield of ∼50% with selectivity to ethane about ∼70% [19, 20]. Vanadium oxides dispersed on different supports, magnesium vanadates, or molybdates, which are active in ODH of higher alkanes, show relatively poor performance in the reaction of ethane (ethane yields usually below 10%) [12, 13].

7.5.1 Vanadium-Based Catalysts

Numerous research articles discussed the catalytic nature of vanadium-based catalysts on oxidative dehydrogenation of ethane and propane. Table 7.2 shows the brief summary of some significant vanadium-based catalysts used for ODH of ethane. Especially, this table presents the effect of temperature on conversion, selectivity, and yield of ethane and ethylene, respectively. Table 7.2 shows the effect of type of catalyst and their supports for conversion of ethane to ethylene. Maximum conversion and selectivity are obtained for mixed metal support, i.e., Mo–O–V–Nb–Sb–Ca when compared to single metal or other supports. However, there is a slight increase in selectivity when Ca is replaced with Mg for the above catalyst, but the conversion and yield are less [21].

In ethane oxidative dehydrogenation, the activity of vanadium oxide catalyst increases with the weight of V_2O_5, while rates per V atom reach a maximum on VO*x* domains of intermediate size, providing a balance between the activity of surface VO*x* species and their accessibility to reactants. The selectivity of ethylene

Table 7.2 Vanadium-based catalysts

Catalyst	Temp. [°C]	Conversion C_2H_6	Selectivity C_2H_4	Yield C_2H_4	References
Mo–O–V–Nb–Sb–Ca	400	73	71	51.8	[19]
Mo–O–V–Nb–Sb–Mg	400	67	74	49.6	[19]
Sn–V–Sb/Al_2O_3	500	24	44	10.6	[20]
V–Mg–O	560	21	22	4.6	[11]
V_2O_5/Al_2O_3	530	25	54	13.5	[12]
K–V_2O_5/Al_2O_3	530	6	39	2.3	[13]
V_2O_5/SiO_2	540	30	22	6.6	[13]

is maximum for intermediate values of active loading, which corresponds to the development of the monolayer structure. Vanadium oxide-supported catalyst activity data of ethane follows Mars-van Krevelen redox mechanism when compared to LHHW and Eley Riedal mechanism.

7.5.2 Molybdenum-Based Catalysts

The activity data for molybdenum-based catalysts for different supports are presented in Table 7.3. The table represents the effect of supports and temperature at different W/F ratios. The performance of molybdenum-based catalysts is less when compared to vanadium-based catalysts, regardless of the support used [22]. Alumina contributes to primary oxidation and dehydrogenation routes of ethane in alumina-supported catalysts for the formation of CO*x* and coke. The molybdenum has participated in ODH of ethane and further oxidation of ethylene to CO*x* [23]. The decrease in catalytic activity observed at higher loadings due to the growth of

Table 7.3 Molybdenum-based catalysts [21]

S. No.	T (°C)	W/F (g s ml^{-1})	Catalyst	References
1	400	1.80	Mo/V/Sb/O	[40]
2	510	0.04	V_2O_5–Al_2O_3	[41]
3	500	11.25	Mo/V/O	[42]
4	580	0.06	V_2O_5–Al_2O_3 mesop	[43]
5	700	0.10	V/Mg/O mesop	[44]
6	280	–	Mo/V/Nb/O	[45]
7	340	0.55	Mo/V/Te/O	[46]
8	580	0.06	V/Mo/O–Al_2O_3 mesop	[43]
9	580	0.06	V/Mo/O–Al_2O_3	[43]

Al_2MoO_4 crystallites. Conversion and selectivity increase with catalyst loading up to 15 wt% and then remain constant. The maximum performance of the catalyst can be obtained with greatly dispersed two-dimensional molybdenum fully encapsulated the alumina surface [21, 24].

Most of the research studies have dealt with light alkanes like C_2 to C_5 activation by ODH to olefins over different metal oxides like molybdates, antimonates, or vanadates, chromium, gallium heteropoly acids. So far, the performance of solid catalysts related to metals, metal oxides, or metal complexes immobilized in zeolites supported by silica and non-silica material or polymeric resins was carried for oxidative dehydrogenation of ethane [25].

7.5.3 Chromium-Based Catalysts

The activity data for chromium-based catalysts for different supports are presented in Table 7.4. Chromium-based catalysts supported by silica and non-silica materials are most suitable for oxidative dehydrogenation of ethane due to their high catalytic activity. The metal oxide- or silica-supported chromium catalysts showed excellent performance for the dehydrogenation of ethane with carbon dioxide as an oxidant. These catalysts were normally prepared by fully dispersing Cr species on supports with high surface areas [26]. The main supports include inorganic oxides like SiO_2, ZrO_2, Al_2O_3, TiO_2 and mesoporous materials like SBA-15, SBA-16, MSU-*x*, and MCM-41. The chromium loading and the properties, structures of different supports greatly influence the oxidation state, redox status, and dispersion of chromium species on the support.

7.6 Synthesis of Catalysts by Various Methods

7.6.1 Impregnation/Deposition

In this procedure, a required volume of solution with a known amount of the precursor of the active phase is contacted with a previously weighed solid support. The amount of metal ions that interactively remain bound to the surface of support rely on the adsorption capacity, period of impregnation and temperature of impregnation. The selection of wet impregnation or incipient wetness impregnation method depends on the volume of solution. Normally, wet impregnation method is used for the preparation of the catalyst in which an excess of solution is used. After a certain period of time, the solid is separated and the excess amount of solvent is removed by drying. In the other method, i.e., incipient wetness impregnation, the volume of solution is equal to or slightly less than the pore volume of the support further the amount of metal ions removed by drying.

Table 7.4 Chromium-based catalysts

S. No	Catalyst name	Temp (°C)/ Time	Conversion C_2H_6	Selectivity C_2H_4	Yield C_2H_4	Feed composition	References
1.	5Cr–10Ce/SBA–15	700/12 h	55.0	96.0	33.9	1:3	[37]
2.	Ce-based monolithic catalysts SBA–15/ Al_2O_3/FeCrAl	750/1130 h	63.9	87.2	55.7	1:4	[10]
3.	Na_2WO_4/Co(2)–Mn/SiO_2(Co loading)	750/10 h	60.3	90.7	54.7	1:5 (influence of the total flow rate)	[27]
4.	5% Cr/SiO_2	700	30.7	96.5	29.6	1:7	[6]
5.	Cr_2O_3/SiO_2	650	56:1	92.9	52.1	1:5	[47]
	5 wt% Cr_2O_3/Al_2O_3		19:2	96.5	18.5		
	5 wt% Cr_2O_3/ZrO_2		57:3	60.4	34.6		
6.	Cr_2O_3	650 (550–650)	22.5	87.0	19.6	1:5	[48]
	Cr_2O_3/SiO_2		56.1	92.9	52.1		
	Cr_2O_3/SO_4–SiO_2		67.2	81.8	55.0		
7.	9Fe–9Mn/Si–2	800/150 h	68.6	92.3		1:1	[49]
8.	Cr_2O_3/SBA–15	675/16 h	61.2	82.2	50.3	1:6	[50]

7.6.2 Hydrothermal Method

In this method, based on the type of catalyst, the precursor solution is mixed with an alkali (KOH) in a stainless steel autoclave reactor (Fig. 7.2) at the required temperature for a specific time. For a typical process, the temperature for autoclave is maintained at 70–200 °C for a period of 10–24 h depending on the process and the obtained solution air-cooled to ambient temperature. The resulting precipitate is collected by filtration, washed, and finally dried.

7.6.3 Precipitation

In the precipitation method, the metal salts are dissolved in water for a specific period of time and further the precipitation is carried out to maintain the pH by the slow addition of a required amount of precipitating agents like ammonium hydroxide or sodium carbonate at room temperature. The resultant precipitate is filtered after washing with distilled water and dried overnight at 100–120 °C. After precipitation/impregnation, the catalyst mass is normally subjected to the following treatments, namely drying and calcination.

7.6.4 Sol–Gel Method

In this method, primarily a stable colloidal solution consists of solid particles ranging 1 nm–1 micron is formed by hydrolysis and partial condensation of precursors like metal oxide or inorganic salt. Further, it produces a gel material by condensation of solution particles into a three-dimensional network. The resultant

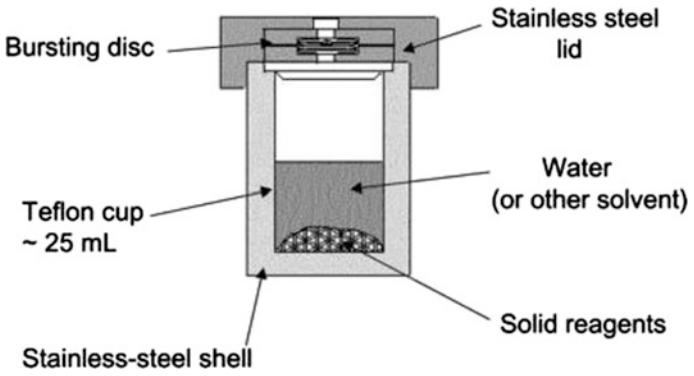

Fig. 7.2 Hydrothermal Teflon bottle schematic diagram

gel is a diphasic material in which the solvent encapsulated by solids. The removal of the encapsulated liquid from a gel can be done either by evaporative drying or with supercritical drying/extraction. When the gels are dried by evaporation, the solid products are known as xerogel; whereas the gels are dried by supercritical drying, the dried gel is called aerogel.

7.7 Preparation and Characterization of Metal Oxide-Supported Chromium (Cr_2O_3/Al_2O_3) Catalyst

7.7.1 Catalyst Preparation

Al_2O_3-supported Cr_2O_3 catalysts were prepared by adopting wet impregnation method using commercially available alumina. Four catalysts were prepared by varying the weight percentage (5–20%) of Cr_2O_3. The required weight of commercially available Cr $(NO_3)_3 \cdot 9H_2O$ was dissolved in minimum amount of water and further this solution was added to the Al_2O_3 support with constant stirring. Water was used to remove excess water, and the catalyst masses were dried in an air oven at 120 °C for 12 h. Finally, 5–20 wt% Cr_2O_3 supported alumina catalysts were obtained by calcination at 650 °C for 6 h [27].

7.7.2 BET Specific Surface Area

Table 7.5 shows the specific surface areas of the prepared catalysts. The specific surface area of Al_2O_3 was 205 m^2/g. It can be observed from the surface area values that there is a marginal decrease of surface area with increasing chromia loading up to 15 wt% which is due to clogging of alumina pores by chromia species [28]. Significant reduction in surface area is noticed in 20 wt% Cr_2O_3/Al_2O_3 catalyst due to the creation of crystalline Cr_2O_3 species. Similar kind of observation was made by Cherian et al. [29], and this observation was supported by XRD where crystalline Cr_2O_3 observed at higher loadings.

It has been reported that the molecular structure of Cr_2O_3 species mainly depends on the surface hydroxyl chemistry and support surface. The chemical

Table 7.5 BET specific surface areas of four different Cr wt% catalysts

S. No.	Catalyst	Surface area (m^2/g)
1	Al_2O_3	205
2	5 wt% Cr_2O_3/Al_2O_3	191
3	10 wt% Cr_2O_3/Al_2O_3	172
4	15 wt% Cr_2O_3/Al_2O_3	154
5	20 wt% Cr_2O_3/Al_2O_3	109

properties of a support also play a major role in the chromium dispersion and its anchoring capacity with the support [16]. Wang et al. [30] elucidated the dispersion and anchoring capacity of chromium species with different oxide supports such as SiO_2, ZrO_2, TiO_2, and Al_2O_3 by using point of zero charge (PZC). This study revealed that the support with the low PZC value (SiO_2 acidic hydroxyl groups) have poor anchoring capacity with chromium oxide, while the support with high PZC value (Al_2O_3 basic hydroxyl groups) shows high anchoring capacity, which leads to high dispersion of chromium oxide species. In the present case, the catalysts with lower loadings possessed Cr in its higher oxidation states as correlated with the previous results [16], where Cr^{3+} ions were oxidized to their higher oxidation states due to the removal of adsorbed water molecules on the support.

7.7.3 *X-Ray Diffraction Analysis of the Cr_2O_3/Al_2O_3 Catalysts*

Figure 7.3 shows the XRD patterns of Cr_2O_3/Al_2O_3 catalysts with different Cr_2O_3 loadings calcined at a heating rate of 650 °C/6 h. All the four catalysts exhibited two characteristic peaks at 2θ of 45.8° and 66.8° corresponding to γ-Al_2O_3 (JCPDS 29-0063), the intensity of the peaks decreased with increase in Cr_2O_3 loading, the reason could be due to the clogging of alumina by chromium species. One could notice from Fig. 7.3 that different types of chromium oxide species were formed on the alumina surface. The XRD results recommend that the chromium can be stabilized on alumina with different oxidation states ranging from +5 to +6 at lower loadings, and upon increasing the chromium content to above 10 wt%, chromium can be stabilized with its highly stable oxidation state +3 in addition to its higher

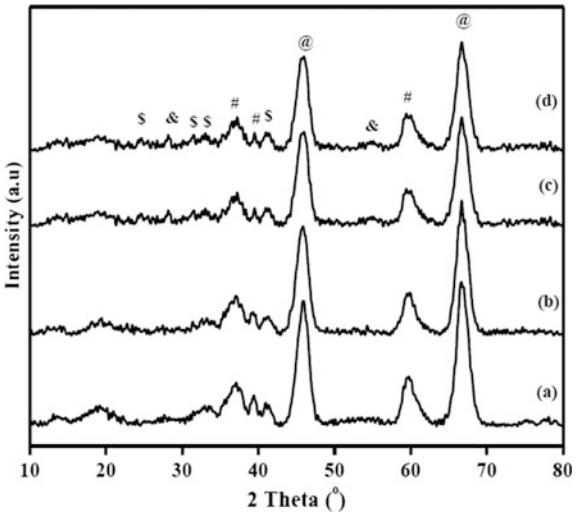

Fig. 7.3 XRD patterns of catalysts calcined at 650 °C/6 h **a** 5% Cr_2O_3/Al_2O_3, **b** 10% Cr_2O_3/Al_2O_3, **c** 15% Cr_2O_3/Al_2O_3, and **d** 20% Cr_2O_3/Al_2O_3; (@) Al_2O_3, (#) CrO_3, ($) Cr_2O_5, and (&) Cr_2O_3

oxidation stages [31]. This suggests that the phase and dispersion of chromium species mainly rely upon the surface area, nature of support, and chromium content.

7.7.4 Temperature-Programmed Reduction Profiles of the Catalysts

The temperature-programmed reduction profiles of chromium supported by Al_2O_3 catalysts with changing loadings (5–20 wt%) calcined at a heating rate of 650 °C/6 h are shown in Fig. 7.4. All four catalysts exhibit a single-stage reduction in the temperature range of 379–415 °C. The reduction may be due to the reduction of the chromium species Cr^{+6} to Cr^{+3} [32, 33] according to the following reaction:

$$2CrO_3 + 3H_2 \rightarrow Cr_2O_3 + 3H_2O \quad (2)$$

The reduction in temperature of 5 wt% Cr_2O_3 is centered at 415 °C. This temperature shifts toward lower side (379 °C) when the weight of Cr_2O_3 increased to 15 wt% and it remained constant above 15 wt% Cr_2O_3 loading, and these observations are similar to the earlier reports [32–34]. Oxygen is strongly bound to the support at lower loadings due to strong chromium-support interactions. For the reduction of chromium, it requires a higher temperature, whereas in higher loadings chromium-support interactions become weaker due to the accumulation of chromia. The consumption of hydrogen is high comparatively at lower temperatures to undergo reduction [33, 34]. In the present case, 5 wt% Cr_2O_3/Al_2O_3 catalyst showing high reduction temperature might be due to the formation of

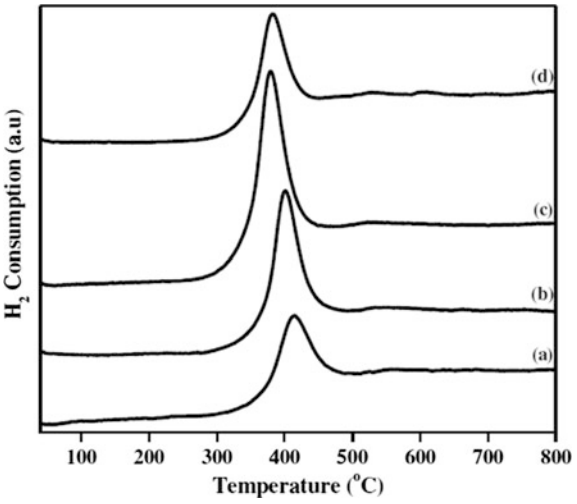

Fig. 7.4 TPR profiles of catalysts calcined at 650 °C/6 h **a** 5% Cr_2O_3/Al_2O_3, **b** 10% Cr_2O_3/Al_2O_3, **c** 15% Cr_2O_3/Al_2O_3, and **d** 20% Cr_2O_3/Al_2O_3

monochromate-like species, whereas low reduction temperature was observed in higher loadings due to the formation of polychromate-like species.

7.8 Catalytic Performance

The performance of catalysts was evaluated in a fixed-bed downflow reactor at atmospheric pressure. About 1 g weight (18/25) of the catalyst is used in each run. The catalyst was diluted with equal amount of quartz beads and was suspended between two quartz wool plugs at the middle of the reactor. Before starting the reaction, the catalyst was pre-treated with an inert gas [helium flow (30 ml/min)] at a temperature of 500 °C for 1 h. The reactants, oxidant along with inert gas, were fed through mass flow controllers to the reactor to maintain the volume ratio of 15/15/30 and reactor temperature maintained with a PID controller. On-line Nucon5765 GC equipped with TCD using Molecular sieve 5A and Porapak Q columns was used to analyze the effluent gas stream. No conversion of ethane was observed with quartz wool (in the absence of catalyst) in the studied temperature range of 550–650 °C.

7.8.1 Effect of Temperature

The effect of temperature on conversion and selectivity of catalysts with varying chromium loading was shown in Fig. 7.5. From the above figure, it can be seen that the ethane conversion increases with increase in temperature from 550 to 650 °C for all four catalysts. The conversion is maximum, i.e., 32.01% for 15% chromium catalyst when compared to the other three catalysts. The conversion of ethane

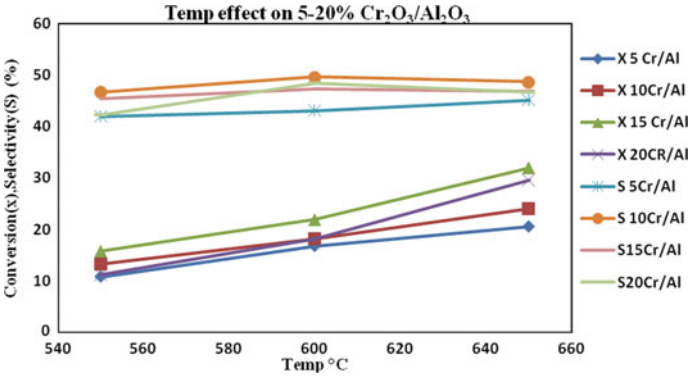

Fig. 7.5 Temperature versus conversion and selectivity of 5–20 wt% Cr_2O_3/Al_2O_3 in ODH of ethane with CO_2

Table 7.6 BET specific surface areas of the chromia catalysts and their catalytic functionality at 650 °C

Catalyst	Surface area of support (m^2/g)	Surface area of catalyst (m^2/g)	X-C_2H_6 (%)	X-CO_2 (%)	S-C_2H_4 (%)	S-CH_4 (%)
Cr_2O_3/Al_2O_3	205	154	32.0	21.3	46.2	53.8
Cr_2O_3/ZrO_2	57	33	42.2	37.4	36.0	64.0
Cr_2O_3/Al_2O_3–ZrO_2 (1:1)	138	97	36.0	29.1	56.2	43.8

X conversion; S selectivity

increases with increase in chromium weight percentage up to 15 and then drop in conversion observed for further increase in chromium loading, i.e., for 20% (Table 7.5).

7.8.2 *Effect of Metal Oxide Supports on Catalytic Activity*

The effect of adding metal oxide support, i.e., mixed oxides on chromium metal, was discussed elsewhere [35]. Addition of metal oxide support, i.e., ZrO_2, to the existing catalyst will increase the conversion and selectivity. Surface areas of the metal oxide support measured in Quanta Chrome Surface area analyzer are presented in Table 7.6. Al_2O_3 has the largest surface area when compared to ZrO_2 and mixed oxide supports. The performance of mixed oxide-supported chromium is high when compared to Al_2O_3 and ZrO_2 supports, and this may be due to the availability of more surface area, i.e., 97 m^2/g.

7.8.3 *X-Ray Diffraction Analysis of the Cr_2O_3/Al_2O_3–ZrO_2 Catalysts*

The XRD patterns of aluminum oxide, zirconium oxide, and mixed metal oxide-supported Cr_2O_3 catalysts are presented in Fig. 7.6. Al_2O_3-supported Cr_2O_3 exhibits two peaks at 2θ of 45.8° and 66.8° corresponding to γ-Al_2O_3. Chromia is stabilized on Al_2O_3 support with different oxidation states. ZrO_2-supported Cr_2O_3 shows both monoclinic and tetragonal and phases of ZrO_2. Crystalline phases of Cr_2O_3 could not be identified clearly due to the dominance of the ZrO_2 phases. The addition of Al_2O_3 to ZrO_2 delays this phase transformation as represented previously [36].

Al_2O_3 supported chromia catalyst exhibits a single-stage reduction of chromia by means of h peak at 379 °C in TPR profile as shown in Fig. 7.7. This may due to the transformation of Cr^{+6} to Cr^{+3} according to the following reaction:

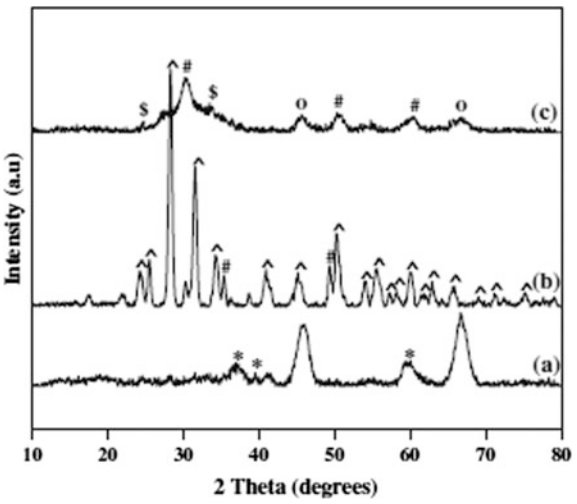

Fig. 7.6 XRD patterns of catalysts **a** Cr_2O_3/Al_2O_3, **b** Cr_2O_3/Zr_2O_3, **c** Cr_2O_3/Al_2O_3–Zr_2O_3 (1:1)

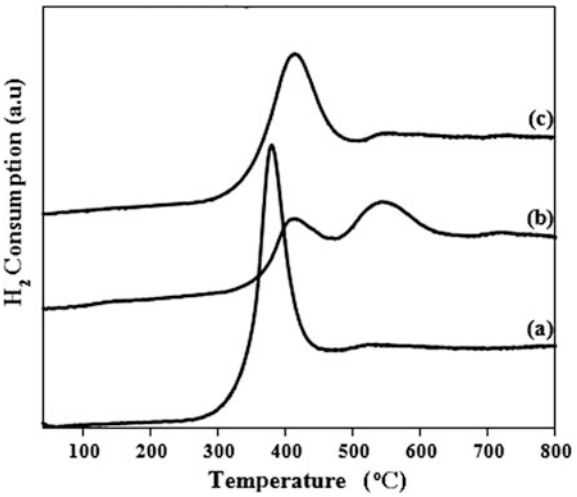

Fig. 7.7 TPR profiles of the catalysts **a** Cr_2O_3/Al_2O_3, **b** Cr_2O_3/ZrO_2, **c** Cr_2O_3/Al_2O_3–ZrO_2 (1:1)

$$2CrO_3 + 3H_2 \rightarrow Cr_2O_3 + 3H_2O \quad (3)$$

While for Cr_2O_3/ZrO_2, the reduction stages occur between 320–470 °C and 480–625°C. The two peaks correspond to the chromia reduction of Cr^{+6} to Cr^{+3} and Cr^{+3} to Cr^{+2}, respectively. The maximum peak in temperature might be due to the direct reduction of bulk chromia species to lower oxidation state; i.e., Cr^{+3} may be to Cr^{+2} [35].

7.8.4 Performance Evaluation Metal Oxide-Supported Chromia

The performance of catalysts for ODH of ethane with carbon dioxide is presented in the table. Single metal oxide support, i.e., Cr_2O_3/Al_2O_3, gives 32 and 21% conversion for ethane and CO_2, respectively, while the ethylene selectivity is 46%. The performance of Cr_2O_3/ZrO_2 catalyst is high for ethane conversion, i.e., 42%, but the selectivity of ethylene decreases to 36%. It reveals that the performance of Cr_2O_3 is high in the activation of CO_2 at large temperatures. But the mixed metal oxides, i.e., $Cr_2O_3/Al_2O_3–ZrO_2$, show higher conversion (36%) for ethane and CO_2 (29%) when compared to only Al_2O_3 and it is lower than Cr_2O_3/ZrO_2. The performance variation of metal oxide-supported chromia catalysts is due to the difference in redox property as explained by Wang et al. [35, 37]. Both Cr^{3+} and Cr^{2+} ions play a major role in the catalytic reaction as active sites [37]. The higher basicity of Al_2O_3 when compared to ZrO_2 could be the reason for the decrease in performance [35].

7.9 Effect of Oxidizing Agent

7.9.1 Oxidative Dehydrogenation Using O_2 as an Oxidant

Oxidative dehydrogenation of ethane using O_2 as oxidant over metal oxide-supported chromia catalyst produces ethylene and water. The reactions involved in this process are as follows:

$$C_2H_6 + 0.5O_2 \rightarrow C_2H_4 + CO + H_2O \quad (4)$$

$$C_2H_6 + 3.5O_2 \rightarrow 2CO_2 + 3H_2O \quad (5)$$

Formation of water removes the constraint on equilibrium conversion, but the formation of carbon oxides due to total or partial combustion of ethane is one of the challenges associated with this process. Thermal runaway can take place due to the exothermic nature of these reactions [6]. A highly selective catalyst is required to make ODH an attractive process with higher product selectivity and yield.

7.9.2 Oxidative Dehydrogenation Using CO_2 as an Oxidant

Currently, the use of CO_2 as a mild oxidizing agent in ODH process is found to be promising attractive in this perspective.

The reactions involved when CO_2 used as an oxidizing agent are as follows:

$$\text{Main reaction} \quad C_2H_6 + CO_2 \rightarrow C_2H_4 + CO + H_2O \tag{6}$$

$$\text{Side reactions} \quad C_2H_6 \rightarrow C_2H_4 + H_2 \tag{7}$$

$$C_2H_6 + 2CO_2 \rightarrow 4CO + 3H_2 \tag{8}$$

$$H_2 + CO_2 \rightarrow CO + H_2O \tag{9}$$

$$C_2H_6 + H_2 \rightarrow 2CH_4 \tag{10}$$

All the above reactions are endothermic in nature, but CO_2 ODH reaction is favorable due to thermodynamic constraints. Ethylene is produced by direct dehydrogenation reaction (7) and also by the oxidative dehydrogenation process (1). Reverse water gas shift (RWGS) reaction (9) aids in the dehydrogenation of alkane resulting in the formation of the alkene. Equations (8) and (10) represent the reforming and hydrocracking reactions, respectively. The lower oxidizing ability of CO_2 reduces the undesirable products of total oxidation [38] and selectivity may be improved.

7.9.3 *Performance of Cr_2O_3/Al_2O_3-ZrO_2 Catalyst in the Presence of Carbon Dioxide or Oxygen as the Oxidant*

Performance of Cr_2O_3/Al_2O_3–ZrO_2 catalyst was evaluated at various reaction temperatures in the presence of carbon dioxide as well as oxygen. The results obtained show that the conversion of reactant, i.e., ethane, increases with increase in temperature. The oxidizing agent has no effect on conversion with respect to temperature. The similar trend was observed for the selectivity of ethylene, while for the case of CO_2 as an oxidant, the ethylene selectivity increases with temperature up to 600 °C and almost remained constant with further increase in temperature. The ethane conversion is always higher with oxygen when compared to CO_2 in the entire gamut of temperature. But the ethylene selectivity is very low when the O_2 is oxidant. The secondary oxidation of ethylene may be the reason for the difference in ethylene selectivity. Oxygen has more oxidizing ability when compared to carbon dioxide. But the ethylene selectivity is more forcarbon dioxide when compared to Oxygendue to its mild oxidizing nature. Thesecondary oxidation of ethylene may be thereason for the difference in ethyleneselectivity, this can be explained by TPDE (Table 7.7).

7.9.4 *Temperature-Programmed Decomposition (TPD) of Ethylene*

Figure 7.7 shows temperature-programmed decomposition experiment profiles observed on mixed metal oxide catalyst. From Fig. 7.7, it can be seen that the product ethylene desorbed is higher with oxygen as the oxidant (161 μ mol/g) when compared to carbon dioxide (98 μ mol/g). From the results, it is observed that the amount of ethylene formed is more with oxygen, as ethylene stays for a longer time on the surface due to strong interaction, and ethylene is subjected to secondary oxidation, thus leading to the reduction in ethylene selectivity [35] (Fig. 7.8).

7.10 Challenges and Future Scope of ODE

There are many challenges to apply oxidative dehydrogenation process.

Table 7.7 Effect of oxidizing agent on catalytic activity for Cr_2O_3/Al_2O_3–ZrO_2 (1:1)

Catalyst	Temp (° C)	Presence of CO_2		Presence of O_2	
		X-C_2H_6 (%)	S-C_2H_4 (%)	X-C_2H_6 (%)	S-C_2H_4 (%)
Cr_2O_3/Al_2O_3–ZrO_2 (1:1)	550	15.6	52.9	33.2	5.8
	600	22.7	57.2	40.7	9.9
	650	36.0	56.2	50.3	18.2

X conversion; S selectivity

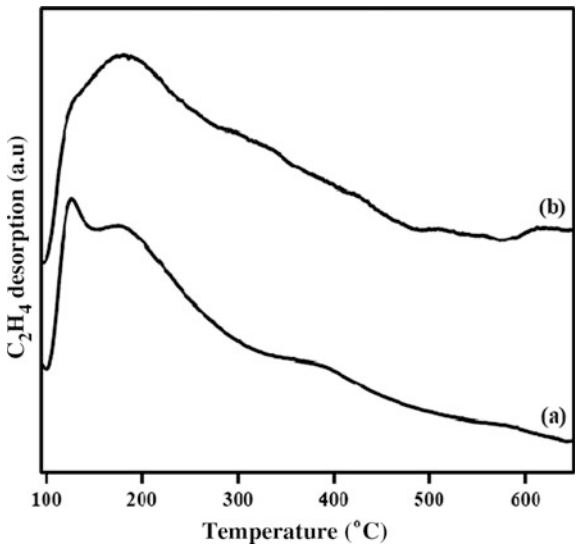

Fig. 7.8 C_2H_4 temperature-programmed desorption profiles of 15 wt% Cr_2O_3/Al_2O_3–ZrO_2 (1:1) catalyst treated at 650 °C for 1 h **a** C_2H_6 + CO_2 treated **b** C_2H_6 + CO_2 treated

(1) The oxidative dehydrogenation of alkanes produces a significant amount of oxides of carbon.
(2) Thermal runaway of the reaction due to exothermic in nature.
(3) Difficulty in controlling the selectivity of ethylene due to side reactions.

ODH of ethane to ethane has not been commercialized yet. However, in view of the very good advantages, oxidative dehydrogenation process has become a prime research area in recent years. The main objective is to achieve maximum ethane conversion and ethylene selectivity at lower temperatures. It is well-known fact that the oxides of carbon are thermodynamically more stable than ethylene; thus, the selected catalysts should control the reaction for achieving highest selectivity to ethylene and to prevent the formations of the by-products, i.e., carbon oxides.

The high reactivity of alkenes poses a challenging task in developing an appropriate catalyst. Recent technologies are developing two-step redox-based chemical looping-oxidative dehydrogenation (Cl-ODH) process in an oxygen-free environment.

References

1. Arakawa H, Aresta M, Armor JN, Barteau MA, Beckman EJ, Bell AT, Domen K et al (2001) Catalysis research of relevance to carbon management: progress, challenges, and opportunities. Chem Rev 101(4):953–996
2. EPA Office of Compliance sector Notebook Project (2014) Profile of the organic chemical industry, 2nd edn, www.epa.gov/compliance/resources/publications/assistance/sectors/notebooks, Accessed 10 Nov 2004
3. Corma A, García H (2002) Lewis acids as catalysts in oxidation reactions: from homogeneous to heterogeneous systems. Chem Rev 102(10):3837–3892
4. Ansari MB, Park SE (2012) Carbon dioxide utilization as a soft oxidant and promoter in catalysis. Energy Environ Sci 5(11):9419–9437
5. Chang JS, Vislovskiy VP, Park MS, Yoo JS, Park SE (2003) Utilization of carbon dioxide as soft oxidant in the dehydrogenation of ethylbenzene over supported vanadium–antimony oxide catalysts. Green Chem 5(5):587–590
6. Kumar ASH, Prasad P (2014) Cracking and oxidative dehydrogenation of ethane to ethylene: process and intensification options. In: Industrial catalysis and separations: innovations for process intensification, p 287
7. Yoo JS, Lin PS, Elfline SD (1993) Gas-phase oxygen oxidations of alkylaromatics over CVD Fe/Mo/borosilicate molecular sieve. II. The role of carbon dioxide as a co-oxidant. Appl Catal A Gen 106(2):259–273
8. Pieck CL, Banares MA, Fierro JLG (2004) Propane oxidative dehydrogenation on VOx/ZrO_2 catalysts. J Catal 224(1):1–7
9. Gao X, Wachs IE (2000) Investigation of surface structures of supported vanadium oxide catalysts by UV–vis–NIR diffuse reflectance spectroscopy. J Phys Chem B 104(6):1261–1268

10. Watson RB, Lashbrook SL, Ozkan US (2004) Chlorine modification of Mo/silica-titania mixed-oxide catalysts for the oxidative dehydrogenation of ethane. J Mol Catal A Chem 208 (1–2):233–244
11. Jones A (2014) Tempature-programmed reduction for solid materials characterization. CRC Press, Boca Rotan
12. Malet P, Caballero A (1988) The selection of experimental conditions in temperature-programmed reduction experiments. J Chem Soc Faraday Trans 1 Phys Chem Condens Phases 84(7):2369–2375
13. Tran K, Hanning-Lee MA, Biswas A, Stiegman AE, Scott GW (1995) Electronic structure of discrete pseudotetrahedral oxovanadium centers dispersed in a silica xerogel matrix: implications for catalysis and photocatalysis. J Am Chem Soc 117(9):2618–2626
14. Haber J (1994) Supported vanadium oxide catalysts: molecular structural characterization and reactivity properties. Crit Rev Surf Chem 4(3/4):141–187
15. Newbury DE, Joy DC, Echlin P, Fiori CE, Goldstein JI (1986) Electron channeling contrast in the SEM. In: Advanced scanning electron microscopy and X-ray microanalysis. Springer, Boston, MA, pp 87–145
16. McDonald AM (1998) Environmental scanning electron microscopy. Mater World 6:399–401
17. Koeppel RA, Nickl J, Baiker A (1994) 5 Characterization of V_2O_5/TiO_2 Eurocat samples by temperature-programmed reduction. Catal Today 20(1):45–52
18. Hurst NW, Gentry SJ, Jones A, McNicol BD (1982) Temperature programmed reduction. Catal Rev Sci Eng 24(2):233–309
19. Monti DA, Baiker A (1983) Temperature-programmed reduction. Parametric sensitivity and estimation of kinetic parameters. J Catal 83(2):323–335
20. Cvetanović RJ, Amenomiya Y (1972) A temperature programmed desorption technique for investigation of practical catalysts. Catal Rev 6(1):21–48
21. Cavani F, Ballarini N, Cericola A (2007) Oxidative dehydrogenation of ethane and propane: how far from commercial implementation? Catal Today 127(1–4):113–131
22. Heracleous E, Lee AF, Wilson K, Lemonidou AA (2005) Investigation of Ni-based alumina-supported catalysts for the oxidative dehydrogenation of ethane to ethylene: structural characterization and reactivity studies. J Catal 231(1):159–171
23. Heracleous E, Lemonidou AA (2006) Ni–Nb–O mixed oxides as highly active and selective catalysts for ethene production via ethane oxidative dehydrogenation. Part I: Characterization and catalytic performance. J Catal 237(1):162–174
24. Heracleous L (2003) Strategy and organization: realizing strategic management. Cambridge University Press, Cambridge
25. Solsona B, Vázquez MI, Ivars F, Dejoz A, Concepción P, Nieto JL (2007) Selective oxidation of propane and ethane on diluted Mo–V–Nb–Te mixed-oxide catalysts. J Catal 252(2):271–280
26. Rao TM, Sayari A (2009) Ethane dehydrogenation over pore-expanded mesoporous silica-supported chromium oxide: 2 Catalytic properties and nature of active sites. J Mol Catal A Chem 301(1–2):159–165
27. Thirumala bai P, Manokaran V, Saiprasad PS, Srinath S (2015) Studies on heat and mass transfer limitations in oxidative dehydrogenation of ethane over Cr_2O_3/Al_2O_3 Catalyst. Procedia Eng 127:1338–1345
28. Grzybowska B, Słoczyński J, Grabowski R, Wcisło K, Kozłowska A, Stoch J, Zieliński J (1998) Chromium oxide/alumina catalysts in oxidative dehydrogenation of isobutane. J Catal 178(2):687–700.
29. Cherian M, Rao MS, Yang WT, Jehng JM, Hirt AM, Deo G (2002) Oxidative dehydrogenation of propane over Cr_2O_3/Al_2O_3 and Cr_2O_3 catalysts: effects of loading, precursor and surface area. Appl Catal A 233(1–2):21–33

30. Kung HH (1994) Oxidative dehydrogenation of light (C_2 to C_6) alkanes. Adv Catal 40(1)
31. Weckhuysen BM, Wachs IE, Schoonheydt RA (1996) Surface chemistry and spectroscopy of chromium in inorganic oxides. Chem Rev 96(8):3327–3350
32. Shen Z, Liu J, Xu H, Yue Y, Hua W, Shen W (2009) Dehydrogenation of ethane to ethylene over a highly efficient Ga_2O_3/HZSM-5 catalyst in the presence of CO_2. Appl Catal A 356 (2):148–153
33. Mentasty LR, Gorriz OF, Cadus LE (1999) Chromium oxide supported on different Al_2O_3 supports: catalytic propane dehydrogenation. Ind Eng Chem Res 38(2):396–404
34. Mentasty LR, Gorriz OF, Cadus LE (2001) A study of chromia–alumina interaction by temperature-programmed reduction in dehydrogenation catalysts. Ind Eng Chem Res 40 (1):136–143
35. Ramesh Y, Bai PT, Babu BH, Lingaiah N, Rao KR, Prasad PS (2014) Oxidative dehydrogenation of ethane to ethylene on Cr_2O_3/Al_2O_3–ZrO_2 catalysts: the influence of oxidizing agent on ethylene selectivity. Appl Petrochem Res 4(3):247–252
36. Klimova T, Rojas ML, Castillo P, Cuevas R, Ramírez J (1998) Characterization of Al_2O_3–ZrO_2 mixed oxide catalytic supports prepared by the sol-gel method. Microporous Mesoporous Mater 20(4–6):293–306
37. Wang S, Murata K, Hayakawa T, Hamakawa S, Suzuki K (2001) Effect of promoters on catalytic performance of Cr/SiO_2 catalysts in oxidative dehydrogenation of ethane with carbon dioxide. Catal Lett 73(2–4):107–111
38. Yoo JS (1998) Selective gas-phase oxidation at oxide nanoparticles on microporous materials. Catal Today 41(4):409–432
39. Rogelj J, Schaeffer M, Meinshausen M, Shindell DT, Hare W, Klimont Z, Schellnhuber HJ et al (2014) Disentangling the effects of CO_2 and short-lived climate forcer mitigation. Proc Natl Acad Sci 111(46):16325–16330
40. Bai PT, Srinath S, Upendar K, Sagar TV, Lingaiah N, Rao KR, Prasad PS (2017) Oxidative dehydrogenation of ethane with carbon dioxide over Cr_2O_3/SBA-15 catalysts: the influence of sulfate modification of the support. Appl Petrochem Res 7(2–4):107–118
41. Botella P, Dejoz A, Nieto JL, Concepción P, Vázquez MI (2006) Selective oxidative dehydrogenation of ethane over MoVSbO mixed oxide catalysts. Appl Catal A 298:16–23
42. Martinez-Huerta MV, Gao X, Tian H, Wachs IE, Fierro JLG, Banares MA (2006) Oxidative dehydrogenation of ethane to ethylene over alumina-supported vanadium oxide catalysts: relationship between molecular structures and chemical reactivity. Catal Today 118(3–4):279–287
43. Osawa T, Ruiz P, Delmon B (2000) New results on the oxidative dehydrogenation of ethane to ethylene: promoting catalytic performance of Mo-V- and Ni-V-oxide by α–Sb_2O_4. Catal Today 61(1–4):309–315
44. Solsona B, Dejoz A, Garcia T, Concepción P, Nieto JL, Vázquez MI, Navarro MT (2006) Molybdenum–vanadium supported on mesoporous alumina catalysts for the oxidative dehydrogenation of ethane. Catal Today 117(1–3):228–233
45. Chao ZS, Ruckenstein E (2004) V–Mg–O prepared via a mesoporous pathway: a low-temperature catalyst for the oxidative dehydrogenation of propane to propene. Catal Lett 94(3–4):217–221
46. Roussel M, Bouchard M, Karim K, Al-Sayari S, Bordes-Richard E (2006) MoVO-based catalysts for the oxidation of ethane to ethylene and acetic acid: influence of niobium and/or palladium on physicochemical and catalytic properties. Appl Catal A 308:62–74
47. Zhu J, Qin S, Ren S, Peng X, Tong D, Hu C (2009) $Na_2WO_4/Mn/SiO_2$ catalyst for oxidative dehydrogenation of ethane using CO_2 as oxidant. Catal Today 148(3–4):310–315

48. Ge X, Zhu M, Shen J (2002) Catalytic performance of silica-supported chromium oxide catalysts in ethane dehydrogenation with carbon dioxide. React Kinet Catal Lett 77(1):103–108
49. Wang S, Murata K, Hayakawa T, Hamakawa S, Suzuki F (2000) Dehydrogenation of ethane with carbon dioxide over supported chromium oxide catalysts. Appl Catal A 196(1):1–8
50. Wang S, Murata K, Hayakawa T, Hamakawa S, Suzuki K (1999) Oxidative dehydrogenation of ethane by carbon dioxide over sulfate-modified Cr_2O_3/SiO_2 catalysts. Catal Lett 63(1–2):59–64

Chapter 8
Electrochemical Reduction of Carbon Dioxide into Useful Low-Carbon Fuels

Raghuram Chetty, Sunita Varjani, G. Keerthiga, S. Srinath and K. S. Rajmohan

Abstract In this chapter, preliminary discussion on the need for mitigation of greenhouse gas emissions in today's scenario is emphasized, followed by the foundation to the conversion of CO_2 into useful chemicals. Various techniques employed for CO_2 sequestration are introduced, and in the midst of these approaches, electrochemical reduction of CO_2 is emphasized, owing to its advantages in product selectivity, operation at ambient conditions without supplementary chemical requirements, environmental compatibility, relatively simple modularity and quick scalability. Different types of catalysts reported in the literature for activating and reducing CO_2 are critically analysed. To start with, metallic electrodes in aqueous solutions and nanoporous materials are discussed. The reaction mechanism and effect of supporting electrolytes, pressure, and temperature are summarized. Combination of various techniques such as bio-electrochemical reduction and photocatalytic technologies have been accentuated. Furthermore, limitations and outlook of electrochemical reduction of CO_2 are presented, in which development of modules similar to that of commercially available H_2O electrolysers could pave the way for commercialization of electrocatalytic reduction of CO_2.

Keywords CO_2 sequestration · Electrochemical reduction · Energy carrier Hydrocarbon · Energy conversion

R. Chetty · G. Keerthiga · K. S. Rajmohan
Department of Chemical Engineering, Indian Institute of Technology Madras, Chennai 600036, India

S. Varjani
Gujarat Pollution Control Board, Gandhinagar 382010, Gujarat, India

S. Srinath · K. S. Rajmohan (✉)
Department of Chemical Engineering, National Institute of Technology Warangal, Warangal 506004, Telangana, India
e-mail: rajmohan@nitw.ac.in

F. Winter et al. (eds.), *CO_2 Separation, Purification and Conversion to Chemicals and Fuels*, Energy, Environment, and Sustainability,
https://doi.org/10.1007/978-981-13-3296-8_8

Nomenclature

ADH	Alcohol dehydrogenase
AldDH	Aldehyde dehydrogenase
AMS	American Meteorological Society and Environmental Technology
ARCI	International Advanced Research Centre for Powder Metallurgy and New Materials, Hyderabad
BAU	Business-as-usual
BP	British Petroleum oil and gas company
CNT	Carbon nanotubes
Cu/Zn-H	Zn deposited from high concentration (1 M) on Cu substrate
Cu/Zn-L	Zn deposited from low concentration (0.1 M) on Cu substrate
DNV group	Det Norske Veritas group
FDH	Formate dehydrogenase
FE	Faradaic efficiency
G. *Sulfurreducens*	*Geobacter sulfurreducens*
GAB	Genetically altered bacteria
GDE	Gas diffusion electrodes
GHG	Greenhouse gas
HEO	Hydrogen evolution overvoltage
IEA	International Energy Agency
IPCC	Intergovernmental panel on climate change
MoU	Memorandum of Understanding
NCCR	National Centre for Catalysis Research
NOAA	National Oceanic Atmospheric Administration
NRC-ICPET	National Research Council-Institute of Chemical Process
SHE	Standard hydrogen electrode
SPE	Solid polymer electrolyte
STEP	Solar thermal electrochemical photo
USA	United States of America
XRD	X-ray diffraction

8.1 Introduction

Combustion of solid, liquid and gaseous fuels leads to air pollution in the environment. Depending upon the composition of fuel, NO_x, SO_x and CO_2 emissions vary. Anthropogenic emissions have increased the concentration of CO_2 in the atmospheric following a hockey-stick curve, and the atmospheric CO_2 has crossed its upper safe limit (350 ppm) as shown in Fig. 8.1a [1].

According to NOAA and the American Meteorological Society (AMS), the global atmospheric carbon dioxide is 409 ± 0.1 ppm in 2018, a new record high.

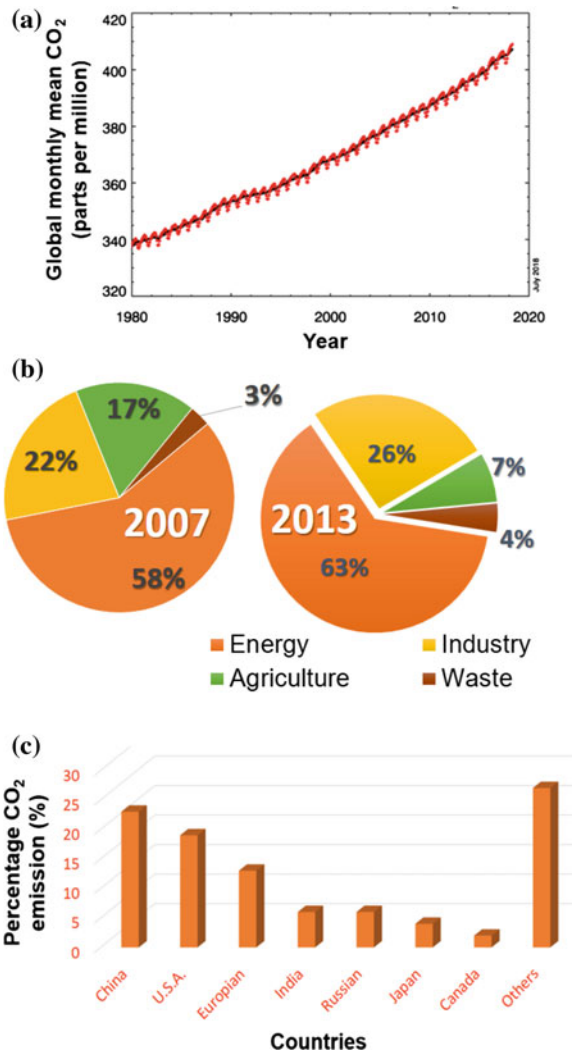

Fig. 8.1 **a** Atmospheric CO_2 concentration [1], **b** comparison of sectoral percentage share of greenhouse gas emissions between 2007 and 2013, **c** CO_2 emissions by selected countries

Between 2016 and 2017, the global annual mean of CO_2 increased by 2.2 ± 0.1 ppm, which was slightly less than the increase between 2015 and 2016 of 3.0 ppm per year.

Hence, stabilization of CO_2 levels is inexorable to achieve carbon-neutral society and to cope up with the Earth's climate. Numerous routes for CO_2 capture and reduction are being investigated. The increasing demand for renewable energy has motivated researchers to look for energy from other sources including waste. The use of CO_2 as feedstock to synthesize fuels is considered as an alternative to solve the current energy problem.

CO_2 is highly stable and has limited applications in fire extinguishers and beverages. CO_2 is the most oxidized form of carbon. Technologies including biochemical, photochemical, electrochemical, solar thermochemical and chemical sequestration are employed to transform CO_2 into valuable chemicals. Electrochemical reduction of CO_2 is generally performed on metal surfaces which are catalytically active with the involvement of clean electrons. In comparison to various methods of CO_2 reduction, electrochemical reduction technique offers several advantages such as high product selectivity, ambient condition operation without supplementary chemical requirements, environmental compatibility, relatively simple modularity and quick scalability. Moreover, reduction of CO_2 in aqueous solution is also feasible using electrolyte of high CO_2 solubility and conductivity. Electrochemical CO_2 reduction, especially coupling with renewable energy, can play an important role in realizing sustainable energy future, which also contribute to decreasing greenhouse emissions.

The electrocatalytic reduction of CO_2 into valuable products depends on choice of the electrode material, applied potential and electrolyte. The selection of electrocatalysts for CO_2 reduction ranges from metals, its oxides, metal alloys, complexes, enzymes, organic molecules and polymers/clusters. In this chapter, the catalytic activity, stability, Faradaic efficiency, possible CO_2 reduction mechanisms and product selectivity are discussed. Lastly, some insight on future development and towards commercialization of electrochemical CO_2 reduction methodology is suggested.

8.2 Energy and Climate Change

Global primary energy consumption is predicted to be approximately 76,663 TW-h by 2050 and expected to be tripled (343 PW-h) by 2100 [2]. If the fossil fuels usage continue at the same trend to serve energy at a low cost, then the quality of human life will be affected with continuing greenhouse emissions contributing to the global warming.

8.2.1 Carbon Cycle and Greenhouse Emissions

Carbon is transformed or cycled among Earth's seas, atmosphere, biological system and geosphere. Carbon is the basic building block of life and an essential segment of numerous chemical processes. Every living being is inbuilt with carbon materials. It is available in the air basically as carbon dioxide (CO_2), yet additionally as less extent gases such as methane (CH_4). CO_2 present in the atmosphere behaves like a blanket and traps the longwave radiation within the planet and keeps it warm. With the increase in the CO_2 concentration, the earth gets warmer and thus CO_2 contributes towards global warming.

In 1896, Svante Arrhenius, a Swedish physicist, reported that carbon dioxide (CO_2) has a role to play in the greenhouse effect and unnatural weather change across the globe. These days, a worldwide temperature alteration is the most critical environmental concern. CO_2 constitutes 63% of the greenhouse gases (GHGs) followed by methane (24%) and N_2O (3%) [3]. The climatic change, for the most part of the world, happened because of ozone-depleting substances (such as chlorofluorocarbons) emanating from anthropogenic emissions such as combustion of fossil fuels, automobiles and refrigeration [4]. According to the IEA report, there was an exponential increase in CO_2 emissions from 1971 (14.1 Gt) to 2017 (32.5 Gt) with global energy-related CO_2 emissions rose by 1.4% in 2017 [2].

8.2.2 *Sources of CO_2 Emission*

Assessment report of the Indian government in 2017 summarized the greenhouse gas emissions due to anthropogenic activities from energy, industry, agriculture and waste [5]. In comparison to the previous report, the industrial sector has increased from 58 to 63% whereas agriculture, forest and other land use sector have decreased from 17 to 7% as shown in Fig. 8.1b. In addition, the customary treatment of wastewater, along with degradation of organic contaminants, has contributed extraordinary amount of CO_2 discharged into the atmosphere, which is assessed to be 1.21×10^4 t d^{-1} in 2025 [6]. Deforestation, inappropriate agriculture and cutting of trees in the name of infrastructure development have significantly increased the CO_2 level in the atmosphere and in turn, the biosphere is turning out to be a carbon source than a sink (absorption). The atmospheric CO_2 concentration is alarmingly increasing as shown in Fig. 8.1a.

In view of controlling the increasing global temperature, Kyoto protocol earnestly asked thirty-seven industrialized nations as well as European Union to cut GHG emissions by 5% from 1990 levels by 2010. Later, in the Copenhagen agreement several nations agreed to work towards keeping the rise in global temperatures to below 2 °C past the pre-industrial level. Earlier, in 2012, IEA demonstrated that 43×10^{12} kg of CO_2 should be reduced to 14×10^{12} kg keeping in mind the end goal to acquire the ±2 °C target proportional to 450 ppm of CO_2 [7].

In view of the challenges pertaining to global climate change, countries that contribute majorly to CO_2 emission are China and USA as shown in Fig. 8.1c. China, USA, India and Russia accounted for 9040.74, 4997.50, 2066.01 and 1468.99 million metric tons of CO_2 emissions from fuel combustion which amounts to 28, 15, 6 and 5%, respectively [8]. In the past two decades, China has doubled its CO_2 emission, whereas India has seen two-thirds increase mainly due to the production of energy from fossil fuels to meet the demands of industrialization and population growth. Developed and developing nations release higher concentrations of CO_2 per capita. For instance, USA which has just 5% of the world population has generated 15% of the global emission. The Asian economies accounted

Table 8.1 CO_2 emissions per capita of selected countries

Country	Qatar	USA	China	Germany	Australia	UK	India
CO_2 per capita (metric ton)	23.4	9.5	4.55	5.6	9.37	3.66	1.12
% global emission	0.25	14.34	26.51	2.16	1.24	1.11	6.81

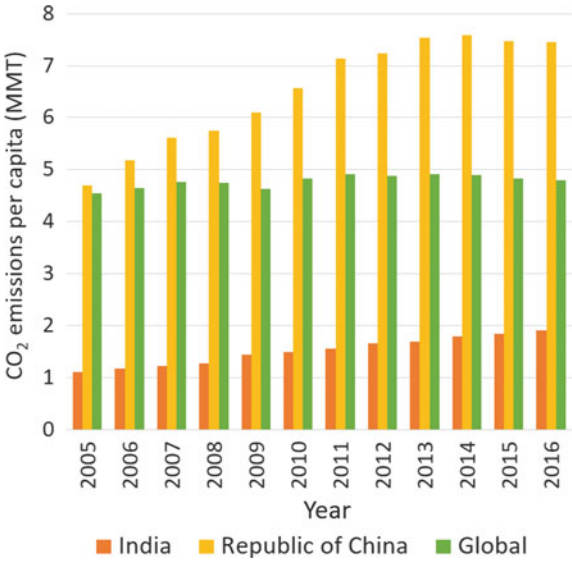

Fig. 8.2 Recent trends in CO_2 emissions per capita in India, China and global level

for two-thirds of the global increase in carbon emissions. As on January 2018, CO_2 production per capita of few countries is listed in Table 8.1. The value for China and India is less because of its high population. Figure 8.2 depicts the trend in CO_2 emission per capita at India and China in comparison to the global level.

Considering the available oil reserves, British Petroleum (BP) energy outlook 2030 predicts that oil may remain to be the major energy source for several years to come; however, CO_2 emission associated with fossil fuel combustion will pose a severe environmental concern. Intergovernmental panel on climate change (IPCC) reported that power plants with fossil fuels as feedstock contribute majorly (85%) to CO_2 emissions (10,000 Mt $year^{-1}$) followed by cement manufacturing units, steel industries, refineries and petrochemical industries [9]. Global CO_2 emissions may reach 57 Gt $year^{-1}$ by 2050 with business-as-usual (BAU) emission projections.

8.3 CO_2 Physical and Chemical Properties

Carbon dioxide (carbonic anhydride, carbonic acid) gas results from the reaction between carbon and oxygen. It exists in solid and gas states. Solid CO_2 is generally referred as dry ice since it directly changes from solid phase into gas. CO_2 is a colourless, odourless and tasteless gas. CO_2 is an indispensable food for all living things. CO_2 is soluble in water, ethanol and acetone. 1 kg of CO_2 occupies 550 L of volume. Solubility of CO_2 in various solvents is listed in Table 8.2. CO_2 gas is one among the five topmost gases present in the atmosphere. In the 1750s, Joseph Black observed that when limestone (calcium carbonate) is treated/heated with acids, it resulted in a gas which was denser than air and later found as carbon dioxide. In general, CO_2 is the major product formed when fossil fuels are combusted, when a liquid undergoes fermentation and from our breathing, which in turn is assimilated by plants to release oxygen.

Carbon dioxide, CO_2, is a linear molecule with its valence shell containing sixteen bonding electrons. Except oxygen 2s energy (−32.4 eV), the energies associated with the atomic orbitals of carbon 2s (−19.4 eV), carbon 2p (−10.7 eV) and oxygen 2p (−15.9 eV) are in the close range [10]. An irreversible reduction takes place upon structural change from linear to bend due to single electron transfer.

Constituting a weak Lewis base-oxygen atoms and an electrophilic carbon, CO_2 is a very stable linear molecule. Two oxygen atoms and one carbon atom will share each electron to form covalent bond and make an O=C=O molecule. With four electrons sharing, carbon and oxygen can count eight electrons in the outer shell, making it a stable CO_2 molecule not ready to react with oxygen or carbon atoms any further. They are not ionic since the bond is shared not transferred, and the description of the structure of a molecule does not end without molecular orbital theory.

Separation of carbon dioxide from the combustion product is difficult when oxygen-fuel technologies are used. Once separated, conversion of CO_2 is the next challenge because of their physical and chemical properties listed below.

Figure 8.3 represents the energy barrier diagram for CO_2 reduction. Thermodynamically, CO_2 is a highly stable compound which necessitates highly active catalysts and high energy for conversion into targeted products [12]. Also,

Table 8.2 Solubility of CO_2

CO_2 in a particular system	Solubility (mol L^{-1}) atm. pressure and at 298 K
Water	0.033
KC–water	0.028
$KHCO_3$–water	0.027
Methanol	0.194
80 mmol/dm^3 KOH in methanol	0.677

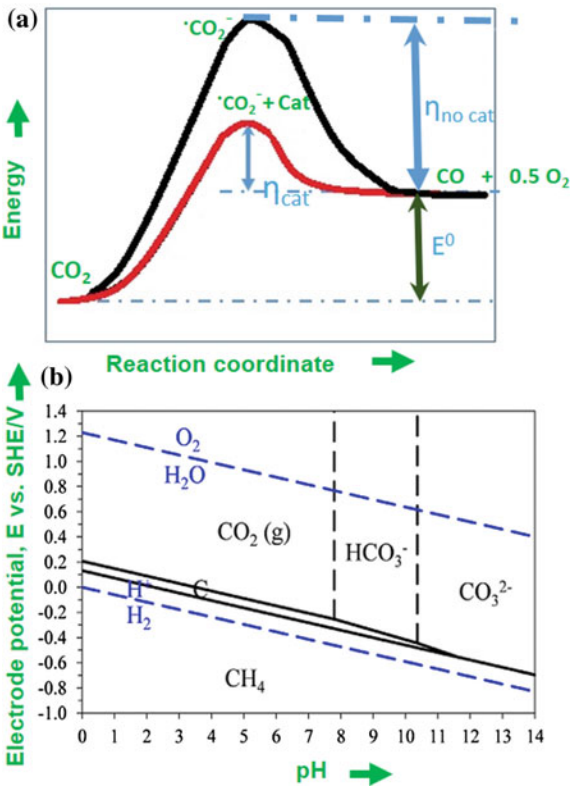

Fig. 8.3 **a** Energy barrier diagram for CO_2 reduction reaction. **b** Pourbaix diagram for CO_2 reduction (25 °C and 10^5 Pa [11])

carbonates, carbamates, and carboxylates can be formed by catalytically reacting CO_2 into organic molecules. However, they do not find large-scale applications for fuels or product production.

The enthalpy term (ΔH_0) helps in evaluating thermodynamic stability as well as the feasibility of CO_2 transformations into useful chemicals and represented by Gibbs–Helmholtz correlation

$$\Delta G_0 = \Delta H_0 - T\Delta S_0 \tag{8.1}$$

ΔG_0 represents the Gibbs free energy between the reactants and the products of a chemical reaction, and $T\Delta S_0$ is the entropy term which does not help much in accessing the thermodynamic driving force for the chemical reactions involving CO_2. A strong indication of a CO_2 molecule's stability can thermodynamically be identified with a high negative standard Gibbs free energy of formation value ($\Delta G_f^o = -349.67$ kJ mol^{-1}) when compared to other molecules [13]. The structure changes from linear to bend on transferring one electron to the CO_2 molecule [14]. In the presence of water, electrochemical reduction of CO_2 is competed by hydrogen evolution reaction. Hence, the suppression of hydrogen evolution is

Table 8.3 Applications of CO_2 by processes [17]

Processes	Applications
Chemicals and pharmaceuticals	Production of salicylic acid and aspirin, etc., used for product storage/transportation at low temperature
Beverage	Carbonation of beverages such as beer, mineral water, soft drinks, etc. Also used as shielding gas for preserving the drink quality
Safety	CO_2 snow for fire extinguishers
Coolant	In chemistry for controlling reactor temperatures

important because the applied energy is consumed by hydrogen evolution rather than for CO_2 reduction [15].

The equilibrium potential versus pH of CO_2 is represented by Pourbaix diagram in Fig. 8.3b. The dissolved CO_2 exists in three different states ($CO_{2(g)}$, HCO_3^- and CO_3^{2-}) as a function of pH. Bumroongsakulsawat and Kelsall [11] refer to the formation of CO at pH less than 4.1 and formic acid at pH greater than 4.1. The multi-electron charge transfer reductions of CO_2 are carried out at much more positive potential than required for one-electron reduction. Moreover, protonating the reduction product will help in reducing the thermodynamic barrier for CO_2 reduction. Thus, understanding the thermodynamics of the CO_2 reduction is indeed necessary.

CO_2 is a stable molecule requiring to overcome Gibbs energy of formation: $\Delta G^{o}_{298\,K}$, $(CO_2) = -394.4$ kJ mol^{-1}. The action of a suitable catalyst, energy input and a reductant may form methane and methanol.

Currently, CO_2 is being used in several processes. The concept of producing methanol using CO_2 was conceived in the 1920s, and the same is described in a recent book [16]. The reduction of CO_2 to hydrocarbons fuels and alcohols using nuclear energy or other renewable energy sources may deliver a future energy distribution system based on gaseous or liquid fuels without a net upsurge in atmospheric CO_2. Some of its important applications are listed below in Table 8.3 [17]. The various chemical reactions associated with CO_2 are listed in Table 8.4.

8.4 Health Concerns Due to CO_2

While burning food for energy, the human body produces carbon dioxide as a waste gas and the blood takes it to the lungs, and we exhale it and breathe oxygen. The CO_2 level in the blood is approximately 26 milliequivalent units per litre of blood. If the lungs cannot remove CO_2, and high CO_2 in blood, it may lead to organ failures including respiratory failure.

When the CO_2 concentration in the atmosphere exceeds 100× times its maximum limit of 350 ppm, it can be toxic to animal life. Depending upon the levels of CO_2, various potential hazards are reported as shown in Table 8.5. For instance, 5000 ppm is the maximum limit for workplace exposures on a daily basis whereas beyond 40,000, it is extremely harmful since there will be no O_2 to inhale.

Table 8.4 Reactions involving CO_2 conversion into hydrocarbon/fuels

Name of the reaction	Reaction	Eqn. no.	ΔH° at 298.15 K (kJ mol^{-1})
CO_2 reforming of methane	$CO_{2(g)} + CH_{4(g)} \rightarrow 2H_{2(g)} + 2CO_{(g)}$ (Simultaneous consumption of two major greenhouse gases)	8.2	247.3
Methane decomposition	$CH_{4(g)} \rightarrow C_{(s)} + 2H_{2(g)}$	8.3	74.8
Boudouard equilibrium	$2CO_{(g)} \rightarrow C(s) + CO_2(g)$	8.4	−172.5
Reverse water gas shift (RWGS)	$CO_{2(g)} + H_2(g) \leftrightarrow CO(g) + H_2O(g)$	8.5	41.2
CO_2 Hydrogenation/ methanation	$CO_{2(g)} + 4H_{2(g)} \rightarrow CH_{4(g)} + 2H_2O_{(g)}$	8.6	−113.6
Steam reforming	$CH_{4(g)} + H_2O_{(g)} \rightarrow CO_{(g)} + 3H_{2(g)}$	8.7	206.1
Hydrogenation of CO_2 to methanol	$CO_{2(g)} + 3H_{2(g)} \rightarrow CH_3OH_{(g)} + H_2O_{(g)}$	8.8	−49.5
Direct synthesis of Dimethyl ether using CO_2/H_2	$2CO_{2(g)} + 6H_{2(g)} \rightarrow CH_3OCH_{3(g)} + 3H_2O_{(g)}$	8.9	–
CO_2 hydrogenation to formic acid	$CO_{2(g)} + H_{2(g)} \rightarrow HCOOH_{(l)}$	8.10	32.9
CO_2 hydrogenation to higher alcohols	$2CO_{(g)} + 4H_{2(g)} \rightarrow C_2H_5OH_{(g)} + H_2O_{(g)}$	8.11	−255.5
CO_2 hydrogenation to higher alcohols	$2CO_{2(g)} + 6H_{2(g)} \rightarrow C_2H_5OH_{(g)} + 3H_2O_{(g)}$	8.12	−173.1
CO_2 reforming of ethanol and higher alcohols	$C_2H_5OH_{(g)} + CO_{2(g)} \rightarrow 3CO_{(g)} + 3H_{2(g)}$	8.13	
Oxidative dehydrogenation in the presence of CO_2	$C_6H_5 - C_2H_{5(g)} \rightarrow C_6H_5 - CH = CH_{2(g)} + H_{2(g)}$ $CO_{2(g)} + H_{2(g)} \leftrightarrow CO_{(g)} + H_2O_{(g)}$	8.14	
Oxidative dehydrogenation (ODH) for C_2H_4 production	$C_2H_6 + CO_2 \rightarrow C_2H_4 + CO + H_2O$	8.15	ΔH°_{983} = +135

Table 8.5 Potential health hazards associated with levels of CO_2 in the air

CO_2 level (ppm)	Remarks
1000–2000	Drowsiness
2000–5000	Sleepiness, headaches, loss of attention, poor concentration, slight nausea and increased heart rate
5000	Toxicity or oxygen deprivation
40,000	Harmful due to lack of O_2

8.5 Technologies Available for CO_2 Reduction

Developing economically feasible technologies to convert CO_2 into useful chemicals and fuels has a significant contribution to address the global warming challenge. Also, research on capturing and storing CO_2 is equally significant. To mitigate CO_2 emission to a possible extent, several treaties and MoUs have been signed by several nations and organizations. For instance, protocols for NO_x emission as well as SO_x emission and certified emission reductions are in force to stabilize the situation [18].

Figure 8.4a illustrates the different strategies to control CO_2 emission into the atmosphere. Conservation practices include reducing carbon-based fuels or

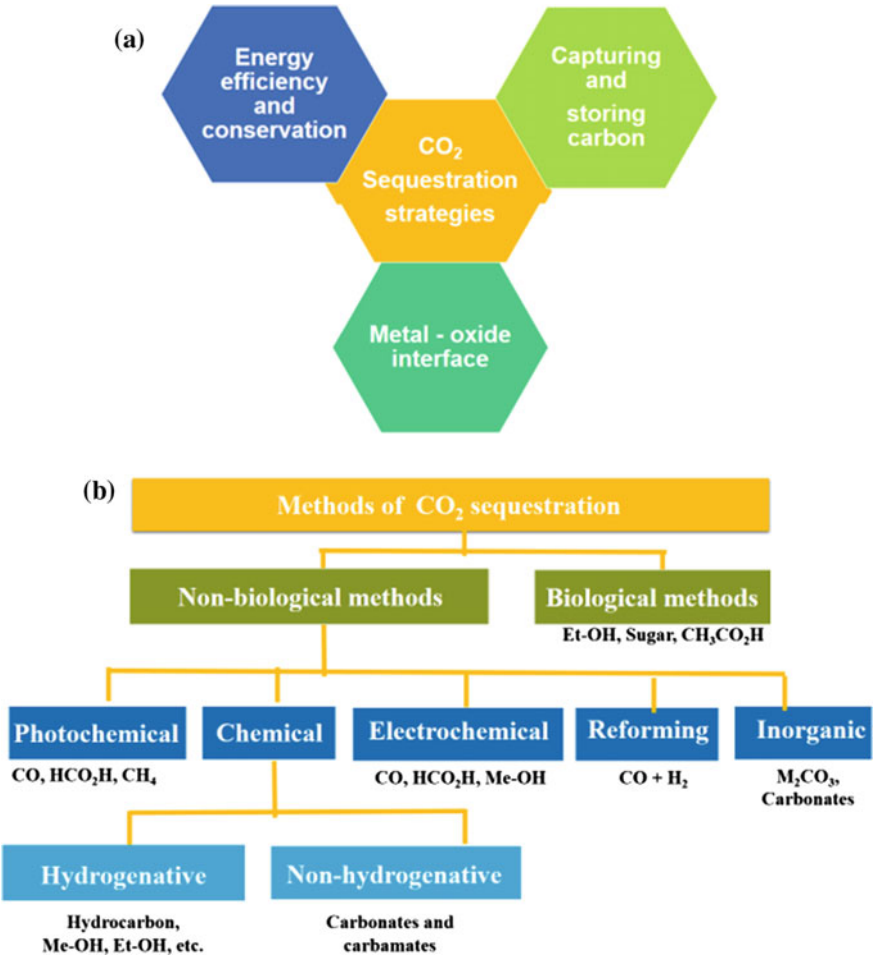

Fig. 8.4 **a** Strategies for CO_2 management and **b** methods of CO_2 sequestration

employing reduced carbon sources of energy such as natural gas. The last strategy is to capture and store CO_2. Potentially, CO_2 can be utilized as an alternative, non-toxic and efficient feedstock for production of few polymers or new chemicals that could help in carbon balance [18].

To convert CO_2 into products, it requires an input of energy which can be derived from solar as a sustainable source. Thus, photocatalytic splitting gains interest to convert CO_2 into useful fuels.

Various techniques for CO_2 conversion to achieve high energy density chemicals are under investigation, including thermochemical, chemical, photochemical, photoelectrochemical, biochemical, bio-photoelectrochemical and electrochemical routes. Various techniques in the research and development stage can be grouped as biological processes and non-biological processes as shown in Fig. 8.4b. Some of the emerging technologies which focus on these aspects are

- Biochemical reduction of CO_2
- Chemical sequestration of CO_2
- Thermochemical sequestration of CO_2
- Photochemical reduction of CO_2
- Electrochemical reduction of CO_2

Preferably, the upcoming progress in these techniques should use renewable energy source and need to be economic.

In comparison to heterogeneous photocatalysts for CO_2 conversion in the liquid phase, homogeneous catalysts can uniformly supply CO_2 to active sites. Homogeneous catalysts are costly metals and necessitate reductants that are sacrificial in nature. Challenges in developing novel reactant materials are reported elsewhere [14]. Carbon dioxide dissolved in the aqueous phase may be electrochemically reduced to form oxygenates, hydrocarbons or carbon monoxide utilizing both homogeneous as well as heterogeneous catalysts. This approach will be attractive when the source of power is wind or photovoltaic. Another alternative to specifically functionalize CO_2 is hydrogenation of CO_2 to low molecular weight hydrocarbons or oxygenates by means of modified methanol and Fischer–Tropsch (FT) synthesis [19, 20]. Such procedures have a more prominent potential to be extended to commercial scale contrasted with the electrocatalytic or photocatalytic transformation. The challenge in implementing CO_2 hydrogenation is the requirement for pure H_2 at an affordable cost. On the other hand, CO_2 can react with CH_4 to yield a blend of CO and H_2 gas (synthesis gas) [21].

A brief introduction, working principle along with pros and cons of the various technologies are given below.

8.5.1 Biochemical Reduction of CO_2

US researchers have proved that bacteria can turn CO_2 into fuel. Though it was known that microalgae can consume CO_2, there were no good processes to produce fuels from them. Recently, Liao team has developed a genetically altered bacteria (GEB) to consume CO_2 and produce isobutanol and isobutyraldehyde [22]. The genome of the Synechococcus elongates, a cyanobacterium was modified by combining four genes from a different bacteria, and this can act as a reaction vessel for CO_2 reduction. The authors claim that their process is faster than hydrogen production by one degree of the higher order and about ten degrees of the higher order than ethanol produced using genetically modified micro-organisms. However, this method offers low yields at the expense of sophisticated laboratory practices. Spinner et al. [23] have reviewed the bio-electrochemical conversion of CO_2 using enzyme catalysts like AldDH, FDH and ADH. The enzyme selectivity and addition of electron mediator to improve the selectivity were discussed. Similarly, Soussan et al. [24] have obtained reduction current up to 30 A m^{-2} by carrying out CO_2 reduction using *G. sulfurreducens*. The glycerol was the product obtained from the medium of formate which was extricated from the cells by applying pressure. Following this work, Lovley and Nevin [25], studied electrode-to-microbe electron transfer for the manufacture of fuels and other useful chemicals from CO_2 [25]. The author discussed in detail about the application of biotechnology in combination with electrochemical energy for the production of fuels and chemicals from CO_2. Though this process ensures new promises on conversion of CO_2, excessive operation time and requirement of close monitoring of the operating parameters make it less attractive among various methods of CO_2 conversion.

8.5.2 Chemical Sequestration of CO_2

Carbon sequestration refers to the chemical processes through which CO_2 may be discharged from the environment and stowed in a suitable carbonate mineral forms. It can be exclusively done as CO_2 removal, a known form of geoengineering. In carbon capture and storage process, CO_2 is separated from various sources and stored in underground reservoirs.

Naturally, the weathering of rock in several centuries could have formed by the reaction between CO_2 with abundantly available calcium oxide (CaO) or magnesium oxide (MgO) to form stable carbonates following Eqs. 8.16 and 8.17 [26].

$$CaO + CO_2 \rightarrow CaCO_3 \tag{8.16}$$

$$MgO + CO_2 \rightarrow MgCO_3 \tag{8.17}$$

Calcium and magnesium silicates are present in nature and reacts with CO_2 as in Eqs. 8.18 and 8.19.

$$Mg_2SiO_4 + 2CO_2 = 2MgCO_3 + SiO_2 \tag{8.18}$$

$$Mg_3Si_2O_5(OH)_4 + 3CO_2 = 3MgCO_3 + 2SiO_2 + 2H_2O \tag{8.19}$$

It is felt that the energy requirements of sequestration processes are significant. A recent publication reports that sequestration consumes one-fourth of the output capacity of a power plant (600 MW) [27]. For instance, the efficiency of a 600 MW coal-fired power plant has reduced from 41 to 31.2% after including CO_2 capture and sequestration. It is also expected that the expense of carbon sequestration may tend to increase over time. All these will have an impact on the cost of energy produced, which may be as high as twice the costs of modern coal technology. Hence, alternative measures are investigated.

8.5.3 Solar Thermochemical Reduction of CO_2

CO_2 reduction through sunlight was developed as a novel solar thermal electrochemical photo (STEP) process, which converts CO_2 into carbon monoxide or carbon [28]. CO_2 was broken down in molten lithium carbonate electrolyte at high temperatures in electrolysis cell powered by sunlight. The process for reducing CO_2 to CO was substantially improved via oxidation of zinc in a two-step Zn/ZnO solar thermochemical cycle [29]. Few authors reported the decomposition of gaseous CO_2 in molten salts such as molten LiCl–Li_2O or the molten $CaCl_2$–CaO at 1173 K which on thermal reduction yields amorphous carbon or rod-like graphite crystals [30]. The scope for producing higher energy density fuels is less, and the high-temperature operation makes such a process of reducing CO_2 less viable.

8.5.4 Photochemical Reduction of CO_2

Photochemical reduction of carbon dioxide is an attractive method for CO_2 conversion as it makes use of sunlight which is in abundance and freely available. Photocatalysis uses catalysts under visible light or UV to oxidize or reduce the pollutants to innocuous compounds, generally at ambient conditions. It was also adapted to mimic nature's photosynthesis process [20]. In this process, photogenerated electrons are used for the reduction of CO_2, whereas holes are utilized for the oxidation of water. CO_2 undergoes a single electron transfer reaction at −1.85 V versus SHE to form $CO_2^{\cdot-}$ due to the alteration in hybridization of C from sp^2 to sp^3 [31].

Heterogeneous photocatalysis deals with visible light-activated photocatalysts which could split water and reduce CO_2. Past research dealt with modifying a

photocatalyst with a suitable co-catalyst, and substantial advancement in this area was achieved. To date, more than 100 metal oxides based on photocatalytic systems have been reported to be active for water splitting. Carbon nanotube (CNT)-supported TiO_2 [32, 33], Cu, Pt co-catalysed N-doped TiO_2 nanotube arrays [34, 35], Ag/Cu-TiO_2-coated optical fibre [36, 37], $SrTiO_3$ [38, 39], supramolecular or biphasic ionic liquid [40] and other tantalates [41] were tested for CO_2 by photoreduction. Moreover, dye-sensitized TiO_2 films were also investigated, which produced formic acid, formaldehyde and methanol as products [42].

Negligible pressure drop during the operation of photocatalytic reactors makes it a flexible choice. But some of the limitations of the process were due to its low yields of producing single carbon product. Moreover, the reason for the shorter lifetime and poor selectivity of components needs to be addressed. The catalyst should have a large band gap which fits in the negative potential range of conduction band (donor) as well as the positive potential range of valence band (acceptor) [20]. Recent research is focused on producing stable catalysts which are economically viable, environmentally inert and visible light active.

Commercially, Mantra Venture Group runs a carbon (CO_2) reduction machine which converts 1 kg of CO_2 per day to formic acid, profitably and which can be reused in steel plants. Interface Europe achieves 90% CO_2 reduction in their process using 100% renewable energy and has attained zero negative impact on the environment.

8.6 Electrochemical Technique

In the electrochemical technique, gaseous CO_2 carbon dioxide and protons from aqueous electrolytes are utilized to produce a variety of low-carbon fuels.

By comparing the reactivity of various processes, the reactivity of electrocatalytic reduction of CO_2 is stated to be higher than bio- and photochemical processes [43]. The electrochemical reduction of CO_2 proceed by adsorbing and activating CO_2 on metal surfaces and Table 8.6 shows the basic anodic and cathodic reactions during the reduction of CO_2.

8.6.1 Advantages of Electrochemical CO_2 Reduction

Electrochemical CO_2 reduction offers numerous benefits in comparison to rest of the technologies like (i) directing the intermediates towards reduction, (ii) modular and quick industrial upgradation, (iii) less formation of by-products, (iv) operation at ambient conditions without any supplementary chemical requirements, (v) avoids complex start-up processes, (vi) offers a simpler and flexible process, (vii) avoids costly high pressure/temperature reactors, (viii) enables the process production rate to be quickly varied with easily switch on/off [20, 44, 45] and (ix) the products of

Table 8.6 Reduction potentials of reactions involved during CO_2 reduction at pH = 7 and unit activity [20]

	E_o, V (vs. NHE)	Eqn. no.
Cathodic reaction		
$2H^+ + 2e^- \rightarrow H_2$	−0.41	8.20
$CO_2 + e^- \rightarrow CO_2^-$	−1.90	8.21
$CO_2 + H^+ + e^- \rightarrow HCO_2^-$	−0.49	8.22
$CO_2 + 2H^+ + 2e^- \rightarrow CO + H_2O$	−0.53	8.23
$CO_2 + 8H^+ + 8e^- \rightarrow CH_4 + 2H_2O$	−0.24	8.24
$2CO_2 + 12H^+ + 12e^- \rightarrow C_2H_4 + 4H_2O$	−0.33	8.25
Anodic reaction		
$2H_2O \rightarrow O_2 + 4H^+ + 4e^-$	+0.82	8.26

electrocatalytic CO_2 reduction rarely need separation, as the mixture of hydrocarbon (methane, ethane) obtained can be used as "hythane" a mixture of hydrogen/natural gas, as a clean alternative fuels in existing transportation sectors [46].

Scale-up studies demonstrated on Sn electrode shows profitable production of formic acid [47, 48]. Interestingly, the capital cost to be invested in the electrochemical reduction of CO_2 is less than carbon capture and storage. The products formed from in this process are easily separable, and its installation is economical than compared to other sophisticated methods like biochemical process. The electrochemical reduction of CO_2 can be made energy (grid) independent by combining with solar, to outperform as a photoelectrochemical reduction in a photovoltaic cell.

8.6.2 Metallic Electrodes in Aqueous Solutions

In general, activation is a reversible alteration of a molecule into a closely identical chemical or physical state that shows an improved tendency to undergo a chemical reaction [49]. Unlike other molecules, CO_2 needs high activation energy for reduction. The applied potential (volts) for the reduction of CO_2 is more negative than the equilibrium values, primarily due to high reorganizational energy among linear molecule and bent radical anion of CO_2. Hence, the one-electron reduction reaction of CO_2 to $CO_2^{\cdot-}$ occurs at −1.9 V, and the rate-determining step has to be achieved before further reactions take place.

Activation and reduction of CO_2 molecule can be subdivided and studied under various subsections such as an electrode, electrolyte and reaction conditions like temperature, pressure and the products formed. Any metal or a semiconductor to be an electrode should have the desired properties shown in Fig. 8.5a.

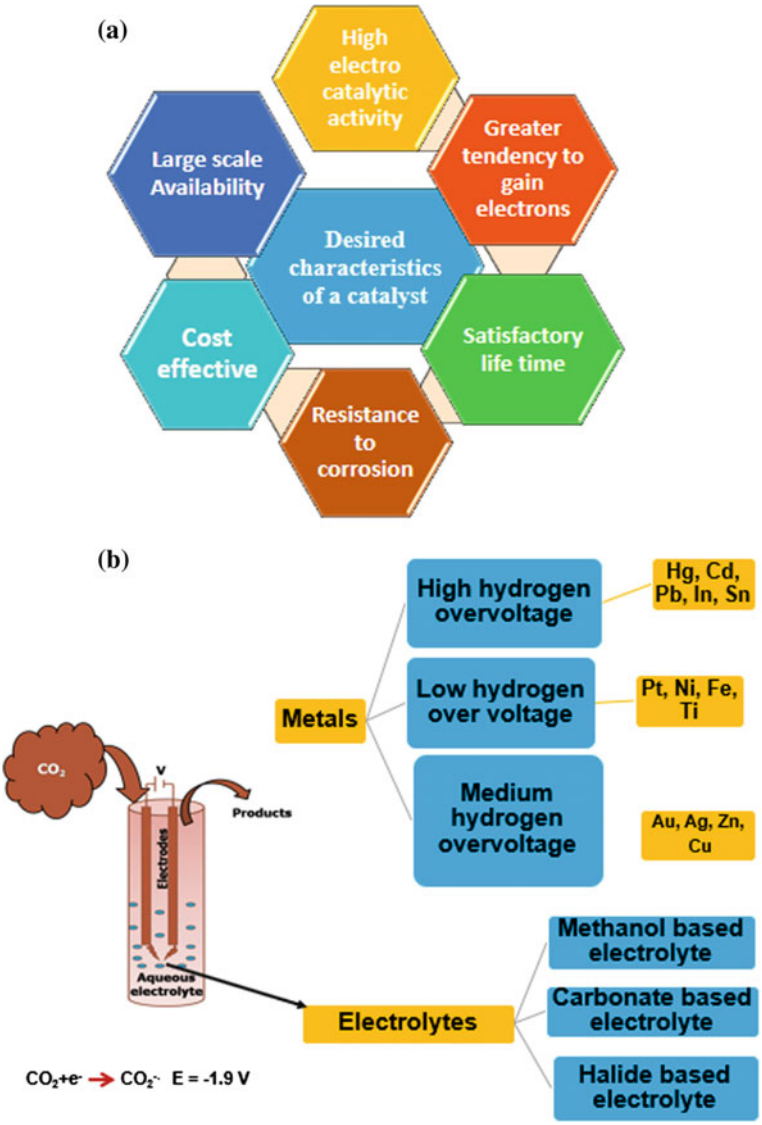

Fig. 8.5 **a** Desired characteristics for electrodes for CO_2 reduction and **b** electrodes classification and electrolytes for electrochemical reduction of CO_2

8.6.3 Classification of the Electrode Material

Homogeneous and heterogeneous catalysts are employed for electrochemical reduction of CO_2. The metallic electrodes can be categorized into four groups based

on the hydrogen overvoltage characteristics for reducing CO_2, in aqueous electrolyte system [17, 50].

- High hydrogen evolution overvoltage metal
- Medium hydrogen evolution overvoltage metal
- Cu-unique metal
- Low hydrogen evolution overvoltage metal

The above classification is schematically represented in Fig. 8.5b. The individual classification of each category is discussed below.

8.6.3.1 High Hydrogen Evolution Overvoltage Metal

Metals like Hg, Pb, Sn, In, Tl, Bi and Cd with high hydrogen evolution overvoltage (HEO) characteristics promote the formation of formate (Table 8.7). They have negligible CO adsorption and hence graded as a poor catalyst towards CO_2 reduction [47, 51]. In this category, Sn and Pb showed promising results to yield formic acid in significant amount [52–54] as discussed in detail below. Formic acid obtained from CO_2 through electrochemical reduction may function as a useful fuel as well as an energy-storage medium owing to its technical feasibility and potential scope for commercial applications. Methanol is commonly used as a CO_2 absorbent in industries, and its solubility in CO_2 is high, approximately five times greater than water. CO_2 dissolved in methanol with Pb electrode was reported for its conversion into formic acid [55]. The product was predominant between −1.8 and −2.5 V versus Ag/AgCl. Other products formed were CO and methane. The partial current density for CO_2 reduction was twenty-two times higher than hydrogen evolution, while the Tafel plot revealed no limitation towards mass transfer in the tested potential range.

8.6.3.2 Medium Hydrogen Evolution Overvoltage Metals

Metals like Zn, Cu, Ga, Au, Pd and Ag, with medium HEO characteristics property, promote the formation of fuel precursor CO. They have weak CO adsorption bond and allow CO to desorb. CO was assumed to be the first intermediate formed on Ag and Au electrode [64–66], while other metals were less exploited towards CO_2 reduction. A summary of the electrochemical reduction of CO_2 on medium hydrogen overvoltage metals like Pd, Ag and Au reported in the literature is presented in Table 8.8.

Table 8.7 Summary of electrochemical reduction of CO_2 on high hydrogen overvoltage metals

Electrode	Electrolyte conditions	Products formed	References
Pb	Methanol	HCOOH	[55]
High hydrogen overvoltage metals	Aqueous	HCOOH	[56]
Pb	K_2CO_3	HCOOH	[57]
Sn–Cu	Aqueous	Formate and H_2, CO, CH_4, C_2H_4	[58]
Pb, Zn on Cu	Methanol	Absence of Cu-HCOOH, CO Presence of Cu-hydrocarbons	[59]
Pb	Aqueous	Formic acid	[60]
Pb in-situ IR studies	Propylene carbonate	Oxalate	[60]
Pb, In-Continuous	Polymer electrolyte	Formate	[51]
Sn (Pilot plant)	NaOH	HCOOH, Formate	[47]
Sn, SnO_x on Ti	$NaHCO_3$		[61]
Sn	$KHCO_3$, K_2SO_4, KCl, Na_2SO_4, Cs_2SO_4, $NaHCO_3$ and $CsHCO_3$		[62]
Sn	Aqueous	Formate	[63]

Table 8.8 Summary of electrochemical reduction of CO_2 on medium hydrogen overvoltage metals

Electrode	Electrolyte conditions	Products formed	References
Pd on Pt wire	$KHCO_3$	Formate	[67]
Pd	$KHCO_3$	HCOOH	[68]
Au, Ag	KOH + methanol electrolyte	HCOOH, CO	[66]
Au microdisc	Dimethyl sulphoxide	Kinetic parameters and charge transfer coefficient study	[69]
Ag	Three phase	CO	[70]
Au film deposited on a polymer membrane		CO	[71]
Ag in ion exchange membrane	K_2SO_4	CO	[72]
Nitrogen-based organometallic Ag-GDE		CO	[73]
Nanoporous Ag	KOH solution	CO	[74]
Oxide-derived Au	$NaHCO_3$	CO	[61]

8.6.3.3 Low Hydrogen Evolution Overvoltage Metal

Metals like Fe, Ni, Ti, Pt, Rh, Co and Ir which exhibit low HEO characteristics and display strong CO adsorption [75]. The literature report in Table 8.9 lists the electrochemical reduction of CO_2 performed on various metals/metal oxides including Ru, Ru/Cu, Ru/Cd and RuO_2/TiO_2. Due to the low turnover of adsorbed CO, they could only evolve hydrogen as the primary product. Some of these metals employed as electrocatalysts for CO_2 conversion are discussed in detail below.

8.6.4 Cu Electrodes

Cu is unique for the reduction of CO_2 as it can favour the breaking of C–O bond in CO_2 and hence facilitate hydrocarbon formation. It was basically derived from the medium HEO group due to its excellent ability to adsorb and desorb metal–carbon bond in electrochemical CO_2 reduction. Comparison of Faradaic efficiency of the products obtained with Cu electrode in various electrolytes is listed in Table 8.10. The key products formed during the electrochemical reduction of CO_2 are hydrocarbons (CH_4) and alcohols [88, 89]. Research has grown in this field using Cu as base metal and understanding CO_2 reduction by varying the supporting electrolyte [66], lowering temperature [59], increasing pressure [90], and also modification by

Table 8.9 Summary of electrochemical reduction of CO_2 on low hydrogen overvoltage metals

Electrode	Electrolyte/ Experimental conditions	Products formed	References
RuO_2/TiO_2	$NaHCO_3$	Methanol	[76]
Ru, Ru/Cu, Ru/Cd	$NaHCO_3$	Methanol	[77]
Ti and hydrogen-storing Ti electrodes	KOH in methanol	Formic acid, CO	[78]
Platinum/Nafion on reticulated vitreous carbon (RVC) electrodes	$HClO_4$, CV and CO adsorption experiments	–	[79]
Modified platinum mesh electrode	KCl + 10% propylene carbonate	Ethanol and lactic acid	[80]
Pt-GDE at high pressures (<50 atm)	$KHCO_3$	Methane, ethanol	[81]
Platinum nanoparticles on carbon black	–	Hydrocarbons > C_5	[82]
Pt/CNT, Fe/CNT	$KHCO_3$	Isopropanol	[83]
Pt/C–TiO_2	0.2 M NaF + 10 mM pyridine	Methanol	[84]

Table 8.10 Comparison of Faradaic efficiency of the products for with Cu electrodes

References	Experimental conditions	Potential (V) versus Ag/AgCl	Faradaic efficiency (%)			
			CH4	Ethylene	Ethane	H_2
[44]	KCl	−1.9	4.1	NA	38.5	61.1
[65]	Cu mesh 3 M KCl (GLS-pH 3)	−2.4	5.1	40.0	0.3	53.2
[44]	$KHCO_3$	−2	19.6	NA	8.9	62.5
[86]	$KHCO_3$	−1.9	Trace	20	Trace	40
[87]	Pulsed electrolysis—$KHCO_3$	−1.8 to −3.2	33.3	25.5	NA	20.5
[85]	Methanol	−3	7.5	6	NA	NA
[59]	LiCl/methanol at 248 K, 10 atm	−2	8	12	NA	5

oxidation [91] and deposition [86]. Figure 8.6a shows various the possibilities of modifying the catalyst surface.

Some of the recent reviews also demonstrate the role of Cu towards CO_2 reduction. The possible modes of adsorption of CO_2 on metal surface as described in Fig. 8.6b can be either by (a) carbon coordination—with the carbon bonded to the electrode surface, (b) oxygen coordination—with either single oxygen or two oxygen bonded to the electrode surface, (c) mixed coordination—with a carbon and oxygen bonded to the electrode surface [92]. Later, Schouten et al. [93] proposed a new mechanistic pathway leading to methane and ethylene with high selectivity during the electrochemical reduction of CO_2 on Cu electrode.

8.6.5 Other Electrodes Towards CO_2 Reduction

Researchers have analysed all possible metals in the periodic table towards CO_2 reduction and based on the behaviour of reduction, a unique grouping of metals was established. Molecular electrocatalysts including bimetallic Cu complexes, rhenium bipyridine complexes, Ni macrocyclic complexes, palladium triphosphine complexes are used [89, 94, 95]. Hara et al. [81] have studied Au, Ag, Zn and In as well as group 8-10 metals comprising Fe, Ni, Rh, Co, Pt and Pd towards CO_2 reduction. The final product composition varied with electrode type and the operating conditions.

Electrochemical reduction of CO_2 in aqueous solution is competed by hydrogen evolution reaction. To overcome this limitation, in our studies, Zn-based electrode was prepared by constant potential deposition on Cu substrate, with high (6 M) concentration (Cu/Zn-H) and low concentration (0.6 M) deposit (Cu/Zn-L). The products from the reduction of CO_2 were methane, ethane and hydrogen. Comparison of the effect of electrode potential for the products formed on Cu/Zn-H and Cu/Zn-L revealed the tendency of high hydrogen evolution (≈59%) and low

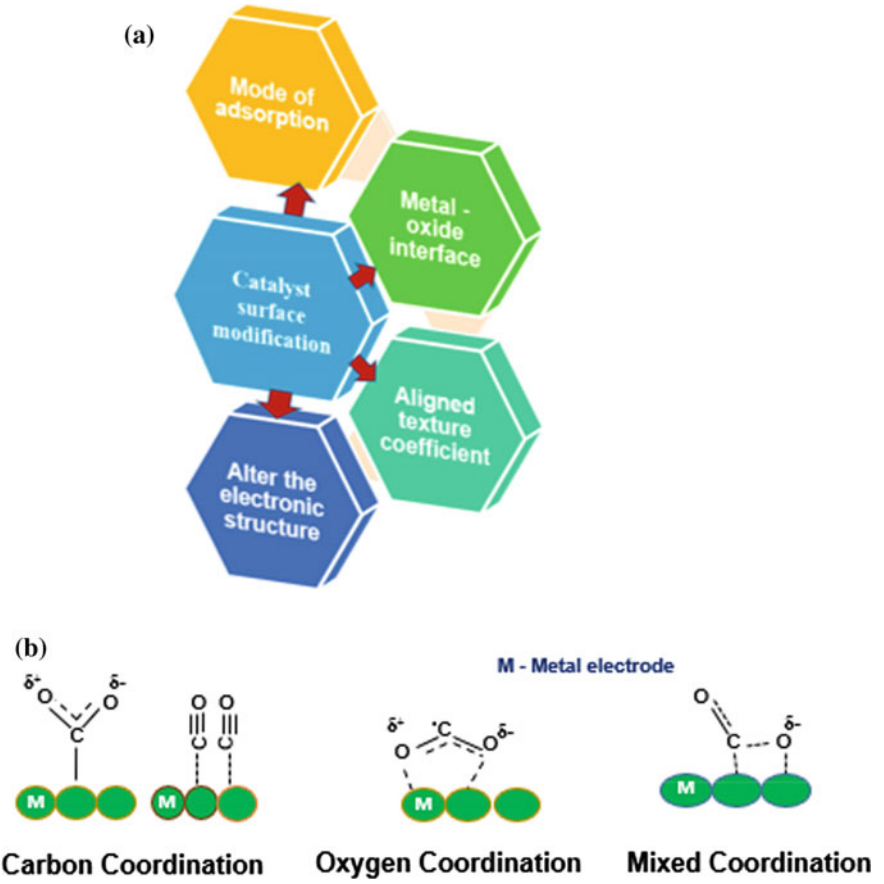

Fig. 8.6 **a** Modification of catalyst surface, **b** possible structure for adsorbed $CO_2^{\delta-}$ on metals surface [82, 92]

methane formation (<15%) on low concentration deposit of Zn on Cu (Cu/Zn-L). High concentration deposit of Zn on Cu (Cu/Zn-H) showed enhanced Faradaic efficiency of methane on Cu/Zn-H (52%) compared to bare Cu (23%) electrodes. Moreover, the efficiency of hydrogen on Cu/Zn (3%) was significantly reduced than Cu electrode (53%). It was proposed that the feasible reaction on Zn electrode is protonation rather than the coupling of carbons to get higher hydrocarbons like Cu electrode [45].

Other than metals, gas diffusion electrodes, semiconductor electrodes, macrocyclic complexes and conducting polymers are also investigated for CO_2 reduction. Among homogeneous and heterogeneous catalysts, the former shows high selectivity and tunability whereas the later show robustness and ease of purification of products. There is an interest to combine these two catalyst surfaces by covalent

bonds by addressing the selectivity issue. Table 8.11 shows the product formed with different metallic structure as the catalyst.

8.6.6 Reaction Mechanism

As listed in Table 8.8, various products are formed in different cathode–electrolyte systems following the reactions listed in Table 8.4. To activate the catalyst surface and reduce CO_2, usually the choice of electrode and electrolyte plays an important role which influences the adsorption of CO_2. KCl and $KHCO_3$ are widely studied for understanding the reaction mechanism [62, 73]. The schematic shows the adsorption of ions on the Cu surface in KCl and $KHCO_3$ electrolytes. Adsorption of KCl and $KHCO_3$ electrolyte on Cu surface which dissociates into K^+, Cl^- and K^+ and HCO_3^- ions as shown in Fig. 8.7. Illustrating the case of KCl electrolyte, the carbon atom of CO_2 links with the Cu atom through Cl^- ion; moreover, Lewis acid of [K^+] or [H^+] links with the oxygen atom of CO_2, initiating the formation of first intermediate CO_2^- in the CO_2 reduction reaction [73]. Incidentally, the drastic change in magnitude of pH before and after the reaction (i.e. from 4.3 to 6.4) favours ethane formation in KCl [17]. Whereas, in $KHCO_3$, equilibrium is maintained between HCO_3^- ions and CO_2 as shown in Fig. 8.7b, and hence, it provides sufficient local dissolved CO_2 between the interface and the electrode [62]. Smaller change in pH (7.2–8.5) was noticed to yield methane as the predominant product. Sequence of mechanistic steps (Eqs. 8.27–8.32) to form methane and ethane during the ECR of CO_2 at Cu electrode are listed in the Table 8.12. Initial rate-determining step of CO_2 reduction (Eq. 8.27) takes place with the aid of electrolyte, and hence, the activation of CO_2 occurs. Once the CO_2 molecule is activated by multipoint adsorption configurations, CO as an intermediate is formed.

Adsorption involving one carbon and one oxygen as shown in Fig. 8.6b as mixed coordination appears to be the most probable mode of adsorption of CO_2 based on the IR spectroscopic investigation [96]. Following this rate-limiting step, $CO_{(ads)}$ through electronation process forms carbon which may clog the active reaction sites. This could be the reason for drop in the activity of the catalyst during

Table 8.11 Products formed at the surface of various cathodes for electrochemical reduction of CO_2

Metal	Product
Hg, Pb, Sn, Cd, In	Formic acid
Zn, Au, Ag	CO
Cu	C_2H_4, CH_4, HCOOH, CO and alcohols
Pt and Pd	Adsorbed CO
Ru	Low yield of alcohols, hydrocarbons and formaldehyde
Fe, Mo, Cr, Nb, Ti,	Poor performance

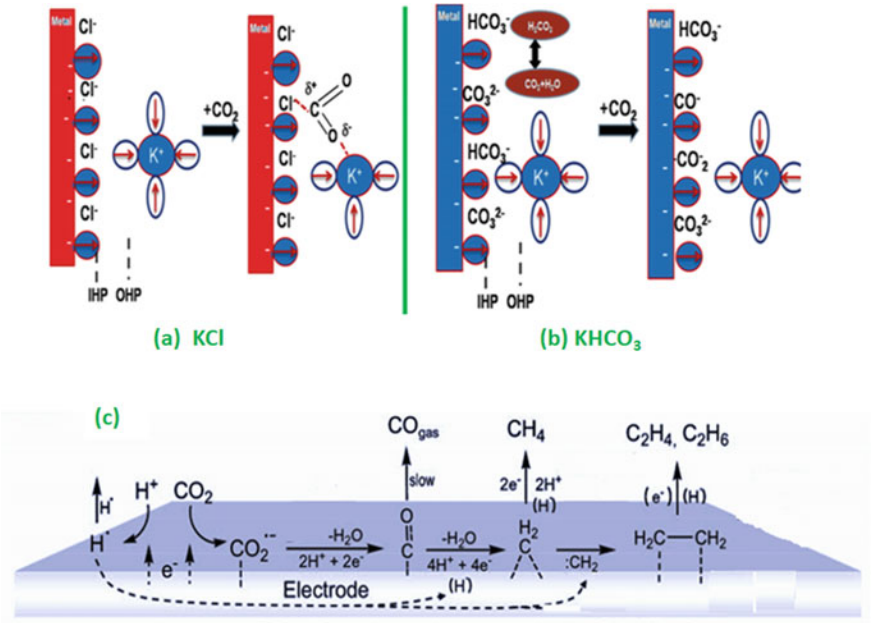

Fig. 8.7 Schematic showing adsorption of ions on the Cu surface in **a** KCl, **b** $KHCO_3$ electrolytes and **c** mechanism for product formation [50]

Table 8.12 Reaction mechanism at Cu electrode during the electrochemical reduction of CO_2

Reaction mechanism	Eqn. no.
$CO_{2(aq)} + e^- \rightarrow CO^{\cdot-}_{2(ads)}$	8.27
$CO^{\cdot-}_{2(ads)} + 2H^+ + e^- \rightarrow CO_{(ads)} + H_2O$	8.28
$CO_{(ads)} + 2H^+ + e^- \rightarrow C_{(ads)} + H_2O$	8.29
$CO_{(ads)} + 4H^+ + e^- \rightarrow \cdot CH_2 + H_2O$	8.30
$\cdot CH_2 + 2H^+ + e^- \rightarrow CH_4$	8.31
$\cdot CH_2 + \cdot CH_2 + 2H^+ + e^- \rightarrow C_2H_6$	8.32

reaction. However, $CO_{(ads)}$ through protonation forms a $^{\cdot}CH_2$ group which tends to stabilize as methane [64]. Based on the crystal planes, pH of the system and applied potential, it can either dimerize with $^{\cdot}CH_2$ group to form ethylene, or dimerization followed by protonation to form ethane [59] as shown in Eqs. 8.31 and 8.32.

8.6.7 Solid Polymer Electrolyte Reactors for Large-Scale CO_2 Sequestration

To overcome the limitations such as high ohmic resistance, mass transfer limitations, increased competitive reactions and possible leakages associated with an aqueous electrolyte, the concept of the solid polymer electrolyte (SPE) is employed. SPE provides good tensile strength, low ohmic resistance, increased electrode life and ease of separation of products [52, 53, 97]. For instance, tin-based gas diffusion electrode (GDE) was used for electrocatalytic reduction of CO_2 [54]. The reduction was carried out in zero gap cell which showed formic acid as the major product. The Faradaic efficiency of formic acid was 18% in the initial 5 min and decreased to 12% at 1 h. Though the formate production was effectively low, the X-ray diffraction analysis proved that the electrode was stable over hours in GDE mode. Economically, electrochemical methods are attractive in terms of operating costs while operating in continuous mode. Solid polymer electrolytic reactors can be employed for processing several tonnes of CO_2 continuously.

8.6.8 Effects of Pressure, Temperature and Supporting Electrolyte

Studies on temperature effect on electrochemical reduction of CO_2 have shown that the formation of hydrocarbon on an oxidized copper electrode was significantly enhanced with increase in temperature, but at the same time, the hydrogen evolution on the electrodes increased indicating that the rate of competitive reaction (by-product formation) is greater than the rate of desired reaction [44]. Hara et al. [81] reported that electroreduction of CO_2 at 30 atm in aqueous $KHCO_3$ solution yielded formic acid and CO as main products 1 atm pressures. Formic acid and CO are the major products under high pressure (30 atm) and hydrogen at 1 atm pressure. Thus, in general, the selectivity of products depended mainly on the balance of the supply of CO_2 to the electrode, the current density and the type of electrode.

Usually, a supporting electrolyte is added to enhance the ionic conductivity of the aqueous solution in which CO_2 is dispersed so as to eliminate the transport of electroactive species by ion migration in the electric field, to eliminate IR drop and to uphold constant ionic strength [11]. The electrolyte medium, which consists of solvent and the supporting electrolyte, exerts a major influence on the nature of the electrochemical processes. The chemical properties of the electrolyte medium affect the electrochemical reaction mechanism. It is understood that the supporting electrolytes influence both the solubility and mechanism of reaction in the course of electroreduction of CO_2. The key electrolytes that are employed for CO_2 reduction can be classified as methanol/supporting salt (KOH, CsOH, RuOH, LiCl, LiBr) added methanol electrolyte, carbonate-based electrolyte ($KHCO_3$, Na_2SO_4, $NaHCO_3$, etc.), halide-based electrolyte (KCl, KBr, KI, etc.).

8.6.9 Hybrid Processes to Enhance Electrochemical Reduction of CO_2

Often a combination of two or more processes make a hybrid system, which makes use of the advantages of the individual processes for enhanced conversion of CO_2. Processes like solar thermochemical reduction of CO_2, photoelectrochemical and bio-photoelectrochemical methods are employed to activate and reduce CO_2 into fuels, and chemicals are also being investigated [14].

For instance, in a relatively new concept known as electrobiocommodities and is in the infancy of development, electrons are straightaway supplied to electrotrophs (micro-organisms) [98, 99], which couples the reduction of carbon dioxide and direct electron consumption [100, 101]. This has the scope of being the straightforward and energy efficient technologies to produce biocommodities using electrical energy. There are numerous vulnerabilities identified by versatility and business aggressiveness forms. Anaerobic techniques in which CO_2 itself can act as an electron acceptor need to be developed rather than developing micro-organisms on electrochemically produced electron donors with O_2 as the electron acceptor. Further understanding of electrode-to-microbe electron exchange mechanism is needed.

8.6.10 Recent Advancements and Future Scope

At the International level, DNV research and innovation of USA has set up a profitable large-scale electrochemical reduction process of CO_2 to formic acid and formate salt conversion. On the other hand, Stanford University focuses on lowering the overpotential of CO_2 reduction towards formic acid using Cu_2O and Ag films. Penn State Institutes of Energy and Environment (EMS energy institute), Princeton University and Iowa State University (Catalysis and Electrochemical Energy Laboratory) in the USA focus on CO_2 conversion and application for sustainable development to fuels and chemicals. The University of Illinois at Urbana—Champaign and International Institute for Carbon-Neutral Energy Research works on Electroreduction of CO_2 as a key component of artificial photosynthesis. NRC-ICPET of Canada looks into the electrocatalytic conversion of carbon dioxide to hydrocarbons in view of upgrading biogas and storage.

Environmental preservation centre of Mie University, Yamaguchi University, Chiba University and Tokyo Institute of Technology, Japan, looks into various aspects of the electrocatalytic conversion of CO_{-2} using CH_3OH as supporting electrolyte (varying electrode and reaction conditions). Long carbon-chain hydrocarbons are derived from CO_2 by Laboratory of Catalysis for Sustainable Production and Energy (CASPE), University of Messina, Italy. Delft University of Technology, the Netherlands, reported an innovation wherein paraffin, as well as olefins up to C_6 hydrocarbons, was produced from CO_2.

In India, government and research institutions are looking at the challenges and strategies of CO_2 reduction and budding out with the ways and means to utilize and mitigate CO_2. Indian Institute of Technology Delhi focuses on the direct electrochemical gaseous reduction of CO_2 on solid polymer electrolytes which yields hydrocarbons and methanol as the product [52, 102, 103]. Indian Institute of Technology Madras along with NCCR, Chennai, focuses on advancement in the electrochemical CO_2 reduction to hydrocarbons on surface-modified Cu and Zn electrodes in aqueous electrolytes [44, 45, 104, 105]. National Institutes and private institutions have taken initiatives to reduce CO_2. Sajjan India Limited, Mumbai, has got its CDM project registered with the United Framework Convention on Climate Change (UNFCCC) under the Kyoto Protocol where it aims to reduce CO_2 emission significantly. Centre for Photoelectrochemical (PEC) Cells and Advanced Ceramics (ARCI, Hyderabad) works on utilizing the solar energy to convert CO_2 into methanol.

Development and characterization of tailored catalysts and studies on the reaction mechanisms in the electrochemical reduction of CO_2 can be the focus areas of research. Effects of heteroatom doping and molecular hybrids are important in carbon as well as the metal–organic framework (MOF)-based catalysts, which are being investigated for the electrochemical reduction of CO_2. Medium hydrogen overvoltage metals such as Cu, Ag, Zn and Au are promising electrocatalysts for the CO_2 reduction. If the challenges such as low electrochemical stability and high overpotential associated with copper and Cu-based materials are addressed, Cu will be the practical catalyst for CO_2 reduction reaction. The parameters that influence the electrochemical activity of the catalyst, such as, particle size, crystal facet, grain boundary, metal valence, oxidation state, heteroatom configuration and organic hybrid also need detailed investigation. Arriving at an innovative electrocatalyst with its optimized parameters of reduction (electrolyte, potential and time of reduction) will be a gateway in dealing with the complicated process of reducing CO_2. CO_2 sequestration needs to be evaluated and applied properly to protect our environment and resources.

8.7 Conclusion and Perspectives

In this chapter, a general introduction to the recent energy and environmental scenario is addressed. A brief overview of CO_2 emission with a detailed description of CO_2 molecule and the ways and means available for its mitigation is discussed. The need for mitigation of greenhouse gas emissions in today's scenario is highlighted, followed by the foundation to the conversion of CO_2 into useful chemicals. Various techniques employed for CO_2 sequestration are introduced, and electrochemical reduction of CO_2 is selected owing to its technological advantages and simplicity. Background and application of electrochemical reduction of CO_2 using homogeneous and heterogeneous catalysts are discussed. In aqueous solution, electrochemical reduction of CO_2 is competed by hydrogen evolution reaction. In

an attempt to mitigate the hydrogen evolution, deposition of Zn on Cu showed enhanced Faradaic efficiency of methane (52%) compared to bare Cu (23%) electrode. Moreover, the Faradaic efficiency of hydrogen on Cu/Zn (3%) was significantly reduced than on a Cu electrode (53%). Development of efficient electrocatalyst and prototype modules similar to that of commercially available H_2O electrolyser will pave the way for commercialization of CO_2 reduction. Furthermore, direct reduction of CO_2 in solid polymer electrolyte reactors has the potential for large-scale treatment and industrial applications. Combination of hybrid process such as the photoelectrocatalytic and/or bio-electrochemical processes may assist in addressing the economic and productivity challenges. Arriving at an innovative electrocatalyst with optimized parameters of reduction (electrolyte, potential and time of reduction) will be a gateway in the reduction of CO_2.

References

1. Dlugokencky E, Tans P (2016) NOAA/ESRL. www.esrl.noaa.gov/gmd/ccgg/trends/. Retrieved on 4th Aug 2018
2. Li M (2017) World energy 2017–2050: annual report
3. Chen Y, Jiang W, Liang DT, Tay JH (2008) Biodegradation and kinetics of aerobic granules under high organic loading rates in sequencing batch reactor. Appl Microbiol Biotechnol 79 (2):301–308
4. Parry M, Parry ML, Canziani O, Palutikof J, Van der Linden P, Hanson C (eds) (2007) Climate change 2007-impacts, adaptation and vulnerability: working group II contribution to the fourth assessment report of the IPCC, vol 4. Cambridge University Press, Cambridge
5. GHG Platform India (2017) Trend analysis of GHG emissions in India, Sept 2017. http://www.ghgplatform-india.org. Retrieved on 4th July 2018
6. Rosso D, Stenstrom MK (2008) The carbon-sequestration potential of municipal wastewater treatment. Chemosphere 70(8):1468–1475
7. ElMekawy A, Hegab HM, Mohanakrishna G, Elbaz AF, Bulut M, Pant D (2016) Technological advances in CO_2 conversion electro-biorefinery: a step toward commercialization. Biores Technol 215:357–370
8. Intergovernmental Panel on Climate Change (IPCC) (2018) Assessments of climate change. http://www.ipcc.ch. Retrieved on 07.08.2018
9. Metz B (ed) (2005) Carbon dioxide capture and storage: special report of the intergovernmental panel on climate change. Cambridge University Press, Cambridge
10. Housecroft CE, Sharpe AG (2008) Inorganic chemistry, 3rd edn. Prentice Hall, New Jersey
11. Bumroongsakulsawat P, Kelsall GH (2014) Effect of solution pH on CO: formate formation rates during electrochemical reduction of aqueous CO_2 at Sn cathodes. Electrochim Acta 141:216–225
12. MacDowell N, Florin N, Buchard A, Hallett J, Galindo A, Jackson G, Fennell P (2010) An overview of CO_2 capture technologies. Energy Environ Sci 3(11):1645–1669
13. Green DW (2008) Perry's chemical engineers' handbook. McGraw Hill, New York
14. Scibioh MA, Viswanathan B (2004) Electrochemical reduction of carbon dioxide: a status report. In: Proceedings of national academy of science, vol 70, pp 1–56
15. Song C (2006) Global challenges and strategies for control, conversion and utilization of CO_2 for sustainable development involving energy, catalysis, adsorption and chemical processing. Catal Today 115(1–4):2–32

16. Olah GA, Goeppert A, Prakash GS (2011) Beyond oil and gas: the methanol economy. Wiley, New Jersey
17. Gattrell M, Gupta N (2006) A review of the aqueous electrochemical reduction of CO_2 to hydrocarbons at copper. J Electroanal Chem 594(1):1–19
18. Viswanathan B (2011) Reflections on the electrochemical reduction of carbon dioxide on metallic surfaces. Indian J Chem Sec A 51:166–174
19. Zhang HB, Liang XL, Dong X, Li HY, Lin GD (2009) Multi-walled carbon nanotubes as a novel promoter of catalysts for CO/CO_2 hydrogenation to alcohols. Catal Surv Asia 13 (1):41–58
20. Smith YR, Subramanian V, Viswanathan B (2012) Photo-electrochemical and photo-catalytic conversion of carbon dioxide. Photo-Electrochem Photo-Biol Sustain 1:155–182
21. Yagi F, Kanai R, Wakamatsu S, Kajiyama R, Suehiro Y, Shimura M (2005) Development of synthesis gas production catalyst and process. Catal Today 104(1):2–6
22. Atsumi S, Higashide W, Liao JC (2009) Direct photosynthetic recycling of carbon dioxide to isobutyraldehyde. Nat Biotechnol 27(12):1177
23. Spinner NS, Vega JA, Mustain WE (2012) Recent progress in the electrochemical conversion and utilization of CO_2. Catal Sci Technol 2(1):19–28
24. Soussan L, Riess J, Erable B, Delia ML, Bergel A (2013) Electrochemical reduction of CO_2 catalysed by *Geobacter sulfurreducens* grown on polarized stainless steel cathodes. Electrochem Commun 28:27–30
25. Lovley DR, Nevin KP (2013) Electrobiocommodities: powering microbial production of fuels and commodity chemicals from carbon dioxide with electricity. Curr Opin Biotechnol 24(3):385–390
26. Herzog H (2002) Carbon sequestration via mineral carbonation: overview and assessment. Massachusetts Institute of Technology, Laboratory for Energy and the Environment, Cambridge, Massachusetts
27. Spath PL, Mann MK (2004) Biomass power and conventional fossil systems with and without CO_2 sequestration—comparing the energy balance, greenhouse gas emissions and economics (No. NREL/TP-510-32575). National Renewable Energy Lab, Golden, CO (US)
28. Licht S, Wang B, Ghosh S, Ayub H, Jiang D, Ganley J (2010) A new solar carbon capture process: solar thermal electrochemical photo (STEP) carbon capture. J Phys Chem Lett 1 (15):2363–2368
29. Loutzenhiser PG, Meier A, Gstoehl D, Steinfeld A (2010) CO_2 splitting via the solar thermochemical cycle based on Zn/ZnO redox reactions. In: Advances in CO_2 conversion and utilization, vol 1056, pp 25–30. American Chemical Society, Washington
30. Otake K, Kinoshita H, Kikuchi T, Suzuki RO (2012) CO_2 decomposition using electrochemical process in molten salts. J Phys Conf Ser 379(1):012038
31. White JL, Baruch MF, Pander JE III, Hu Y, Fortmeyer IC, Park JE, Zhang T, Liao K, Gu J, Yan Y, Shaw TW (2015) Light-driven heterogeneous reduction of carbon dioxide: photocatalysts and photoelectrodes. Chem Rev 115(23):12888–12935
32. Habisreutinger SN, Schmidt-Mende L, Stolarczyk JK (2013) Photocatalytic reduction of CO_2 on TiO_2 and other semiconductors. Angew Chem Int Ed 52(29):7372–7408
33. Xia XH, Jia ZJ, Yu Y, Liang Y, Wang Z, Ma LL (2007) Preparation of multi-walled carbon nanotube supported TiO_2 and its photocatalytic activity in the reduction of CO_2 with H_2O. Carbon 45(4):717–721
34. Wang J, Ji G, Liu Y, Gondal MA, Chang X (2014) Cu_2O/TiO_2 heterostructure nanotube arrays prepared by an electrodeposition method exhibiting enhanced photocatalytic activity for CO_2 reduction to methanol. Catal Commun 46:17–21
35. Varghese OK, Paulose M, LaTempa TJ, Grimes CA (2009) High-rate solar photocatalytic conversion of CO_2 and water vapour to hydrocarbon fuels. Nano Lett 9(2):731–737
36. Mao J, Li K, Peng T (2013) Recent advances in the photocatalytic CO_2 reduction over semiconductors. Catal Sci Technol 3(10):2481–2498

37. Wu JC, Wu TH, Chu T, Huang H, Tsai D (2008) Application of optical-fiber photoreactor for CO_2 photocatalytic reduction. Top Catal 47(3–4):131–136
38. Arai T, Sato S, Kajino T, Morikawa T (2013) Solar CO_2 reduction using H_2O by a semiconductor/metal-complex hybrid photocatalyst: enhanced efficiency and demonstration of a wireless system using $SrTiO_3$ photoanodes. Energy Environ Sci 6(4):1274–1282
39. Halmann M, Ulman M, Aurian-Blajeni B (1983) Photochemical solar collector for the photoassisted reduction of aqueous carbon dioxide. Sol Energy 31:429–431
40. Grills DC, Fujita E (2010) New directions for the photocatalytic reduction of CO_2: supramolecular, $scCO_2$ or biphasic ionic liquid—$scCO_2$ systems. J Phys Chem Lett 1 (18):2709–2718
41. Iizuka K, Wato T, Miseki Y, Saito K, Kudo A (2011) Photocatalytic reduction of carbon dioxide over Ag cocatalyst-loaded $ALa_4Ti_4O_{15}$ (A=Ca, Sr, and Ba) using water as a reducing reagent. J Am Chem Soc 133(51):20863–20868
42. Qin G, Zhang Y, Ke X, Tong X, Sun Z, Liang M, Xue S (2013) Photocatalytic reduction of carbon dioxide to formic acid, formaldehyde, and methanol using dye-sensitized TiO_2 film. Appl Catal B 129:599–605
43. Shibata H (2009) Electrocatalytic CO_2 reduction: catalysis engineering and reaction mechanism. Doctoral dissertation, TU Delft, Delft University of Technology
44. Keerthiga G, Viswanathan B, Chetty R (2015) Electrochemical reduction of CO_2 on electrodeposited Cu electrodes crystalline phase sensitivity on selectivity. Catal Today 245:68–73
45. Keerthiga G, Chetty R (2017) Electrochemical reduction of carbon dioxide on zinc-modified copper electrodes. J Electrochem Soc 164:H164–H169
46. Ortenzi F, Chiesa M, Scarcelli R, Pede G (2008) Experimental tests of blends of hydrogen and natural gas in light-duty vehicles. Int J Hydrogen Energy 33(12):3225–3229
47. Agarwal AS, Zhai Y, Hill D, Sridhar N (2011) The electrochemical reduction of carbon dioxide to formate/formic acid: engineering and economic feasibility. Chemsuschem 4 (9):1301–1310
48. Dominguez-Ramos A, Singh B, Zhang X, Hertwich EG, Irabien A (2015) Global warming footprint of the electrochemical reduction of carbon dioxide to formate. J Clean Prod 104:148–155
49. Vayenas CG, Bebelis S, Pliangos C, Brosda S, Tsiplakides D (2001) Electrochemical activation of catalysis: promotion, electrochemical promotion, and metal-support interactions. Springer Science & Business Media, Berlin
50. Gattrell M, Gupta N (2007) Electrochemical reduction of CO_2 to hydrocarbons to store renewable electrical energy and upgrade biogas. Energy Convers Manage 48(4):1255–1265
51. Narayanan SR, Haines B, Soler J, Valdez TI (2011) Electrochemical conversion of carbon dioxide to formate in alkaline polymer electrolyte membrane cells. J Electrochem Soc 158 (2):A167–A173
52. Aeshala LM, Uppaluri RG, Verma A (2013) Effect of cationic and anionic solid polymer electrolyte on direct electrochemical reduction of gaseous CO_2 to fuel. J CO_2 Utilization 3:49–55
53. Aeshala LM, Rahman SU, Verma A (2012) Effect of solid polymer electrolyte on electrochemical reduction of CO_2. Sep Purif Technol 94:131–137
54. Machunda RL, Ju H, Lee J (2011) Electrocatalytic reduction of CO_2 gas at Sn based gas diffusion electrode. Curr Appl Phys 11(4):986–988
55. Kaneko H, Nozaki K, Ozawa T, Oku K, Shimanuki T, Koga Y (1988) U.S. patent no. 4,732,827. U.S. Patent and Trademark Office, Washington, DC
56. Chaplin RPS, Wragg AA (2003) Effects of process conditions and electrode material on reaction pathways for carbon dioxide electroreduction with particular reference to formate formation. J Appl Electrochem 33(12):1107–1123
57. Köleli F, Balun D (2004) Reduction of CO_2 under high pressure and high temperature on Pb-granule electrodes in a fixed-bed reactor in aqueous medium. Appl Catal A 274(1–2):237–242

58. Li H, Oloman C (2005) The electro-reduction of carbon dioxide in a continuous reactor. J Appl Electrochem 35(10):955–965
59. Kaneco S, Katsumata H, Suzuki T, Ohta K (2006) Electrochemical reduction of carbon dioxide to ethylene at a copper electrode in methanol using potassium hydroxide and rubidium hydroxide supporting electrolytes. Electrochim Acta 51(16):3316–3321
60. Innocent B, Liaigre D, Pasquier D, Ropital F, Léger JM, Kokoh KB (2009) Electro-reduction of carbon dioxide to formate on lead electrode in aqueous medium. J Appl Electrochem 39(2):227
61. Chen Y, Li CW, Kanan MW (2012) Aqueous CO_2 reduction at very low overpotential on oxide-derived Au nanoparticles. J Am Chem Soc 134(49):19969–19972
62. Wu J, Risalvato FG, Ke FS, Pellechia PJ, Zhou XD (2012) Electrochemical reduction of carbon dioxide I. Effects of the electrolyte on the selectivity and activity with Sn electrode. J Electrochem Soc 159(7):F353–F359
63. Alvarez-Guerra M, Del Castillo A, Irabien A (2014) Continuous electrochemical reduction of carbon dioxide into formate using a tin cathode: comparison with lead cathode. Chem Eng Res Des 92(4):692–701
64. Kaneco S, Iiba K, Hiei NH, Ohta K, Mizuno T, Suzuki T (1999) Electrochemical reduction of carbon dioxide to ethylene with high Faradaic efficiency at a Cu electrode in CsOH/methanol. Electrochim Acta 44(26):4701–4706
65. Yano H, Tanaka T, Nakayama M, Ogura K (2004) Selective electrochemical reduction of CO_2 to ethylene at a three-phase interface on copper (I) halide-confined Cu-mesh electrodes in acidic solutions of potassium halides. J Electroanal Chem 565(2):287–293
66. Kaneco S, Hiei NH, Xing Y, Katsumata H, Ohnishi H, Suzuki T, Ohta K (2002) Electrochemical conversion of carbon dioxide to methane in aqueous $NaHCO_3$ solution at less than 273 K. Electrochim Acta 48(1):51–55
67. Podlovchenko BI, Kolyadko EA, Lu S (1994) Electroreduction of carbon dioxide on palladium electrodes at potentials higher than the reversible hydrogen potential. J Electroanal Chem 373(1–2):185–187
68. Yoshitake H, Kikkawa T, Muto G, Ota KI (1995) Poisoning of surface hydrogen processes on a Pd electrode during electrochemical reduction of carbon dioxide. J Electroanal Chem 396(1–2):491–498
69. Welford PJ, Brookes BA, Wadhawan JD, McPeak HB, Hahn CE, Compton RG (2001) The electro-reduction of carbon dioxide in dimethyl sulfoxide at gold microdisk electrodes: current|voltage waveshape analysis. J Phys Chem B 105(22):5253–5261
70. Yano H, Shirai F, Nakayama M, Ogura K (2002) Electrochemical reduction of CO_2 at three-phase (gas| liquid| solid) and two-phase (liquid| solid) interfaces on Ag electrodes. J Electroanal Chem 533(1–2):113–118
71. Stevens GB, Reda T, Raguse B (2002) Energy storage by the electrochemical reduction of CO_2 to CO at a porous Au film. J Electroanal Chem 526(1–2):125–133
72. Hori Y, Ito H, Okano K, Nagasu K, Sato S (2003) Silver-coated ion exchange membrane electrode applied to electrochemical reduction of carbon dioxide. Electrochim Acta 48 (18):2651–2657
73. Tornow CE, Thorson MR, Ma S, Gewirth AA, Kenis PJ (2012) Nitrogen-based catalysts for the electrochemical reduction of CO_2 to CO. J Am Chem Soc 134(48):19520–19523
74. Lu X, Leung DY, Wang H, Leung MK, Xuan J (2014) Electrochemical reduction of carbon dioxide to formic acid. ChemElectroChem 1(5):836–849
75. Marcos ML, González-Velasco J, Bolzán AE, Arvia AJ (1995) Comparative electrochemical behaviour of CO_2 on Pt and Rh electrodes in acid solution. J Electroanal Chem 395(1–2):91–98
76. Qu J, Zhang X, Wang Y, Xie C (2005) Electrochemical reduction of CO_2 on RuO-/TiO_2 nanotubes composite modified Pt electrode. Electrochim Acta 50(16–17):3576–3580
77. Popić JP, Avramov-Ivić ML, Vuković NB (1997) Reduction of carbon dioxide on ruthenium oxide and modified ruthenium oxide electrodes in 0.5 M $NaHCO_3$. J Electroanal Chem 421 (1–2):105–110

78. Mizuno T, Kawamoto M, Kaneco S, Ohta K (1998) Electrochemical reduction of carbon dioxide at Ti and hydrogen-storing Ti electrodes in KOH–methanol. Electrochim Acta 43 (8):899–907
79. Huang M, Faguy PW (1996) Carbon dioxide reduction on platinum |Nafion®| carbon electrodes. J Electroanal Chem 406(1–2):219–222
80. Ogura K, Endo N (1999) Electrochemical Reduction of CO_2 with a functional gas-diffusion electrode in aqueous solutions with and without propylene carbonate. J Electrochem Soc 146 (10):3736–3740
81. Hara K, Kudo A, Sakata T (1995) Electrochemical reduction of carbon dioxide under high pressure on various electrodes in an aqueous electrolyte. J Electroanal Chem 391(1–2):141–147
82. Centi G, Perathoner S, Winè G, Gangeri M (2007) Electrocatalytic conversion of CO_2 to long carbon-chain hydrocarbons. Green Chem 9(6):671–678
83. Gangeri M, Perathoner S, Caudo S, Centi G, Amadou J, Begin D, Schlögl R (2009) Fe and Pt carbon nanotubes for the electrocatalytic conversion of carbon dioxide to oxygenates. Catal Today 143(1–2):57–63
84. de Tacconi NR, Chanmanee W, Dennis BH, MacDonnell FM, Boston DJ, Rajeshwar K (2011) Electrocatalytic reduction of carbon dioxide using Pt/C-TiO_2 nanocomposite cathode. Electrochem Solid-State Lett 15(1):B5–B8
85. Ohya S, Kaneco S, Katsumata H, Suzuki T, Ohta K (2009) Electrochemical reduction of CO_2 in methanol with aid of CuO and Cu_2O. Catal Today 148(3–4):329–334
86. Goncalves MR, Gomes A, Condeço J, Fernandes TRC, Pardal T, Sequeira CAC, Branco JB (2013) Electrochemical conversion of CO_2 to C_2 hydrocarbons using different ex situ copper electrodeposits. Electrochim Acta 102:388–392
87. Yano J, Morita T, Shimano K, Nagami Y, Yamasaki S (2007) Selective ethylene formation by pulse-mode electrochemical reduction of carbon dioxide using copper and copper-oxide electrodes. J Solid State Electrochem 11(4):554–557
88. Jiang Z, Xiao T, Kuznetsov VÁ, Edwards PÁ (2010) Turning carbon dioxide into fuel. Philos Trans Roy Soc Lond A Math Phys Eng Sci 368(1923):3343–3364
89. Wu J, Zhou XD (2016) Catalytic conversion of CO_2 to value added fuels: current status, challenges, and future directions. Chin J Catal 37(7):999–1015
90. Hara K, Tsuneto A, Kudo A, Sakata T (1994) Electrochemical reduction of CO_2 on a Cu electrode under high pressure factors that determine the product selectivity. J Electrochem Soc 141(8):2097–2103
91. Li CW, Kanan MW (2012) CO_2 reduction at low overpotential on Cu electrodes resulting from the reduction of thick Cu_2O films. J Am Chem Soc 134(17):7231–7234
92. Kabir K (2016) Surface acoustic wave based sensors for selective detection of low concentration elemental mercury vapour
93. Schouten KJP, Kwon Y, Van der Ham CJM, Qin Z, Koper MTM (2011) A new mechanism for the selectivity to C_1 and C_2 species in the electrochemical reduction of carbon dioxide on copper electrodes. Chem Sci 2(10):1902–1909
94. Ogura K, Ferrell JR III, Cugini AV, Smotkin ES, Salazar-Villalpando MD (2010) CO_2 attraction by specifically adsorbed anions and subsequent accelerated electrochemical reduction. Electrochim Acta 56(1):381–386
95. Kondratenko EV, Mul G, Baltrusaitis J, Larrazábal GO, Pérez-Ramírez J (2013) Status and perspectives of CO_2 conversion into fuels and chemicals by catalytic, photocatalytic and electrocatalytic processes. Energy Environ Sci 6(11):3112–3135
96. Ryczkowski J (2001) IR spectroscopy in catalysis. Catal Today 68:263–381
97. Rajmohan KS, Chetty R (2017) Enhanced nitrate reduction with copper phthalocyanine-coated carbon nanotubes in a solid polymer electrolyte reactor. J Appl Electrochem 47(1):63–74
98. Wang J (2006) Analytical electrochemistry. Wiley, New Jersey
99. Lovley DR (2011) Powering microbes with electricity: direct electron transfer from electrodes to microbes. Environ Microbiol Rep 3(1):27–35

100. Nevin KP, Woodard TL, Franks AE, Summers ZM, Lovley DR (2010) Microbial electrosynthesis: feeding microbes electricity to convert carbon dioxide and water to multicarbon extracellular organic compounds. MBio 1(2):e00103–e00110
101. Nevin KP, Hensley SA, Franks AE, Summers ZM, Ou J, Woodard TL, Snoeyenbos-West OL, Lovley DR (2011) Electrosynthesis of organic compounds from carbon dioxide catalyzed by a diversity of acetogenic microorganisms. Appl Environ Microbiol 77 (9):2882-2886. https://doi.org/10.1128/AEM.02642-10
102. Malik K, Singh S, Basu S, Verma A (2017) Electrochemical reduction of CO_2 for synthesis of green fuel. Wiley Interdisc Rev Energy Environ 6(4):e244
103. Singh S, Gautam RK, Malik K, Verma A (2017) Ag-Co bimetallic catalyst for electrochemical reduction of CO_2 to value added products. J CO_2 Utilization 18:139–146
104. Keerthiga G, Viswanathan B, Chetty R (2018) Effect of bicarbonate and chloride electrolytes on product distribution for CO_2 electrochemical reduction on Cu electrode. Catal Green Chem Eng 1(2)
105. Keerthiga G, Viswanathan B, Pulikottil CA, Chetty R (2012) Electrochemical reduction of carbon dioxide at surface oxidized copper electrodes. Bonfring Int J Ind Eng Manage Sci 2 (1):41–43

Chapter 9
The Utilization of CO_2, Alkaline Solid Waste, and Desalination Reject Brine in Soda Ash Production

Dang Viet Quang, Abdallah Dindi and Mohammad R. M. Abu Zahra

Abstract Conventional Solvay process, which utilizes CO_2 to synthesize sodium carbonate, has been well-known for more than a century, but the only purpose of this process is to produce soda ash. Annually, significant amounts of CO_2 are converted into soda ash using Solvay process; however, this conventional process does not sustain CO_2 and waste cycle. Increasing the awareness of global warming and climate change linking to CO_2 emission has pressured this industry to move for a more eco-friendly process that should exploit its potential for CO_2 utilization and sequestration and thus contribute to both CO_2 emission and waste management. In conventional Solvay process, to produce one mole of Na_2CO_3, at least one mole of CO_2 might be emitted to atmosphere due to the use of CaO. Therefore, a number of studies have been done to explore novel processes or to modify the Solvay process in order for it to engage more in CO_2 mitigation. This chapter introduces the most up-to-date modified Solvay process and novel pathways to produce soda ash and baking soda in the consideration of waste and CO_2 utilization. Simultaneous waste and CO_2 utilization offers a great opportunity for shifting to a green production, not only soda ash industry but others where their exhausted CO_2, alkaline solid wastes, or reject brine can be utilized. However, there are challenges which require further research and technological development initiatives for the idea to be industrially implemented.

Keywords Soda ash · CO_2 utilization · CO_2 emission · Reject brine
Slag · Fly ash · Layered double hydroxide · Hydrotalcite · Solvay process

D. V. Quang · A. Dindi · M. R. M. Abu Zahra (✉)
Department of Chemical Engineering, Khalifa University of Science and Technology, Masdar City P.O. Box 54224, Abu Dhabi, United Arab Emirates
e-mail: mabuzahra@masdar.ac.ae

F. Winter et al. (eds.), *CO_2 Separation, Purification and Conversion to Chemicals and Fuels*, Energy, Environment, and Sustainability,
https://doi.org/10.1007/978-981-13-3296-8_9

Nomenclature

C_3A	$Ca_3Al_2O_6$
H	H_2O
AN	NH_4NO_3
AC	NH_4Cl
AA	CH_3COONH_4
AS	$(NH_4)_2SO_4$
MAE	Methyl aminoethanol
LDH	Al layered double hydroxide
HT	Hydrotalcite-like materials
Cl–HT	Chloride-form hydrotalcite
AOD	Argon oxygen decarburization
BOF	Basic oxygen furnace
BF	Blast furnace
EAF	Electric arc furnace
MW	Municipal solid waste
XRD	X-ray diffraction
EDS	Energy dispersive X-ray spectroscopy

9.1 Potential Contribution of Inorganic Waste in CO_2 Emission Mitigation

9.1.1 Carbon Utilization with Alkaline Solid Waste

Industrial wastes such as slag or fly ash may have composition similar to cement; therefore, they have great potential to use as active additives to replace a certain fraction of cement in concrete [1–3]. Recent study indicated that the strength of cement mortar can be significantly enhanced by adding carbonated slag or fly ash [4, 5]. These wastes contain significant amount of CaO and MgO which has been extensively investigated for CO_2 sequestration [6]. The most effective CO_2 sequestration for those wastes is gas–liquid method in which slag is dispersed in water and then CO_2 gas is introduced into the slurry. Divalent ions such as Ca^{2+} leached from slag react with dissolved CO_2 according to Eqs. 9.1–9.3 to form calcium carbonate [7–9]. The $CaCO_3$ reacts with $Ca_3Al_2O_6$ (C_3A) phase in concrete as shown in Eq. 9.4 that results in the formation of calcium carboaluminate hydrate ($C_3A \cdot CaCO_3 \cdot 11H$, where H stands for H_2O) and ($C_3A \cdot 0.5CaCO_3 \cdot 0.5Ca(OH)_2 \cdot 11.5H$). The formation of calcium carboaluminate hydrate could contribute to enhance the mechanical strength of concrete [4]. With an estimated 400 million tonnes of iron and steel slag (for every tonne of steel produced, two tonnes of CO_2 emission, 400 kg of blast and basic oxygen furnace slag, and 200 kg of electric arc furnace slag are generated) [10], 750 million tonnes of fly ash from coal-fired power plant [11], and huge quantity of

alkaline waste from other industries' discharges annually, this alternative could contribute to reduce a great amount of CO_2 emission.

$$H_2O + CO_2 \rightarrow H_2CO_3 \rightarrow 2H^+ + CO_3^{2+} \tag{9.1}$$

$$CaO + H_2O \rightarrow Ca^{2+} + 2OH^- \tag{9.2}$$

$$Ca^{2+} + CO_3^{2-} \rightarrow CaCO_3 \tag{9.3}$$

$$\begin{aligned} 2C_3A + 1.5\ CaCO_3 + 0.5Ca(OH)_2 + 22.5H \rightarrow C_3A \cdot CaCO_3 \cdot 11H \\ + C_3A \cdot 0.5CaCO_3 \cdot 0.5Ca(OH)_2 \cdot 11.5H \end{aligned} \tag{9.4}$$

Global phosphate industry, mainly fertilizer producers, discharges approximately over 200 million tonnes of phosphogypsum annually (4.5–5.5 tonnes for one tonne of P_2O_5 produced), and about 85% of this is disposed without any treatment [12, 13]. This waste is dumped in large stockpile causing serious environmental impact. Phosphogypsum has high content of calcium sulfate, about 24–34 wt% as CaO and 48–58 wt% as SO_3. This make it high potential for CO_2 utilization and sequestration [14–20]. However, not only sequestration, this solid waste could be converted to marketable $(NH_4)_2SO_4$ fertilizer [21]. CO_2 utilization and $(NH_4)_2SO_4$ fertilizer production is based on the conventional Merseburg process in which $CaSO_4$ reacts with $(NH_4)_2CO_3$ to form $CaCO_3$ and $(NH_4)_2SO_4$ as Eq. 9.5 [22, 23].

$$CaSO_4 \cdot 2H_2O + (NH_4)_2CO_3 \rightarrow (NH_4)_2SO_4 + CaCO_3 + 2H_2O \tag{9.5}$$

$$CaSO_4 \cdot 2H_2O + 2NH_4OH + CO_2 \rightarrow (NH_4)_2SO_4 + CaCO_3 + 3H_2O \tag{9.6}$$

Conventionally, $(NH_4)_2CO_3$ that previously produced by bubbling CO_2 into ammonium solution is added into the slurry of gypsum or phosphogypsum. Recent studies reveal that bubbling CO_2 or flue gas directly into ammonium-saturated phosphogypsum solution helps reduce reaction process from two steps to one step which could result in saving expense and lower production cost [8, 24, 25]. This modified Merseburg process is chemically described in Eq. 9.6. Accordingly, for every tonne of $(NH_4)_2SO_4$ produced, 0.9 tonnes of $CaCO_3$ is generated which can permanently sequester 0.4 tonnes of CO_2, and 1.6 tonnes of waste gypsum is consumed [25]. With over 200 million tonnes of phosphogypsum from phosphate industry together with significant amount gypsum from flue gas desulfurization process in power plant [24], its reveals the high potential of gypsum waste and CO_2 utilization to produce marketable products such as $CaCO_3$ and $(NH_4)_2SO_4$.

9.1.2 CO_2 Utilization with Aqueous Inorganic Waste

Beside the solid alkaline wastes that contain mainly Ca^{2+} and Mg^{2+} with the large capacity of CO_2 sequestration, there are also aqueous solution wastes that have high

concentration of Na^+, Mg^{2+}, and Ca^{2+} such as reject brine from desalination plant [26, 27], saline brine from CO_2 storage sites [28] or textile industry [29]. High demand on clean water due to the world population growth and scarcity of freshwater has driven the increase in the deployment of desalination plants worldwide. Desalination has become an important source of drinking water production with the capacity of estimated >86 million m^3/day from >18,000 plants in 2015 [28]. Over 15,000 desalination plants were installed in 2009 in which reverse osmosis technology accounted for 80% and global market for reverse osmosis alone is predicted to reach $8.1 billion by 2018 [30–32]. Desalination is the most viable way that can produce enough clean water to meet the high demand. However, this method faces some issues that are high energy consumption and reject brine management and disposal. According to Dawoud and Mulla, every 1 m^3 clean water produced results in 2 m^3 of reject brine [33]. Advanced technologies may enhance the water recovery and reduce the reject flow, but the reject volume still remains very large. Reject brine disposal is a costly process which accounts for 3–33% of the total cost of desalination depending on the selection of disposal method [34]. The major constituents in reject brine comprise of calcium, magnesium, sodium cations, sulfate and chloride anions, and sometime antiscalants. Their concentrations are dependent on the water sources, desalination technologies, and water recovery ratio or concentration factor [27, 34]. Seawater desalination plant recovery is typically limited to 40–65%, and its total dissolved solid concentration usually ranges from 65,000 to 85,000 mg/l [27]. Reject brine disposal either inland or into the sea may result in negative environmental impact due to locally increasing in temperature and salinity; hence, a proper management and treatment procedure is required for the disposal [31, 35]. A number of methods such as solar evaporation, membrane distillation, electrodialysis, forward osmosis, zero liquid discharge, salt recovery have been proposed to reduce and eliminate the brine disposal in which the methods that combine brine treatment with the recovery of valuable component have drawn significant interest [31, 32, 35–37]. Recently, several studies have considered the recovery of salt and minerals from rejected brine in the context of CO_2 capture and utilization [38–42]. Simultaneous CO_2 and brine utilization is based on the reaction between CO_2 and major inorganic cations prevailed in the rejected brine. Generally, CO_2 utilization with brine can be divided into two methods: direct precipitation of earth alkaline cations of Ca^{2+} and Mg^{2+} by CO_2 gas to form $CaCO_3$ and $MgCO_3$ [43–46] and indirect precipitation of Na^+ to form sodium bicarbonate [41]. In the former method, less soluble carbonates removed from water can be value-added products; nevertheless, with the low Ca^{2+} and Mg^{2+} concentrations of several hundred to several thousand ppm, this method is potentially used for brine pre-treatment other than the recovery of $CaCO_3$ for marketing [45], whereas, the latter method makes up a core technology for the industrial production of soda ash (Na_2CO_3) [47]. Soda ash is an important raw material used in many industries such as glass, chemicals, soaps and detergents, metallurgy, water treatment, pulp, and paper. Producing soda ash from rejected brine and CO_2 is an opportunity for at the same time utilizing two waste streams in one product. By producing soda ash, CO_2 can be sequestered in the way that generates the added value for CO_2 captured.

In the following section, the CO_2 utilization in the most updated sodium bicarbonate ($NaHCO_3$) and sodium carbonate production process will be introduced; especially, its relevance to CO_2 mitigation strategy and brine and solid waste treatment will be considered.

9.1.3 *Conventional Solvay Process and Its Potential for CO_2 Utilization*

Solvay process developed in 1861 by Ernest Solvay is the most commercially accepted process for soda ash production due to its low investment and maintenance costs compared to others. This process produces soda ash from brine (NaCl) and limestone ($CaCO_3$) with the overall reaction given in Eq. 9.7 [48]. In fact, it is more complicated and goes through many different steps that are schematically described in Fig. 9.1. Brine after purification is ammoniated and carbonated by passing the CO_2 gas (Eq. 9.8). The carbonation leads to the precipitation of bicarbonate ($NaHCO_3$) that is subsequently filtered and calcined to produce soda ash (Eq. 9.9). Filtrate mainly consisting of NH_4Cl and residual NaCl is mixed with CaO in the distillation process to regenerate NH_3 that is returned to ammoniation process (Eq. 9.10). CaO reacts with NH_4Cl and NaCl in the filtrate to form $CaCl_2$ as a major chemical species in distiller waste (Eqs. 9.10 and 9.11). Limestone is burned to supply CaO for NH_3 regeneration and CO_2 for carbonation process (Eq. 9.12). The conventional Solvay process faces a significant problem of waste management [48–50]. To ease its impact on the environment, the waste utilization is usually added into the traditional Solvay process in which $CaCl_2$ can be converted to $CaCO_3$, calcium phosphate, magnesium phosphate, or gypsum that are commercializable by-products [50–55]. The Solvay process itself does not substantially contribute to reduce CO_2 emission due to the burning fossil fuel for CaO and CO_2. This process consumes a significant amount of CO_2 because of the high demand on soda ash and therefore has high potential for CO_2 utilization and sequestration, but it can become reality only when the whole process is revised with the replacement of CaO and CO_2 sources. These chemicals are abundant in many industrial wastes such as fly ash, slag, and flue gas. Thus, the exploration of those wastes as major sources for CaO and CO_2 instead of burning $CaCO_3$ should be considered. This strategy does not only reduce CO_2 emission but also mitigate other wastes to be discharged to the environment. In the following parts of this chapter, the modified Solvay method and related methods to produce $NaHCO_3$ and Na_2CO_3 in the consideration of waste and CO_2 utilization will be introduced.

$$2NaCl + CaCO_3 \rightarrow Na_2CO_3 + CaCl_2 \tag{9.7}$$

$$NaCl + CO_2 + NH_3 + H_2O \rightarrow NaHCO_3 + NH_4Cl \tag{9.8}$$

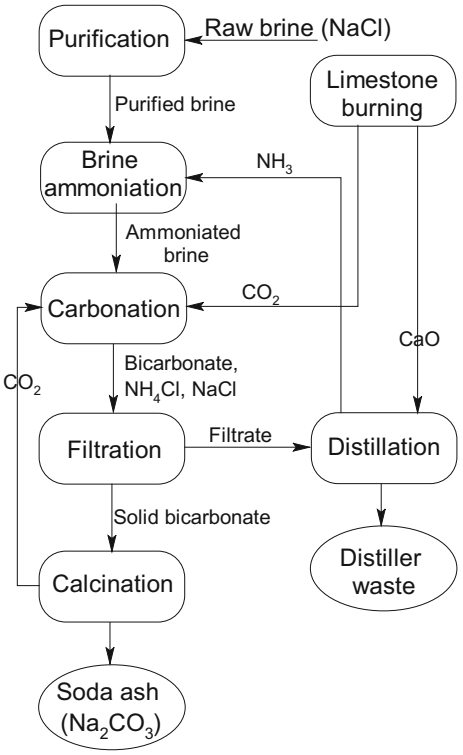

Fig. 9.1 Schematic diagram of a traditional Solvay process

$$2NaHCO_3 \rightarrow Na_2CO_3 + H_2O + CO_2 \tag{9.9}$$

$$2NH_4Cl + CaO \rightarrow CaCl_2 + 2NH_3 + H_2O \tag{9.10}$$

$$2NaCl + CaO + H_2O \rightarrow CaCl_2 + 2NaOH \tag{9.11}$$

$$CaCO_3 \rightarrow CaO + CO_2 \tag{9.12}$$

9.2 Modified Solvay Process and Solid Waste Utilization

9.2.1 Solid Waste Utilization in a Modified Solvay Process

Looking at the Solvay process as shown in Fig. 9.1, we can find a number of precursors or process steps where the traditional sources can be partially or even completely replaced by wastes. First of all, let us analyze the CO_2 cycle in the process; every mole of Na_2CO_3 produced requires one mole of CO_2 from burned $CaCO_3$ fed into system. This process looks like a carbon neutral one emission

because CO_2 in a close loop, however, there is a hidden event, i.e., $CaCO_3$ burning process that combusts fossil fuel and generate significant amount of CO_2 [56]. The emission from fossil fuel combustion in lime production may vary with the type of kiln and fuel, but according to Shan et al., an average of 56.55 million tonnes CO_2 emitted for the production of 207.5 million tonnes lime in China in 2012 [56]. This means that every tonne of CaO produced generates 0.27 tonnes CO_2 that are not used in soda ash production. Steinhauser indicated that the production of one tonne of soda ash emits from 0.2 to 0.4 tonnes of CO_2 [48]. This makes the traditional Solvay process not attractive in the term of CO_2 emission. CO_2 is however very abundant in flue gas from power plant or industry that burns fossil fuel as energy source. Flue gas from coal-fired power plant, for example, contains approximately 15 vol.% of CO_2 that can be a viable CO_2 supply for soda ash industry. The issue now lies in the CaO source because burning $CaCO_3$ does not only provide CO_2 but also provide CaO. Stop burning $CaCO_3$ means the alternatives for CaO source must be taken into account. Fortunately, as discussed in earlier section, a variety of alkaline solid wastes such as ash and slag which have high content of CaO are available from coal-fired power plants and other industries that burn coal for energy as well. Depending on industry, technology, and type of coal, chemical composition and alkaline contents of solid wastes can be varied. In the industrial process, e.g., steelmaking illustrated in Fig. 9.2, slag can be collected from different process steps with different quantities and qualities. Table 9.1 shows the chemical composition of major alkaline wastes that are available from the literatures [6, 7, 57, 58]. The slag collected from blast furnace (BF slag) contains about 38–42 wt% CaO, while that collected from basic oxygen furnace (BOF slag) has 46.3–55.9 wt% CaO. As can be seen in this table, there are a number of wastes that have high CaO content with maximum above 50 wt% such as municipal solid waste (MW) incinerator bottom ash (53 wt%), fly ash class C (54.8 wt%), blended hydraulic slag cement (56.9 wt %), air pollution control residue (60 wt%), argon oxygen decarburization (AOD) slag from steel industry (60.7 wt%), and paper sludge incineration ash (69

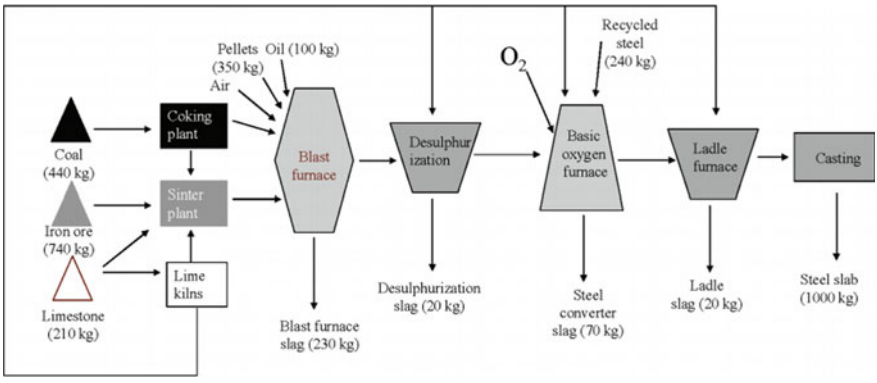

Fig. 9.2 Flowchart of a typical integrated steelmaking process. Reprinted with permission from [59], copyright 2008 American Chemical Society

Table 9.1 Chemical composition of different alkaline solid wastes

Wastes	Chemical composition (wt%)								References
	CaO	MgO	SiO_2	Fe_2O_3	Al_2O_3	Na_2O	K_2O	LOI	
Fly ash (class C)	15.1–54.8	0.1–6.7	11.8–46.4	1.4–15.6	2.6–20.5	0.2–2.8	0.3–9.3	0.3–11.7	[57]
Fly ash (class F)	0.5–14.0	0.3–5.2	37.0–62.1	2.6–21.2	16.6–35.6	0.1–6.3	0.1–4.1	0.3–32.8	[57]
Blast furnace slag (BF)	38.0–42	5.0–8.2	33.0–36.7	0.2–0.5	13.5–15.5	–	0	–	[58]
Steel slag (BOF)	46.3–55.9	2.1–6.3	9.3–12.9	22.7–25.3	1.1–2.0	0.3	0.1	–	[58]
Steel slag (EAF)	25.0–47.0	4.0–15.0	27.0	1.6	–	–	–	–	[6]
AOD process slag	60.7	5.83	27.6	0.21	–	–	–	–	[6]
Desulfurization and ladle slag	43–58	1.0–6.0	16.0–19.0	10.0–20.0	–	–	–	–	[7]
Cement kiln dust	38.0–50.0	0–2.0	11.0–16.0	1.0–4.0	3.0–6.0	–	–	–	[58]
Biomass and wood ash	24.0–46.0	8.0–9.0	5.17	1.0–1.3	–	0.5	14.0–21.0	–	[6]
Recycled concrete aggregate	15.0–24.0	2.03	–	–	–	0.1	0.2	–	[6]
Incinerator sewage sludge ash	9.0–37.0	3.0	40.0	5.6	–	0.7	2.3	–	[6]
MW incinerator bottom ash	32.0–53.0	2.8	4.0–30.0	1.0–7.9	–	2.2–5.7	0.8–2	–	[6]
Pulverized-fuel ash	1.3–10	1–3	56	13.8	–	0.5	0.1	–	[6]
Oil shale ash	42.0–50.0	5.0–6.5	22.0	4.0	–	–	–	–	[6]
Air pollution control residue	50.0–60.0	8.0	10.0	0.5–1.5	–	–	2.0–6.0	–	[6]
Paper sludge incineration ash	45–69	1.3–5.3	10–25	1–4.7		0–1	0–2		[6]
Blended hydraulic slag cement	51.4–56.9	2.5–5.4	25–28	1.5–3.7	8.4–9.3	–	–		[58]
Waste concrete	35.7	3.0	25.1	1.2	3.4	–	–		[60]

BF Blast furnace; *BOF* Basic oxygen furnace; *EAF* Electric arc furnace; *AOD* Argon oxygen decarburization; *MW* Municipal solid waste

wt%). These two waste streams, flue gas and alkaline solid waste, could be perfect alternatives for CO_2 and CaO sources and positive contribution to CO_2 emission and solid waste mitigation.

In the Solvay process, thermal energy consumption accounts for 30% of production cost and considerable fraction of it comes from firing $CaCO_3$ for CaO [63]. The use of solid waste instead of CaO does not only reduce CO_2 emission but also directly contributes to lower the cost of product thanks to the reduction in energy consumption and low cost of solid waste. In order to improve the input parameters such as energy and material cost and diminish the amount of waste in conventional process, Carvalho Pinto et al. proposed a modified Solvay process as shown in Fig. 9.3 where lime used in the regeneration of ammonia is partially replaced by steel slag milk [63]. The steel slag having 40.1 wt% CaO was utilized in the laboratory investigation. The effect of various conditions such as temperature, time, NH_4Cl concentration, and slag/NH_4Cl ratio on the extraction of Ca^{2+} ions from slag was investigated. The maximum Ca^{2+} extraction efficiency reaches 5 wt% at the optimum condition of NH_4Cl 1.5 mol/L at 90 °C for 60 min with a solid-to-liquid ratio of 2 wt%. The Ca^{2+} leaching is however significantly affected by the $NaHCO_3$ concentration remained in the filtrate from the Solvay process after solid $NaHCO_3$ is separated. For a better Ca^{2+} leaching, it requires a thermal treatment to decompose $NaHCO_3$ prior to the addition of alkaline waste [54, 63]. By thermal treatment, the Ca^{2+} concentration is improved from 192 to 1520 mg/L, which is close to leaching efficiency of pure NH_4Cl (1840 mg/L). NH_3 recovery also varies with reaction conditions and is possible to reach a maximum of 40 wt%. The study at bench scale indicated that the maximum NH_3 recovery of 40 wt% can be reached only when multi-recovery stages is applied.

It is easily understandable that the success of alkaline solid wastes as alternatives to CaO depends on the amount of Ca^{2+} ions that can be extracted as active components. The extraction is controlled by several factors including the type of solid waste, CaO content of waste, the nature of calcium in solid waste, extracting solution, and temperature [7, 59–62, 65, 68–71, 73]. CaO content in solid waste is a primary parameter to evaluate the potential of a waste utilization. The CaO content greatly varies with the type of solid waste. As shown in Table 9.1, CaO contents in

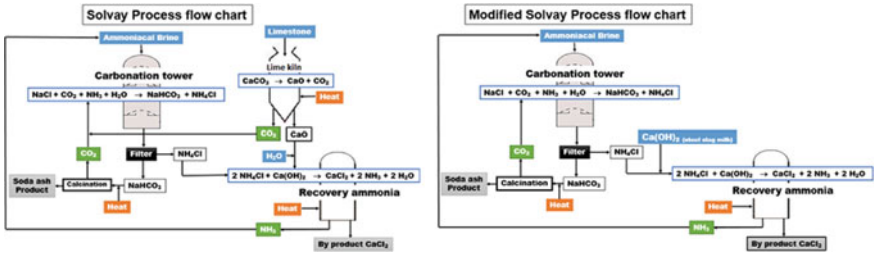

Fig. 9.3 Conventional Solvay process and its modified one by partial replacement of CaO with steel slag. Reprinted with permission from [63], copyright 2015 Springer Nature publisher

different solid wastes are variable, the higher CaO wastes are usually expected to have more amount of Ca^{2+} extracted, but it also depends on which type of crystalline phase existing in the wastes. In a research to extract Ca^{2+} from steel slag containing 40.1 and 30.5 wt% CaO using NH_4Cl solution and the filtrate of the Solvay process conducted by de Carvalho Pinto et al., the maximum Ca^{2+} extraction reached only 22 wt%, much lower compared to many others as shown in Table 9.2 [54, 63]. Even though only 22 wt% calcium was extracted, 84.3 wt% of the NH_3 inlet can be recovered, demonstrating a great potential of solid waste use in a modified Solvay process. Therefore, the key to the success of this process now lies on calcium extraction method. In the following section, the essential parameters for effective calcium extraction using the NH_4Cl solution or the filtrate from the Solvay process will be intensively discussed based on the available literatures.

9.2.2 *Calcium Extraction by Extracting Agent*

The number of studies has been conducted to extract the calcium from solid waste for a purpose of CO_2 sequestration and calcium carbonate production [6, 7, 58, 61, 65, 67, 70, 73, 74]. The calcium extraction efficiency is used as a major parameter to evaluate the effectiveness of an extraction system. The extraction efficiency is defined as the percentage of Ca extracted by extracting solution to the total calcium in the solid waste used in the test as expressed in Eq. 9.13. Pure water has very poor calcium extraction because it can dissolve only part of free CaO in solid waste. In a research conducted by Said et al. [61], only 0.81 wt% of calcium in steel-converted slag was extracted by pure water. However, in another research, He et al. can extract more than 10 wt% of calcium from fly ash using pure water even though the fly ash contains less CaO, 30.47 wt% (Table 9.2) [62]. The difference in calcium extraction efficiency is probably due to the different contents of free calcium oxide or the waste microstructure that prevents the migration of Ca^{2+} into water phase. The calcium extraction efficiency offered by water is usually far below the requirement for an application, and thus, it needs a more effective method. Various extracting agents such as acids (HCl, HNO_3, CH_3COOH, and CH_3CH_2COOH) [59, 74–76] and ammonium salts (NH_4Cl, NH_4NO_3, CH_3COONH_4, and $(NH_4)_2SO_4$) [59–62, 71] have been used to improve the Ca^{2+} extraction. Recent works have indicated that the addition of these extracting agents helps enhance the Ca^{2+} extraction significantly thanks to their possibility to selectively dissolve some calcium compounds in solid waste, e.g., the dissolution of calcium silicate and calcium ferrite phases given in Eqs. 9.14 and 9.15 [65, 66, 68, 70, 72].

$$\text{Ca extraction efficiency}(\%) = \frac{m_{Ca}(g)}{m_t(g) \times \frac{C_{CaO}(\%)}{100} \times \frac{M_{Ca}\left(\frac{g}{mol}\right)}{M_{CaO}\left(\frac{g}{mol}\right)}} \times 100 \tag{9.13}$$

Table 9.2 Calcium extraction by NH_4Cl solution in the literature

No.	Waste	CaO (wt%)	Extracted (wt%)	Selectivity (%)	NH_4Cl concentration (mol/L)	Solid–liquid ratio (g/L)	Particle size (micro)	Ca in leachate (g/L)	Temperature (°C)	Time (Min)	References
1	Steel slag	44.9	0.81	–	Water	0.0	0–125	–	30	60	[61]
2	Fly ash	30.47	10	–	Water	50.0	<100	–	40	60	[62]
3	Steel slag	40.1	5.9[a]	–	0.1	20.0	–	0.34	85	45	[63]
4	Steel slag	40.1	3.7[a]	–	0.1	50.0	–	0.53	85	45	[63]
5	Steel slag	40.1	2.1[a]	–	0.1	100.0	–	0.61	85	45	[63]
6	Steel slag	40.1	0.8[a]	–	0.1	300.0	–	0.69	85	45	[63]
7	Steel slag	41.1	0.5[a]	–	0.1	500.0	–	0.75	85	45	[63]
8	Steel slag	40.1	4.8[a]	–	1	400.0	–	5.52	85	45	[63]
9	Steel slag	30.5	22.1	93.9[a]	2.8	50.0	–	1.28	85	45	[54]
10	Steel slag (BOF)	40	52.5[a]	75.38[a]	2	100.0	–	15.00	60	120	[64]
11	Steel slag (BOF)	44.9	56	–	1	20.0	0–125	–	30	60	[61]
12	Steel slag (BOF)	51.4	78	–	1	100.0	<250	–	20	30	[65]
13	Steel slag (BOF)	36	62.1[a]	–	1.8	83.3	250–500	13.30	53	68	[66]
14	Steel slag (BOF)	45.9	about 70	–	2	20.0	74–125	–	20	60	[67]
15	Desulphurization slag	58	50	–	2	20.0	–	–	20	60	[67]
16	Ladle slag	49.4	about 15	–	2	20.0	–	–	20	60	[67]
17	Steel slag (BF)	34.5	<10	–	2	20.0	–	–	20	60	[67]
18	Steel slag (BOF)	34.4	20.4[a]	97.0	2	100.0	150–500	5.01	–	120	[68]
19	Steel slag (BOF)	34.4	34.4[a]	97.0	2	100.0	<150	8.46	–	120	[68]
20	Ladle slag	38.2	15.4[a]	97.0	2	100.0	150–500	4.21	–	120	[68]
21	Ladle slag	38.2	30.7[a]	96.0	2	100.0	<150	8.37	–	120	[68]

(continued)

Table 9.2 (continued)

No.	Waste	CaO (wt%)	Extracted (wt%)	Selectivity (%)	NH_4Cl concentration (mol/L)	Solid–liquid ratio (g/L)	Particle size (micro)	Ca in leachate (g/L)	Temperature (°C)	Time (Min)	References
22	Desulphurization slag	39.3	22.2[a]	97.0	2	100.0	150–500	6.24	–	120	[68]
23	Desulphurization slag	39.3	39.9[a]	95.0	2	100.0	<150	11.19	–	120	[68]
24	Hazelwood fly ash	32.4	32	–	4	166.7	<150	–	80	30	[69]
25	Yallourn fly ash	9.4	37	–	4	166.7	<150	–	80	30	[69]
26	Fly ash	30.47	35	–	1	50.0	<100	–	25	120	[62]
27	Steel slag	47	35.0[a]	96.1[a]	2	100.0	–	11.75	45	30	[70]
28	Granulated slag (BF)	22.5	49.0	–	1	10.0	–	–	30	30	[71]
29	Granulated slag (BF)	22.5	52	–	2	10.0	–	–	30	60	[71]
30	Air-cooled slag (BF)	32.9	11	–	1	10	–	–	30	30	[71]
31	Air-cooled slag (BF)	32.9	13.7	–	2	10.0	–	–	30	60	[71]
32	Steel slag (EAF)	39	75[b]	–	2	50.0	–	–	100	60	[72]
33	Steel slag (EAF)	39	85[b]	–	2	50.0	–	–	100	60	[72]
34	Steel slag (EAF)	39	95[b]	–	2	50.0	–	–	100	60	[72]
35	Concrete	35.7	19.4[a]	95.3[a]	0.5	50.0	<149	2.48	20	240	[60]
36	Concrete	35.7	32.0[a]	98.0[a]	1	50.0	<149	4.08	20	240	[60]

[a]Estimation based on the ion concentration in the leachate,

[b]Estimation from the figure of corresponding references. The concept basic oxygen furnace slag (BOF) and steel converter slag are unified as steel slag (BOF) in this table

where m_{Ca} is the mass of Ca extracted by the extracting solution (g), m_t is the mass of solid waste used (g), C_{CaO} is the CaO content in solid waste (wt%), M_{Ca} is molecular weight of calcium (g/mol), and M_{CaO} is molecular weight of CaO (g/mol).

$$2CaO_{(S)} \cdot SiO_{2(s)} + 4NH_4Cl_{(aq)} \leftrightarrow 2CaCl_{2(aq)} + SiO_{2(s)} + 4NH_{3(g)} + 2H_2O_{(l)} \tag{9.14}$$

$$Ca_2Fe_2O_{5(s)} + 2NH_4Cl_{(aq)} \leftrightarrow 2Ca^{2+}_{(aq)} + 2Cl^{-}_{(aq)} + 2NH_{3(g)} + Fe_2O_{3(s)} + H_2O_{(l)} \tag{9.15}$$

The calcium extraction from fly ash by water and ammonium salts at different temperatures was reported by He et al. [62] (Fig. 9.4). It is evident that the calcium extraction improves significantly by adding those extracting agents. Temperature also contributes to the improvement, but it should be controlled in a moderate range. The higher temperatures do not significantly improve the extraction but incur the water vaporization that causes the loss of solvent, difficult process control, and energy intensiveness. In another research, Lee et al. showed the effect of ammonium salts on two types of slag, granulated slag and air-cooled slag [71]. They again confirm the extraction efficiency caused by the type of both extracting solvent and solid waste. NH_4NO_3, NH_4Cl, and CH_3COONH_4 have a comparable extraction efficiency, approximately 49–52 wt% for granulated slag and 11–17 wt% for air-cooled slag (Fig. 9.5). $(NH_4)_2SO_4$ has worse extraction among four ammonium salts due to the formation of less soluble $CaSO_4$ on the outer layer of slag granules that prevents the dissolution of Ca^{2+} into liquid phase. Using 2 mol/L of NH_4Cl, NH_4NO_3, and CH_3COONH_4, Said et al. can extract from 45 to 54% calcium from BOF slag that has the particle size of 74–125 μm. Similar results were observed by

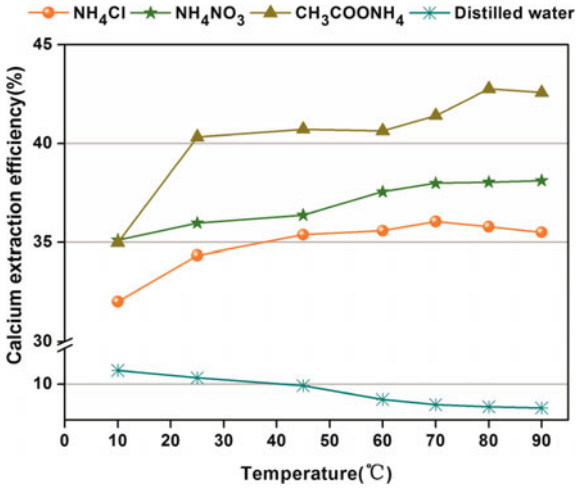

Fig. 9.4 Influence of temperature and the type of extraction solution on Ca^{2+} extraction efficiency (ammonium salt concentration: 1 mol/L, solid-to-liquid ratio: 50 g/L, mixing rate: 500 rpm, time: 60 min). Reprinted with permission from [62], copyright 2013 American Chemical Society

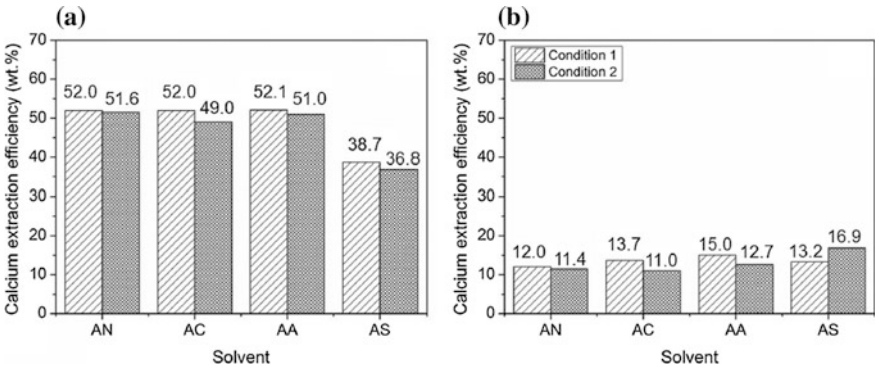

Fig. 9.5 Calcium extraction efficiency of (**a**) granulated slag, and **b** air-cooled slag when different ammonium salts are used. Solvent concentration (mol/L), reaction temperature (°C), reaction time (min), and solid-to-liquid ratio are 2 mol/L, 30 °C, 60 min, and 10 for the condition 9.1 and 1 mol/L, 30 °C, 30 min, and 10 for the condition 9.2, respectively. Further detail on the condition 9.1 and 9.2 can be found in Table 9.2. Abbreviations for the solvents: AN: NH_4NO_3, AC: NH_4Cl, AA: CH_3COONH_4, and AS: $(NH_4)_2SO_4$. Reprinted with permission from [71], copyright 2016 Elsevier

Sanni et al. in which acids that form soluble salts with calcium such as CH_3COOH, HNO_3, and CH_3CH_2COOH possess the highest extraction efficiency (85–100%) followed by ammonium salts (NH_4NO_3, NH_4Cl, and CH_3COONH_4) with the efficiency ranging from 50 to 80%, while $(NH_4)_2SO_4$, $(NH_4)_2HPO_4$, and $NH_4H_2PO_4$ showed a poor extraction [67]. For cement waste, 1 mol/L solution of NH_4NO_3 and CH_3COONH_4 has the extraction efficiency of $\sim$69% that is better than NH_4Cl and $(NH_4)SO_4$ with only 32 and 4%, respectively [60]. Generally, ammonium salts of NH_4Cl, NH_4NO_3, and CH_3COONH_4 were recognized as the best solution for extracting calcium from solid waste thanks to their high extraction efficiency and NH_3 recyclability.

Variety of agents have proved to be effective for calcium extraction, however, to apply in the Solvay process, and only NH_4Cl is a suitable candidate because it is the main component in the filtrate that will react with CaO for NH_3 recovery. In a typical Solvay process, NH_4Cl concentration in the filtrate is around 3.6–4.9 mol/L, but it could not directly apply for calcium extraction because of the presence of HCO_3^+ in the filtrate that reacts with Ca^{2+} to form insoluble $CaCO_3$ [54, 55, 63]. The $CaCO_3$ may form the less soluble carbonated shell around slag particles that prevents the dissolution of Ca^{2+} ions [7, 9, 58]. Thermal treatment can decompose the HCO_3^+ to release CO_2, but also remove NH_4^+ as NH_3 in the gas phase; this causes the decrease in the NH_4Cl concentration. The reduction in NH_4Cl concentration may influence the extraction capacity of the filtrate. Recent researches have indicated that NH_4Cl concentration plays a very important role in the calcium extraction [60–63, 65, 67, 70, 72]. Table 9.2 shows the calcium extraction from various solid wastes using NH_4Cl in the literatures. In this table, numerous parameters including NH_4Cl concentration, solid-to-liquid ratio, particle size,

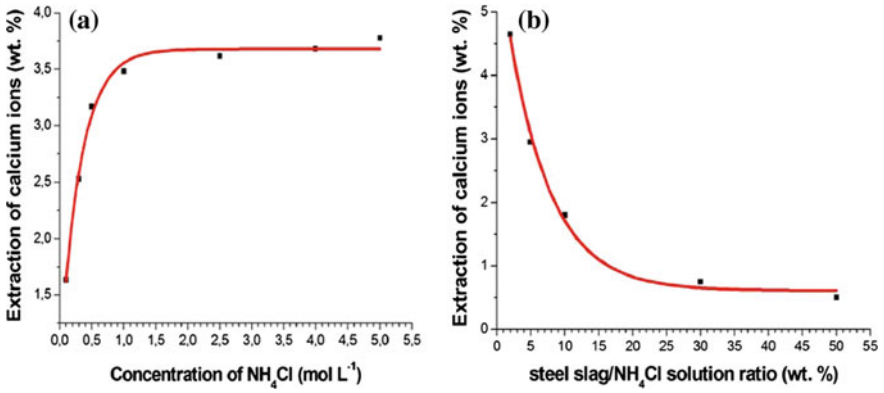

Fig. 9.6 Effect of NH_4Cl concentration (**a**) and solid-to-liquid ratio (**b**) on the calcium extraction efficiency. Reprinted with permission from [63], Springer Nature publisher

temperature, and extraction time and their influence on the extraction efficiency, calcium selectivity, and calcium concentration in leachate are introduced. A good agreement among published works is that the extraction efficiency improved with the increase in NH_4Cl concentration; however, its concentration above 1 mol/L would be preferable. A rapid increase in the extraction efficiency was observed at the NH_4Cl ranging from 0 to 1 mol/L. Above 1 mol/L, the increase is not significant (Fig. 9.6a). The decrease in NH_4^+ concentration due to thermal treatment of the filtrate has been verified by de Carvalho Pinto et al. [54, 63]. By boiling the filtrate containing NH_4Cl 4.2 mol/L for 30 min, they can recover 16.7% NH_3 which causes the NH_4Cl concentration decrease to 3.5 mol/L [63]. In another study, the reduction on the NH_4Cl concentration from 3.6 to 2.8 mol/L was found by boiling the filtrate [54]. These suggest that a fraction of NH_3 can be recovered by thermal treatment, but it does not influence on the following extraction activity because the NH_4Cl concentration is remained in preferable range. By boiling the filtrate for 30 min prior to the addition of slag, de Carvalho Pinto et al. can enhance the calcium extracted into filtrate solution from 192 to 1520 mg/L [63] confirming the effectiveness of the thermal treatment.

9.2.3 Type of Solid Waste

Types of solid waste and the crystalline phases existing in solid waste are the most influent factors that decide the success of extraction using NH_4Cl. CaO content and its compounds in waste vary with the waste sources and directly affect the extraction efficiency. The calcium extraction from different wastes under various conditions is provided in Table 9.2. In general, BOF slag has a high extraction efficiency. Most of BOF slag samples show the extraction efficiency above 50 wt%,

while only few samples of desulphurization lag and BF slag attain 50 wt% calcium extraction. Investigating on the calcium extraction from different slags, Sanni et al. recognized that free lime in BOF and desulphurization slags contributes to high extraction with about 70 and 50%, respectively, while all calcium in BF and ladle slags exists in silicate form that explains for a poor extraction with a efficiency below 15% [67]. According to Lee et al., air-cooled slag contains higher CaO content (32.9 wt%) compared to granular slag (22.5 wt%) but the extraction efficiency is much lower, 11–17 wt% compared to 49–52 wt%, respectively [71]. The differences are attributed to the crystallinity of these two slags caused by collecting methods. Granular slag is generated by rapid cooling using water produced about 50% amorphous phase and 50% crystalline phases including mainly wustite (15.23%), $Ca_2Fe_2O_5$ (13.32%), beta-Ca_2SiO_4 (13.10%), and magnetite (10.96%), whereas air-cooled slag is obtained by slow cooling under an ambient atmosphere containing mostly crystalline phases, which account for the poor extraction from this slag. To demonstrate the high extraction contributed by free CaO in solid waste, the comparison between MgO + CaO mixture and fly ashes was made by Hosseini et al. [69]. Two fly ashes collected from electrostatic precipitator of coal power plant that are Hazelwood fly ash (32.4 wt% CaO) containing mainly $CaSO_4$, CaO, calcium ferrite ($CaFe_2O_4$), and silicate and Yallourn fly ash (9.4 wt% CaO) containing mostly magnesia ferrite, quartz, and amorphous CaO were tested. As shown in Fig. 9.7, above 80 wt% of calcium in MgO + CaO mixture can be extracted, while only 32 and 37 wt% of calcium was leached from Hazelwood and Yallourn fly ash in the first cycle using NH_4Cl, respectively.

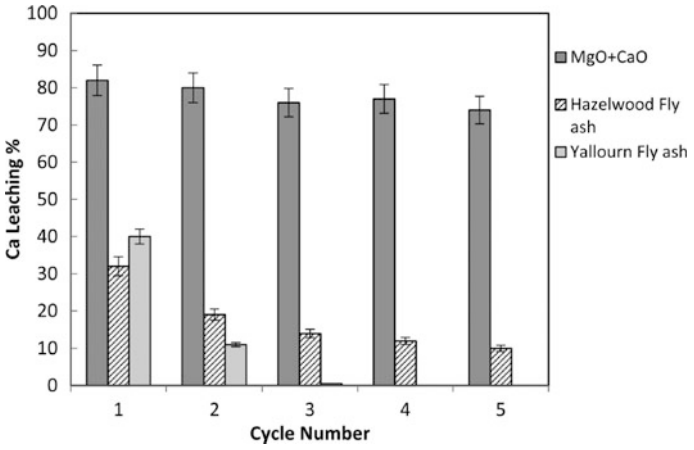

Fig. 9.7 Calcium extraction efficiency for five leaching-carbonation cycles at optimum conditions (80 °C and 30 min) using MgO + CaO mixture, Hazelwood and Yallourn fly ash. Reprinted with permission of [69], copyright 2014 American Chemical Society

9.2.4 Particle Size and Microwave Treatment

Particle size distribution is another crucial characteristic that influences on the calcium extraction. Data on the effect of size on the calcium extraction can be found in Table 9.2. Investigating the calcium leaching from various slags with size <150 and 150–500 μm by Hall et al. indicated an impressive increase in extraction efficiency by size reduction with a maximum 50% higher in small size samples [68]. By reducing the size of slag from 250–500 to 0–125 μm, Said et al. can improve almost 50% of the extraction efficiency of a steel converter slag which contains the majority of $CaSiO_4$, $Ca_2Fe_2O_5$, $Fe_{0.925}O$, and Fe_3O_4 without free CaO (Fig. 9.8) [61]. Further extraction improvement can be executed by the application of microwave [72], ball milling, and heat treatment [70]. Tong et al. found that the calcium leaching can be improved about 10% by the combination of NH_4Cl extracting agent with microwave treatment on electric arc furnace slag [72]. The research indicated that Ca_2SiO_3, Ca_2SiO_4, and Ca_3SiO_5 can be dissolved by NH_4Cl solution generating leaching Ca^{2+} and SiO_2. Lee et al. showed a calcium extraction improvement by combining NH_4Cl extracting agent with ball milling [70]. The improvement is attributed to the particle size reduction that decreased from <10 to 1–5 μm by ball milling.

9.2.5 Solid-to-Liquid Ratio

Solid-to-liquid ratio (g/L) for extraction is another key parameter. Most of studies agree that lower solid-to-liquid ratio offers better extraction efficiency (Table 9.2) [61–63, 65]. The relation was clarified by de Carvalho Pinto et al. as shown in Fig. 9.6b; the extraction efficiency drastically declines as the slag concentration increases [63]. This is in congruence with the observation by Said et al. where the

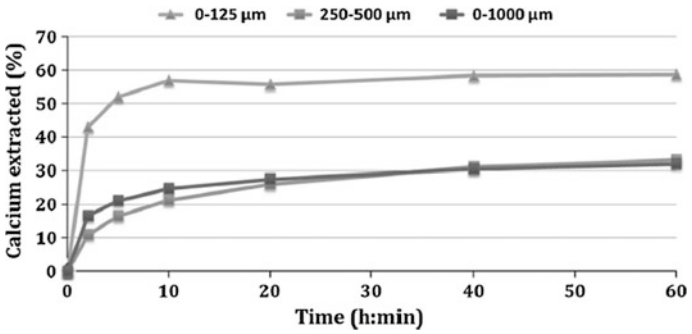

Fig. 9.8 Effect of particle size on calcium extraction from steel converter slag in NH_4Cl solution 1 mol/L (solid-to-liquid ratio: 20 g/l). Reprinted with permission from [61], copyright 2012 Elsevier

calcium extraction from BOF slag by ammonium salts reached a maximum (73%) at the lowest solid concentration (5 g/L) and the lowest extraction (6%) by the highest solid concentration (100 g/L) [61]. The analogous effect was also observed when calcium was extracted from fly ash [62]. The reason for this reduction in the extraction efficiency is most likely due to the high viscosity causing the low mobility of solution that prevents proper mixing and consequently reducing calcium extraction. It is also believed that the higher buffer effect of the NH_4^+/NH_3 couple is attained at pH = 9.25. At this pH, NH_4^+ and NH_3 concentrations are equal and their interconversion occurs that prevents the further Ca^{2+} extraction [63]. In contrast to the extraction efficiency, the Ca^+ concentration in the liquid increased a long with the increase in solid-to-liquid ratio; this relation is illustrated by He et al. in Fig. 9.9. In a practical application, an optimum solid-to-liquid ratio must be determined to balance the extraction efficiency, Ca^{2+} concentration, and water consumption for efficient production.

9.2.6 *Extraction Selectivity*

Since solid waste has a diverse chemical composition, the extraction may simultaneously leach various metal ions into solution. Selectivity of a metal is a fraction of its concentration to total metal concentration in the leachate. A good solid waste should generate high selectivity for Ca over others. Impurity leached into the filtrate does not impact on the quality of resulting $NaHCO_3$ or Na_2CO_3 product, but it may affect the NH_3 recovery efficiency and relate to the strategy for later waste management. High selectivity of unreactive species toward NH_4Cl or metal ions that form stable complexes with NH_3 will result in low NH_3 recovery. In general, ammonium salt solution shows a good selectivity for calcium against undesired

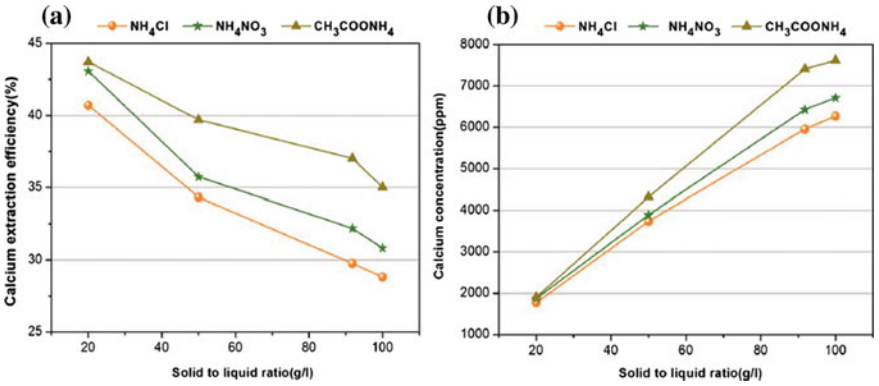

Fig. 9.9 Effect of solid-to-liquid ratio on calcium extraction efficiency (**a**) and Ca^{2+} concentration in leachate (**b**) at 25 °C for 60 min with the NH_4Cl concentration of 1 mol/L and mixing rate 500 rpm. Reprinted with permission from [62], copyright 2013 American Chemical Society

species (Table 9.2) [54, 60, 65, 68, 70]. Relatively small quantity of undesired metals, e.g., Mn, Fe, Ni, Al, Si are detected in the leachate. A study by Jo et al. on the calcium extraction from cement waste using ammonium salts showed that most of ammonium salts have a good selectivity for calcium, which is greater at higher salt concentration, reached above 98% at the salt concentration of 1.0 mol/L (Fig. 9.10) [60]. Other studies on steel slag by Hall et al. and Lee et al. show that the calcium extraction can attain more than 95% selectivity [68, 70]. Sun et al. found only 75.7% Ca selectivity when extracting it with NH_4Cl 2 mol/L from oxy furnace steel slag; however, total selectivity for two alkaline metals of Ca and Mg reached 96% [64]. Since magnesium could contribute well for NH_3 recovery in the Solvay process, the high selectivity for these two elements is acceptable.

9.3 Modified Solvay Process with Amines and Reject Brine Utilization

Finding a way to prevent or mitigate sea disposal of concentrated brine wastes has huge environmental benefits. The idea to combine CO_2 utilization with waste brine treatment derives from the unique opportunity provided by the availability of vast amounts of brine wastes from desalination plant. Due to its ability to treat two environmental wastes, CO_2 utilization with brine is a promising technology for solving the problem of desalination brine wastes [36]. Over the years, different ideas have been proposed to accomplish this kind of process, most of which are based on the Solvay process first developed by Ernst Solvay in 1861 [77]. Recently, methods involving the use of CaO and layered double hydroxides have also been

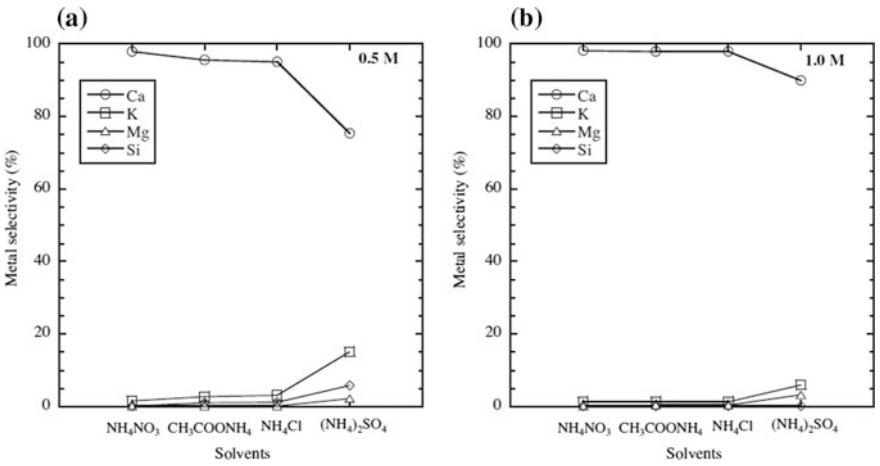

Fig. 9.10 Selectivity of major metal ions in different ammonium salts at the concentration of **a** 0.5 mol/L and **b** 1.0 mol/L. Reprinted with permission from [60], copyright 2014 Elsevier

shown to give promising results with regard to this process. The goal of the following sections is to provide a more detailed description of these processes and their performances with respect CO_2 utilization and reject brine treatment.

The conventional Solvay process involves reacting CO_2 with ammonia/brine solution to produce $NaHCO_3$ and ammonium chloride (Fig. 9.1). The $NaHCO_3$ is precipitated and separated, while the ammonium chloride solution (filtrate) is reacted with lime to produce ammonia, which is recycled, and $CaCl_2$ as a waste product. While this process scheme can be applied directly for CO_2 utilization and brine treatment as demonstrated by El-Naas [78, 79], it is not very appropriate for the processes where sodium removal is the main goal due to its low sodium conversion. This, in addition to the volatility of ammonia at the temperatures at which CO_2 capture processes operate, poses a problem for the application of Solvay process for CO_2 utilization and brine treatment [80, 81]. Also, Solvay process applies CaO for the regeneration of ammonia. This is counterproductive for the CO_2 capture process due to the fact the production of CaO is CO_2 intensive. For every two moles of CO_2 from power plants captured, one mole of CO_2 from calcination of limestone is released [82].

Modifications of the Solvay process for CO_2 capture and utilization processes have been mostly focused on the replacement of volatile ammonia with alcohol amines which are stable at the temperature range of CO_2 capture processes. Alcohol amines also tend to give better performance results (Na conversion/removal) than ammonia with dilute CO_2 streams such as flues gas as shown in Table 9.3.

Huang et al. used a sterically hindered alcohol amine and methyl aminoethanol (MAE), in the place of ammonia, and reported a CO_2 capacity of 0.9 mol/mol MAE and a $NaHCO_3$ yield of 14.3 g $NaHCO_3$/mole MAE ($\sim$17.14 g/kg solution) at MAE and NaCl concentration of 1.2 and 3.4 M, respectively [82]. In similar vein, Dindi et al. investigated the use of different classes of alcohol amines as replacement for ammonia and found that secondary or sterically hindered amines such as 2-amino, 2-propanol-amine gave the best performance [83, 86]. The reaction of amines with CO_2 could follow either a carbamate or the bicarbonate route depending on the class of the amine. Primary and secondary amines react with CO_2 to form carbamates following the zwitterion mechanism Eq. 9.16, while tertiary and sterically hindered amines react with CO_2 to form bicarbonates according to Eq. 9.17 [87].

Table 9.3 Na conversion in brine treatment with the Solvay process

Alkali	NaCl conc.	Alkali/NaCl	Na conversion (%)	References
AMP	0.6	0.57	60	[83]
AMP	1.8	1.87	85	[83]
NH3	Actual brine	2	42	[79]
NH3	4.5	1.74	82.2	[84]
NH3	Actual brine	2	75.8	[85]

Reprinted with permission from [83], copyright 2015 Elsevier

$$2R_1R_2NH + CO_{2(aq)} \leftrightarrow R_1R_2NCOO^- + R_1R_2NH_2^+ \quad (9.16)$$

$$R_1R_2R_3N + CO_{2(aq)} + H_2O \leftrightarrow R_1R_2R_3NH^+ \cdot HCO_3^- \quad (9.17)$$

$$R_1R_2NCOO^- + R_1R_2NH_2^+ + H_2O \rightarrow R_1R_2NH_2^+ \cdot HCO_3^- + R_1R_2NH \quad (9.18)$$

$$R_1R_2NH_2^+ \cdot HCO_3^- + NaCl \rightarrow NaHCO_3 + R_1R_2NH_2^+ \cdot Cl^- \quad (9.19)$$

$$R_1R_2R_3NH^+ \cdot HCO_3^- + NaCl \rightarrow NaHCO_3 + R_1R_2R_3NH^+ \cdot Cl^- \quad (9.20)$$

Primary or secondary amines react with CO_2 to form carbamate (Eq. 9.16) accordingly, two molecules of amine are needed to capture one mole of CO_2. For this reason, the CO_2 absorption capacity of such amines cannot exceed 0.5 mol CO_2 per mole of amine theoretically. Meanwhile, the tertiary or sterically hindered amines which follow the bicarbonate pathway have the potential of reaching a capacity of 1 mol CO_2 per mol amine as shown in Eq. 9.17, although they may be prevented from reaching this capacity due to kinetic limitations of the bicarbonate pathway. Sometimes, the capacity of primary or secondary amines exceeds the theoretical limit due to the carbamate hydrolysis (Eq. 9.18) which releases an amine to react with more CO_2, thereby increasing the CO_2 absorption capacity beyond the theoretical limit. This effect is even more pronounced in the presence of brine.

The CO_2 absorption capacity of amines increases as a result of precipitation of $NaHCO_3$. Na in the brine reacts with HCO_3^- generated in Eq. 9.17 (tertiary amines) and Eq. 9.18 (primary/secondary amines), thereby shifting the equilibrium to the right and causing more CO_2 to be absorbed and more $NaHCO_3$ to be precipitated in Eqs. 9.19 and 9.20 [88]. The process continues until the solution pH reduces below 9 in which case $NaHCO_3$ cannot be precipitated and equilibrium is reached or until all the amine is consumed to form an amine chloride. This explains why amines give better CO_2 absorption results in the presence of NaCl [82, 83].

Although amines give better results during the carbonation stage, a major drawback of the use of amines in the Solvay process is the difficulty of regenerating the free amine from the amine chloride by-product produced during the carbonation step. Although Huang proposed a method for regenerating ammonia from NH_4Cl using activated carbon as a means of avoiding the use of CaO for ammonia regeneration, no method was proposed for regenerating the MAE chloride [82]. The activated carbon was used to remove HCl from a solution of NH_4Cl with the liberation of ammonia according to Eq. 9.21.

$$NH_4Cl + AC \leftrightarrow NH_3 + AC \cdot HCl \quad (9.21)$$

The HCl-loaded activated carbon was then regenerated with water and used repeatedly to produce about 0.0012 mol HCl per cycle. In addition, the ultra-high lime with aluminum (UHLA) method was proposed by Dindi et al. to recover AMP from the AMP-HCl formed during the carbonation step. However, the efficiency of

this process was limited by increasing amine concentration and by the presence CO_2 in the solution [83]. No other method for regenerating amines from amine chlorides has been reported in the literature. Hence, this constitutes a major obstacle in the application of the amine-based Solvay process for brine treatment and CO_2 capture and utilization

Recently, El-Naas proposed a process in which the CaO was used to replace NH_3 in the Solvay process. The CaO is dispersed in brine to increase its pH and then applied for CO_2 capture. The higher pH facilitates absorption of CO_2 into the brine and subsequently the precipitation of $NaHCO_3$. The system was effective for CO_2 capture and Na removal with an optimum temperature of 10 °C and CaO concentration of 20 g/L. Beyond this concentration, Na removal was reduced due to competitive formation of $CaCO_3$. The modified process had a maximum CO_2 capture capacity of 1.44 mol/L and sodium removal efficiency of 35%, while the conventional process had a maximum CO_2 capacity of 1.14 mol/L and a 29% sodium removal efficiency. The modified process is also potentially less costly than the conventional process due to the elimination of energy-intensive ammonia regeneration, fewer unit operations, and lower costs of CaO relative to the cost of ammonia [89].

9.4 Layered Double Hydroxide Process

Due to the shortcomings of the modified Solvay processes for the simultaneous treatment of desalination brines and CO_2 utilization, a new, layered double hydroxide (LDH)-based process has been recently proposed which has the potential to perform better than modified Solvay processes [90]. LDHs, also known as hydrotalcite, are clay materials consisting of alternating layers of mixed metal hydroxides and anion-bearing interlayers, similar to structure of the hydrotalcite mineral as shown in Fig. 9.11 [46]. The mixed metal hydroxides layer are made up of positively charged di or trivalent cations, while the anion layer contains negatively charged balancing anions which combine to give the formula $\left[M^{2+}_{1-x}M^{3+}_{x}(OH)_2\right]_x + (A^-)\ x/n \cdot mH_2O$. M^{2+} represents divalent cations like Mg, Fe, Co, Cu, Ni, or Zn, M^{3+} represents trivalent cations like Al, Cr, Ga, Mn or Fe, and A^- is the interlayer anion such as CO_3^{-2}, HCO_3^-, SO_4^{-2}, Cl^-, or OH^-. The value of x is equal to the molar ratio of $M^{2+}/(M^{2+} + M^{3+})$ and is generally in the range 0.2–0.33.

Carbonate LDHs, in which a CO_3^{2-} ion exists within the layers, are the most common LDH forms due to the strong affinity of the LDHs for the CO_3^{2-} ion. While LDHs can exchange their interlayer ions with other ions present in a solution, this is not always possible depending on the relative affinity of the anion to the LDH. However, when calcined, they release the interlayer anion and OH groups to produce mixed metal oxides, which can reconvert to the original LDH structure when being dispersed in an aqueous solution of the appropriate anion, making them

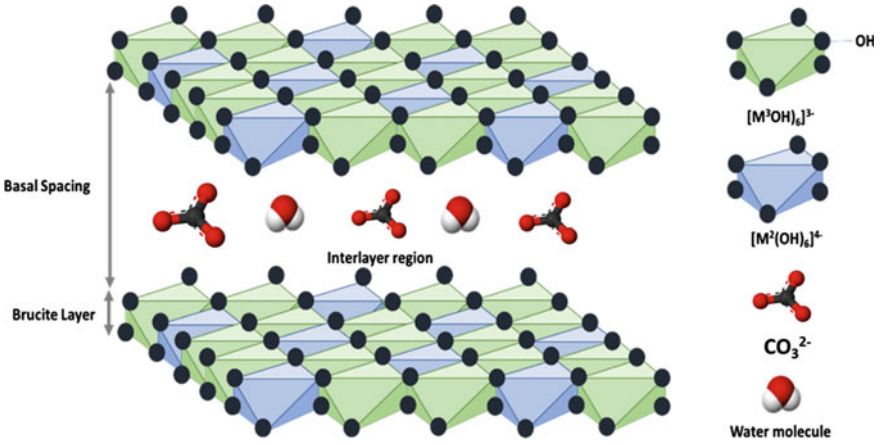

Fig. 9.11 Hydrotalcite structure. Reprinted with permission from [90], copyright 2018 Elsevier

excellent materials for the sorption anions. This property of LDHs has been harnessed for the removal of different kinds of contaminants from wastewater like iodide [91], silicate [92], chlorides [93], heavy metals [94], and rare earth elements [95].

In the case of reject brine treatment, the objective is to reduce chloride and sodium concentrations to levels that are safe for disposal. LDHs can be used to remove chloride from brine as shown in several studies by Kameda and co-workers [93, 96, 97]. Given that the removal of chlorides from brines by Mg–Al–O also results in the increase in OH^- ions in the solution leading to a rise in solution pH, this increased alkalinity can then be employed for CO_2 absorption and precipitation of $NaHCO_3$ which ultimately leads to sodium removal from the brine. In this way, CO_2 capture/utilization and reject brine treatment are combined in one single process as further described in the following section.

9.4.1 Process Description

The process consists of three major stages which are the chloride removal, carbonation, and regeneration stages as shown in Fig. 9.12. In the chloride removal stage, Mg–Al mixed metal oxide, derived from Mg–Al hydrotalcite, is dispersed in the brine to remove the chloride ions via an ion exchange process. Chloride moves from the liquid phase to the solid phase, while the solution is enriched in OH^- ions due to the solvation of the mixed metal oxide. When the slurry is separated, the brine solution becomes more alkaline while mixed metal oxide is transformed to a chloride-form hydrotalcite, Cl^-–HT, according to Eq. 9.22. The resulting alkaline brine solution, a mixture of NaOH and NaCl, is then sent to the carbonation stage

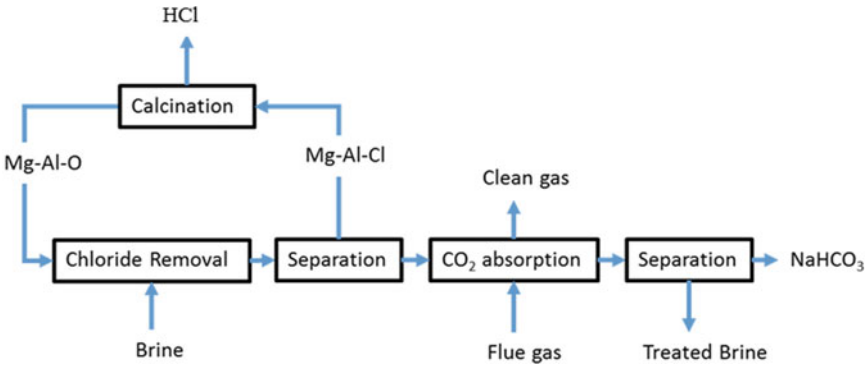

Fig. 9.12 Schematic diagram of the proposed process

for the precipitation of $NaHCO_3$. Depending on the initial concentration of the brine and the extent of chloride removal, a concentration step may be required to bring this solution to a concentration high enough to precipitate NaHCO3.

In the carbonation stage, the CO_2 captured from flue gas reacts with the alkaline solution to precipitate $NaHCO_3$, removing the Na^+ from the brine in the process as described in Eqs. 9.23–9.28. The liquid effluent from this stage has reduced salinity and can therefore be disposed as treated brine, while the $NaHCO_3$ can be dried and packaged for sale. To ensure efficiency of the process, the spent Cl–HT must be reused. This is done thermally in the regeneration stage.

Chloride removal step:

$$Mg_{0.8}Al_{0.2}O_{1.10} + 0.2NaCl + 1.1H_2O \rightarrow Mg_{0.8}Al_{0.2}(OH)_2Cl_{0.2} + 0.2NaOH \tag{9.22}$$

Carbonation step:

$$CO_{2(g)} \leftrightarrow CO_2(aq) \tag{9.23}$$

$$CO_{2(aq)} + OH^- \leftrightarrow HCO_3^-(aq) \tag{9.24}$$

$$HCO_3^- + OH^- \leftrightarrow H_2O(l) + CO_3^{2-}(aq) \tag{9.25}$$

At high pH,

$$Na^+(aq) + CO_3^{2-}(aq) \rightarrow Na_2CO_3(aq) \tag{9.26}$$

At low pH when OH^- has been depleted by reaction 9.24,

$$Na^+(aq) + HCO_3^-(aq) \rightarrow NaHCO_3(aq) \tag{9.27}$$

$$NaHCO_3(aq) \rightarrow NaHCO_3(s) \downarrow \tag{9.28}$$

During the regeneration, the Cl–HT is calcined at above 450 °C to produce the original Mg–Al mixed metal oxide (Mg–Al–O) by releasing Cl, OH, and CO_2 present in the Cl–HT structure. The mixed metal oxide is then returned to the chloride removal stage and the process loop continues, while the released chloride, on the other hand, provides opportunity for the production of Cl-based products which brings additional value to the process. Overall, the process results in a more extensive treatment of the brine because of the removal of both Na and Cl ions while creating more potential for revenue through the sale of CO_2- and Cl^--based chemical products.

9.4.2 Process Evaluation and Performance

A detailed assessment of the proposed process has been presented in [90]. The process was evaluated based on its ability to accomplish the two process objectives of brine treatment and CO_2 utilization. The performance indices for the evaluation of brine treatment were expressed as overall chloride and sodium removal efficiencies, and for CO_2 capture and utilization, as CO_2 absorption capacity and yield of $NaHCO_3$, respectively. Firstly, hydrotalcite and mixed metal oxide were synthesized; thereafter, cyclic tests were carried out to determine the performance indices. Conversion between hydrotalcite and the mixed metal oxide in a process cycle can be demonstrated by XRD investigation (Fig. 9.13).

The Mg–Al–O was found to be effective for the removal chloride from the brine across the six cycles tested as shown in Fig. 9.14. Chloride removal efficiencies

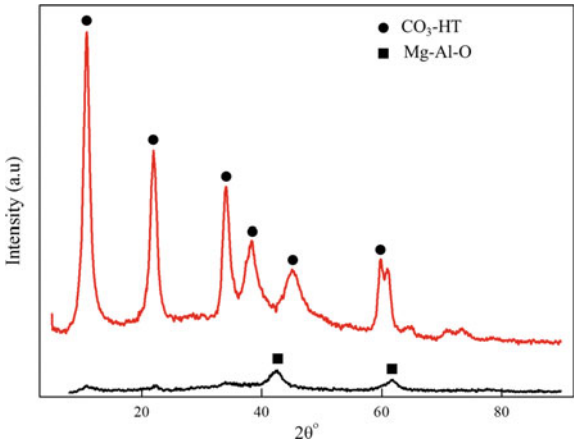

Fig. 9.13 XRD spectra and of the synthesized CO_3–HT and Mg–Al–O. Reprinted with permission from [90], copyright 2018 Elsevier

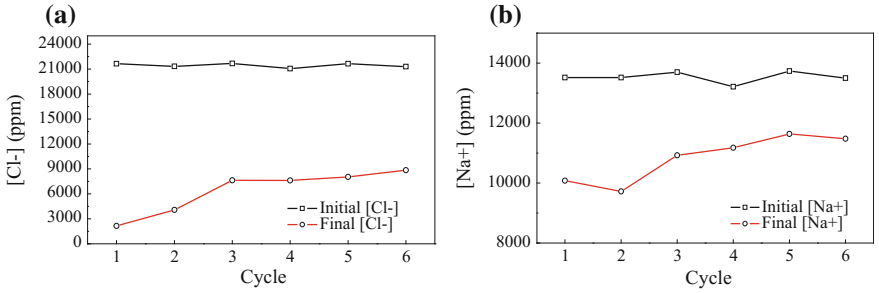

Fig. 9.14 Initial and final concentrations of Cl^- (**a**) and Na^+ (**b**) in brine. Reprinted with permission from [90], copyright 2018 Elsevier

varied from 90 to 58%, from the first cycle to the sixth cycle, with an average of 70% across six cycles. The extent of sodium removal from the brine, due to precipitation of $NaHCO_3$, varied from 26 to 17% from the first cycle to the sixth cycle, with an average of 20% across six cycles, while an average $NaHCO_3$ yield of 44 g/kg carbonated solution was also obtained over six cycles of the process. The characterization of the produced $NaHCO_3$ confirmed that a pure $NaHCO_3$ product can be obtained from the process as presented in Fig. 9.15. Based on these results,

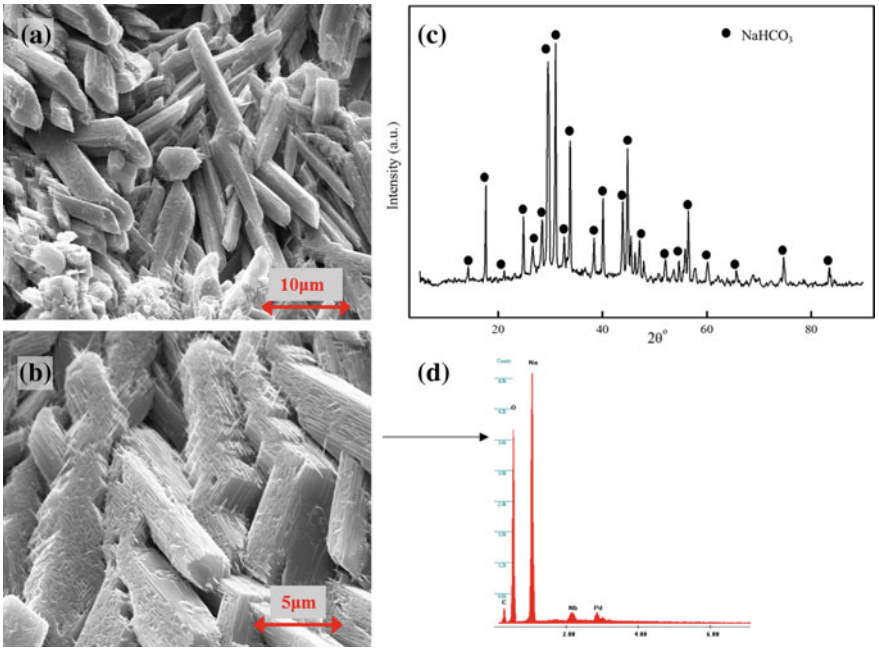

Fig. 9.15 SEM images at different magnifications (**a**, **b**), XRD spectra (**c**), and EDS spectra (**d**) of precipitated $NaHCO_3$. Reprinted with permission from [90], copyright 2018 Elsevier

the proposed process was found to be feasible for the simultaneous treatment of the reject brine and CO_2 utilization.

The proposed process concept is an important contribution to research efforts on brine treatment and CO_2 utilization. It promises to be more effective than earlier processes because it is able to remove both Na and Cl ions from brine, whereas other proposed processes remove only Na ions. Also, in many regions where reject brines are generated in large volumes, desalination plants are usually integrated with power plants; hence, there will be little logistical constraint to the implementation of this process and the potential cost savings from the combined treatment of two industrial wastes as well as the revenue from the sale of two chemical products might justify the investment in this technology. Nonetheless, a detailed techno-economic study is required to determine the economic viability of the proposed process concept.

9.5 Conclusion

Current progress has been demonstrated promising outcomes from solid waste, reject brine, and CO_2 utilization for greener soda ash production. No doubt that the waste and CO_2 utilization in an integrated process has huge potential on the mitigation of CO_2 emission and waste management. Instead of burning $CaCO_3$ for CO_2 and CaO in the conventional Solvay process, those agents can be extracted from the waste streams of power plant or steel plant in a modified Solvay process. The process can further integrate with reject brine treatment from desalination plant to create process that completely consumes wastes as raw materials. This process is suitable to combine with other industries such as power plant or steel plant so that it can at the same exploit both waste material and waste heat for a marketable product production. The revenue received may be partially offset the cost of waste treatment and CO_2 capture that will encourage the effort toward waste and CO_2 emission mitigation.

The calcium extraction from solid waste is influenced by multiple parameters including CaO content and its crystalline phase, particle size distribution, extracting agent concentration (NH_4Cl), and solid-to-liquid ratio. CaO content, particularly free CaO, and the size of solid waste has the most decisive role for an efficient extraction. While the NH_4Cl concentration in the filtrate of the Solvay process is usually in the range of optimum concentration for extraction (>1 mol/L), the solid-to-liquid ratio becomes a very important parameter for balancing Ca^{2+} concentration in the filtrate and extraction efficiency. Recent initiative reveals that steel slag can partly replace CaO in the Solvay process to recover 40% NH_3 [63]; however, it could be significantly improved with a more suitable solid waste (high CaO content with low crystallinity and small particle size).

The modified Solvay process by replacing NH_3 with alcohol amine may render high soda ash recovery, but it faces the critical problem of amine recyclability. The layered double hydroxide process using Al_2O_3–MgO mixture to adsorb Cl^- ions

generating NaOH solution that can capture CO_2 for soda ash production is novel and promising route, but it is still in the research stage.

To accelerate the waste and CO_2 utilization in the soda ash production, several challenges must be solved in future research, i.e., (1) to recognize the waste sources that are most suitable for NH_4Cl extraction and NH_3 recovery, (2) to find calcium extraction assistant method to effectively boost the extraction, (3) to revise the extractor, e.g., using multiple stage or combine mixing with microwave, (4) to look for an efficient way to recycle alcohol amine in modified Solvay process, (5) to prevent the formation of spinel phase during calcination of the layered double hydroxide for the long recyclability of Al_2O_3–MgO system, and finally, an economic evaluation for the proposed process is necessary.

References

1. Salman M, Cizer Ö, Pontikes Y, Santos RM, Snellings R, Vandewalle L, Blanpain B, Van Balen K (2014) Effect of accelerated carbonation on AOD stainless steel slag for its valorisation as a CO_2 sequestering construction material. Chem Eng J 246:39–52
2. Pan S-Y, Chen Y-H, Chen C-D, Shen A-L, Lin M, Chiang P-C (2015) High-gravity carbonation process for enhancing CO_2 fixation and utilization exemplified by the steelmaking industry. Environ Sci Technol 49:12380–12387
3. Chen K-W, Pan S-Y, Chen C-T, Chen Y-H, Chiang P-C (2016) High-gravity carbonation of basic oxygen furnace slag for CO_2 fixation and utilization in blended cement. J Clean Prod 124:350–360
4. Pan S-Y, Chung T-C, Ho C-C, Hou C-J, Chen Y-H, Chiang P-C (2017) CO_2 mineralization and utilization using steel slag for establishing a waste-to-resource supply chain. Sci. Rep. 7:17227
5. Pei S-L, Pan S-Y, Gao X, Fang Y-K, Chiang P-C (2018) Efficacy of carbonated petroleum coke fly ash as supplementary cementitious materials in cement mortars. J Clean Prod 180:689–697
6. Sanna A, Dri M, Hall MR, Maroto-Valer M (2012) Waste materials for carbon capture and storage by mineralisation (CCSM)—a UK perspective. Appl Energy 99:545–554
7. Sanna A (2015) Reduction of CO_2 emissions through waste materials recycling by mineral carbonation. Handb Clean Energy Syst
8. Xie H, Yue H, Zhu J, Liang B, Li C, Wang Y, Xie L, Zhou X (2015) Scientific and engineering progress in CO_2 mineralization using industrial waste and natural minerals. Engineering 1:150–157
9. Ukwattage NL, Ranjith PG, Li X (2017) Steel-making slag for mineral sequestration of carbon dioxide by accelerated carbonation. Measurement 97:15–22
10. W.S. Association (2016) Steel industry by-products, vol 2
11. Blissett RS, Rowson NA (2012) A review of the multi-component utilisation of coal fly ash. Fuel 97:1–23
12. Tayibi H, Choura M, López FA, Alguacil FJ, López-Delgado A (2009) Environmental impact and management of phosphogypsum. J Environ Manage 90:2377–2386
13. Saadaoui E, Ghazel N, Ben Romdhane C, Massoudi N (2017) Phosphogypsum: potential uses and problems—a review. Int J Environ Stud 74:558–567
14. Hammas I, Horchani-Naifer K, Férid M (2013) Solubility study and valorization of phosphogypsum salt solution. Int J Miner Process 123:87–93

15. Ennaciri Y, Bettach M, Cherrat A, Zegzouti A (2015) Conversion of phosphogypsum to sodium sulfate and calcium carbonate in aqueous solution. J Mater Environ Sci 7:1925
16. Mattila HP, Zevenhoven R (2015) Mineral carbonation of phosphogypsum waste for production of useful carbonate and sulfate salts. Front Energy Res 3
17. Zhao H, Li H, Bao W, Wang C, Li S, Lin W (2015) Experimental study of enhanced phosphogypsum carbonation with ammonia under increased CO_2 pressure. J CO_2 Utilization 11:10–19
18. Romero-Hermida I, Santos A, Pérez-López R, García-Tenorio R, Esquivias L, Morales-Flórez V (2017) New method for carbon dioxide mineralization based on phosphogypsum and aluminium-rich industrial wastes resulting in valuable carbonated by-products. J CO_2 Utilization 18:15–22
19. Cárdenas-Escudero C, Morales-Flórez V, Pérez-López R, Santos A, Esquivias L (2011) Procedure to use phosphogypsum industrial waste for mineral CO_2 sequestration. J Hazard Mater 196:431–435
20. Azdarpour A, Asadullah M, Junin R, Manan M, Hamidi H, Mohammadian E (2014) Direct carbonation of red gypsum to produce solid carbonates. Fuel Process Technol 126:429–434
21. Bao W, Zhao H, Li H, Li S, Lin W (2017) Process simulation of mineral carbonation of phosphogypsum with ammonia under increased CO_2 pressure. J CO_2 Utilization 17:125–136
22. Kandil A-HT, Cheira MF, Gado HS, Soliman MH, Akl HM (2017) Ammonium sulfate preparation from phosphogypsum waste. J Radiat Res Appl Sci 10:24–33
23. Abbas KK (2011) Study on the production of ammonium sulfate fertilizer from phosphogypsum. Eng Technol J 29:814
24. Chou M-IM, Bruinius JA, Benig V, Chou S-FJ, Carty RH (2005) Producing ammonium sulfate from flue gas desulfurization by-products. Energy Sour 27:1061–1071
25. Msila X, Billing DG, Barnard W (2016) Capture and storage of CO_2 into waste phosphogypsum: the modified Merseburg process. Clean Technol Environ Policy 18:2709–2715
26. Ahmed M, Shayya WH, Hoey D, Mahendran A, Morris R, Al-Handaly J (2000) Use of evaporation ponds for brine disposal in desalination plants. Desalination 130:155–168
27. Voutchkov N (2011) Overview of seawater concentrate disposal alternatives. Desalination 273:205–219
28. Kaplan R, Mamrosh D, Salih HH, Dastgheib SA (2017) Assessment of desalination technologies for treatment of a highly saline brine from a potential CO_2 storage site. Desalination 404:87–101
29. Krishnaveni V, Palanivelu K (2013) Recovery of sodium bicarbonate from textile dye bath effluent using carbon dioxide gas. Ind Eng Chem Res 52:16922–16928
30. Greenlee LF, Lawler DF, Freeman BD, Marrot B, Moulin P (2009) Reverse osmosis desalination: water sources, technology, and today's challenges. Water Res 43:2317–2348
31. Morillo J, Usero J, Rosado D, El Bakouri H, Riaza A, Bernaola F-J (2014) Comparative study of brine management technologies for desalination plants. Desalination 336:32–49
32. Joo SH, Tansel B (2015) Novel technologies for reverse osmosis concentrate treatment: a review. J Environ Manage 150:322–335
33. Dawoud MA (2012) Environmental impacts of seawater desalination: Arabian Gulf case study
34. Ahmed M, Shayya WH, Hoey D, Al-Handaly J (2001) Brine disposal from reverse osmosis desalination plants in Oman and the United Arab Emirates. Desalination 133:135–147
35. Pérez-González A, Urtiaga AM, Ibáñez R, Ortiz I (2012) State of the art and review on the treatment technologies of water reverse osmosis concentrates. Water Res 46:267–283
36. Giwa A, Dufour V, Al Marzooqi F, Al Kaabi M, Hasan SW (2017) Brine management methods: recent innovations and current status. Desalination 407:1–23
37. Ahmad N, Baddour RE (2014) A review of sources, effects, disposal methods, and regulations of brine into marine environments. Ocean Coast Manag 87:1–7

38. Dziedzic D, Gross KB, Gorski RA, Johnson JT (2006) Feasibility study of using brine for carbon dioxide capture and storage from fixed sources. J Air Waste Manag Assoc 56:1631–1641
39. Bang J-H, Yoo Y, Lee S-W, Song K, Chae S (2017) CO_2 mineralization using brine discharged from a seawater desalination plant. Minerals 7:207
40. Breunig HM, Birkholzer JT, Borgia A, Oldenburg CM, Price PN, McKone TE (2013) Regional evaluation of brine management for geologic carbon sequestration. Int J Greenhouse Gas Control 14:39–48
41. El-Naas MH, Al-Marzouqi AH, Chaalal O (2010) A combined approach for the management of desalination reject brine and capture of CO_2. Desalination 251:70–74
42. Vito CD, Mignardi S, Ferrini V, Martin RF (2011) Reject brines from desalination as possible sources for environmental technologies. In: Ning RY (ed) Expanding issues in desalination
43. Druckenmiller ML, Maroto-Valer MM (2005) Carbon sequestration using brine of adjusted pH to form mineral carbonates. Fuel Process Technol 86:1599–1614
44. Soong Y, Fauth DL, Howard BH, Jones JR, Harrison DK, Goodman AL, Gray ML, Frommell EA (2006) CO_2 sequestration with brine solution and fly ashes. Energy Convers Manag 47:1676–1685
45. Zhao Y, Zhang Y, Liu J, Gao J, Ji Z, Guo X, Liu J, Yuan J (2017) Trash to treasure: seawater pretreatment by CO_2 mineral carbonation using brine pretreatment waste of soda ash plant as alkali source. Desalination 407:85–92
46. Wang W, Hu M, Zheng Y, Wang P, Ma C (2011) CO_2 Fixation in Ca^{2+}/Mg^{2+} rich aqueous solutions through enhanced carbonate precipitation. Ind Eng Chem Res 50:8333–8339
47. Wagialla KM, Al-Mutaz IS, El-Dahshan ME (1992) The manufacture of soda ash in the Arabian Gulf. Int J Prod Econ 27:145–153
48. Steinhauser G (2008) Cleaner production in the Solvay process: general strategies and recent developments. J Clean Prod 16:833–841
49. Jadeja RN, Tewari A (2009) Effect of soda ash industry effluent on agarophytes, alginophytes and carrageenophyte of west coast of India. J Hazard Mater 162:498–502
50. Kasikowski T, Buczkowski R, Cichosz M, Lemanowska E (2007) Combined distiller waste utilisation and combustion gases desulphurisation method: the case study of soda-ash industry. Resour Conserv Recycl 51:665–690
51. Kasikowski T, Buczkowski R, Cichosz M (2008) Utilisation of synthetic soda-ash industry by-products. Int J Prod Econ 112:971–984
52. Kasikowski T, Buczkowski R, Dejewska B, Peszyńska-Białczyk K, Lemanowska E, Igliński B (2004) Utilization of distiller waste from ammonia-soda processing. J Clean Prod 12:759–769
53. Kasikowski T, Buczkowski R, Lemanowska E (2004) Cleaner production in the ammonia–soda industry: an ecological and economic study. J Environ Manage 73:339–356
54. de Carvalho Pinto PC, da Silva TR, Linhares FM, de Andrade FV, de Oliveira Carvalho MM, de Lima GM (2016) A integrated route for CO_2 capture in the steel industry and its conversion into $CaCO_3$ using fundamentals of Solvay process. Clean Technol Environ Policy 18:1123–1139
55. Trypuć M, Białowicz K (2011) $CaCO_3$ production using liquid waste from Solvay method. J Clean Prod 19:751–756
56. Shan Y, Liu Z, Guan D (2016) CO_2 emissions from China's lime industry. Appl Energy 166:245–252
57. Hemalatha T, Ramaswamy A (2017) A review on fly ash characteristics—towards promoting high volume utilization in developing sustainable concrete. J Clean Prod 147:546–559
58. Pan S-Y, Chang EE, Chiang P-C (2012) CO_2 Capture by accelerated carbonation of alkaline wastes: a review on its principles and applications. Aerosol Air Qual Res 12:770–791
59. Eloneva S, Teir S, Salminen J, Fogelholm C-J, Zevenhoven R (2008) Steel converter slag as a raw material for precipitation of pure calcium carbonate. Ind Eng Chem Res 47:7104–7111

60. Jo H, Park S-H, Jang Y-N, Chae S-C, Lee P-K, Jo HY (2014) Metal extraction and indirect mineral carbonation of waste cement material using ammonium salt solutions. Chem Eng J 254:313–323
61. Said A, Mattila H-P, Järvinen M, Zevenhoven R (2013) Production of precipitated calcium carbonate (PCC) from steelmaking slag for fixation of CO_2. Appl Energy 112:765–771
62. He L, Yu D, Lv W, Wu J, Xu M (2013) A novel method for CO_2 sequestration via indirect carbonation of coal fly ash. Ind Eng Chem Res 52:15138–15145
63. de Carvalho Pinto PC, de Oliveira Carvalho MM, Linhares FM, da Silva TR, de Lima GM (2015) A cleaner production of sodium hydrogen carbonate: partial replacement of lime by steel slag milk in the ammonia recovery step of the Solvay process. Clean Technol Environ Policy 17:2311–2321
64. Sun Y, Yao M-S, Zhang J-P, Yang G (2011) Indirect CO_2 mineral sequestration by steelmaking slag with NH_4Cl as leaching solution. Chem Eng J 173:437–445
65. Said A, Laukkanen T, Järvinen M (2016) Pilot-scale experimental work on carbon dioxide sequestration using steelmaking slag. Appl Energy 177:602–611
66. Yong S, Ping ZJ, Lian Z (2016) NH4Cl selective leaching of basic oxygen furnace slag: optimization study using response surface methodology. Environ Progress Sustain Energy 35:1387–1394
67. Sanni E, Sebastian T, Hannu R, Justin S, Arshe S, Carl-Johan F, Ron Z (2009) Reduction of CO_2 emissions from steel plants by using steelmaking slags for production of marketable calcium carbonate. Steel Res Int 80:415–421
68. Hall C, Large DJ, Adderley B, West HM (2014) Calcium leaching from waste steelmaking slag: significance of leachate chemistry and effects on slag grain mineralogy. Miner Eng 65:156–162
69. Hosseini T, Selomulya C, Haque N, Zhang L (2014) Indirect carbonation of victorian brown coal fly ash for CO_2 sequestration: multiple-cycle leaching-carbonation and magnesium leaching kinetic modeling. Energy Fuels 28:6481–6493
70. Lee SM, Lee SH, Jeong SK, Youn MH, Nguyen DD, Chang SW, Kim SS (2017) Calcium extraction from steelmaking slag and production of precipitated calcium carbonate from calcium oxide for carbon dioxide fixation. J Ind Eng Chem 53:233–240
71. Lee S, Kim JW, Chae S, Bang JH, Lee SW (2016) CO_2 sequestration technology through mineral carbonation: An extraction and carbonation of blast slag. J CO_2 Utilization 16:336–345
72. Tong Z, Ma G, Zhang X, Cai Y (2017) Microwave-supported leaching of electric arc furnace (EAF) slag by ammonium Salts. Minerals 7:119
73. Mattila HP, Zevenhoven R (2014) Chapter ten—production of precipitated calcium carbonate from steel converter slag and other calcium-containing industrial wastes and residues. In: Aresta M, van Eldik R (eds) Advances in inorganic chemistry. Academic Press, pp 347–384
74. Sun Y, Parikh V, Zhang L (2012) Sequestration of carbon dioxide by indirect mineralization using victorian brown coal fly ash. J Hazard Mater 209–210:458–466
75. Jo H, Lee M-G, Park J, Jung K-D (2017) Preparation of high-purity nano-$CaCO_3$ from steel slag. Energy 120:884–894
76. Park HK, Bae MW, Nam IH, Kim S-G (2013) Acid leaching of $CaOSiO_2$ resources. J Ind Eng Chem 19:633–639
77. Solvay E (1882) Manufacture of soda by the ammonia process. USA
78. El Naas M (2011) Reject brine management, desalination, trends and technologies. InTech, Croatia, pp 237–252
79. El-Naas M, Ali A-M, Omar C (2010) A combined approach for the management of desalination reject brine and capture of CO_2. Desalination 251:70–74
80. Joris K, Andrea R, Toon VH, Arjan VH, Wim T, Andre F (2010) The impact of CO_2 capture in the power and heat sector on the emission of SO_2, NOx, particulate matter, volatile organic compounds and NH3 in the European Union. Atmos Environ 44:1369–1385
81. Dave N, Do T, Puxty G, Rowland R, Feron PHM, Attalla MI (2009) CO_2 capture by aqueous amines and aqueous ammonia—a comparison. Energy Procedia 1:949–954

82. Huang HP, Shi Y, Li W, Chang SG (2001) Dual alkali approaches for the capture and separation of CO_2. Energy Fuels 15:263–268
83. Dindi A, Quang DV, Abu-Zahra MR (2015) Simultaneous carbon dioxide capture and utilization using thermal desalination reject brine. Appl Energy 154:298–308
84. Abdel-Aal HK, Ibrahim AA, Shalabi MA, Al-Harbi DK (1996) Chemical separation process for highly saline water 1. Parametric Exp Invest Ind Eng Chem Res 35:799–804
85. Abdel-Aal H, Ibrahim A, Shalabi M, Al-Harbi D (1997) Dual-purpose chemical desalination process. Desalination 113:19–25
86. Dindi A, Quang DV, El Hadri N, Rayer A, Abdulkadir A, Abu-Zahra MR (2014) Potential for the simultaneous capture and utilization of CO_2 using desalination reject brine: amine solvent selection and evaluation. Energy Procedia 63:7947–7953
87. Vaidya PD, Kenig EY (2007) CO_2-alkanolamine reaction kinetics: a review of recent studies. Chem Eng Technol 30:1467–1474
88. Conway W, Wang X, Fernandes D, Burns R, Lawrance G, Puxty G, Maeder M (2013) Toward the understanding of chemical absorption processes for post-combustion capture of carbon dioxide: electronic and steric considerations from the kinetics of reactions of CO_2 (aq) with sterically hindered Amines. Environ Sci Technol 47:1163–1169
89. El-Naas MH, Mohammad AF, Suleiman MI, Al Musharfy M, Al-Marzouqi AH (2017) A new process for the capture of CO_2 and reduction of water salinity. Desalination 411:69–75
90. Dindi A, Quang DV, AlNashef I, Abu-Zahra MR (2018) A process for combined CO_2 utilization and treatment of desalination reject brine. Desalination 442:62–74
91. Theiss FL, Sear-Hall MJ, Palmer SJ, Frost RL (2012) Zinc aluminium layered double hydroxides for the removal of iodine and iodide from aqueous solutions. Desalin Water Treat 39:166–175
92. Nenoff TM, Sasan K, Brady PV, Krumhansl JL, Paap S, Heimer B, Howe K, Stoll Z, Stomp J (2017) Waste water for power generation via energy efficient selective silica separations. Sandia National Lab. (SNL-NM), Albuquerque, NM (United States)
93. Kameda T, Yabuuchi F, Yoshioka T, Uchida M, Okuwaki A (2003) New method of treating dilute mineral acids using magnesium–aluminum oxide. Water Res 37:1545–1550
94. Setshedi K, Ren J, Aoyi O, Onyango MS (2012) Removal of Pb (II) from aqueous solution using hydrotalcite-like nanostructured material. Int J Phys Sci 7:63–72
95. Douglas G, Wendling L, Pleysier R, Trefry M (2010) Hydrotalcite formation for contaminant removal from Ranger mine process water. Mine Water Environ 29:108–115
96. Kameda T, Yoshioka T, Hoshi T, Uchida M, Okuwaki A (2005) The removal of chloride from solutions with various cations using magnesium–aluminum oxide. Sep Purif Technol 42:25–29
97. Kameda T, Oba J, Yoshioka T (2017) Simultaneous removal of Cl^- and SO_4^{2-} from seawater using Mg–Al oxide: kinetics and equilibrium studies. Appl Water Sci 7:129–136